



HAL
open science

Évaluation du compactage par pétrissage et des performances à long terme des sols traités à la chaux

Geetanjali Das

► **To cite this version:**

Geetanjali Das. Évaluation du compactage par pétrissage et des performances à long terme des sols traités à la chaux. Géotechnique. Ecole Centrale de Nantes, 2021. English. NNT : . tel-03678919v1

HAL Id: tel-03678919

<https://hal.science/tel-03678919v1>

Submitted on 26 Apr 2022 (v1), last revised 25 May 2022 (v2)

HAL is a multi-disciplinary open access archive for the deposit and dissemination of scientific research documents, whether they are published or not. The documents may come from teaching and research institutions in France or abroad, or from public or private research centers.

L'archive ouverte pluridisciplinaire **HAL**, est destinée au dépôt et à la diffusion de documents scientifiques de niveau recherche, publiés ou non, émanant des établissements d'enseignement et de recherche français ou étrangers, des laboratoires publics ou privés.

THESE DE DOCTORAT DE

L'ÉCOLE CENTRALE DE NANTES

ÉCOLE DOCTORALE N° 602
Sciences pour l'Ingénieur
Spécialité : Génie Civil

Par

Geetanjali DAS

Evaluation of kneading compaction method and the long-term performances of lime-treated soils.

Thèse présentée et soutenue à Nantes, le 03-12-2021

Unité de recherche : Département Géotechnique, Environnement, Risques naturels et Sciences de la terre (GERS), Université Gustave Eiffel, Campus de Nantes

Rapporteurs avant soutenance :

Enrique ROMERO MORALES Directeur de recherche, Universitat Politècnica de Catalunya, Barcelone
Francesca CASINI Associate Professeur, Università degli Studi di Roma Tor Vergata

Composition du Jury :

Président :	Emmanuel ROZIERE	Professeur des universités, École Centrale de Nantes
Examineurs :	Bertrand FRANÇOIS	Associate Professeur, Université de Liège
	Rabah HAMZAOUI	Directeur de recherche, Ecole Spéciale des Travaux Publics, Paris
Dir. de thèse :	Dimitri DENELEE	Directeur de recherche, Université Gustave Eiffel, Bouguenais
Co-encadrant :	Andry RAZAKAMANANTSOA	Chargé de recherche, Université Gustave Eiffel, Bouguenais

Invité

Daniel PUIATTI

Ingénieur, DPST Consulting, Villemomble

ACKNOWLEDGMENT

I would like to graciously express my gratitude to Dr. Andry Razakamanantsoa, Dr. Gontran Herrier, Dr. Didier Lesueur, and Dr. Dimitri Deneele for providing me this opportunity to work as a Ph.D. student in France. I particularly thank Dr. Andry Razakamanantsoa for his valuable guidance and constant supervision in all experimentations and for writing Peer-reviewed journals during the accomplishment of this thesis. I also thank Dr. Gontran Herrier and Dr. Dimitri Deneele for their supervision in finalizing the novelty of my works through Peer-reviewed journals.

I express my sincere thanks to Mr. Erwann Rayssac, Mr. Daniel Bondenes, Mrs. Sophie Ricordel, Mr. Denis Courtier-Murias, Mrs. Nadege Caubriere, and Mr. Martin Guillon, Laboratory instructors at Université Gustave Eiffel, for their support in conducting laboratory experimentations at Université Gustave Eiffel.

My wholehearted thanks to Dr. Andry Razakamanantsoa for providing me the '*Laboratory proposed kneading device*,' which possesses the novelty for most of my Peer-reviewed Journals. I also thanks Dr. Gontran Herrier, who always supported me in the completion of experiments required to be conducted at Lhoist R&D, Belgium. I thank Mrs. Gaetane Sioen, Laboratory instructor at Lhoist R&D, Belgium, who performed microstructural tests to complete a part of my experimental works.

I would like to express my thanks to Arthur Antoine, a Master's student from Polytech Nantes, who helped me finish my Patent application by building the proposed device, which work has been submitted for publication. I also thank Dr. Lucile Saussaye, Researcher at Cerema, Blois, for her support in completing my first Peer-reviewed article. I thank Dr. Harifidy Ranaivomanana, Professor at Université de Nantes, Saint-Nazaire, and Dr. David Bulteel, Professor at IMT Lille Douai, who have approved the official progress of my thesis during each year.

Finally, I express my deepest thanks to my Parents and friends, who fully supported me mentally during the accomplishment of this thesis.

GEETANJALI DAS

TABLE OF CONTENTS

TABLE OF CONTENTS	iv
LIST OF FIGURES	x
LIST OF TABLES	xiv
NOMENCLATURE & ABBREVIATIONS	xvi
GENERAL INTRODUCTION	4
Objectives	5
Scope and Organization of the thesis	5
Chapter 1	5
STATE OF ART	5
General	5
1.1 Introduction	5
1.2 Soil-lime reactions	7
1.3 Modifications in soil pore-structure due to soil-lime reactions	8
1.4 Long-term performances of lime-treated soil	13
1.4.1. Implementation parameters and their contribution towards hydromechanical performances... 16	
1.4.1.1. Lime content and curing conditions	16
1.4.1.2. Compaction	20
1.4.1.3. Mellowing	23
1.4.2. Lime leaching from lime-treated soil	26
1.5 Discussions	28
1.5.1 Field Investigations of lime-treated soil structures	28
1.5.2 Lime content and Compaction conditions effect on lime-treated soil	29
1.5.3. Leaching mechanism of compacted lime-treated soil	29
1.5.4 Long-term performance evaluation of lime-treated soil	30
1.6 Research gaps and Proposals	31
Chapter 2	33
MATERIALS AND EXPERIMENTAL PROCEDURES	33
General	33
2.1 Materials	33
2.1.1. Soil used and its properties.	33
2.1.2 Lime used and its properties.	33

2.2 Experimental Procedures	34
2.2.1 Determination of Lime Modification Optimum.....	34
2.2.2. Determination of compaction parameters	35
2.2.3. Specimen preparation for compaction	36
2.2.4 Compaction tests	36
2.2.4.1 Standard Static Compaction.....	36
2.2.4.2 Kneading compaction	36
2.2.5 Curing of specimens.....	38
2.2.6 Unconfined Compressive Strength.	38
2.2.7 Hydraulic Conductivity test.	38
2.2.8 Physicochemical Investigations.	40
2.2.8.1. Water Content and suction measurement.....	40
2.2.8.2 pH and Electric Conductivity measurement	41
2.2.8.3 Inductive Coupled Plasma Optical Emission spectroscopy test.....	41
2.2.9 Volume and Mass measurement.	42
2.2.10 Microstructural investigations.....	42
2.2.10.2 Pore structure measurements by MIP.	43
2.2.10.3. Micro X-ray Fluorescence (μ -XRF)	44
2.2.10.4. Scanning Electron Microscope (SEM).....	44
Chapter 3.....	45
EVALUATION OF THE LONG-TERM EFFECT OF LIME TREATMENT ON A SILTY SOIL EMBANKMENT AFTER SEVEN YEARS OF ATMOSPHERIC EXPOSURE: MECHANICAL, PHYSICOCHEMICAL, AND MICROSTRUCTURAL STUDIES (PROPOSAL 1).	45
General.....	45
3.1 Studied embankments and specimens sampling.....	45
3.2 Laboratory Tests	49
3.3 Results.....	50
3.3.1 Unconfined Compressive Strength.	50
3.3.2 SEM observations.	51
3.3.3. Physicochemical properties.....	51
3.3.4. Pore size distributions.	56
3.3.5. Distribution of SSA.....	57
3.4 Discussions.	59
3.4.1 Evaluation of the UCS measured from the in-situ cured lime-treated specimens.....	59
3.4.2 Contribution of mesopores generation towards strength evolution in lime-treated soil	59
3.4.3 Long-term effect of lime treatment on the water content and pH distribution at the core of the embankments.	60

3.4.4 Effect of lime treatment on the evolution of suction at the core of the embankments.....	61
3.4.5 Effectiveness of lime treatment on the upper layer of the embankment submitted to atmospheric exposure.....	62
3.4.6. Evaluation of pore structures measured between the untreated and the lime-treated soil.....	63
3.4.7. Comparison between the volume of mesopores measured by MIP and BJH.	64
3.4.8 Long-term effect of lime treatment on the SSA.....	64
3.5 Conclusions.....	65
Chapter 4.....	67
EFFECT OF KNEADING ACTION ON THE COMPRESSIVE STRENGTH AND MICROSTRUCTURE EVOLUTION OF LIME-TREATED SILTY SOIL (PROPOSAL 2).....	67
General.....	67
4.1 Materials.	68
4.1.1 Sample preparations.....	68
4.2 Laboratory tests.....	69
4.3 Results.....	69
4.3.1 UCS of kneading compacted specimens.....	69
4.3.2. Comparison of UCS evolution.....	70
4.3.3 Comparison of microstructural modifications.	71
4.4 Discussions.	76
4.5 Conclusions.....	81
Chapter 5.....	83
INFLUENCE OF PORE FLUID-SOIL STRUCTURE INTERACTIONS ON COMPACTED LIME-TREATED SILTY SOIL (PROPOSAL 3).....	83
General.....	83
5.1 Materials.	83
5.1.1 Sample preparations.....	84
5.2 Laboratory tests.....	84
5.2.1 Hydraulic conductivity test.	84
5.2.2 Unconfined compressive strength (UCS) test.	85
5.2.3 Pore structure determination.	85
5.3 Results.....	85
5.3.1 Comparative evaluation of UCS in the lime-treated unleached and leached soil.	85
5.3.2 Comparative evolution of Pore size distribution.....	86
5.3.3 Hydraulic conductivity measurements in untreated and lime-treated soil.	88
5.3.4 Evolution of calcium concentrations in the effluents of untreated and lime-treated soils.	92
5.4 Discussions.	93
5.4.1 Influence of pore fluid-soil structure interaction on the UCS evolution of lime-treated soil.....	93

5.4.2 Influence of pore fluid-soil structure interaction on the hydraulic behavior of lime-treated soil.	94
5.5 Conclusions.....	97
Chapter 6.....	99
INFLUENCE OF DIFFERENT WETTING-DRYING CYCLES TESTING CONDITIONS ON THE PHYSICOCHEMICAL AND MICROSTRUCTURE EVOLUTION OF LIME-TREATED SOIL (PROPOSAL 4).....	99
General.....	99
6.1 Materials.	100
6.2 Sample preparations.....	100
6.3 Testing conditions for Wetting and drying cycles.	100
6.4 Laboratory Experiments.....	101
6.5 Results.....	102
6.5.1 W-D/D-W cycle influence on UCS evolution.	102
6.5.2 W-D/D-W cycle influence on volume variations.....	102
6.5.3 W-D/D-W cycle influence on physicochemical evolution in the specimens.....	103
6.5.4 W-D/D-W cycle influence on pore structure modifications.	106
6.6 Discussions.	107
6.7 Conclusions.....	111
CHAPTER 7	113
INFLUENCE OF WETTING FLUIDS ON THE COMPRESSIVE STRENGTH, PHYSICOCHEMICAL, AND PORE-STRUCTURE EVOLUTION IN LIME-TREATED SOIL SUBJECTED TO WETTING AND DRYING CYCLES (PROPOSAL 5).	113
General.....	113
7.1 Materials and Methodologies.....	114
7.1.1 Soil, Lime, and fluid properties.	114
7.1.2 Sample preparations.....	114
7.1.3 Laboratory tests.....	114
7.2 Results.....	115
7.2.1 UCS evolution at the end of W-D cycle.....	115
7.2.2 Physicochemical evolution at the end of W-D cycle.	116
7.2.3 Pore structure evolution at the end of W-D cycle.....	118
7.3 Discussions	120
7.4 Conclusions.....	121
Chapter 8.....	123
CONCLUSIONS, CONTRIBUTIONS AND FUTURE SCOPE.	123
General.....	123
8.1 Conclusions.....	123

8.2 Contributions.....	125
8.3 Future scope.....	125
BIBLIOGRAPHY	127
APPENDIX-I	144
Peer reviewed Journals	144
Conferences (National & International).....	144
Patent	144

LIST OF FIGURES

Fig. 1-1 Lime Applications.....	6
Fig. 1-2 Soil-lime physico-chemical reactions.....	9
Fig. 1-3 Pore size distribution in untreated and 5% lime-treated expansive clay soil (after Tran et al., 2014).....	10
Fig. 1-4 SEM micrographs obtained from untreated and lime-treated soils (a-c) (modified after Rosone et al., 2019); (d) XRD pattern obtained from untreated and lime-treated impersol (d) (modified after Al-Mukhtar et al., 2010) subjected to different curing times.....	12
Fig. 1-5 Pore size distribution (PSD) by MIP analysis (after Rosone et al., 2019) (a) and SSA by BET analysis (b & c) obtained from untreated and lime-treated soils subjected to different curing durations...	13
Fig. 1-6 Height variations of lime-treated materials subjected to 5 successive W-D cycles (after Cuisinier et al., 2014) (a), Evolution of porosity in lime-treated soil with respect to a number of F-T cycles (b) (Han et al., 2021), Evolution of UCS (c) and Hydraulic conductivity (d) in lime-treated soil subjected to 12 W-D cycles (Cuisinier et al., 2020).....	15
Fig. 1-7 Flow chart interlinking durability, hydromechanical behaviors, implementation parameters and microstructure modifications in lime-treated soil.....	16
Fig. 1-8 UCS evolution with respect to lime content (a) and curing time (b).....	18
Fig. 1-9 Hydraulic conductivity evolution with respect to lime content.....	19
Fig. 1-10 UCS evolution in different lime-treated soil after about 1 month of curing time as a function of compaction moisture contents.....	21
Fig. 1-11 UCS evolution as a function of mellowing durations reported by Sivapullaiah et al. (1998) (a); Osinubi and Nwaiwu (2006) (b); Ali and Mohamed (2017) (c); and Al-Ne'aimi and Hussain (2011) (d).25	
Fig. 1-12 SEM images of 5% hydrated lime-treated soil immediately after mixing (a), 48 hours after mixing (b) (modified after Di Sante et al., 2015).....	25
Fig. 1-13 Evolution of hydraulic conductivity in lime-treated soil compacted immediately after mixing and after 7 days of mellowing (after Moghal et al., 2020).....	26
Fig. 2-1 LMO of MLD soil.....	34
Fig. 2-2 Laboratory designed Mini Proctor compaction tool.....	35
Fig. 2-3 Laboratory used Standard Static compaction tool.....	37
Fig. 2-4 Laboratory Kneading compaction tool.....	37
Fig. 2-5 Schematic diagram of flexible wall permeameter setup.....	39
Fig. 2-6 WP4C Dewpoint Potentiometer (Decagon device) (modified from Haghverdi et al., 2020).....	41

Fig. 2-7 Schematic diagram showing excitement of electrons, thus jumping to a high-level energy after absorbing energy, and again returning to the low-level energy by releasing light of specific wavelength (after Fassel and Kniseley, 1974)..... 41

Fig. 2-9 Schematic diagram showing nitrogen gas adsorption and desorption phases during the BET test (modified from Mohammadi et al., 2020)..... 43

Fig. 3-1 Trench excavated in the lime-treated embankment (T2) for the sampling of specimens..... 46

Fig. 3-2 Plan view, Front view along with Cross-sectional view of the excavated trench made for sample collections from the Untreated embankment (*All units in meter*) 47

Fig. 3-3 Plan view, Front view along with Cross-sectional view of the excavated trenches made for sample collections from the lime-treated embankment (*All units in meter*) 48

Fig. 3-4 UCS measured from the field- and laboratory-cured specimens..... 50

Fig. 3-5 SEM images of specimens Nat 2 (0.45 m) (a) and T1-1 (0.30 m) (b-d) at different magnifications sampled from the core of the embankments. 51

Fig. 3-6 Contour plots showing the distributions of water content (%) in the untreated (a) and the cross-sections T1 (b), T2 (c), T3 (d), and T4 (e) of the lime-treated embankments measured during deconstruction. 52

Fig. 3-7 Water content (%) measured on specimens sampled from the upper layer of the lime-treated embankment during deconstruction. 53

Fig. 3-8 Contour plot showing the distribution of pH in the untreated (a) and the cross-sections T1 (b), T2 (c), T3 (d), and T4 (e) of the lime-treated embankments measured during deconstruction..... 55

Fig. 3-9 pH measured on specimens sampled from the upper layer of the lime-treated embankment during deconstruction. 56

Fig. 3-10 PSD and Cumulative (Cum.) pore volume observed between untreated (Nat & Nat 2) and lime-treated specimens (T2-2 & T2-3) at a depth of 0.15 m & 0.45 m normal to the slope by MIP (a-d) & BJH (e-h) methods. 57

Fig. 3-11 Contour plot showing the distribution of SSA (m^2/g) in the untreated (a), and cross-sections T1 (b), T2 (c), T3 (d), and T4 (e) of the lime-treated embankments during deconstruction..... 58

Fig. 3-12 Evolution of mesopores distribution (a) and cumulative pore volume (b) between T1-1 & T2-4 by BJH method. 60

Fig. 3-13 Water retention plot obtained from the present soil compared to the one obtained from Nguyen et al. (2015). 62

Fig. 3-14 Evolution of SSA with respect to the presence of pore volume in the mesopore range of pore diameter 25-75 Å. 65

Fig. 4-1 Strength evolution of 1%, 2.5% and 4% lime-treated kneading compacted specimens at OMC-28 days (a), WMC-28 days (b), OMC-90 days (c), WMC-90 days (d), OMC-180 days (e), and WMC-180 days (f).	70
Fig. 4-2 UCS measured from 1%, 2.5% and 4% lime-treated specimens subjected to static and kneading compactions at OMC-28 days (a), WMC-28 days (b), OMC-90 days (c), WMC-90 days (d), OMC-180 days (e), and WMC-180 days (f).	71
Fig. 4-3 Evolution of pore structure after addition of 1%, 2.5%, and 4% lime in the untreated statically compacted specimens at OMC and after 28 days of curing.	72
Fig. 4-4 Analysis of pore structure by MIP for 1%, 2.5% and 4% lime-treated specimens compacted by kneading and static compaction at OMC, and WMC and after 28 days (a-d) and 90 days (e, f) of curing at 20°C.	73
Fig. 4-5 Evolution of isotherms in 1%, 2.5%, and 4% lime-treated OMC, and WMC kneading and statically compacted specimens after 28 days (a-d) and 90 days (e, f) of curing at 20°C.	74
Fig. 4-6 Percentage of cumulative mesopores volume measured in 1%, 2.5%, and 4% lime-treated OMC, and WMC kneading and statically compacted specimens after 28 days (a-f) and 90 days (g-i) of curing at 20°C.	75
Fig. 4-7 μ -XRF image highlighting calcium distributions in 1%, 2.5%, and 4% lime-treated static (a, b, & c) and kneading compacted (d, e, & f) specimens prepared at OMC after 28 days of curing time at 20°C.	76
Fig. 4-8 Diagonal Crack in kneading compacted (a), and vertical crack in statically compacted (b) specimens after UCS test at 1% lime treatment, compacted at OMC and after 28 days curing.	78
Fig. 4-9 Schematic diagram showing the difference in the effect of kneading and static compaction on aggregates deformation and lime-dispersion.	79
Fig. 4-10 Comparative evolution of UCS in in-situ core sampled and laboratory-accelerated cured soil of dimension of l/d ratio of 1 (a) and 2 (b).	79
Fig. 4-11 Comparison of PSD obtained by BJH in 2.5% lime-treated kneaded specimens obtained between laboratory accelerated cured specimen and 7 years in-situ atmospherically cured specimens.	80
Fig. 5-1 Comparative evolution in UCS obtained in the 28 days cured and leached statically (a) and Kneading (b) compacted specimens.	86
Fig. 5-2 Comparative evolution of PSD in the 1% (a), 2.5% (b), and 4% (c) lime-treated statically and Kneading compacted 28-days cured specimens.	86
Fig. 5-3 Comparative evolution of PSD between 1%, 2.5%, and 4% lime-treated unleached and leached statically compacted (a-c) and kneading compacted specimens (d-f).	87

Fig. 5-4 Evolution in hydraulic conductivity of untreated and 1%, 2,5%, and 4% lime-treated DW and LW submitted statically (a-c), and kneading (d-f) compacted specimens.	89
Fig. 5-5 Percentage of life expectancy that can be reached in a unit height earth structure if subjected to 40 PVF of DW (a) and LW (b) in kneading-and statically-compactd soil.....	91
Fig. 5-6 Concentration of Ca leached from the untreated and 1%, 2.5%, and 4% lime-treated DW & LW submitted statically (a-c) and kneading (d-f) compacted specimens.	92
Fig. 5-7 Schematic diagram showing differences in lime-treated compacted soil matrices after being subjected to static and kneading compactions and the expected flow paths of permeant solution during hydraulic test.....	95
Fig. 6-1 UCS evolution in the lime-treated specimens subjected to W-D/D-W cycles as per AP, RP, and DP testing conditions.	102
Fig. 6-2 Average volume variations (a-c), and water content variations (d-f) recorded from the specimens subjected to W-D/D-W cycles as per AP, RP, and DP testing conditions.....	104
Fig. 6-3 Soil suction (a) and pH (b) measured in the initial and UCS subjected specimens during W-D/D-W cycles as per AP, RP, and DP testing conditions.	104
Fig. 6-4 Calcium concentration (a) and Electric Conductivity (b) measured in the effluents collected from the specimens subjected to W-D/D-W cycles as per AP, RP, and DP testing conditions.	105
Fig. 6-5 Comparative PSD by MIP (a-c), and Cum. (cumulative) pore volume evolution by BJH (d-f) between untreated and 10 months cured lime-treated specimen with the lime-treated specimens subjected to W-D/D-W cycles as per AP, RP, and DP testing conditions.....	106
Fig. 6-6 Comparative evolution of calcium concentration and electric conductivity in the specimens subjected to W-D/D-W cycles.	110
Fig. 7-1 Lime-treated specimens placed in four different fluids for 1 st wetting during the W-D cycles. .	115
Fig. 7-2 Unconfined Compressive Strength obtained after 5 W-D cycles.....	116
Fig. 7-3 Soil suction and soil pH measured at the end of 5 W-D cycles along with the reference 28 days cured soil.....	117
Fig. 7-4 Final pH measured in the effluents and compared with the initial pH of the respective fluids at the end of 5 W-D cycles.	118
Fig. 7-5 Comparative evaluation of PSD in lime-treated specimens subjected to 0.10 M NaCl (a), MMA (b), 0.60 M NaCl (c), and DW (d) at the end of 5 th W-D cycles with the with the untreated and the reference specimens by MIP.....	119
Fig. 7-6 Comparative evaluation of Cumulative (Cum.) pore volume evolution in the mesopore range 24-250 Å in specimens subjected to different fluids at the end of 5 W-D cycles with the reference and untreated soil by BJH.....	120

LIST OF TABLES

Table 1-1 Field study reported regarding the long-term effect of lime treatment on the strength evolution of earth structures.	14
Table 1-2 Evolution of hydraulic conductivity in different types of lime-treated soil prepared at different lime contents and compaction conditions.	23
Table 1-3 UCS evolution as a function of leaching durations (after Deneele et al., 2016).....	27
Table 1-4 Percent retained strength, and lime leached out after 14 leachate cycles in different types of soils treated with different lime contents (after Chittori et al., 2013)	28
Table 1-5 Literature gaps observed, and proposals made.	31
Table 2-1 Atterberg’s limit and Methylene Blue value of the soil (after Nguyen, 2015).....	33
Table 2-2 Chemical composition of MLD soil (after Nguyen, 2015).....	33
Table 2-3 Chemical composition of Quick lime	34
Table 2-4 Maximum dry density and OMC of untreated and lime-treated silty soil	35
Table 3-1 Test programs with samples identifications and numbers	49
Table 3-2 Suction measured on untreated and lime-treated core-sampled specimens.....	54
Table 3-3 Difference in pore volume measured in the mesopore range of pore diameter 60-250 Å by MIP and BJH methods.	64
Table 4-1 Types and number of specimens prepared by static-and kneading-compactions.	68
Table 4-2 UCS measured in lime-treated kneaded soil subjected to different curing time and temperatures.	70
Table 4-3 Percentage distribution of Calcium (Ca) within the polished surface area of the kneading- and statically-compacted specimens.....	76
Table 4-4 Isotherm peak and cumulative pore volume measured in lime-treated soil.	81
Table 5-1 The pH and Electric Conductivity of solutions.	84
Table 5-2 S_r measured in the lime-treated soil at the end of curing time and at the end of hydraulic test..	88
Table 5-3 Duration of percolation phase in the lime-treated soil to renew 40 PVF of solutions.....	89
Table 5-4 Estimated life expectancy of a unit height in-situ earth structure, if built with the present soil configurations.	91
Table 5-5 Tortuosity calculated from statically and kneading compacted specimens	95
Table 5-6 Comparison of k and life expectancy obtained for in-situ and laboratory cured 2.5% lime-treated kneaded soil, percolated by LW.....	97
Table 6-1 Presentation of testing conditions.....	101

Table 6-2 Estimated average velocity of wetting front and duration required by infiltrated water to flow to the center of a reference in-situ structure..... 109

Table 7-1 The pH and Electric Conductivity of wetting fluids..... 114

Table 7-2 Water content measured during suction measurement. 116

Table 7-3 Cumulative (Cum.) concentration of Ca analyzed in the effluents at the end of 5 W-D cycles in the lime-treated soils. 118

NOMENCLATURE & ABBREVIATIONS

Terms	Representation	
Brunauer–Emmett–Teller	BET	
Barrett-Joyner-Halenda	BJH	
Calcium-aluminate-hydrates	C-A-H	
Calcium-aluminate-silicate-hydrates	C-A-S-H	
Calcium-silicate-hydrates	C-S-H	
California Bearing Ratio	CBR	
Compaction energy higher than standard compaction energy	HE	
Compaction energy lower than standard compaction energy	LE	
Degree of saturation	S_r	%
Demineralized water	DW	
Diameter	d	m
Drying-wetting cycles	D-W cycles	
Dry of optimum	DMC	%
Electric Conductivity	EC	$\mu\text{S}/\text{cm}$
Freeze and Thaw cycles	F-T cycles	
Grain Size Distribution	GSD	
Hydraulic conductivity	k	m/s
Hydraulic tortuosity	T	
Inductive Coupled Plasma Optical Emission spectroscopy	ICP-OES	
Kneading compaction	K	
Length	l	m
Length to diameter ratio	l/d	
Lime modification optimum	LMO	%
Liquid Limit	LL	%
Low-mineralized water	LW	
Marche-les-Dames	MLD	
Maximum dry density	$\rho_{d(max)}$	kN/m^3
Mercury Intrusion Porosimetry	MIP	
Micro X-ray Fluorescence	$\mu\text{-XRF}$	
Optimum moisture content	OMC	%
Plastic Limit	PL	%
Plasticity Index	PI	%
Pore diameter		Å (angstrom)
Pore Size Distribution	PSD	
Pore Volume Flow	PVF	
Quick lime	CaO	
Resilient modulus	M_R	MPa
Scanning Electron Microscopy	SEM	

Specific surface area	SSA	m ² /g
Standard compaction energy	NE	
Static compaction	S	
Stress	σ	MPa
Strain	ϵ	%
Thermogravimetric analysis	TGA	
Unconfined Compressive Strength	UCS	MPa
Unified Soil Classification system	USCS	
Velocity of wetting front	W_f	m/s
Wet of optimum	WMC	%
Wetting-drying cycles	W-D cycles	
X-Ray Diffraction	XRD	

GENERAL INTRODUCTION

Management of natural resources is a critical challenge in any land development project, especially for projects related to earthworks. A cost-effective way to conserve natural resources is to use soil located directly in the land reserved for the project. This makes it essential to improve the engineering properties of the available soil. In this regard, soil improvement by lime is known to be an efficient and economical technique that leads to improved bearing capacity, strength, modulus, etc. (Akula et al., 2020; Al-Mukhtar et al., 2012; Bell, 1996; Diamond and Kinter, 1965; Little, 1995; Osula, 1996).

Soil improvement by lime consists of two primary modification mechanisms: a) the cation exchange reactions and flocculation-agglomeration resulting in a reduction of soil plasticity and increased workability, and b) the long-term pozzolanic-reactions leading to the development of the cementitious compounds, thus improving the soil's hydromechanical performances (Bell, 1996; Diamond and Kinter, 1965; Rogers and Glendinning, 1996). These primary mechanisms bring chemical modifications, which accompanied with appropriate implementation parameters, such as compaction conditions, curing conditions, etc., contribute towards the long-term improvements in lime-treated soil (Asgari et al., 2015; Wang et al., 2017; Le Runigo et al., 2009, 2011).

The long-term performances of lime-treated soil structures are interlinked with the hydromechanical performances of the soil during its service life. The hydromechanical evolution in lime-treated soils is shown to be heavily influenced by numerous implementation parameters, such as lime contents (Al-Mukhtar et al., 2010; Farooq et al., 2011), curing conditions (Asgari et al., 2015; Wang et al., 2017), soil type (Chittori et al., 2013; Little, 1995), compaction conditions (Cuisinier et al., 2011; le Runigo et al., 2009; Mitchell et al., 1965; Watabe et al., 2000), etc. Such influences were extensively investigated through microstructural investigations (Deneele et al., 2016; le Runigo et al., 2011, 2009; Lemaire et al., 2013; Verbrugge et al., 2011).

However, most of these existing studies were obtained from controlled laboratory test results, while the feedback from field performance is limited (Akula et al., 2020; Bicalho et al., 2018; Charles et al., 2012). It is worth noting that the conditions faced by the lime-treated soil under the laboratory- and field-testing environments are relatively different, some of which are as below.

On the field, the usual design-construct of an earthwork project is as follows: the proposed soil materials are initially subjected to a laboratory test to define the compaction parameters required for the design. During the construction, these compaction parameters are achieved by implementing the compaction procedure, which is often adjusted according to the type of soil. Fine-grained soil, particularly clayey soil, is preferred to be compacted by Padfoot roller (Clegg, 1964; Kouassi et al., 2000), which applies kneading action in the soil during compaction. However, this effect of kneading action has not been well investigated in terms of mechanical, hydraulic, and microstructural evolution of lime-treated soil.

Additionally, on the field, lime-treated soil is exposed to numerous stresses produced owing to uncontrolled parameters in the surrounding environment. Such a situation can alter the hydromechanical performances of the lime-treated structure and can lead to reduced lifetime of the same. For an instant, a hydraulic earth structure that remains permanently in contact with water suffers several fluctuations in water level (Chen et al., 2018; Jia et al., 2009; Johansson and Edeskär, 2014; Xiong et al., 2019), which induces ingress or egress of water in the structure. Besides, during such a phenomenon, water infiltrates into the exposed soil resulting in interactions with the lime-treated soil. Since natural water can be constituted of several organic compounds or inorganics compounds or a mixture of both, which control the pH level of the water (Erlandsson et al., 2010; Stockdale et al., 2016), thus, the chemical nature of the infiltrated water

can modify the improvement of the lime-treated soil properties. Soil pH in a lime-treated structure contributes greatly towards the maintenance of the long-term performance of the concerned structure.

At the laboratory scale, the above influence of water fluctuation level is analyzed as per ASTM D559 standard (ASTM 2015). The ASTM procedure involves subjecting the soil to a constant wetting duration at room temperature and then drying durations at an oven using 71°C. Often the soil is subjected to distilled water during the wetting phase. However, how well do these current standard testing conditions, which involves the applied wetting and drying durations, the drying temperature, as well as the wetting fluids, represent the actual field situation a soil is exposed to during the water fluctuation phenomenon, remains less explored.

In the wake of the above discussion, this thesis is focused on presenting hydromechanical, physicochemical, and microstructural evolution in lime-treated soil, which is investigated by subjecting the lime-treated soil to a situation close to the field situation. The investigation involved the use of varying lime contents, curing conditions, and compaction conditions. In the beginning, considering the importance of feedback from the field, the thesis evaluates the evolution of lime-treated soil on being exposed to the atmosphere for several years. Later importance of reproducing a compaction mechanism close to the field was elaborated by comparing the laboratory and field hydromechanical evolution in lime-treated soils. In the end, the thesis highlights the importance to be given to laboratory reproduced testing conditions such as temperature and types of wetting fluids to represent a condition close to the field in order to evaluate the wetting and drying cycles impact on lime-treated soil.

Objectives

A brief objective of this thesis is as follows:

1. Field investigation of a long-term atmospherically exposed lime-treated earth structure.
2. Compressive strength evaluation in lime-treated soil subjected to field practiced kneading compaction mechanism.
3. Hydraulic Conductivity evaluation in lime-treated soil subjected to field practiced kneading compaction mechanism using different ionic strength solution.
4. Influence of wetting-drying cycle's testing conditions on the physicochemical, and microstructure of lime-treated soil.
5. Influence of wetting fluids on the compressive strength, physicochemical, and microstructure of lime-treated soil.

Scope and Organization of the thesis

Having identified the objectives, this thesis is organized chapter-wise as follows:

1. Chapter 1 covers the literature background, followed by additional research required, which has led to five proposals presented for the accomplishment of the above five objectives.
2. Chapter 2 covers the materials and common experimental techniques implemented in this study for accomplishments of the proposals made in Chapter 1.

3. Chapter 3 accomplishes objective 1. This chapter thoroughly evaluates the long-term effect of lime treatment in a seven years atmospherically exposed embankment. The chapter demonstrates that the effect of lime treatment persists significantly throughout the core of the embankment even after seven years of atmospheric exposure. The benefit brought through lime treatment was expressed in terms of significant strength evolution, presence of high soil pH, and cementitious compounds formation in the sampled specimens.
4. Chapter 4 accomplishes objective 2 by investigating the evolution of mechanical performance and microstructural modifications in lime-treated soil subjected to field practiced kneading mechanism. This chapter highlights the relevancy of implementing kneading action in lime-treated soil by presenting a comparative mechanical and microstructural evolution between the specimens sampled from the field and the one produced at the laboratory using kneading action.
5. Chapter 5 accomplishes objective 3 by evaluating the hydraulic conductivity, leaching, and microstructural evolution in lime-treated kneading compacted soil using different ionic strength solutions. This chapter shows the relevancy of life expectancy between lime-treated kneading compacted soil obtained at laboratory scale with the one obtained from the field, thus, again highlighting the importance of the role of kneading action on lime-treated soil. Besides, this chapter also concludes the importance of reproducing a laboratory percolation fluid close to the one lime-treated soil is exposed to under field circumstances.
6. Chapter 6 accomplishes objective 4 by investigating the effect of wetting-drying cycles using different testing conditions on the physicochemical, mechanical, and microstructure evolution of lime-treated soil. This chapter presents the influence of wetting and drying cycles using testing conditions that represent the field conditions. The results obtained were compared with the reference standard testing condition to highlight the importance of reproducing laboratory wetting-drying cycle testing conditions close to the field. This work is performed using a laboratory proposed device.
7. Chapter 7 accomplishes objective 5 by presenting the effect of different wetting fluids on the physicochemical, mechanical, and microstructure evolution of lime-treated soil. In this chapter, a similar configured lime-treated soil was subjected to wetting and drying cycles using four different wetting fluids, and the evolution attained was compared. This chapter highlights the importance of reproducing laboratory wetting fluids close to the one lime-treated soil experienced in the field.
8. Chapter 8 finally summarizes the major conclusions derived from the conclusions obtained during the accomplishment of each objective, contributions made by this thesis, and possible future scope obtained during this study.

Chapter 1

STATE OF ART

General

This chapter presents the literature associated with the long-term performances, hydromechanical evolution, and microstructural modifications on lime-treated soil. The chapter begins with the basic soil-lime reactions and their influence on the soil pore modifications. Then the long-term performances of lime-treated soil are commented, which is shown to be governed by the hydromechanical performances of lime-treated soil, which is again dependent on the implementation parameters. The term hydromechanical performances indicate the combined hydraulic and mechanical performances of a given lime treated soil.

Based on the literature review presented, the additional research required in the future was identified and are reported at the end. Then, proposals made to fulfill the identified research gaps are presented.

1.1 Introduction

With the emerging population, exploitation and consumption of natural resources are moving linearly, hence management of natural resources such as soil is a critical challenge. In every land development project, the use of soil located directly in the worksite is one of the fruitful means of contribution towards such management. However, natural soil, due to its 'low-engineering properties', often fails to sustain the earth structures built with it, owing to the critical competition with the climatic or seasonal variations. Several natural disasters, such as heavy erosion of hydraulic earth structures due to fluctuations of water level, crack propagation in pavements due to swelling-shrinkage of clay soil etc., are commonly encountered (Puppala, 2021; Puppala et al., 2013). These lead to several uneconomic crises.

In this aspect, 'Soil improvement' becomes a common practice. Soil improvement is defined as a process of improving the engineering properties of the soil, chemically and physically, thus making the soil suitable to retain a durable structure. Chemical improvement includes the use of organic or inorganic binders to improve soil properties. Some of them are fly ash produced from coal-burning (Kolias et al., 2005; Show et al., 2003), a mixture of lime and cement (Ojuri et al., 2017; Todingrara et al., 2017), cement kiln dust (Baghdadi et al., 1995; Miller and Azad, 2000), municipal solid waste incinerator ashes (Liang et al., 2020), alkaline activated materials (Cristelo et al., 2012; Zhang et al., 2013), lime (Le Runigo et al., 2011, 2009). Physical improvement involves the execution process such as soil-binder mixing process, using an appropriate binder and water contents during compaction and mixing, implementing the accurate compaction conditions (Cuisinier et al., 2011; Deneele et al., 2016; Makki-Szymkiewicz et al., 2015; Le Runigo et al., 2011, 2009).

Of the several chemicals utilized for soil stabilization, lime is regarded as one of the most versatile chemicals due to its wide applicability in industrial and environmental uses (Dowling et al., 2015). Fig. 1-1 presents the extensive use of lime in different fields, as reported by National Lime Association (2020). Use of lime for soil improvement started somewhere in 1000 B.C (Cherian and Arnepalli, 2015). With the passage of time, lime was reported to be paramount in improving industrial application through environmentally friendly technologies. Besides the versatile and environmental applicability nature of lime, lime was shown to be comparatively cost-effective in several fields (Dowling et al., 2014). During lime

production, the cost of energy use was reported to account for up to half of the gross production costs as per the survey produced by the European Commission, 2014a.

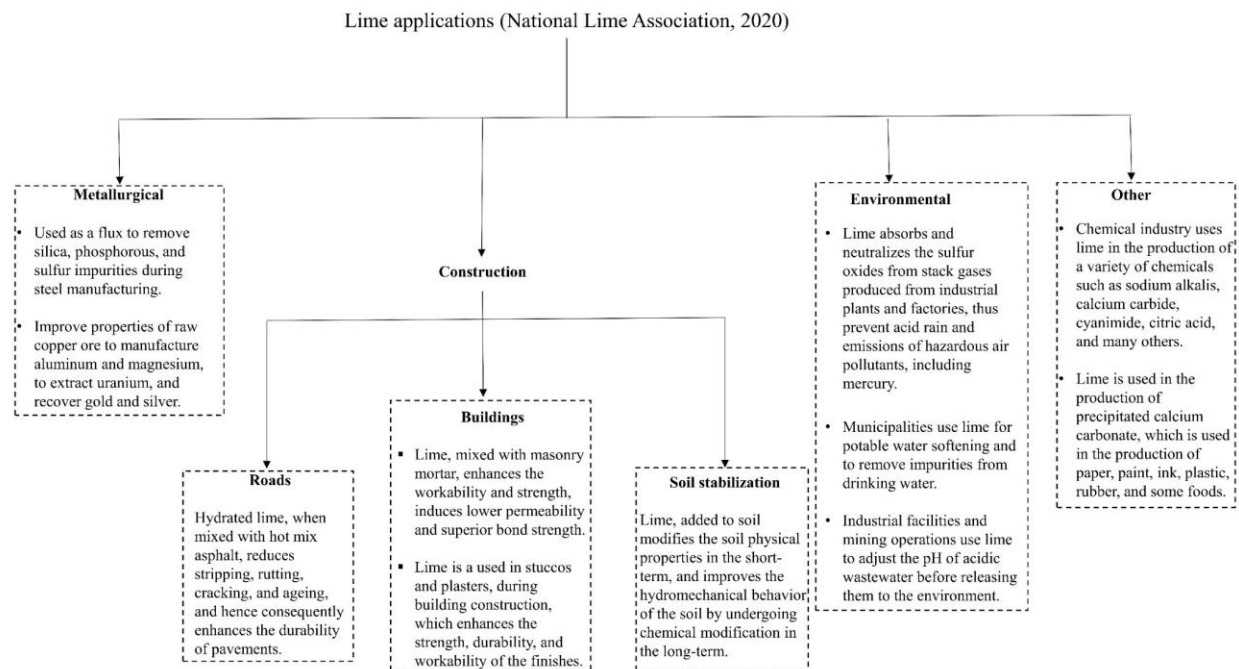


Fig. 1-1 Lime Applications.

Studies concluding the contribution of lime treatment towards improvement from basic soil properties (such as soil plasticity, workability) to geotechnical properties (such as strength and hydraulic conductivity) are extensive (Cuisinier et al., 2011; Le Runigo et al., 2011, 2009; Verbrugge et al., 2011). Not only engineering facts but also the microstructural mechanism responsible for such contribution is extensively investigated (Bin et al., 2007; Deneele, 2016; Han et al., 2021; Vitale et al., 2017).

Sor far, Little (1995) presented an extensive review on stabilization of pavement subgrades and base courses with lime. This review involves hydromechanical performances as well as the mechanism governing such evolution. However, after 1995, there are few reviews available that presents the contribution of lime treatment to earthen structures. For example, Babu and Poulouse (2018) presented a review on the soil-lime reactions of lime-treated soil, Yunus et al. (2014) only focused on factors affecting clay-lime reactions. Recently, Monzoor and Yousuf (2020) presented an overview regarding the lime effect on hydromechanical performances. However, these existing studies does not review essential implementation parameters and microstructural modifications responsible for such evolution.

In this aspect, it becomes essential to present a review that highlights the contribution of lime treatment in geotechnical engineering through facts evidencing hydromechanical performances with an explanation of the involved mechanism. Thus, this chapter reviews the contribution of lime towards soil improvement in terms of hydromechanical evolution and microstructural modifications, which is responsible for the durability of a structure. Essential implementation parameters that contribute towards such evolution, as well as the associated mechanisms, were discussed. The end is then accompanied by a

discussion highlighting major gaps and limitations in the currently available literature, which needs to be focused on future research for efficient and effective application of lime in soil improvement.

1.2 Soil-lime reactions

On addition of lime to the soil-water system, there occur two basic stage chemical reactions as below:

- i. Short-term reaction or modification reaction
- ii. Long-term reaction or pozzolanic reaction

During the Modification reaction or short-term reaction, quick lime (CaO), on being in contact with water, undergoes 'hydration reaction' and forms Ca(OH)₂ (calcium hydro-oxide). Ca(OH)₂ further undergoes 'dissociation reaction' resulting in calcium ions (Ca²⁺) and hydroxide ions (OH⁻). The dissociated Ca²⁺ ions then take place in a cation exchange reaction that leads to soil flocculation/agglomeration (Bell, 1996; Diamond and Kinter, 1965; Little, 1995). This results in a decrease in soil plasticity and improves soil workability. Note that the effectiveness of cation exchange reaction depends on the type of minerals present in the soil (Mitchell and Soga, 2005). On the other hand, the released OH⁻ increases the pH of the soil leading to the alumino-silicate dissolution, thus, releasing Silica (Si), Alumina (Al), Magnesium (Mg) from the soil.

During the second stage reaction, called the 'pozzolanic reaction or long-term reaction,' the available Ca²⁺ ions react with the dissociated Si, Al, and Mg and form pozzolanic/cementitious compounds. Some of the major cementitious compounds commonly formed in lime-treated soil are Calcium-silicate-hydrates (C-S-H), Calcium-aluminate-hydrates (C-A-H), Calcium-aluminate-silicate-hydrates (C-A-S-H) (Bell, 1996; Ingles and Metcalf, 1972; James et al., 2008; Little, 1987).

It is worth noting that the duration of the first-stage reaction is often demonstrated to be comparatively rapid (0-72 hours) (Bell, 1996; Beetham et al., 2015; Croce and Russo, 2003) than the second stage reaction, which takes a longer time (up to several months or years) and plays a major role in improving the hydromechanical, and microstructural properties of the treated soil (Beetham et al., 2015; Diamond and Kinter, 1965; Little, 1995). The above stages of soil-lime-water reactions are briefed in Fig. 1-2.

In addition to the above reactions, exposing a lime-treated soil to an external environment leads to carbonation. Carbonation is defined as a reaction in which CO₂ diffuses through lime-treated soil, gets dissolved in the pore water, reacts with the dissolved Ca²⁺, and produces calcium carbonates (CaCO₃) (Arandigoyen et al., 2006; Vitale et al., 2018). It is a naturally occurring phenomenon that is instigated when any cementitious or pozzolanic compounds come in contact with air (Deneele et al., 2021). During carbonation, precipitation of calcium carbonate occurs with the consumption of available lime for pozzolanic reactions in the short term. While in the long term, carbonation was shown to be detrimental due to the conversion of pozzolanic compounds into CaCO₃, which is regarded as a weak cementitious compound (Deneele et al., 2021). However, the extent of carbonation is shown to be marked by several factors such as temperature, relative humidity (RH), CO₂ concentrations (Xu et al., 2020), soil type and mineralogy (Bandipally et al., 2018; Deneele et al., 2021), binder amount, and curing period (Deneele et al., 2021).

1.3 Modifications in soil pore-structure due to soil-lime reactions

The two basic chemical reactions provided in the preceding section bring significant modification in the soil pore structure. Several microstructural investigations are available in previous studies delineating such modifications and their contribution towards the mechanism of soil improvement. In this chapter, (i) the discussion related to categories of soil pore-structure are made as per the classifications provided by IUPAC (Rouquerol et al., 1994), which categories soil pores in terms of width dimension as macropores ($> 500 \text{ \AA}$), mesopores ($20\text{-}500 \text{ \AA}$), and micropores ($< 20 \text{ \AA}$); and (ii) the classification of soil type was made as per Unified Soil Classification system (USCS) (ASTM D2487-17e1, 1984).

The flocculation and agglomeration that occur during the short-term reactions, after lime addition and compaction, were shown to increase the inter-aggregate pore structure, *i.e.*, the macroporosity of lime-treated soil. Tran et al. (2014) compared the macropores structure obtained from Mercury Intrusion Porosimetry (MIP) test between statically compacted untreated expansive clay soil (CH) and 5% quicklime-treated clay soil after seven days from lime treatment. They observed that the population of inter-aggregates pores in the untreated soil was around the modal size $1.5 \times 10^4 \text{ \AA}$, while for the lime treated soil, it was from $1.5 \times 10^4 \text{ \AA}$ to $3 \times 10^4 \text{ \AA}$ (as presented in Fig. 1-3). They stated that the increased inter-aggregates pores in the lime-treated soil were due to flocculation and agglomeration of soil particles during the modification process. A similar observation was reported by Locat et al. (1996) in Louiseville clay soil (CH) treated with different lime contents. Through Scanning Electron Microscopy (SEM) observations, the macropores structure of uncompacted untreated and 2% lime-treated soil cured for 80 days, and 5% and 10% lime-treated soil cured for 100 days were compared. The inter-aggregates pores in untreated soil were observed to have a radius smaller than $0.5 \times 10^4 \text{ \AA}$, while 2% lime-treated soil have an inter-aggregate pore radius of $1\text{-}5 \times 10^4 \text{ \AA}$, and 5 and 10% lime-treated soils in between 3 and $5 \times 10^4 \text{ \AA}$. However, the extent of development of inter-aggregate pores was dependent on the compaction conditions implemented, which are delineated in later sections.

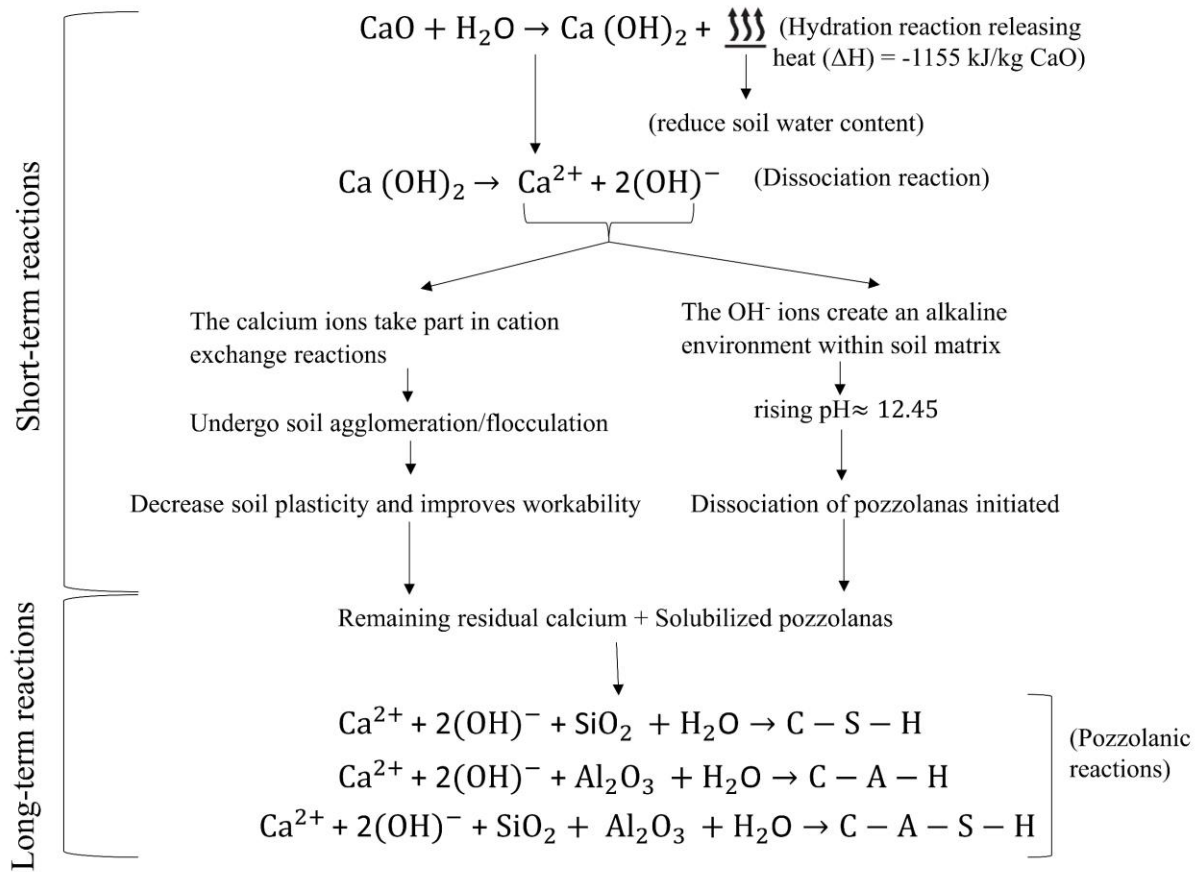


Fig. 1-2 Soil-lime physico-chemical reactions.

Russo and Modoni (2013) compared the soil fabric change induced by 3% of quicklime treatment on OMC-standard proctor compacted alluvial silty soil by using Mercury Intrusion Porosimetry (MIP) analysis. MIP test was performed by injecting mercury in two cycles. The first cycle involves an intrusion followed by extrusion, and the second cycle involves an intrusion of mercury. During each cycle, determination of constricted pore volume was measured, where the constricted pore is defined as the porosity accessible only through pores of the smaller entrance (Delage and Pellerin, 1984). The analysis of MIP was made in terms of the cumulative volume of constricted pores, which is defined as the difference between first and second intrusion volumes (Delage and Lefebvre, 1984; Delage and Pellerin, 1984; Griffiths and Joshi, 1989). A significantly greater number of entrance pore diameters in the large pore range was observed in lime-treated soil compared to the untreated soil, irrespective of the curing time. They stated this observation as a consequence of dimensional growth of the aggregates induced by the flocculation of soil during the short-term reaction.

The increased inter-aggregate pores due to lime treatment during the short-term modification reaction were reported recently by Rosone et al. (2020). Rosone et al. (2020) compared the macroporosity evolution immediately after static compaction in untreated (CH) and 2, 4, and 6% quicklime-treated specimens. They showed that upon lime treatment, the macroporosity of soil increases due to the flocculation reaction. Other studies with a similar conclusion as above involve studies reported by Vitale et al. (2020) and Wang et al. (2016).

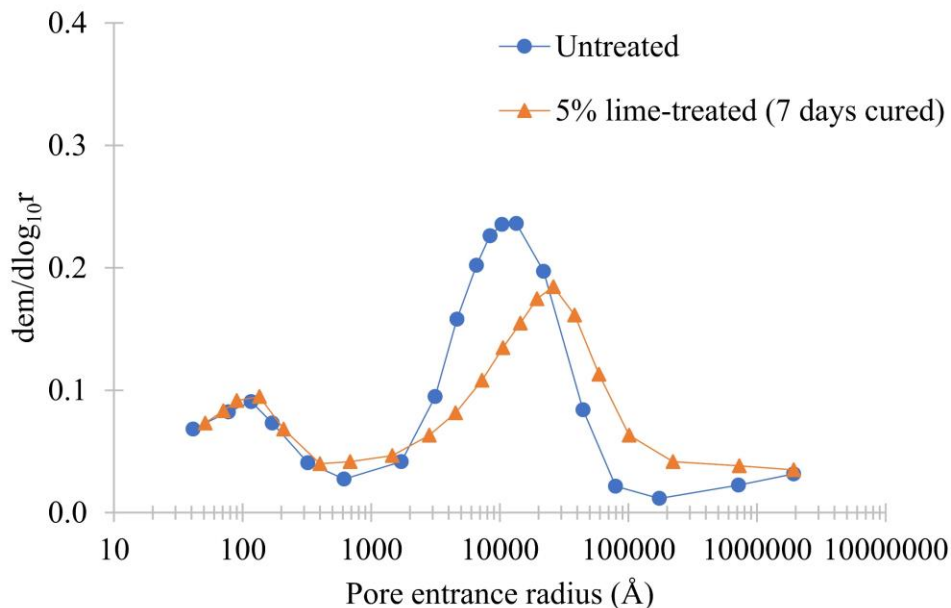


Fig. 1-3 Pore size distribution in untreated and 5% lime-treated expansive clay soil (after Tran et al., 2014)

With the increase in duration from lime treatment, the stabilization reactions or pozzolanic reactions are initiated. Pozzolanic reactions are slow reactions that give rise to several complex cementitious compounds, of which the production of major cementitious compounds is shown in Fig. 1-2. Cementitious materials can be defined as porous solids consisting of a complex mixture of crystalline and gel-like phases

that are formed within the soil pore structure (Jennings et al., 2002). The presence of such compounds was detected mostly through several analyses, of which use of Scanning Electron Microscope (SEM) image analysis and X-Ray Diffraction (XRD) analysis was extensively reported in previous studies for observing the structure and compounds of pozzolanic products (Al-Mukhtar et al., 2010; Bhuvaneshwari et al., 2014; Bin et al., 2007; Dash and Hussain, 2011; Deneele, 2016; Rosone et al., 2019; Tran et al., 2014; Ural, 2021; Vitale et al., 2017; Wang et al., 2016). It is worth noting that XRD mainly detects C-A-H, and C-A-S-H, which are crystalline phases, available as portlandite or calcite, and cannot detect C-S-H, which is amorphous in nature (Tran-Nguyen et al., 2017).

Rosone et al. (2019) performed the SEM micrographs of expansive clay soil (CH) treated with 2, 4, and 6% of quicklime. The obtained SEM micrographs were compared with the one obtained from untreated soil. Fig. 1-4(a-c) provides the difference in soil fabrics between the statically compacted lime-treated and untreated soil and the presence of C-S-H and C-A-S-H after a curing time of 1 month (Fig. 1-4b) and 1 year (Fig. 1-4c). Similarly, the presence of C-S-H within the soil fabric of CH soil after 7 days from treatment with 5% of quicklime was also reported by Tran et al. (2014) in SEM images obtained at high magnification.

Deneele (2016) compared the fabric structure of proctor OMC-compacted untreated silty soil (CL) with 3% quicklime-treated silty soil after 28 days of curing at laboratory temperature. The comparison of the structure was made at both low and high magnification through SEM image analysis. Based on the comparative evaluation Deneele (2016) highlighted the development of cementing compounds linking the soil particles as a result of pozzolanic reactions induced by the high soil pH.

Al-Mukhtar et al. (2010) provided a distinct XRD pattern highlighting several peaks representing the production of cementitious compounds (C-A-H) and availability of lime in impersol (CH) treated with 20% lime. Fig. 1-4d provides a comparative evolution of C-A-H and available lime in 20% lime-treated soil subjected to 7-, 28-, 45-, and 90-days curing periods. Dash and Hussain (2011) presented both SEM and XRD analysis to highlight the development of cementitious compounds in residual soil (CL) treated with 5% and 9% quicklime after 28 days from treatment. Other studies evidencing the development of cementitious compounds through SEM and XRD analysis include studies reported by Di Sante et al. (2020), Jan and Mir (2018), and Ural (2021).

Due to the inter-connected meshes created by the gel-like cementitious compounds within the soil fabrics, smaller pores evolve, as evidenced in several studies through MIP analysis (Cuisinier et al., 2011; Elkady, 2016; Rosone et al., 2019). Rosone et al. (2019) compared the evolution of pores in lime-treated soil treated at different lime contents and subjected to different curing times with the untreated soil. Clay soil (CH) was treated with 2, 4, and 6% of lime, and the evolution of pore-structure of these treated specimens was evaluated by MIP analysis after 7 days, 1 month, and 1 year of curing time. The evolution obtained for the 2% lime-treated soil at different curing times was presented in Fig. 1-5a with the untreated soil. Fig. 1-5a show a gradual increase in pores of smaller diameter with increased curing time, thus evidencing the enhancement of smaller pores evolution. A similar conclusion was provided by Cuisinier et al. (2011) and Elkady et al. (2016), who showed that lime treatment gives rise to the development of pores smaller than 3000 Å.

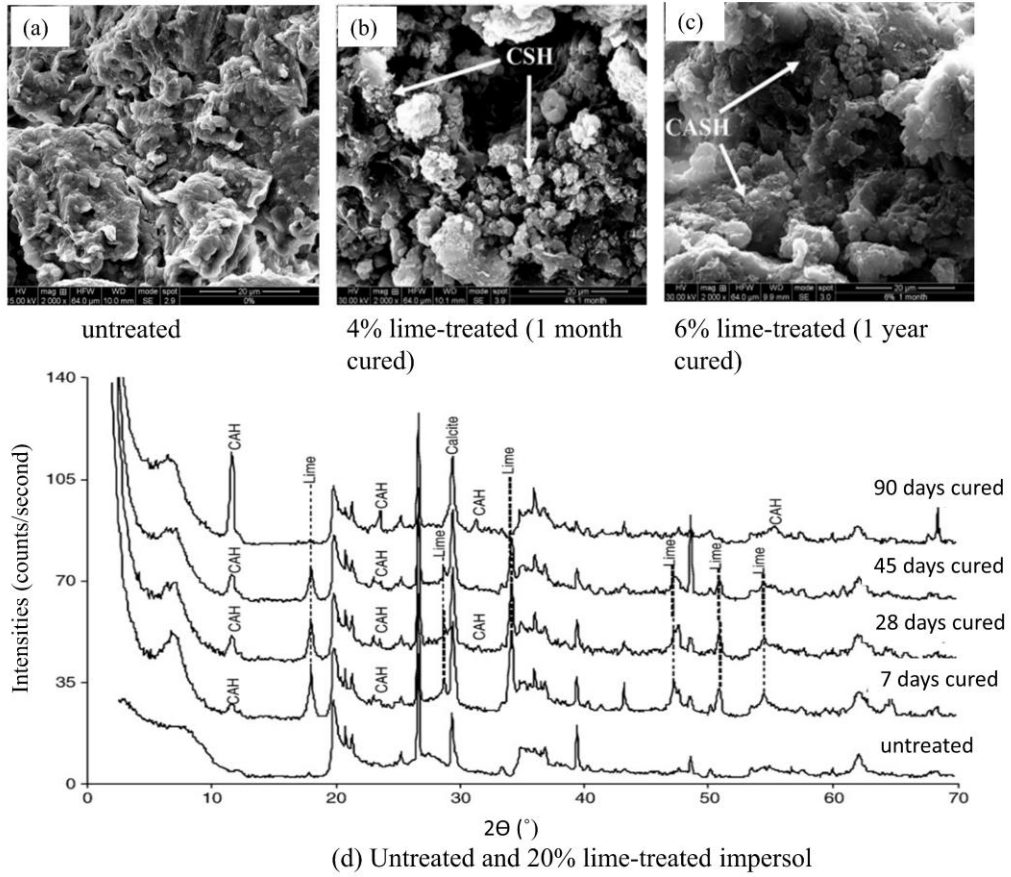
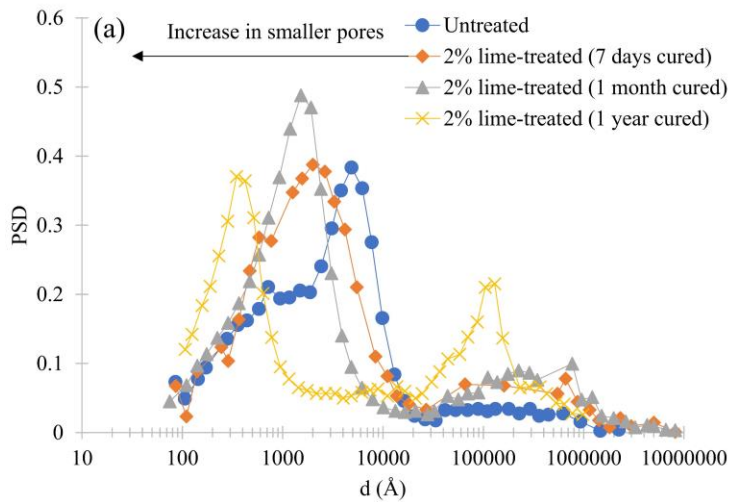


Fig. 1-4 SEM micrographs obtained from untreated and lime-treated soils (a-c) (modified after Rosone et al., 2019); (d) XRD pattern obtained from untreated and lime-treated impersol (d) (modified after Al-Mukhtar et al., 2010) subjected to different curing times.



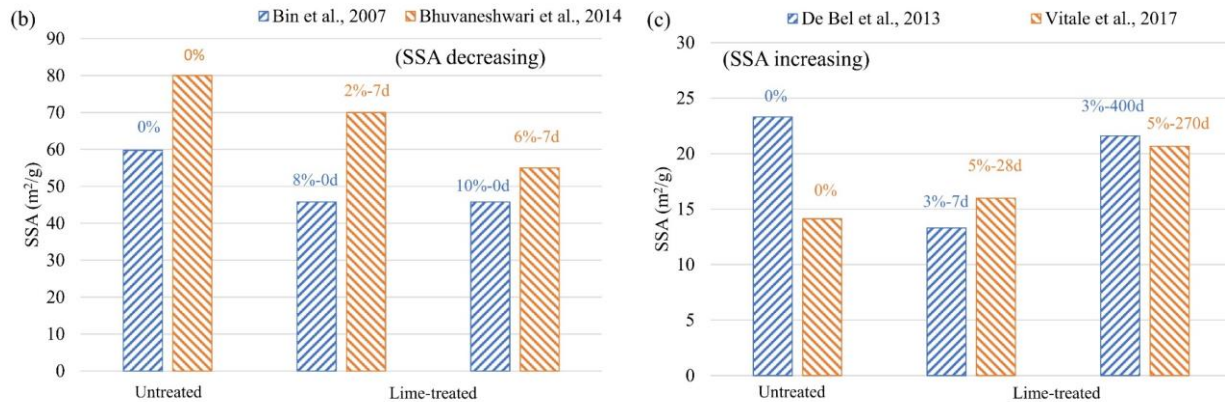


Fig. 1-5 Pore size distribution (PSD) by MIP analysis (after Rosone et al., 2019) (a) and SSA by BET analysis (b & c) obtained from untreated and lime-treated soils subjected to different curing durations.

The evolution of these smaller pores as a consequence of lime treatment was shown to affect the evolution of specific surface area (SSA). The SSA of lime-treated soil was shown to decrease after the addition of lime during short-term curing (Bhuvaneshwari et al., 2014; Bin, 2007). Bin et al. (2007) evaluated the SSA of expansive soil (CH) after mixing it with 8% and 10% of lime by Brunauer–Emmett–Teller (BET) analysis. The obtained SSA was $59.78 \text{ m}^2/\text{g}$, which then decreased to $45.80 \text{ m}^2/\text{g}$ and $45.76 \text{ m}^2/\text{g}$ in the 8% and 10% lime-treated soil, respectively (Fig. 1-5b). Bhuvaneshwari et al. (2014) reported a similar conclusion on expansive soil (CH) treated with 2% and 6% lime and after 7 days from treatment (Fig. 1-5b). This decrease in SSA was explained as a result of modification reaction, during which aggregation of the clay platelets form flocs and reduces the clay size particles (Bhuvaneshwari et al., 2014).

However, after a long time from treatment, the SSA was shown to rise (De Bel et al., 2013; Vitale et al., 2017). This duration taken to show a significant change in the SSA evolution is dependent on the soil type. De Bel et al. (2013) recorded the SSA value of natural silty soil (CL) as $23.3 \text{ m}^2/\text{g}$ by BET analysis. The SSA became $13.3 \text{ m}^2/\text{g}$ after 7 days from treatment with 3% of quicklime (Fig. 1-5c). This SSA was then raised to $21.6 \text{ m}^2/\text{g}$ after 400 days from treatment (Fig. 1-5c). The rise in SSA was also reported in 5% quicklime-treated kaolinite by Vitale et al. (2017), who recorded an SSA of $14.13 \text{ m}^2/\text{g}$ for natural Kaolin. The SSA was observed to fall to $6.74 \text{ m}^2/\text{g}$ after 1 day from treatment. However, it then increased to $15.93 \text{ m}^2/\text{g}$ and $20.66 \text{ m}^2/\text{g}$ after 28 and 270 days from treatment (Fig. 1-5c).

1.4 Long-term performances of lime-treated soil

The long-term performance of lime-treated soil is defined as its resistance against water-induced erosion or resistance to cyclic freezing and thawing (Houben and Guillaud, 1994). Few in-situ studies are available that report the long-term effect of lime treatment in developing significant strength in earthen structures after several years from construction. Some of these studies are presented in Table 1-1.

In addition to these field investigations, extensive controlled laboratory investigations are made in previous studies to evaluate the long-term performances of lime-treated soil. Evaluation of long-term performances of lime-treated soil at laboratory scale is often made by investigating the hydromechanical performances of the soil by subjecting it to successive wetting and drying (W-D) or freeze and thaw (F-T)

cycles (Akcanca and Artemin, 2014; Cuisinier et al., 2020, 2014; Ding et al., 2021; Han et al., 2021; Nguyen et al., 2019). Exposing soil to such cycles is designed to assess the swelling-shrinkage nature and erosion resistance developed in the soil due to lime treatment, which is mainly accounted for the collapsibility of a soil structure (Puppala et al. 2013, 2021).

A significant reduction in the swelling potential and increase in yield stress of a highly expansive problematic soil (CH) was reported by Stoltz et al. (2014) after being treated with 2% and 5% quicklime. However, the same soil being subjected to successive W-D cycles suffered an irreversible shrinkage and swelling behavior and loss in yield stress, as demonstrated by Cuisinier et al. (2014). This irreversible shrinkage and swelling nature were shown in terms of height modifications ($\Delta H/H_0$) of the lime-treated materials as a function of the number of cycles (as presented in Fig. 1-6a). This behavior was obtained for 28 and 180 days cured soils, subjected to W-D cycles using a suction-controlled oedometer, which imposed a suction in the range of 0-8 MPa in the sample. Such a feature was reported to be more significant in the soil treated with low lime content (2%) and subjected to lower curing time (28 days). This was demonstrated to be due to total loss in cementitious bonding, while 5% quicklime-treated and 180 days cured soil maintained some of the cementitious bonding.

Table 1-1 Field study reported regarding the long-term effect of lime treatment on the strength evolution of earth structures.

Type of structures	Lime content	Soil type	Observations	References
Pavements	1%	Cohesive fine-grained	The resilient modulus (M_R) of the base course of Arizona lime-treated pavement increased from approximately 136.5-240 MPa to 376-2806.2 MPa after 1 year from construction.	
	5%	Highly plastic Burleson Clay	The M_R increased from about 6.9 MPa to about 538 MPa, even after constant exposure to a wet climate for 2 years from the time of construction using lime-treated soil.	Little, 1995, 1993, 1992
	4%	Highly expansive Calcium montmorillonite	Unconfined Compressive Strength (UCS) increased from 0.06 MPa to 1.34 MPa after 10 years of construction	
	3%	Clayey gravel	UCS of raw gravel was less than 0.345 MPa. After 14 years of lime treatment, it ranged from a low value of 2.068 MPa to a maximum value of 4.136 MPa.	Dawson and McDowell, 1961
	4%	CL soil	The M_R was increased from 96.5 MPa to 703.2 MPa after 11 years from construction.	Jung and Bobet, 2008
Underground columns	12.5%	Sandy, gravel, and clay soil	The UCS increased threefold after 11 years from construction and remained constant for a further 15 years' curing.	Kitazume and Takahashi, 2009

The irreversible deformation brought in lime-treated soil during W-D cycles, as shown in Fig. 1-6a, was explained at the microscale level by Han et al. (2021). Han et al. (2021) performed 10 F-T cycles, which involved a temperature variation between -15°C to 15°C on CL soil treated with 6% lime and after 180 days of laboratory curing. They analyzed the pore-structure of the soil after 0, 1, 3, 6, and 10 F-T cycles and reported an increased porosity of the lime-treated compacted soil with increased F-T cycles (Fig. 1-6b).

Thus, such a modification can bring changes in the strength and hydraulic performances of lime-treated soils, which was reported by Akcanca and Aytakin (2014), and Cuisinier et al. (2020).

Cuisinier et al. (2020) reported the impact of successive W-D cycles on the strength and hydraulic conduction evolution of CL soil treated with 1% and 3% quicklime. Lime-treated soil after 90 days of laboratory curing was exposed to 12 W-D cycles using the procedure reported in ASTM D559 (ASTM, 2015). The UCS of the 3% lime-treated specimens gradually decreased with increased W-D cycles (Fig. 1-6c), and the obtained UCS at the end of 12 cycles was found to be even lower than the one obtained for the untreated soil. Besides, the magnitude of the hydraulic conductivity was shown to increase by about 2 orders of magnitude (Fig. 1-6d). A similar study was also reported by Nguyen et al. (2019), who showed the influence of F-T cycles on the UCS of lime-treated soils. Three different types of soil consisting of a wide range of plasticity (ML, CL, and MH) were treated with different lime contents, laboratory cured for 7, 28, 90, and 365 days, and were then subjected to 10 F-T cycles. A part of the UCS attained in the soil due to lime treatment was lost during the F-T cycles. However, soil with low plasticity, treated with high lime content, and exposed to longer curing was reported to show a minimal loss in strength.

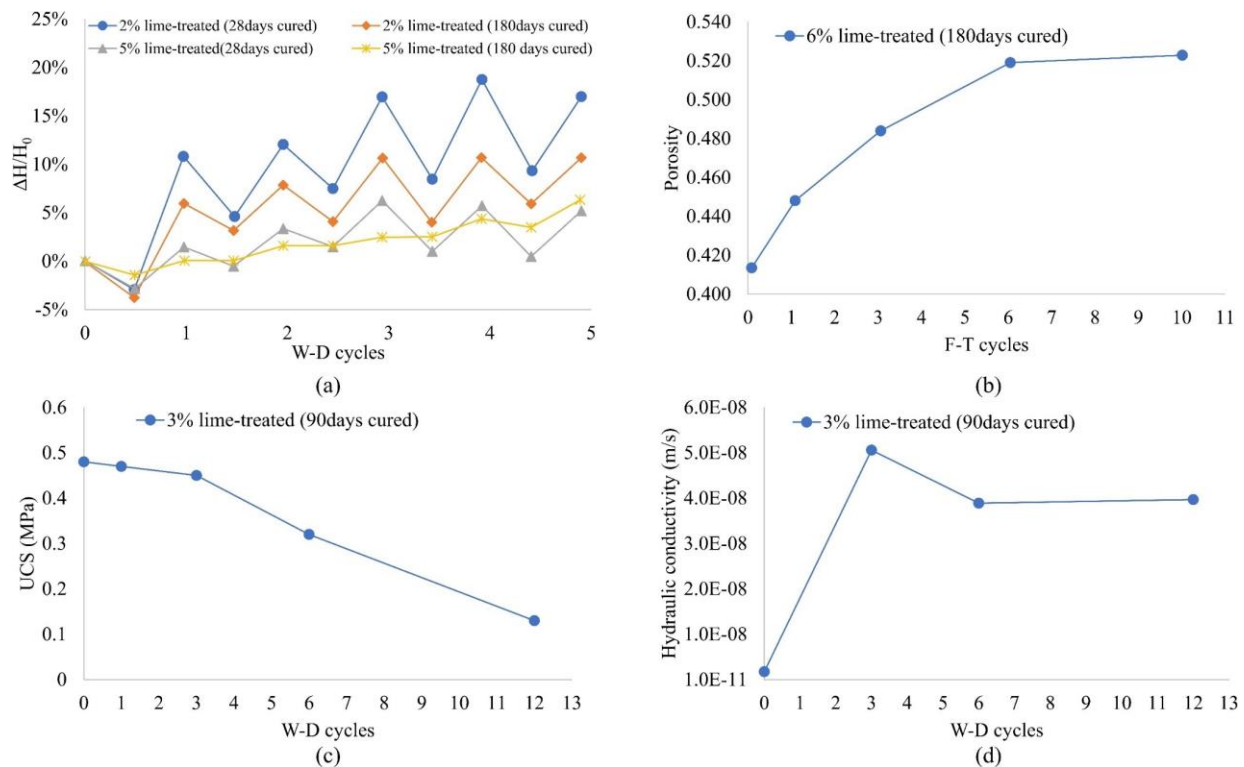


Fig. 1-6 Height variations of lime-treated materials subjected to 5 successive W-D cycles (after Cuisinier et al., 2014) (a), Evolution of porosity in lime-treated soil with respect to a number of F-T cycles (b) (Han et al., 2021), Evolution of UCS (c) and Hydraulic conductivity (d) in lime-treated soil subjected to 12 W-D cycles (Cuisinier et al., 2020).

The above studies reported evidence that the hydromechanical performance of the soil, which governs the long-term performances of a lime-treated soil, is affected by implementation parameters, such as lime contents, curing time, and soil type. Thus, it is essential to understand the influence of implementation parameters on the hydromechanical performances of lime-treated soil, which is discussed

in the following sections. Fig. 1-7 presents a chart diagram showing the interlink associated between durability (long-term performances), hydromechanical behaviors, implementation parameters, and soil microstructure. It is worth noting that among the several implementation parameters available in previous studies, few are reported herein.

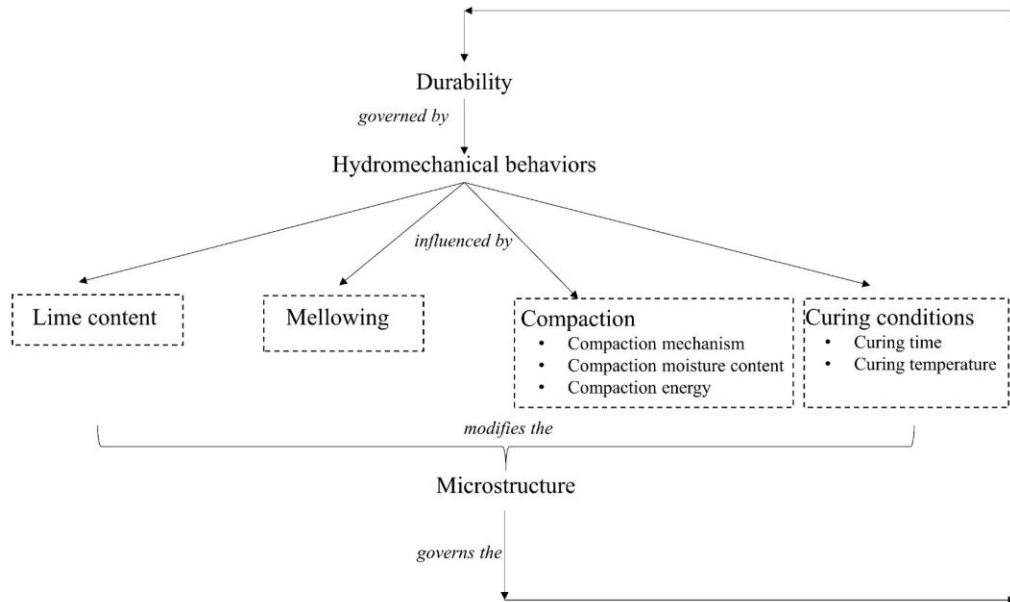


Fig. 1-7 Flow chart interlinking durability, hydromechanical behaviors, implementation parameters and microstructure modifications in lime-treated soil.

1.4.1. Implementation parameters and their contribution towards hydromechanical performances

1.4.1.1. Lime content and curing conditions.

Eades and Grim (1966) introduced the concept of lime modification optimum (LMO) in soil improvement. LMO is defined as the amount of lime that can sufficiently contribute free calcium ions for the short-term improvement of soil (in terms of its workability and plasticity), as well as long-term enhancement of its hydromechanical performances (strength, stiffness, and durability) (Bell, 1996; Cherian and Arnepalli, 2015; Little, 1987). LMO of soil depends primarily on several factors such as the extent of improvement desired, soil type, prevailing environmental conditions, etc. (Bell, 1996; Cherian and Arnepalli, 2015). The methodology for obtaining LMO of soil was suggested by Eades and Grim (1966), which involves mixing air-dried mass of a given soil with distilled water at a mass: volume ratio of 1:5, and then mixing it with different proportions of lime until a pH of 12.4 is reached. The lime content that gives the mixture a pH of 12.4 corresponds to LMO. This method was later modified into ASTM standard D 6276-99a (ASTM, 2006).

Curing is defined as the process of maintaining satisfactory moisture content and temperature in the compacted lime-treated soil for a definite period of time to allow the occurrence of soil lime reactions (Kosmatka et al., 2002). In-situ treated base courses are often cured in two ways: (a) moist curing, which consists of maintaining the surface in a moist condition by light sprinkling and rolling when necessary, and (b) membrane curing, which involves sealing the compacted layer with a bituminous prime coat emulsion,

either in one or multiple applications (Army Corps of Engineers, 1984; Lime manual, 2004). Laboratory curing of the lime-treated specimen is mostly done by wrapping the compacted specimens in any materials that prevent atmospheric interactions and then storing them for a required duration at a constant temperature before testing. Laboratory curing is either done at ambient laboratory temperature or at an elevated temperature (Lemaire et al., 2013; Wang et al., 2017). Curing lime-treated specimens at elevated temperatures accelerated the pozzolanic reactions and enhances the mechanical performances in a short time (Bell, 1996; Little, 1995). Such an approach was often made at the laboratory to attain the maximum improvement in a short time, which helps in the long-term strength prediction of in-situ lime-treated structures.

1.4.1.1a. Impact of lime content and curing conditions on strength evolution of lime-treated soil.

Both lime content and curing time play an interdependent role in governing the long-term hydromechanical performances of lime-treated soils. Though the addition of lime content corresponding to LMO was said to contribute to both short-term and long-term chemical reactions, previously, however, recent studies showed that LMO has limited contribution in the maintenance of the long-term pozzolanic reactions (Le Runigo et al., 2009). Thus, lime content higher than the LMO is recommended to be implemented. Along with higher lime content than LMO, implementing a longer curing time was shown to deliver higher strength to the lime-treated soils. Fig. 1.8 shows the increase in UCS of several different types of lime-treated soil with lime content and curing time, extracted from several reported studies (Al-Mukhtar et al., 2010; Asgari et al., 2015; Bhuvaneshwari et al., 2014; Consoli et al., 2014; Dash and Hussain, 2011; Dhar and Hussain, 2019; Farooq et al., 2011).

Al-Mukhtar et al. (2010) reported an increased UCS in CH soil with increased lime content up to 20% (Fig. 1-8a). The UCS increased with increased lime content in a similar type of soil was also reported by Farooq et al. (2011), Dash and Hussain (2011), Bhuvaneshwari et al. (2014), and Dhar and Hussain (2019). Asgari et al. (2015) reported the UCS increase in CL soil with increased lime content. Fig. 1-8b shows the UCS evolution of the above-reported soils with respect to curing time, presented for selected lime contents. Similar to lime content, the UCS increases with increased curing time. Along with curing time, Nasrizar et al. (2010) and Wang et al. (2017) demonstrated the importance of curing temperature towards UCS evolution. Nasrizar et al. (2010) aimed to examine the effect of curing conditions prevalent in cooler (5°C), semi-arid (30°C), and arid (50°C) regions on the strength of expansive soil (CH) treated with 5% and 7% lime. The study reported that curing at 5°C is not conducive for lime treatment, and the UCS increased with increased curing temperatures in a shorter period. Wang et al. (2017) reported the impact of 40°C and 60°C curing temperatures on sediments treated with 3% and 6% lime. Similar to Nasrizar et al. (2010), Wang et al. (2017) concluded an enhanced UCS evolution at elevated curing temperatures.

A higher lime content enhanced the pozzolanic reactions, which enhanced with increased curing time and temperatures (Diamond and Kinter, 1965; Little 1995). As a consequence, excessive development of cementitious bonding occurs, which triggers an increased cohesion in the treated soil. De Bel et al. (2009) evidenced a significant increase in cohesion from less than 0.10 MPa to more than 0.50 MPa from 50 to 448 days of curing, respectively, in 3% lime-treated CL soil.

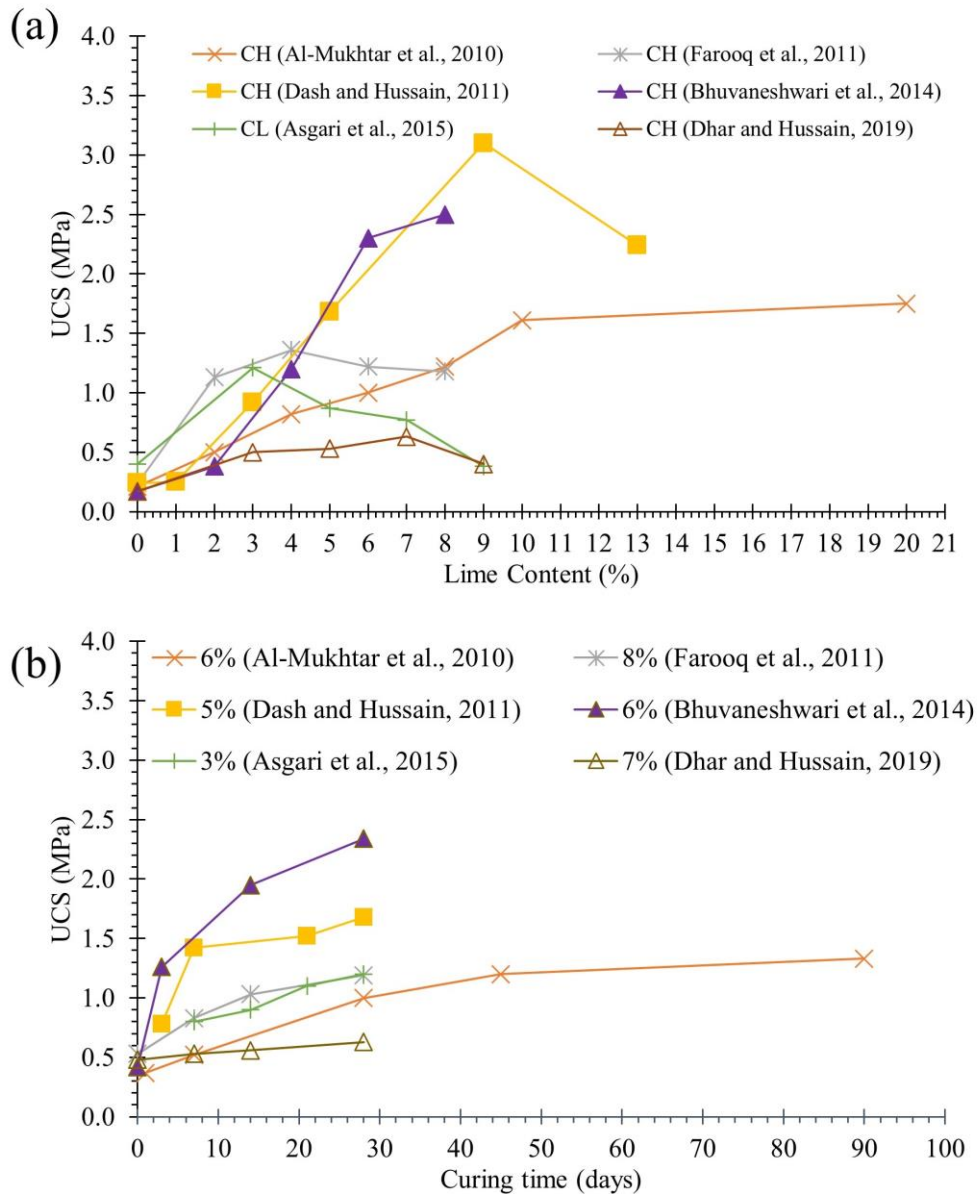


Fig. 1-8 UCS evolution with respect to lime content (a) and curing time (b).

However, Fig. 1-8a show that though the UCS of the soil treated by lime increased with increased lime content, it decreased after a certain lime content in the studies reported by Dash and Hussain (2011), Farooq et al. (2011), Asgari et al. (2015), and Dhar and Hussain (2019). For an instant, the UCS of the soil reported by Dash and Hussain (2011) increased for soil treated with lime content up to 9% and then decreased in the soil treated with 13% lime. Likewise, the UCS increased for the lime-treated soil reported by Farooq et al. (2011) and Asgari et al. (2015), up to 4% and 3%, respectively, and then decreased. Several reasons have been provided for such observations. Bell (1996) stated that since lime has no cohesion or friction, their presence in an excessive amount within the soil particles causes lubrication and thus reduces the strength. Kumar et al. (2007) demonstrated that the decrease in UCS at high lime content was due to the platy shape of unreacted lime particles. Recently, based on the observations made in Fig. 1-8a, Dash and

Hussain (2011) and Dhar and Hussain (2019) demonstrated such occurrence as a consequence of excessive porosity created in the soil structure owing to the excessiveness of cementitious compounds formation.

1.4.1.1b. Impact of lime content and curing conditions on hydraulic conductivity evolution of lime-treated soil.

The magnitude of hydraulic conductivity in lime-treated soil was shown to increase on the addition of lime regardless of the lime content added in comparison to the untreated soil (Awad et al., 2021; El-Rawi et al., 1981; Khattab et al., 2007; Le Runigo et al., 2009; Nalbantoglu and Tuncer, 2001; Osinubi, 1998; Rajasekaran and Rao, 2002). Some of the studies showing the hydraulic conductivity evolution in lime-treated soils as a function of lime content are presented in Fig. 1-9. These soils were compacted at the optimum moisture content (OMC) using standard compaction energy and then cured for 1 month before subjecting to a permeability test.

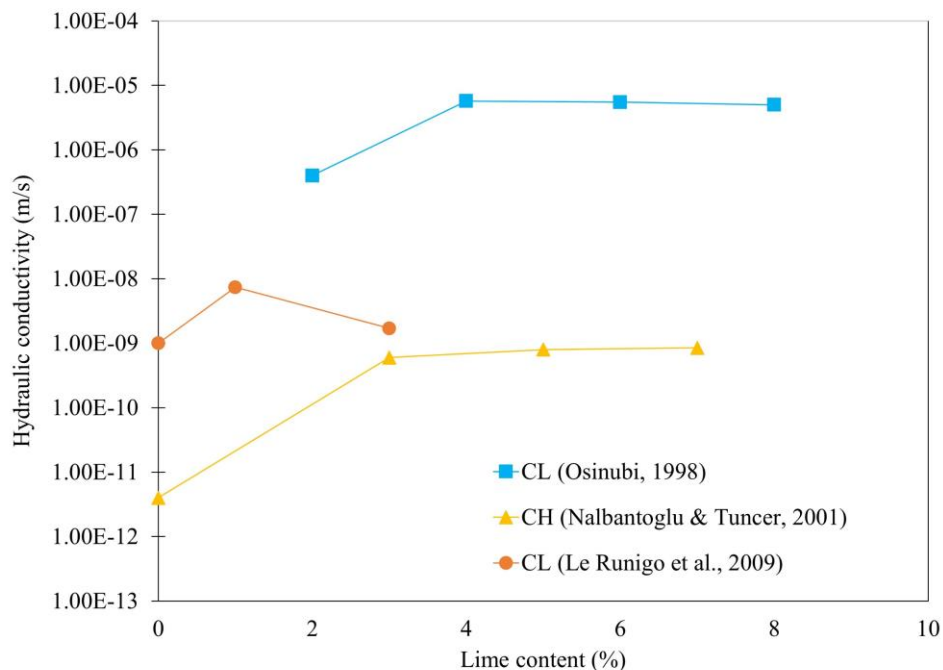


Fig. 1-9 Hydraulic conductivity evolution with respect to lime content.

Fig. 1-9 shows that the magnitude of hydraulic conductivity in different types of lime-treated soils (CH and CL classified soils) increased on lime addition. Similar evolution was also reported by Rajasekaran and Rao (2002), Khattab (2007), and El-Rawi and Awad (1981) for lime-treated soils cured in between 7 to 30 days. This increased hydraulic conductivity in lime-treated soil was demonstrated as a consequence of increased inter-aggregate pores in lime-treated soil, as shown in Fig. 1-3 since hydraulic conductivity is a function of the widest pores present in a given soil (Hunt and Sahimi, 2017).

However, Brandl (1981), De Bel et al. (2005), McCallister and Petry (1992) reported that the magnitude of hydraulic conductivity in lime-treated soil is dependent on the amount of lime added and the curing time. They stated that adding a greater lime content followed by a longer curing duration causes precipitation of cementitious compounds, which block the flow channels and hence reduces the magnitude

of permeability. In addition to the preceding conclusion, Gao et al. (2018) stated that though increased lime content decreased the hydraulic conductivity in lime-treated loess soil (CL), an excessive lime can cause greater porosity and increase the permeability.

On the other hand, Le Runigo et al. (2009) showed that the amount of lime added to silty soil (CL) has minimal impact on the evolution of soil permeability. This is because lime treatment brings changes in pore structure smaller than $1 \times 10^4 \text{ \AA}$, while permeability is controlled by pores greater than $1 \times 10^4 \text{ \AA}$. Cuisinier et al. (2011) compared the impact of lime content and compaction conditions (procedure, moisture content) on the pore structure of ML soil. They stated that the addition of lime does not affect pores larger than $3 \times 10^4 \text{ \AA}$. Pores larger than $3 \times 10^4 \text{ \AA}$ were controlled by the compaction conditions implemented, and hence they concluded the magnitude of hydraulic conductivity as a function of compaction conditions rather than the lime content or curing conditions implemented. Recently, the above conclusion was confirmed through an in-situ permeability test conducted by Makki- Szymkiewicz et al. (2015). Makki- Szymkiewicz et al. (2015) recorded a permeability value of 10^{-9} m/s in an in-situ experimental embankment built using 2.5% quicklime-treated soil (CL) after about 1 month, 6 months, and 1 year from construction. The recorded value of permeability was constant throughout the in-situ curing time. Thus, the study showed that emphasized the importance of compaction conditions on the evolution of hydraulic conductivity of lime-treated soil, which is reported in the following section.

1.4.1.2. Compaction

Compaction is an execution process that plays a vital role in the mechanical improvement of lime-treated soil by compressing the soil mass and decreasing the void ratio (Ikeagwuani and Nwonu, 2019; Kenai et al., 2006). The process of compaction involves compacting the lime-treated soil at a given compaction energy/effort, compaction moisture content, and compaction procedure. These compaction conditions, *i.e.*, compaction energy/effort, moisture content, and procedure, significantly impact the hydromechanical improvement brought by lime treatment in the soil (Cuisinier et al., 2011; Le Runigo et al., 2011, 2009; Makki-Szymkiewicz et al., 2015; Mitchell et al., 1965). Below are some studies highlighting the importance of compaction conditions.

1.4.1.2a. Impact of compaction on strength evolution of lime-treated soil.

Lime-treated soil compacted at different compaction moisture content was shown to influence the evolution in UCS. Le Runigo et al. (2011) studied the UCS evolution in silty soil (CL) treated with 1% and 3% of quicklime. The lime-treated soil was compacted at two initial moisture contents, *i.e.*, at the optimum moisture content (OMC) and 3% higher than OMC (WMC). After about 1 month of curing at laboratory temperature, lime-treated soil compacted at OMC showed greater UCS than the one compacted at WMC (as presented in Fig. 1-10a). Asgari et al. (2015) reported another study regarding the impact of compaction moisture content on the UCS evolution of lime-treated soil after 1 month of curing at laboratory temperature. Their study involves mixing of low plastic soil (CL) with 3%, 5%, 7%, and 9% of hydrated lime and then compacting at water content 2% lower than OMC (DMC), OMC, and 2% more than OMC (WMC). The obtained result showed that maximum UCS was obtained with lime-treated soil compacted at DMC, followed by OMC. At the same time, the minimum was attained with the corresponding WMC compacted soil (Fig. 1-10b).

Yin et al. (2018) demonstrated that this loss in UCS for WMC compacted soil was due to loss in soil grain-to-grain contact owing to excess presence of water. This phenomenon was evident by Deneele (2016) through SEM image observations. Deneele (2016) demonstrated that ML soil treated with 3%

quicklime, cured for 28 days, and compacted at greater water content than OMC shows enhanced dispersion of fine particles (mainly clay particles). Such a dispersion sprayed the development of cementitious compounds during the 28-day curing time and contributed to close porosity and improve binder development throughout the soil matrix.

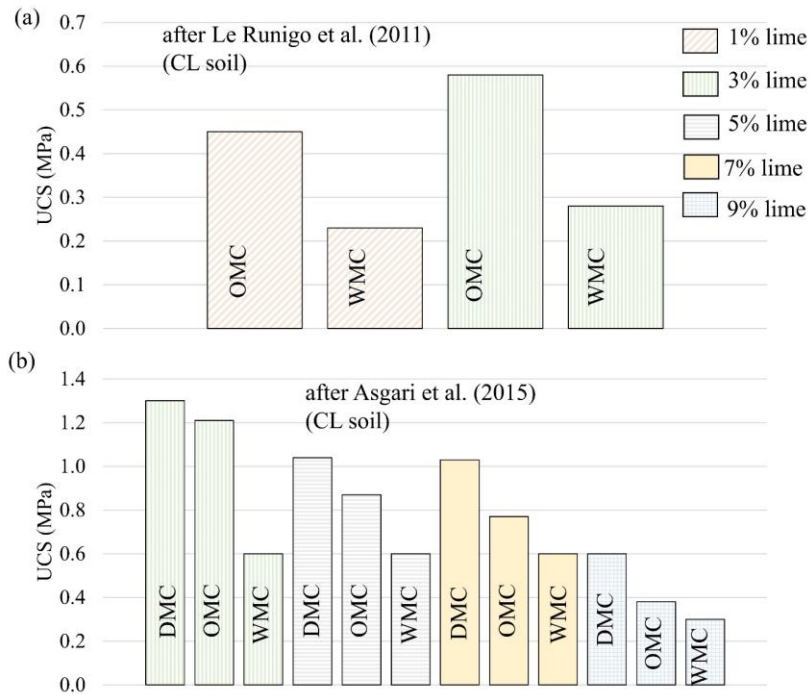


Fig. 1-10 UCS evolution in different lime-treated soil after about 1 month of curing time as a function of compaction moisture contents.

In addition to the impact of compaction moisture content, Le Runigo et al. (2011) demonstrated the importance of compaction effort/energy in the UCS evolution of lime-treated soil. Specimens compacted at the different moisture content was also compacted at compaction energy 50% lower than the standard Proctor energy (LE) and at standard proctor energy (NE) as per NF EN 13286-2 (2010). The result showed that lime-treated soil compacted at LE resulted in lower UCS compared to the one compacted at NE, regardless of the lime content and compaction moisture content used. Little (2000) reported the UCS evolution in three different types of soil having a plasticity index (PI) of 24, 29, and 30%. The soil was treated with 5%, 5.5%, and 6% hydrated lime, compacted at different moisture contents using standard and modified compaction energy, and cured for 7 days at 40°C. The modified compaction energy was approximately 22% greater than the standard compaction energy. The obtained UCS was observed to be higher for all the lime-treated specimens that have been compacted by modified compaction energy, irrespective of the compaction moisture content and soil type. Baldovino et al. (2019) demonstrated such a phenomenon as a consequence of the decrease in soil voids owing to increased compaction effort, which as a result enhances soil particles contact and cementation process. A similar explanation was also provided by Baldovino et al. (2018a, b) and Consoli et al. (2011a, b, 2014).

1.4.1.2b. Impact of compaction on hydraulic conductivity evolution of lime-treated soil.

As per the recent studies stated in section 1.4.1.1b, the hydraulic conductivity of lime-treated soil is governed by the compaction conditions rather than the lime content added or the curing conditions implemented. Studies evidencing the preceding statement are as follows.

Osinubi (1998) showed the hydraulic conductivity evolution in lime-treated lateritic soil compacted using different compaction energies. Lateritic soil treated with 2, 4, 6, and 8% of hydrated lime and compacted by standard Proctor compaction energy (NE) and West African Standard energy was subjected to hydraulic conductivity test after about 1 month of curing. The West African Standard energy (HE) was equivalent to modified compaction energy as per NF EN 13286-2 (2010). The obtained hydraulic conductivity showed that lime-treated soil compacted at HE gave a comparatively lower magnitude of hydraulic conductivity (as presented in Table 1-2).

El-Rawi and Awad (1981) reported that the magnitude of hydraulic conductivity of lime-treated low plastic silty soil was about an order higher in the soil compacted at OMC compared to the one compacted at WMC. A similar conclusion was also drawn by McCallister (1990) with three compacted lime-treated expansive clayey soil.

Le Runigo et al. (2009) performed a hydraulic conductivity test in silty soil (CL) treated with 1% and 3% lime, compacted at different moisture contents and compaction effort/energy. Soil compacted at OMC and WMC (3% higher than OMC) using NE and LE (50% lower than NE) was subjected to 140 days of percolation time after about 1 month of laboratory curing. The obtained results showed the attainment of the minimum magnitude of hydraulic conductivity with the soil compacted at WMC and NE. These results are presented in Table 1-2. Another study was reported by Cuisinier et al. (2011) regarding hydraulic conductivity evolution of untreated and lime-treated silty soil (ML) compacted at OMC and WMC. Soil treated with 2 and 3% of quicklime, compacted at WMC, and cured for about 1 month was shown to have a lower magnitude of hydraulic conductivity (Table 1-2).

Through SEM observation Deneele (2016) reported the decrease in soil agglomeration in the WMC compacted 3% quicklime-treated ML soil compared to the OMC compacted soil. A lower agglomeration led to lower availability of large porosity in the soil, as reported by Tran et al. (2014), and Wang et al. (2017). Thus, a lower magnitude in hydraulic conductivity occurred.

However, though the hydraulic conductivity of WMC compacted lime-treated soil in the above laboratory studies reported was lower than the OMC, it was demonstrated to remain higher than the corresponding untreated soil (Awad et al., 2021). The higher hydraulic conductivity in the lime-treated soil compared to the untreated soil was due to the increased inter-aggregates, as demonstrated in Fig. 1-3. However, Makki-Szymkiewicz et al. (2015) concluded that a similar magnitude of hydraulic conductivity could be obtained in lime-treated and untreated CL soil. They conducted a field evaluation of hydraulic conductivity in an experimental embankment built with 2.5% lime-treated silty soil. For reference, an untreated experimental embankment was also built in the same site near the lime-treated embankment. The magnitude of hydraulic conductivity in the lime-treated embankment was evaluated after 1 year from construction. This magnitude was found to be almost similar to the untreated (Table 1-1). Based on this observation, Makki-Szymkiewicz et al. (2015) stated that due to controlled mixing and compaction conditions implemented during the embankment construction, the hydraulic conductivity of the lime-treated soil remained similar to the untreated soil.

Table 1-2 Evolution of hydraulic conductivity in different types of lime-treated soil prepared at different lime contents and compaction conditions.

Soil ID (soil type as per USCS)	Lime content (%)	Compaction moisture content (%) - compaction effort	Hydraulic conductivity (k) (m/s)	References
Lateritic soil (CL)	2	OMC-NE/OMC-HE	$5.4 \times 10^{-05} / 2.1 \times 10^{-07}$	Osinubi, 1998
	4	OMC-NE/OMC-HE	$5.7 \times 10^{-05} / 4.3 \times 10^{-06}$	
	6	OMC-NE/OMC-HE	$5.5 \times 10^{-05} / 4.0 \times 10^{-06}$	
	8	OMC-NE/OMC-HE	$5.0 \times 10^{-05} / 3.3 \times 10^{-06}$	
Silty soil (CL)	0	OMC-NE	$7.5 \times 10^{-10} < k < 1.0 \times 10^{-09}$	Le Runigo et al., 2009
		OMC-LE	$1.3 \times 10^{-08} < k < 1.9 \times 10^{-08}$	
	1	OMC-NE	$7.1 \times 10^{-10} < k < 7.4 \times 10^{-09}$	
		WMC-NE	$2.5 \times 10^{-10} < k < 3.3 \times 10^{-10}$	
	3	OMC-LE	$1.9 \times 10^{-08} < k < 2.4 \times 10^{-08}$	
		OMC-NE	$1.2 \times 10^{-09} < k < 1.7 \times 10^{-09}$	
Silty soil (ML)	0	OMC-NE	1.1×10^{-08}	Cuisinier et al., 2011
		WMC-NE	1.0×10^{-10}	
	2	OMC-NE	2.7×10^{-08}	
		WMC-NE	8.3×10^{-09}	
	3	OMC-NE	4.2×10^{-08}	
		WMC-NE	5.2×10^{-09}	
Silty soil (CL)	0	WMC-NE	3.0×10^{-09}	Makki-Szymkiewicz et al., 2015
	2.5	WMC-NE	8.5×10^{-09}	

1.4.1.3. Mellowing

Mellowing period of lime-treated soil is defined as the time allowed for the soil-lime-water mixture to stay undisturbed before it is subjected to a compaction test (Sweeney et al., 1988). Mellowing period has been given different terminology, e.g., compaction delay (Ali and Mohamed, 2017), amelioration period (Gallage et al., 2012), and aging period (Sweeney et al., 1988). Mellowing period is important because it is believed to provide better uniformity and workability in the treated soil by breaking down large clay clods through optimization of the chemical reactions between the clay particles and lime (Holt et al., 2000; Bhattacharja and Bhatta, 2003, Al-Rawas and Goosen, 2006, Al-Mukhtar et al., 2012, Lucian, 2013).

1.4.1.3a. Impact of mellowing period on strength evolution of lime-treated soil.

Though the mellowing period is essential in lime-treated soil, however, a longer mellowing duration was shown to be detrimental to the UCS of lime-treated soil by several studies as reported below.

Sivapullaiah et al. (1998) investigated the effect of 0, 24, and 168 hrs mellowing duration on the UCS of Black cotton soil (CH) treated with 2% and 6% hydrated lime. At the end of mellowing durations, soils were compacted by energy equivalent to 60% of standard Proctor energy and at OMC. Specimens were then subjected to 7 days of laboratory curing, which involves 6 days of curing and 1 day of soaking. Cured specimens were then subjected to the UCS test. The comparative UCS difference reported in their study is presented in Fig. 1-11a. The decrease in UCS of lime-treated soil shows a linear trend with the increased mellowing durations. A similar study was reported by Mitchell and Hooper (1961), who showed that 4% hydrated lime-treated organic, expansive clay soil resulted in a loss of 30% in the UCS if mellowed for 24 hours compared to the one which was compacted directly after mixing.

Osinubi and Nwaiwu (2006) demonstrated the impact of compaction delay on soil treated with different lime content, cured for different durations, and compacted using different compaction energy.

Natural reddish-brown lateritic soil (CL) was treated with 3%, 5%, and 8% hydrated lime, mellowed for 0, 1, 2, and 3 hrs, and then compacted using standard Proctor compaction (as per NF EN 13286-2 (2010)), and West African Standard energy. Compacted specimens were cured at laboratory temperature for 7, 14, and 28 days and then subjected to UCS test. The evolution of UCS as a function of mellowing duration for 3% and 5% lime-treated and standard Proctor compacted soil is presented in Fig. 1-11b. The UCS of all the lime-treated soil decreased with increased mellowing duration irrespective of the lime content added and curing time implemented. Similar results were reported for the corresponding soil compacted using West African Standard energy.

Ali and Mohamed (2017) investigated the impact of different mellowing durations on the UCS of lime-treated compacted soil cured for different periods and at different temperatures. Wyoming Sodium Bentonite powder (CH), treated with 7% of hydrated lime, was subjected to mellowing duration of 0, 3, 6, 12, and 24 h. Specimens prepared at standard moisture content were mellowed, compacted by standard Proctor energy, and cured for 1 and 28 days at a temperature of 20°C and 40°C, applied for each curing duration. The obtained UCS is presented in Fig. 1-11c, which showed a similar evolution as the previous studies. Another study was reported by Al-Neaimi, and Hussain (2011), where the effect of compaction delays up to 4 h was shown on the UCS of expansive soil (CH) treated with 3%, 5%, and 8% lime. Similar to the above studies, the UCS of the 7 days cured lime-treated soil decreased with increased compaction delay (as seen in Fig. 1-11d). Other studies that provide a similar conclusion as the above includes studies made by Adefemi and Wole (2013), Ali and Mohamed (2018), Raja and Thyagaraj (2020).

Ali and Mohamad (2017) and Beetham et al. (2014) attributed such a declination in the UCS to be due to the destruction in cementitious bonding formed in the loose state of the lime-treated soil during mellowing periods. An enhanced compaction delay causes a greater number of cementitious bonding formations within the soil particle's contact and between clay flocs, owing to longer pozzolanic reactions. Subjecting the longer mellowed soil to compaction destroys the cementation formed during the loose state, which as a result, causes a decline in the UCS.

1.4.1.3b. Impact of mellowing period on hydraulic conductivity evolution of lime-treated soil.

Similar to the UCS evolution, compaction delay was also shown to negatively impact the hydraulic conductivity evolution in lime-treated soil (Ali and Mohamed, 2017; Di Sante et al., 2015; Moghal et al., 2020).

As mentioned in the preceding section, a longer mellowing duration causes the greater formation of hydrates in the lime-treated soil at a loose state. This feature causes greater soil aggregation, as evidenced by the SEM images provided by Di Sante et al. (2015). Di Sante et al. (2015) compared the SEM images of 5% lime-treated CH soil, compacted immediately after mixing and compacted after 48 hours of mellowing at laboratory temperature. They showed that soil compacted after mellowing showed greater inter-aggregates pore (as seen in Fig. 1-12a & b). Moghal et al. (2020) evidenced the increased inter-aggregates caused by delayed compaction by comparing the cumulative pore volume evolution of two different lime-treated CH soils compacted immediately after mixing and after 7 days from mixing.

As a result of increased inter-aggregates caused by delayed compaction, the magnitude of hydraulic conductivity increased, as reported by Ali and Mohamed (2017) and Moghal et al. (2020). Fig. 1-13 shows comparative differences in the hydraulic conductivity evolution in lime-treated soil compacted immediately and after 7 days from mixing, as reported by Moghal et al. (2020). Both Soil A and Soil B are CH soils, treated with 2% and 4% hydrated lime and statically compacted. Compacted specimens were then subjected to a rigid wall permeameter. The magnitude of hydraulic conductivity increased in both Soil A and Soil B

in the 7 days mellowed soil compared to the soil compacted immediately. The increase was more significant in Soil A than in Soil B, which was demonstrated to be due to the presence of more hydration-enhancing compounds in Soil A, which caused greater cementation during mellowing time.

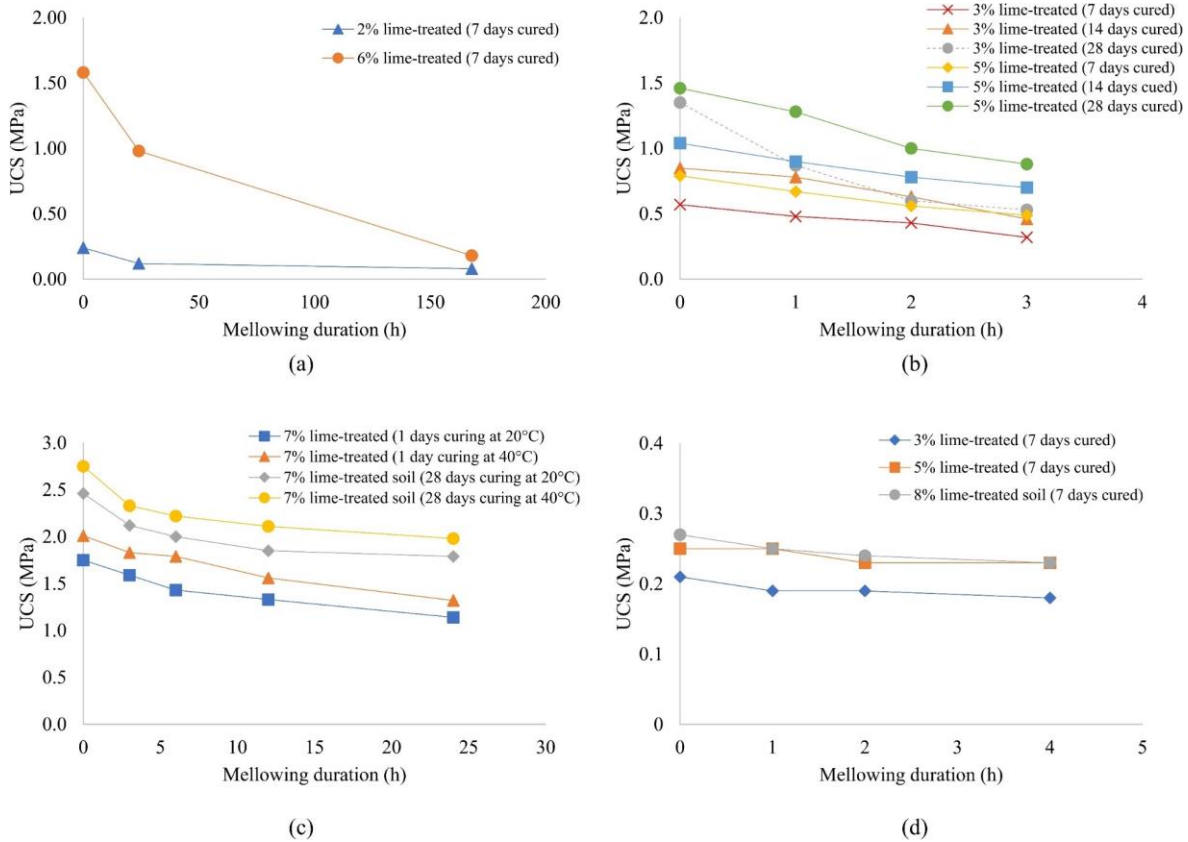


Fig. 1-11 UCS evolution as a function of mellowing durations reported by Sivapullaiah et al. (1998) (a); Osinubi and Nwaiwu (2006) (b); Ali and Mohamed (2017) (c); and Al-Ne'aimi and Hussain (2011) (d).

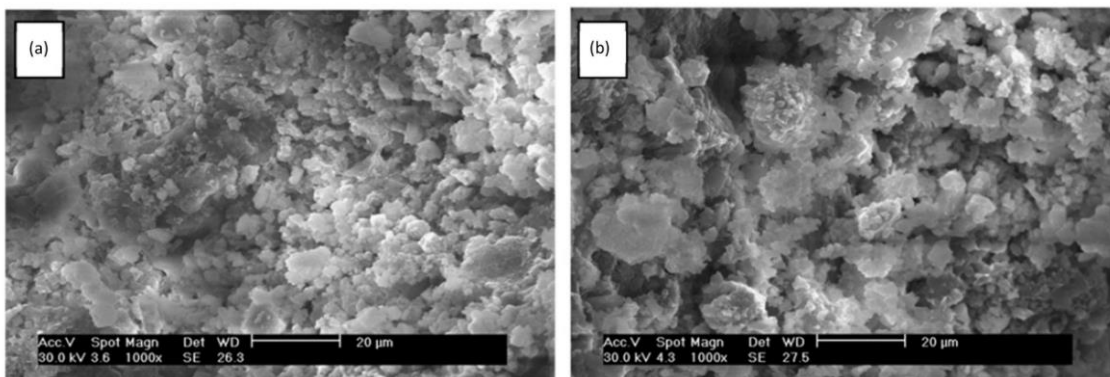


Fig. 1-12 SEM images of 5% hydrated lime-treated soil immediately after mixing (a), 48 hours after mixing (b) (modified after Di Sante et al., 2015).

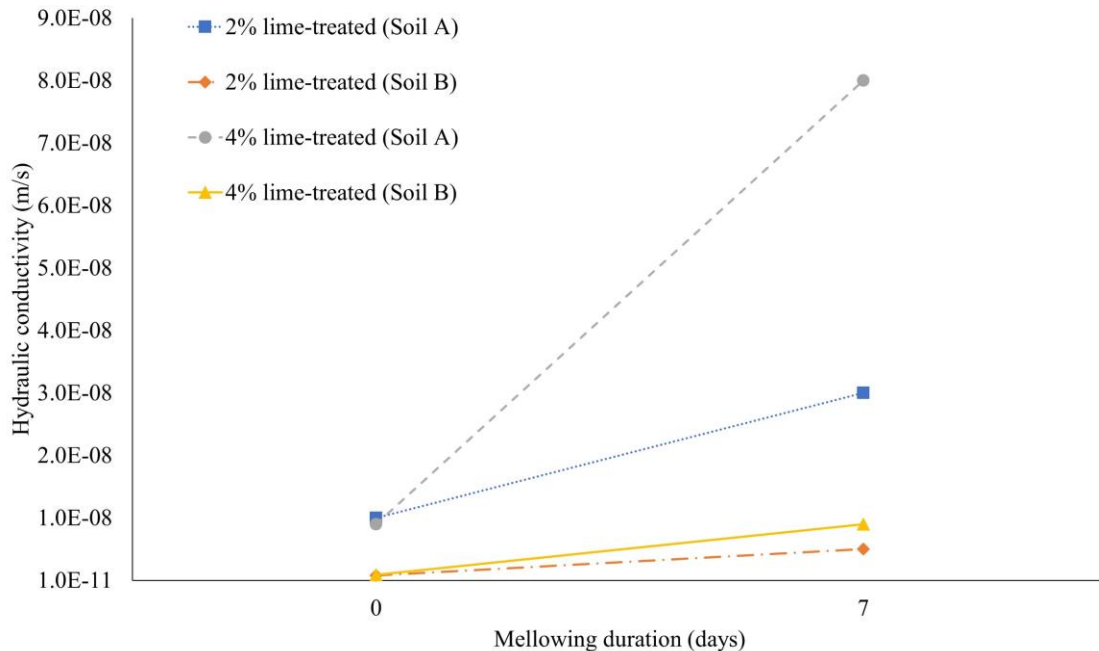


Fig. 1-13 Evolution of hydraulic conductivity in lime-treated soil compacted immediately after mixing and after 7 days of mellowing (after Moghal et al., 2020)

Thus, the above studies conclude that despite the variation in soil type, compaction energy, lime content, curing time, and curing temperature, an increased mellowing duration remained detrimental to the hydromechanical performances of lime-treated soil. Thus, a short mellowing duration of 60 to 90 minutes was proposed as per NF EN 16907-4, which is used in this study.

However, in some cases, mellowing was also shown to be beneficial, such as reduction of sulphate induced swelling in lime-treated expansive soil (Talluri et al., 2013); lime pretreatment (Joel and Otse, 2016) etc. Detailed review on such effect of mellowing is out of the scope of this study.

1.4.2. Lime leaching from lime-treated soil.

Leaching is defined as a process of extracting substances from soil mass by dissolving them in the circulating pore fluid during the process of flow of fluid through a given soil mass (Addiscott and Wagenet, 1985; Razakamanantsoa and Djeran-Maigre, 2016). The leaching phenomenon in natural soil is well investigated in the study demonstrated by Razakamanantsoa and Djeran-Maigre (2016). They investigated the impact of hydro-chemo-mechanical processes in the clayey soil, i.e., Bentonite when subjected to low mineralized water (10^{-3} M NaCl solution) and synthesized leachate. The study shows the positive effect of pre-hydration before hydraulic conductivity test to minimize calcium leaching from natural compacted soil on being subjected to the aggressiveness of synthesized leachate. In lime-treated soil, the presence of calcium and its major component is essential to maintain the long-term durability of the treated structure (Deneele et al., 2016; Le Runigo et al., 2009, 2011). Thus, an enhanced flow rate through lime-treated soil can leach the essential compounds and decline the improvement brought by lime treatment. Concerning this, studies have been conducted to investigate the effect of leaching on the strength and hydraulic evolutions of lime-treated soils.

McCallister and Petry (1992) performed a leach test for 45- and 90-days on lime-treated and OMC-NE compacted clays (CH) after 48 h of curing at 49°C. They stated that leaching does not deteriorate the ability of lime-treated soil to maintain its long-term mechanical performance. Instead, with increased leaching time, they reported a decrease in permeability, which was demonstrated to be due to enhanced development of smaller pores because of cementitious bonding formation. A similar conclusion was reported by Khattab et al. (2007). Khattab et al. (2007) studied the leaching characteristics for over 60 days of percolation in 4% lime treated and OMC-NE compacted FoCa soil (CH) after 7 days of curing at laboratory temperature. Their studies stated that leaching does not reduce the performance of the lime-treated soil, since a minimum quantity of lime was displaced during the percolation time compared to the initial quantity of lime added.

However, Le Runigo et al. (2009) demonstrated that the leaching mechanism has a limited impact on the magnitude of hydraulic conductivity and soil fabric of the lime-treated soil. The influence of leaching on hydraulic conductivity was stated to be dependent on the competition between dissolution and precipitation mechanism of cementitious compounds that takes place during percolation. Such a feature was explained to be influenced by the soil type, lime content, and curing conditions. In their study, silty soil (CL) treated with 1% and 3% lime compacted at OMC-NE were subjected to over 150 days of leaching time after about 1 month of curing at laboratory temperature. 3% lime-treated soil was shown to have developed increased cementitious compounds at the end of leaching time, though there occurred loss in calcium from the lime-treated soil. However, the evolution of hydraulic conductivity remained almost stable over the leaching time, which is not the same case as the one reported by McCallister and Petry (1992) and Khattab et al. (2007). This difference in hydraulic conductivity behavior was demonstrated to be due to the difference in soil type. Given that the soils reported by McCallister and Petry (1992) and Khattab et al. (2007) were CH type, thus, the formation of cementitious compounds was dominant, which have led to a decrease in hydraulic conductivity magnitude.

Though leaching was reported to have an insignificant effect on the soil fabric and hydraulic conductivity evolution, certain studies demonstrated that leaching is detrimental to the UCS evolution of lime-treated soil. De Bel et al. (2005) demonstrated that long-term water circulation through lime-treated silt results in a significant decrease in UCS of the soil. They concluded that a part of this loss in UCS was due to the leaching of calcium from the decalcification of cementitious compounds. A similar study was reported by Hara et al. (2012), who evaluated the leaching effect on the strength of the foundation of an in-situ dike. The dike was constructed with lime-treated Ariake clay (CH). After 20 years from construction, an investigation conducted revealed the occurrence of the degradation of the strength of the dike's foundation due to calcium leaching.

Deneele et al. (2016) evidenced that dissolution of cementitious compounds induces a significant loss in UCS of the lime-treated soil. They performed a percolation test for over 320 days in silty soil (CL) treated with 1% and 3% lime, compacted at OMC-NE, and cured for about 25 days at laboratory temperature. The UCS of the lime-treated soil was shown to decrease gradually with increased leaching time, and this decrease was more significant in the soil treated with low lime content (as shown in Table 1-3).

Table 1-3 UCS evolution as a function of leaching durations (after Deneele et al., 2016)

	UCS of 1% lime-treated soil (MPa)	UCS of 3% lime-treated soil (MPa)
Initial UCS after 25 days curing	0.46	0.58

Leaching durations	90 days	0.09	0.36
	320 days	0.07	0.21

Thus, a part of the above studies explained that the effect of leaching on hydraulic conductivity is limited, while the other part stated the negative effect of leaching on the UCS evolution of lime-treated soil. However, the extent of such effects varied with the soil type and lime content added, as reported by Le Runigo et al. (2009). Considering this, Chittoori et al. (2013) conducted the leaching test on eight soils with different plasticity index (PI) and clay mineralogy treated with different lime contents. These soils are treated with 3%, 4%, 6%, and 8% lime, compacted at OMC by static compaction, and cured for 17 days. The curing process was as per the TxDOT test protocol (TxDOT 2005), which involves 7 days of laboratory curing, followed by 6 h of oven-drying at 40°C and then saturation of the specimens for 10 days by capillary suction. The analysis of UCS evolution and loss of lime was made as a function of the leaching cycle, where, leaching cycle was demonstrated to represent the amount of leaching volume, which is equivalent to the pore void volume of the specimen. Table 1-4 presents the percentage of UCS retained, and lime leached with respect to the initial UCS and lime present in the soil up to 14 leaching cycles. Based on the observations in Table 1-4, Chittoori et al. (2013) demonstrated that during percolation, an insignificant amount of lime was leached (< 0.6%). Thus, most of the UCS retained was higher than 70%. Thus, they concluded that the leaching of lime was limited and was too low to induce significant strength loss in soil regardless of the soil type and lime content used.

Table 1-4 Percent retained strength, and lime leached out after 14 leachate cycles in different types of soils treated with different lime contents (after Chittoori et al., 2013)

Soil ID (soil type-PI)	Lime content added (%)	Percentage of lime leached	Percentage of UCS retained
Austin (CL-34%)	6	0.40	98.8
Bryan (CL-31%)	8	0.40	88.9
El-Paso (CL-16%)	8	0.34	88.5
Fort Worth (CH-29%)	6	0.31	97.0
Keller (CL-11%)	6	0.39	98.8
Paris (CH-36%)	8	0.54	85.0
Pharr-A (CH-45%)	4	0.31	70.0
Pharr-B (CH-37%)	3	0.59	60.9

1.5 Discussions

Until now, the facts reported in this chapter evidenced the impact of numerous parameters on the long-term hydromechanical performances of lime-treated soils. Although extensive studies are made, certain additional investigations are yet needed to be conducted. This section aims to discuss arguments derived from the available facts reported in the literature, followed by the importance of further investigations.

1.5.1 Field Investigations of lime-treated soil structures

It is evident from the existing studies that most studies conducted on soil improvement by lime treatment were obtained from laboratory test results, while the feedback from field performance is less investigated. Table 1-1 provides few field investigations, particularly highlighting the strength evolution. However, the

description related to the influence of implementation parameters and its impact on physicochemical and microstructure modifications, which underlines such strength evolution, was less investigated.

Recently, Akula et al. (2020) presented a study describing the performances of Friant-Kern Canal in California, United States. The bottom and blankets of several sections of the Friant-Kern Canal, initially built with heavy plastic clays, were renovated during the '70s using 4% quicklime by weight. Study up to more than 40 years after the renovation was conducted, which showed stability of a lime-treated hydraulic structure based on physical and microstructural evaluation. The study showed a very low expansion index and high erosion resistance and evidenced the availability of C-S-H by Thermogravimetric analysis (TGA) and XRD analysis on the sampled specimens 40 years after construction. Based on these observations, they have predicted the stability of the hydraulic structure. Other studies include studies reported by Bicalho et al. (2018) and Rosone et al. (2018), who focused on soil suction and water content evolution on the experimental embankments.

Thus, all these studies have demonstrated the effectiveness of lime treatment over time and, to an extent, the effect of the soil atmosphere interaction on the modification of properties of lime-treated soil. Beyond the general behavior mentioned herein, more investigation is needed with respect to strength and microstructural modifications induced by long-term lime treatment on structures cured in the open atmosphere.

1.5.2 Lime content and Compaction conditions effect on lime-treated soil

Available literature indicates that lime content higher than LMO enhances the strength evolution (Fig. 1-8a). At the same time, lime content, if added in excess (above 5-6%), degrades the strength as shown by Dash and Hussain (2019). However, in the aspects of hydraulic conductivity evolution in lime-treated soil, most of the studies showed an increased magnitude of hydraulic conductivity compared to the corresponding untreated soil.

Until recently, Makki-Szymkiewicz et al. (2015) reported that lime-treated and untreated silty soil could show a similar magnitude of hydraulic conductivity if a proper execution mechanism is implemented. On the field, lime-treated fine-grained soil, particularly clayey soil, is preferred to be compacted by Padfoot roller (Kouassi et al., 2000; Willaims, 1949). Padfoot roller develops kneading action by undergoing penetration of the pads in the soil during compaction. However, this effect of kneading action on the hydromechanical performances of lime-treated soil has not been well investigated.

Thus, considering the arguments provided by Makki- Szymkiewicz et al. (2015), it becomes important to reproduce in-situ execution mechanisms, i.e., kneading action at a laboratory scale, to attain a close representation of field hydromechanical performances.

1.5.3. Leaching mechanism of compacted lime-treated soil

So far, the studies explaining the influence of the leaching mechanism on the long-term hydromechanical performances of lime-treated soil seem to be incomplete. Few studies reported that the leaching phenomenon does not degrade the long-term performances, instead improves the hydraulic performances and soil fabric in expansive soil (Khatab et al., 2007; McCallister and Petry, 1992). Other studies reported that leaching degrades the mechanical strength of lime-treated soil in the long term (De Bel et al., 2005; Deneele et al., 2016; Hara et al., 2012). Again, there are studies that deny the above conclusions (Chittori et al., 2013; Le Runigo et al., 2009).

These available studies were mainly focused on understanding the leaching mechanism by varying lime content, soil mineralogy, and curing time. However, since leaching mechanism is associated with the

evolution of hydraulic conductivity, which is governed by the soil pore structure developed based on the implemented compaction conditions. Thus, it becomes important to evaluate the influence of compaction conditions on the leaching phenomenon. As stated in section 1.5.2 regarding the required investigation of the kneading mechanism on the hydromechanical evolution thus, the evolution of the leaching phenomenon should be investigated further. Thus, implementing a field mechanism for evaluating hydraulic conductivity evolution and then understanding the leaching mechanism and its impact on strength evolution is essential to evaluate the actual leaching impact on in-situ structures.

Besides, since lime-treated soil is chemically stabilized soil thus, its interaction with percolating water exhibiting different chemical composition, which occurs in nature, can induce a change in the leaching mechanism and hydromechanical performances. Such an influence should also be analyzed.

1.5.4 Long-term performance evaluation of lime-treated soil

The long-term performance evaluation in lime-treated soil through laboratory investigation is often made either by using the ASTM D559 procedure (ASTM, 2015) or by applying controlled suction to the soil using an oedometer (Cuisinier et al., 2014; Cuisinier and Masrouri, 2005; Delage et al., 1992; Kassiff and Shalom, 1971; Stoltz et al., 2014, 2012; Williams and Shaykewich, 1969). The former method involves wetting a given sample for 5 hours at room temperature and then drying the soil in an oven at 71 °C for 43 hours. In the latter technique, between the unsaturated soil specimen and solution of polyethylene glycol, a semi-permeable membrane is introduced. The semi-permeable membrane prevents the macromolecules movement; however, it allows water movement towards the sample. The water movement is regulated to impose a suction variation of 0-8 MPa in the soil during the wetting and drying cycle. The imposition of suction from 0 to 8 MPa is made since this suction range is considered to represent the realistic suction variations in areas with a Mediterranean climate (Stoltz et al., 2012, 2014).

However, how well these reproduced laboratory methods represent the actual field condition remains less investigated. During the W-D cycles, in a given lime-treated soil, the fluctuation of water level definitely induces a change in the soil saturation level. Such a change in saturation level may modify the soil hydromechanical performances. However, the soil saturation level is generally not considered while investigating the influence of laboratory W-D cycles in lime-treated soil. Besides, drying soil in an oven at an elevated temperature was shown to modify the soil intrinsic structure in the studies reported by Basma et al. (1994) and Sunil and Deepa (2016). Such an observation indicates the necessity of considering the microstructure modification during W-D cycles. Moreover, employing the ASTM procedure also ignore the external fluid and soil sample interactions, as all samples are often soaked in a single cell during wetting. Interaction of pore fluid and soil sample is important since releasing and up-taking of ions can occur during the wetting phase. This, in turn, can modify the swelling and shrinkage in the respective soil. Thus, an inaccuracy in the measured swelling and shrinkage nature can result.

Recently, Cuisinier et al. (2020) reported the detrimental effect of oven-drying in lime-treated soil during W-D cycles. They compared the hydromechanical performances of treated soil by subjecting them to the oven during, which was as per the ASTM procedure, and natural drying during W-D cycles. The natural drying condition involves drying the specimen in a climatic chamber at a temperature of 20 °C and Relative Humidity (RH) of 54%. Based, on the comparison, they concluded that drying treated soil in an oven at elevated temperature bring deleterious effect on the hydromechanical performances. Thus, they proposed the importance of employing a laboratory condition, which bears the relevancy of the field situation. However, the study of Cuisinier et al. (2020) did not consider the physicochemical and microstructural evolution in lime-treated soil, which underlies the hydromechanical performances, as

evident from previous literature. The importance of considering the physicochemical modification was indicated by Elkady et al. (2016), who stated that both suction and cementation mechanisms should be considered to obtain a realistic performance of lime-treated expansive soil. Thus, subjecting a lime-treated soil to an environment where the fluctuation in water level is inhibited by varying the temperature can possibly modify the suction and cementation mechanism.

Besides, during the W-D cycle, the ingress and egress phenomenon of water induces infiltration of water into the soil. Such infiltration of different wetting fluids can possibly modify the hydromechanical performances of lime-treated soils, which remained less investigated.

1.6 Research gaps and Proposals

This chapter presents a comprehensive review of the role of lime in soil improvement with an emphasis on implementation parameters. The influence of soil-lime reactions in the pore structure modification of soil during the short-term modification and long-term pozzolanic reactions has been discussed at the microscale level. Then the contribution of microscale modifications towards the long-term hydromechanical performances of lime-treated soil under the influence of different implementation parameters is critically reviewed. From the review, the discussion section presents the arguments supporting the required additional investigations required to be evaluated to enhance the efficiency and effectiveness of lime treatment towards soil improvement. Following the additional investigations indicated in the discussion section, Table 1-5 presents the research gaps and the proposals made for the accomplishment of this thesis.

Table 1-5 Research gaps observed, and proposals made.

Research gaps	Proposals	Proposal number
Additional field investigation is needed to evaluate the strength and microstructural modifications induced by long-term lime treatment on structures cured in an open atmosphere.	An experimental 2.5% quicklime treated silty soil full-scale embankment was atmospherically cured for 7 years. At the end of 7 years, specimens were sampled to evaluate strength, physicochemical, and microstructural evolution.	1
In-situ executed kneading action during compaction of lime-treated fine-grained soil is less investigated.	A laboratory kneading tool was designed to implement the kneading action on lime-treated soil and then to understand its contribution towards UCS evolution.	2
In-situ execution mechanism, i.e., kneading action and chemical nature of pore fluid, can modify the hydromechanical performances and leaching mechanism of lime-treated soil. Such a phenomenon needs investigation.	Kneading compacted soil was subjected to a hydraulic conductivity test using different pore fluids. The results obtained are compared with those obtained using standard static compaction to differentiate the influence of execution mechanism and pore fluid on hydromechanical and leaching performances.	3
Laboratory implemented duration of wetting and drying cycles does not consider the soil saturation level, and drying was often conducted at 71 ° C, which was much higher than the atmospheric temperature. Such difference in implementation can modify the physicochemical nature of the lime-treated soil, which needs to be studied.	Lime-treated soils were subjected to W-D cycles using different testing conditions that were developed to represent the field situations. The obtained results were compared with the one obtained using the standard ASTM procedure to highlight the influence of testing conditions on the strength, physicochemical, and microstructure modifications.	4
During W-D cycles, water ingress and egress cause infiltration of water into the lime-treated soil. A difference in the chemical nature of such infiltrated	Lime-treated soils were subjected to W-D cycles using different wetting fluids. The physicochemical and	5

water can possibly modify the performances of lime-treated soil, which needs to be evaluated.

microstructural changes brought by such fluids and their contribution towards strength evolution were evaluated.

Chapter 2

MATERIALS AND EXPERIMENTAL PROCEDURES

General

The materials and common experimental techniques implemented in this study are described in this chapter. Additional experimental procedures that are customized for the fulfillment of certain proposals, detailed in Chapter 1 are provided in respective chapters, as needed.

2.1 Materials

2.1.1. Soil used and its properties.

The soil samples used in all the studies made for the completion of this thesis were imported from Marchelles-Dames (MLD), Belgium.

The mineralogy of the soil, obtained by X-Ray Diffraction (XRD), in the studies reported by Nguyen (2015, 2019), was shown to mainly consist of Illite, Kaolinite, Chlorite, Feldspar and Quartz. As per NF P 11-300, the soil is classified as fine soils (type A) (Nguyen, 2015).

The Atterberg's limit and Methylene Blue value of the soil samples were obtained from Nguyen (2015) and are presented in Table 2-1. As per NF P 11-300 standard, soil exhibiting a Methylene Blue Value of 2.39 (<2.5) and the P.I. value of 6.9 (< 12) is classified as A1 soil. The chemical composition of the soil extracted from Nguyen (2015) is presented in Table 2-2.

Table 2-1 Atterberg's limit and Methylene Blue value of MLD soil (after Nguyen, 2015)

Soil fraction < 0.002mm (%)	Methylene Blue Value (g/100g)	Atterberg's limit		
		PL (%)	LL (%)	PI (%)
24	2.4	23.2	30.1	7

Table 2-2 Chemical composition of MLD soil (after Nguyen, 2015)

Elements	% by mass	Elements	% by mass	Elements	% by mass
CaO	1.07	P ₂ O ₅	0.17	Cu	0.01
MgO	1.25	K ₂ O	2.80	Ni	-
Al ₂ O ₃	13.7	SO ₃	0.22	Sr	0.01
SiO ₂	74.00	Cl	0.10	Ti	0.50
Fe ₂ O ₃	4.60	Ba	0.13	Zn	0.01
MnO	0.07	Ce	0.04		
Na ₂ O	1.37	Cr	0.02	Total	99.99

2.1.2 Lime used and its properties.

The lime used in all the studies made for the completion of this thesis is quicklime. It was a Proviacal ® ST supplied by the company Lhoist Sud Europe. Analyzes of this lime were conducted by Lhoist R & D

laboratory (Belgium), and the results are presented in Table 2-3. Table 2-3 shows that the lime complies with the specifications of the requirements of standard NF EN 459-1 and also to the additional criteria of building lime corresponding to the class CL 90-Q.

Table 2-3 Chemical composition of Quick lime

Elements	Requirements EN 459-1 (for CL 90-Q)	Quicklime Proviacal ® ST used
MgO (%)	≤ 5	0.66
CaO + MgO (%)	≥ 90	93.83
CO ₂	≤ 4	3.2
SO ₃	≤ 2	--
CaO available (%)	≥ 80	90.9
t ₆₀ (minutes)	< 10	3.3

2.2 Experimental Procedures

2.2.1 Determination of Lime Modification Optimum.

The LMO test values of the MLD soil are determined by ASTM D 6276-99a (ASTM, 2006). Soil is passed through 425 µm and oven-dried at a temperature ≤ 60°C. The water content of the soil specimen is determined. From the oven-dried specimen, three specimens, each equivalent to 25.0 g, are taken in three 150 ml plastic bottles with an airtight cap. 0.5, 1, and 1.5% of lime equivalent to the dry weight of the soil specimens were added to all three containers, respectively. 100 ml of demineralized water is added to all. This is then followed by continuous shaking of each bottle for 30 seconds repetitively at an interval of 10 minutes for about 60 minutes. In the end, the pH of the soil-lime-water mixture is determined. The lowest percentage of lime that gives a pH of 12.4 is considered the LMO value of the soil.

The LMO value obtained in the present MLD soil is about 1%, as evident from the obtained plot in Fig. 2-1.

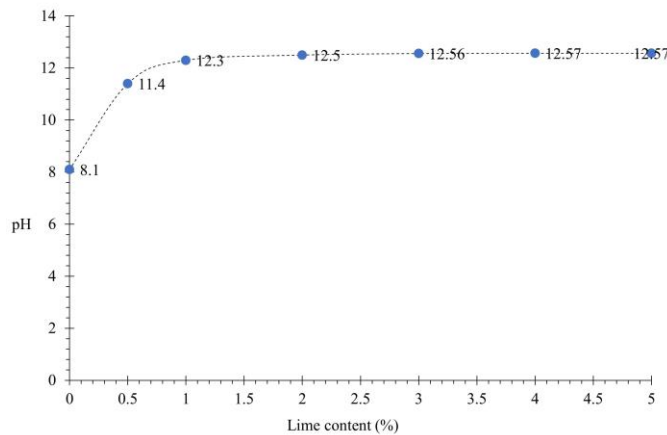


Fig. 2-1 LMO of MLD soil.

2.2.2. Determination of compaction parameters

The maximum dry density, $\rho_{d(max)}$, and Optimum Moisture Content (OMC) of the untreated and the three different lime-treated MLD soils were obtained as per NF P94-093, which follows the same procedure as ASTM, D698-12e2 (ASTM, 2012).

For this purpose, a miniature dynamic Proctor compaction tool (as presented in Fig. 2-2) designed in the laboratory was used. The tool was designed in a way that it applies the standard compaction energy as per ASTM, D698-12e2. Air-dried soil passed through a 5mm sieve and then mixed with the targeted water content were placed inside the mold of internal diameter 70 mm and height 19 mm. Then a cylindrical load of 1.042 kg from a height of 50.5 (± 0.5) mm was applied. A total of 2 layers were compacted, in which each layer was given seven blows. The volume and mass of the compacted soil paste at different water content were recorded and plotted, from which the maximum dry density, $\rho_{d(max)}$, and Optimum Moisture Content (OMC) of the untreated and the lime-treated MLD soils obtained were presented in Table 2-4.

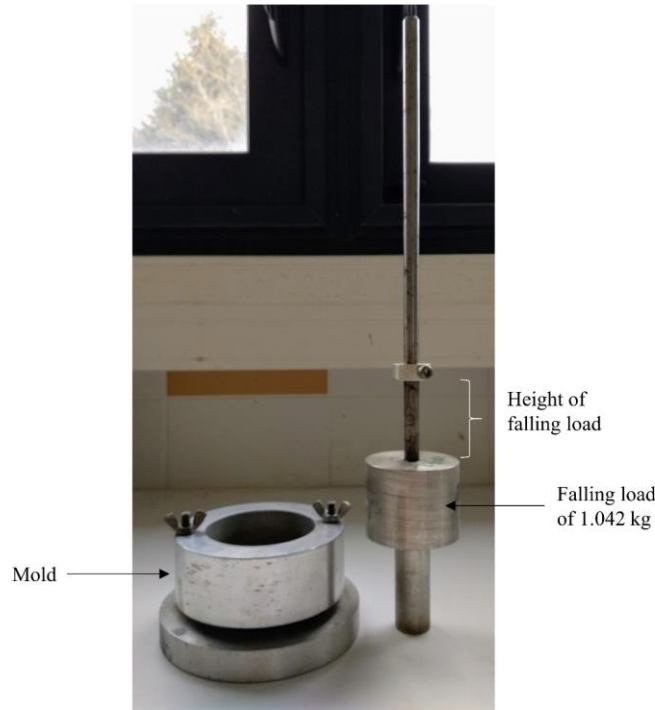


Fig. 2-2 Laboratory designed Mini Proctor compaction tool.

Table 2-4 Maximum dry density and OMC of untreated and lime-treated silty soil

Soil	$\rho_{d(max)}$ (kN/m ³)	OMC (%)
Untreated MLD soil	18.4	14.3
MLD soil treated with 1% lime	17.4	17.6
MLD soil treated with 2.5% lime	17.1	18.5
MLD soil treated with 4% lime	17.0	18.7

2.2.3. Specimen preparation for compaction

Once the characteristics of compaction were deduced, the MLD silt was then air-dried and sieved using a 5 mm-sieve. Soil mixtures were prepared at OMC and at water content 1.1 times higher than OMC *i.e.*, at WMC, and stored in sealed plastic bags for about 24 hours to attain moisture content homogenization. The wet soil and the respective lime were then mixed and rested for 60 to 90 minutes before compaction. The above process of soil preparation was as per the procedure mentioned in the French GTS Technical Guide for soil treatment (2000), which is also a reference for in-situ construction of lime-treated structures.

2.2.4 Compaction tests

Two types of compaction procedures were implemented in this thesis based on the requirement of the proposals made. They are Standard static compaction and Kneading compaction. In each compaction methods, the walls and bottom of the molds were lubricated with oil to avoid sticking of specimens.

2.2.4.1 Standard Static Compaction.

The static compaction involves compression of the specimens from top and bottom, as demonstrated by Holtz et al. (1981). The prepared soil mixture is required to be placed inside the static mold. Then two compressors are placed on the top and bottom of the mold and then using a hydraulic pump, pressure is created to prepare cylindrical compacted soil. Fig. 2-3 presents the laboratory used static device.

2.2.4.2 Kneading compaction

The kneading compaction was conducted by a laboratory-developed kneading tool, which follows the same procedure as demonstrated by Kouassi et al. (2000). However, the present laboratory-developed kneading tool was newly equipped with a dynamic load, as shown in Fig. 2-4. The application of the dynamic load was made successively with the rotation of the 3-kneading feet by an angle of 45° between 2 successive loadings. The applied compaction energy was adjusted as recommended by ASTM D698-91 (Equation 2-1).

$$E = \frac{N \times H \times n \times m \times g}{V} \quad (\text{Equation 2-1})$$

where, E is the potential compaction energy (kN-m/m³); $N = 16$, which is the number of blows per layer; $H = 0.14$ m, *i.e.*, the height of the falling load; $n = 5$, the number of compacted layers; $m = 1.042$ kg, the mass of the falling load (kg), $g =$ acceleration due to gravity (m/s²), $V = 187$ cm³ *i.e.*, the volume of the mold.

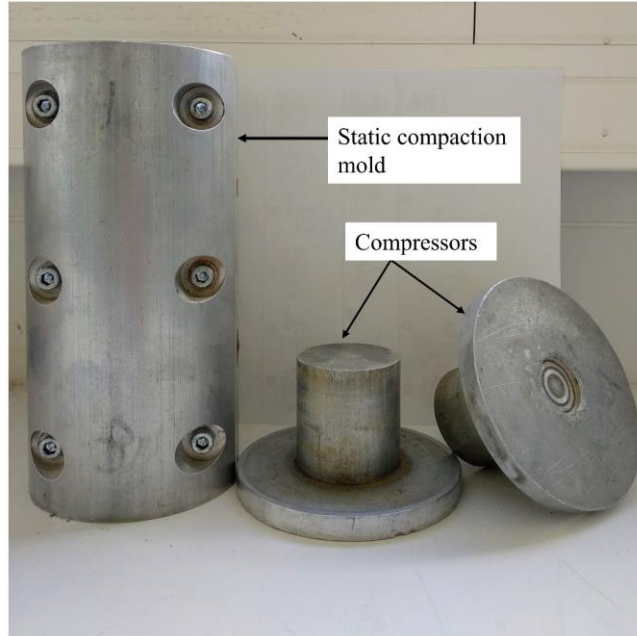


Fig. 2-3 Laboratory used Standard Static compaction tool.

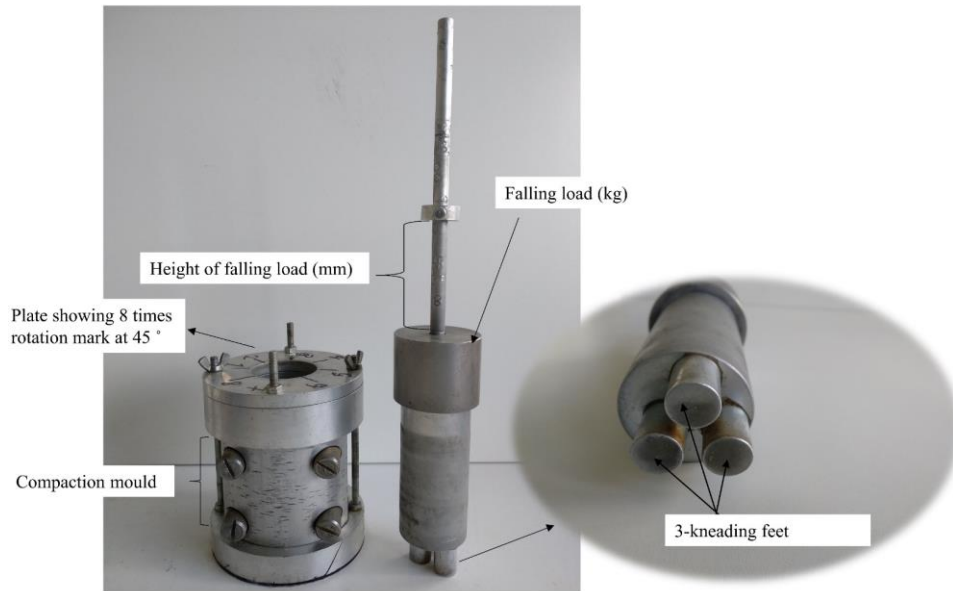


Fig. 2-4 Laboratory Kneading compaction tool.

Soil mixtures for both the kneading and static compaction were prepared at the constant initial compaction characteristics (Table 2-4). After compaction, the bulk density of each specimen was evaluated. The average bulk density of all the kneading and statically compacted specimens was 20.0 kN/m³ and 19.7

kN/m^3 , respectively. Thus, the average bulk density obtained using both compaction methods was similar. Hence, the precision of the kneading tool developed in the laboratory in achieving the targeted bulk density (*i.e.*, obtained from the standard static tool) can be justified.

Cylindrical specimens of dimensions having a length (l) to diameter (d) ratio of both 1 and 2 were prepared using both the compaction methods. Specimens of dimensions having l/d ratio 1 were 0.05 m in length and diameter, and the one of l/d ratio 2 was 0.10 m in length and 0.05 m diameter. The dimensions of specimens prepared vary based on the fulfillment of each proposal provided in Chapter 1.

2.2.5 Curing of specimens

Cylindrical compacted specimens were wrapped using a plastic film followed by a scotch tape. They were then cured in laboratory either in desiccators or using a climatic chamber. The use of desiccator was made when specimens were required to be cured at laboratory ambient temperature and relative humidity. Specimens were cured at climatic chamber to undergo accelerated curing by providing a temperature higher than the laboratory ambient temperature at a controlled relative humidity.

2.2.6 Unconfined Compressive Strength.

Unconfined Compressive Strength is the measure of material strength. It is defined as the maximum axial compressive stress that a material can withstand under unconfined conditions, *i.e.*, the confining stress is zero (Punmia and Jain, 2005). The unconfined compressive strength is also regarded as the uniaxial compressive strength of a material because the application of compressive stress is made along the longitudinal axis of the given sample.

In the present study, UCS analysis was made on compacted untreated and lime-treated specimens using a mechanical press with a load sensor varying between 2.5 to 25 kN. Measurements were performed at a constant deformation rate of 1 mm/min. The presentation of strength evolution is made in terms of the stress-strain curve, where the UCS value corresponds to the peak of the stress-strain curve, where the specimens fail.

2.2.7 Hydraulic Conductivity test.

Hydraulic conductivity test was performed with flexible wall permeameter by a constant hydraulic head. The percolation system established was similar to the one used by Ranaivomanana et al. (2017). A schematic design of the permeability setup is presented in Fig. 2-5.

Specimens were sealed in a cellulose membrane and placed inside cylindrical transparent Polyvinyl chloride (PVC) cell with porous stones on its top and bottom (Fig. 2-5). A water inlet valve was equipped at the center of the PVC cell for applying the confining stress. The PVC cell, along with the membrane and specimen, was then placed within an upper and a lower base plate to avoid vertical deformation. Both the base plate is accompanied by a hole at its center for allowing outflow and inflow of solution in and from the specimen, respectively. The valve connected to the hole at the lower base plate was linked with the Mariotte bottle. During the hydraulic test, the solution from the Mariotte bottle passes through the base of the specimen. This is to ensure uniform flow throughout the specimen by reducing any presence of entrapped air within the compacted specimen. The percolated fluid was collected in an effluent collection bottle linked with the valve connected to the hole in the upper base plate.

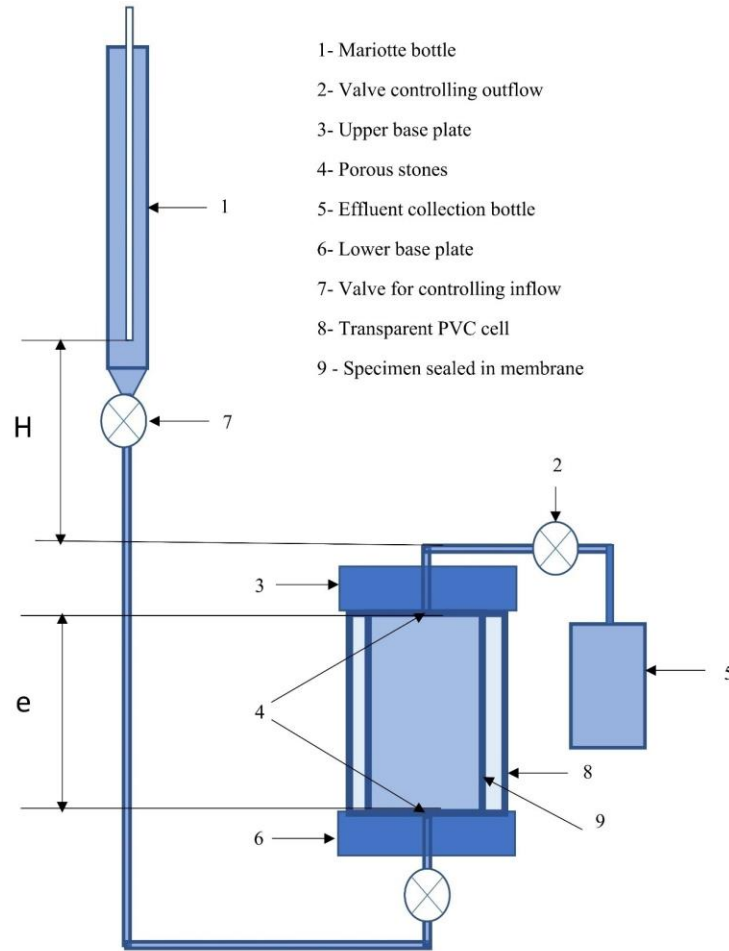


Fig. 2-5 Schematic diagram of flexible wall permeameter setup.

The hydraulic conductivity test was conducted in accordance with the flow conditions provided by Darcy's law. According to Darcy, the hydraulic conductivity, k (m/s) in terms of the total discharge, $Q = dV/dt$, through a specimen; the cross-sectional area of the flow, A (m^2); and the hydraulic gradient, $i = H/e$ can be expressed as follows (Equation 2-2).

$$k = \frac{dV \cdot e}{dt \cdot A \cdot H} \quad \text{(Equation 2-2)}$$

where H is the hydraulic head in m, and e is the specimen thickness in m; dV is the incremental volume of percolated water between two measurements in m^3 ; dt is the time elapsed between two measurements in seconds.

2.2.8 Physicochemical Investigations.

The physicochemical investigations involved in this study include water content measurement, suction measurement, and chemical analysis of different types of fluids as per requirement in the following studies.

2.2.8.1. Water Content and suction measurement.

The water content measurement was conducted as per ASTM D2216-19 (ASTM, 2010). This method involves deducing the gravimetric soil water content, which is the mass of water in the soil, obtained as the difference between the wet soil and the oven-dried soil at 105°C. The gravimetric soil water content is expressed as follows:

$$\text{Gravimetric soil water content (\%)} = \left[\frac{\text{mass of wet soil (g)} - \text{mass of oven-dried soil (g)}}{\text{mass of oven-dried soil (g)}} \right] \times 100$$

The total suction measurements were conducted using the WP4C Dewpoint Potentiometer (Decagon device). The WP4C uses the chilled-mirror dew-point technique to measure the tension of a given soil sample (Haghverdi et al., 2020). Powdered soil specimens are required to be placed in a sample cup of about 15 ml. During the placement of soil specimens, continuous tapping should be done to avoid any entrapment of air. Once filled, the sample cup is sealed inside the sample drawer (as shown in Fig. 2-6). After about 15-20 minutes, the required suction in MPa and corresponding temperature can be seen in the display with simultaneous beeping of the LED light. A total of 3 values were recorded for each specimen to maintain the accuracy in measurement.

The total suction of the soil (Ψ) is dependent on the relative humidity of the subjected specimen as per Kelvin's law (Fredlund and Rahardjo, 1993), as shown in Equation 2-3.

$$\Psi = \frac{-R \times T}{M_w \times \left(\frac{1}{\rho_w}\right)} \times \ln(RH) \quad (\text{Equation 2-3})$$

where R is the universal gas constant (8.31432 J/mol K), T is the absolute measured temperature in degrees Kelvin, M_w is the molecular weight of water (18.016 kg/kmol), ρ_w is the unit weight of water in kg/m³ as a function of T, and RH is the measured relative humidity (partial pressure of porewater vapor in the specimen divided by the saturation pressure of water vapor over a flat surface of water at the same temperature).

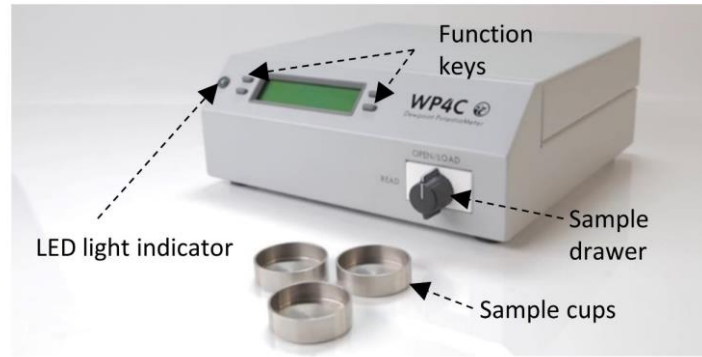


Fig. 2-6 WP4C Dewpoint Potentiometer (Decagon device) (modified from Haghverdi et al., 2020).

2.2.8.2 pH and Electric Conductivity measurement

The pH and Electric conductivity measurements for different fluids, both in an initial state and also as effluent, were done by a digital water quality meter.

The pH was also measured for soil samples. pH measurement for soil specimens was executed as per ASTM D4972-19 (ASTM, 2019). Crushed samples were sieved through a 2 mm mesh size and then suspended in distilled water in a liquid-solid ratio of 5:1 (volume fraction) for 1 hour. The pH of the suspended solution was then recorded.

2.2.8.3 Inductive Coupled Plasma Optical Emission spectroscopy test.

Inductive Coupled Plasma Optical Emission Spectroscopy (ICP-OES) is a technique used to determine the concentration of certain elements present in a given solution. The ICP-OES works on the principle that atoms and ions can absorb energy to move electrons from the ground state to an excited state (Fassel and Kniseley, 1974). During ICP-OES analysis, energy in the form of heat is passed using an argon plasma, which excites the electrons (as shown in Fig. 2-7).

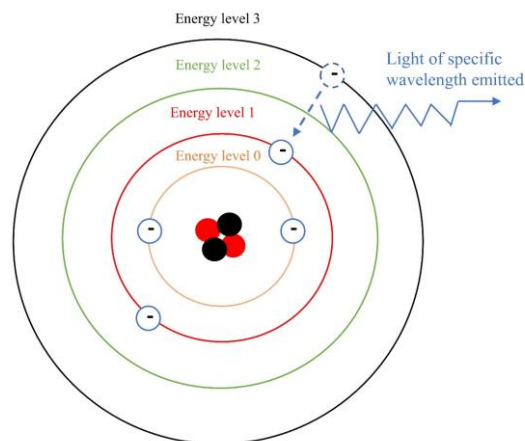


Fig. 2-7 Schematic diagram showing excitement of electrons, thus jumping to a high-level energy after absorbing energy, and again returning to the low-level energy by releasing light of specific wavelength (after Fassel and Kniseley, 1974).

As the atoms and ions return from a higher energy level to a lower energy level, it emits light of a specific wavelength (Fig. 2-7). The amount of light emitted at each wavelength is recorded, and this information is used to calculate the concentration of elements in a given solution based on a calibration graph.

In this study, ICP-OES was used to measure the concentrations of Calcium (*Ca*), Silica (*Si*), and Alumina (*Al*). *Ca*, *Si*, and *Al* are the prime constituents in lime-treated soil, which contributes to the long-term performances, and their analysis allows one to check the lime release and hydrates behavior. Hence, their concentrations were evaluated in fluids percolated through soil during the hydraulic conductivity test (Chapter 5) or was in contact with soil specimens during the wetting drying test (Chapter 6 and Chapter 7).

For each ICP-OES analysis, about 50 ml of solution was collected and then filtered using a 0.45 μm syringe. The solution was then stored in the refrigerator until the required analysis was carried out.

2.2.9 Volume and Mass measurement.

The volume of compacted specimens before and after curing time, after hydraulic conductivity test, and after Wetting and drying cycles was measured. The volume measurement was conducted by Vernier Scale.

The mass measurement of specimens in this study was made by using a laboratory-available weighing machine.

2.2.10 Microstructural investigations.

Untreated compacted specimens and lime-treated compacted specimens after curing and after being subjected to hydraulic conductivity test and wetting and drying cycle were sampled in plastic bags and stored in the freezer to avoid any further possible chemical reactions. These specimens were then freeze-dried and then stored in sealed vacuum bags until microstructural analyses were conducted to avoid any atmospheric interactions.

Following are the microstructural investigations conducted for the completion of this thesis.

2.2.10.1 Specific Surface Area and Pore structure measurements by BET

The Specific Surface Area (SSA) of compacted freeze-dried specimens were analyzed by Brunauer–Emmett–Teller (BET) (Brunauer et al., 1938) test using Micromeritics TriStar II PLUS.

BET uses nitrogen gas to measure the specific surface area in soil (Westermarck, 2000). Freeze-dried samples were evacuated or degassed at 50°C. Nitrogen gas at temperature, T of 77K, and pressure (p) lower than the equilibrium/saturation gas pressure (p_0) was then injected. At this temperature, the nitrogen gas condenses on the surface of the particles. At the initial state, the first adsorbed layer, also regarded as a monolayer, is formed. Since the size of the gas atom/molecule is known thus, the amount of adsorbed (condensed) gas is assumed to correspond to the total surface area of the particles, including pores at the surface.

Once the saturation pressure (p_0) was reached, the completion of the adsorption phase occurred, and the desorption phase was initiated, in which the gas was progressively withdrawn until the initial point of the adsorption phase was achieved. The amount of gas adsorbed by the soil during the adsorption and desorption phases was recorded as a function of relative pressure (p/p_0) of the adsorptive gas. Both the adsorption and desorption branch of isotherms was used to obtain the Pore Size Distribution (PSD) by using the Kelvin equation (Equation 2-4).

$$r_k = \frac{2 \cdot V_m \cdot \gamma \cdot \cos \theta}{R \cdot T \cdot \ln \left(\frac{p}{p_0} \right)} \quad \text{(Equation 2-4)}$$

where r_k is the radius of curvature of the condensed gas inside the pore, γ is the surface tension, V_m is the molar gas volume of an ideal gas, θ is the contact angle, and R is the gas constant.

The above procedure of obtaining the PSD from the isotherm branch obtain from BET is regarded as Barrett-Joyner-Halenda (BJH) method (Barrett et al., 1951). Fig. 2-8 presents a schematic representation of the adsorption and desorption process during the BET test.

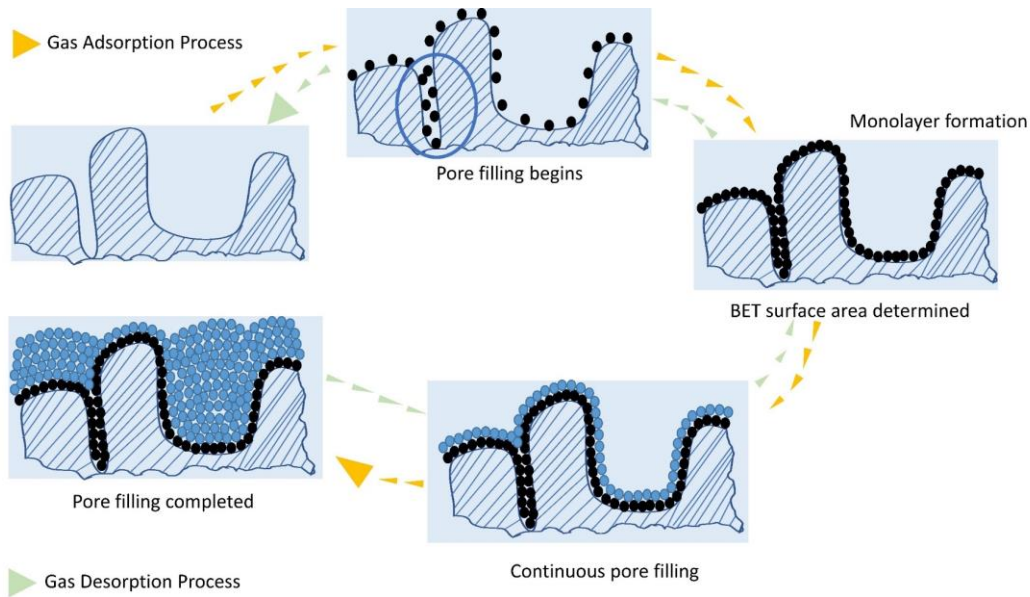


Fig. 2-8 Schematic diagram showing nitrogen gas adsorption and desorption phases during the BET test (modified from Mohammadi et al., 2020).

2.2.10.2 Pore structure measurements by MIP.

The procedure of the Mercury Intrusion Porosimetry (MIP) test involves the evacuation of freeze-dried samples via heating inside a sealed penetrometer. Mercury (a non-wetting liquid) was then progressively introduced into the samples through incremental hydraulic pressure. The volume of mercury intruded, and the applied pressure, p (MPa), was registered (Romero and Simms, 2008). By measuring the pressure p required to be applied to force the mercury into a cylindrical pore of diameter, D , pore sizes can be obtained according to the Washburn equation (Equation 2-5).

$$D = \frac{4 \cdot \gamma \cdot \cos \theta}{p} \quad \text{(Equation 2-5)}$$

D is the diameter of the entrance pore where mercury intrudes, γ is the surface tension of mercury ($\gamma = 0.484 \text{ N/m}$ at 25°C), and θ represents contact angle between mercury and pore wall (Romero and Simms, 2008). The contact angle is known to be significantly vary based on the surface roughness of the intruded medium. It was usually considered between 139° to 147° for clay minerals (Diamond, 1970).

2.2.10.3. Micro X-ray Fluorescence (μ -XRF)

The μ -XRF is a non-destructive analytical technique used to determine the elemental composition of materials. It works on the same principles as X-ray Fluorescence (XRF). During XRF, the subjected sample is excited by a high-energy x-ray beam, following which fluorescent (or secondary) X-ray is emitted from the subjected specimen. Each of the types of elements present in the subjected specimen produces characteristics of fluorescent X-rays, which is unique for that specific element. Thus, the qualitative and quantitative analysis of the material composition can be made (Vitale, 2016).

During XRF, the distribution of the x-ray beam was made on a large sample (20-60mm). While, during μ -XRF, the x-ray beam is restricted to the targeted area (0.025-0.1mm), and a microscopically small area on the surface of a large sample is analyzed (Vitale, 2016).

In this study, the elemental analysis was made using a micro-XRF M4 Tornado spectrometer (Bruker AXS microanalysis) equipped with an energy dispersive detector (SDD) and rhodium X-ray source. It was made in lime-treated kneading, and statically compacted specimens were performed to analyze the distribution of calcium under the influence of two different compaction mechanisms, which is detailed in Chapter 4.

2.2.10.4. Scanning Electron Microscope (SEM)

SEM image analysis is a technique that uses an electron beam to image the subjected samples at a resolution of nanometer scale. The electrons are emitted from a filament in the form of a beam, which is then focused on the surface of the subjected sample by a set of lenses in the electron column to generate a variety of signals at the surface of the specimen. The signals that are derived from the electron-samples interactions provide information that consists of the texture of the sample, its chemical composition, and crystalline structure and orientation of the material composing the sample.

In this study, SEM image analysis was performed in freeze-dried untreated and lime-treated compacted specimens coated with gold or carbon to show the presence of cementitious bonding due to lime treatment.

Chapter 3

EVALUATION OF THE LONG-TERM EFFECT OF LIME TREATMENT ON A SILTY SOIL EMBANKMENT AFTER SEVEN YEARS OF ATMOSPHERIC EXPOSURE: MECHANICAL, PHYSICOCHEMICAL, AND MICROSTRUCTURAL STUDIES (PROPOSAL 1).

Das, G., Razakamanantsoa, A., Herrier, G., Saussaye, L., Lesueur, D., & Deneele, D. (2021). Evaluation of the long-term effect of lime treatment on a silty soil embankment after seven years of atmospheric exposure: Mechanical, physicochemical, and microstructural studies. *Engineering Geology*, 281, 105986. <https://doi.org/10.1016/j.enggeo.2020.105986>

General

The present chapter is focused on the fulfillment of Proposal 1, which aims to present a thorough evaluation of the long-term influence of lime treatment in an atmospherically cured experimental embankment. This study involves the assessment of a 2.5% lime-treated embankment after seven years of exposure to wet environmental conditions. The embankment was constructed on 2011, Rouen, France, by MLD soil treated with 2.5% quicklime. It was earlier investigated by Makki-Szymkiewicz et al. (2015) at an early age (up to 1 year from construction) to assess its hydraulic performance. The present chapter demonstrates an extended investigation regarding the long-term effect of lime treatment in compressive strength, physicochemical, and microstructure evolution. The evaluation was done by comparison of (i) the mechanical performance of the field sampled specimens with laboratory cured specimens and (ii) the physicochemical and microstructural properties of the samples from the lime-treated embankment with specimens obtained from an untreated embankment constructed near to it as a reference embankment.

The chapter begins with an explanation detailing the construction of the embankment and then the process of specimens sampling, followed by laboratory testing. Then the first part of the results presented is focused on (i) evaluating the UCS of the lime-treated soil, (ii) examining the presence of cementitious bonding within the fabric of the lime-treated soil, and (iii) investigating the long-term effect of lime treatment on water content, suction, and pH. The second part presents the effect of lime treatment on pore structure and specific surface area modifications. The end is then accompanied by an elaborative discussion of the presented results.

3.1 Studied embankments and specimens sampling.

This section explains the two deconstructed embankments, which include compaction details, *i.e.*, compaction moisture content and compaction procedure, and the details of sample collection (location and process of sampling).

Both the untreated and the lime-treated embankments were compacted by a pad foot roller at a moisture content of about 1.1 times of OMC during construction in 2011. The lime-treated and the untreated embankment were compacted in 6 and 3 layers, respectively. The average water content recorded after completion of compaction of the untreated and the lime-treated embankment was 17.0 % and 19.4 %, respectively.

The embankments were deconstructed in October 2018. During deconstruction, at first, few specimens were gathered at different depths from the surface up to a depth of 0.12 m (*i.e.*, in the regions

close to the surface) to understand the impact of seasonal variation and vegetation roots in the lime-treated embankment. Then the soil near the surface was removed to limit the effect of weathering and plant roots. Later, trenches were excavated (as shown in Fig. 3-1) for sampling soil specimens at different depths throughout the core of the embankment.

A single trench was made on the untreated embankment (Fig. 3-2). Four trenches were excavated across the lime-treated embankment: T1 and T2 located towards the South-West, and T3 and T4 were located towards the North-East (Fig. 3-3). Specimens were collected throughout the trenches described in Figs. 3-2 and 3-3 for the untreated and lime-treated embankments, respectively.



Fig. 3-1 Trench excavated in the lime-treated embankment (T2) for the sampling of specimens.

The following nomenclature is used here to identify the various specimens. The specimens collected from the trench excavated in the untreated embankment are referred to as ‘Nat’, followed by the number displayed in the cross-section (Fig. 3-2). Similarly, specimens collected from the trench of the lime-treated embankment are referred to as ‘T1’, ‘T2’, ‘T3’, and ‘T4’, followed by the number in the corresponding cross-section (Fig. 3-3).

The trenching of the untreated embankment was relatively easy to perform, as the compacted soil was damp and less cohesive. However, block-cutting was not possible due to the low cohesion of the soil.

In the lime-treated embankment, two types of sampling were carried out. A compacted cubic block of about 0.40 m³ volume was cut from trenches using an excavator. It is worth noting that the process of block sampling was particularly complicated due to the rigidness of the soil. The second type of sampling consists of recovering smaller samples taken from each point of sample collection of the four trenches (Fig. 3-3). All specimens sampled were packed in a sealed bag and transported to the laboratory with care.

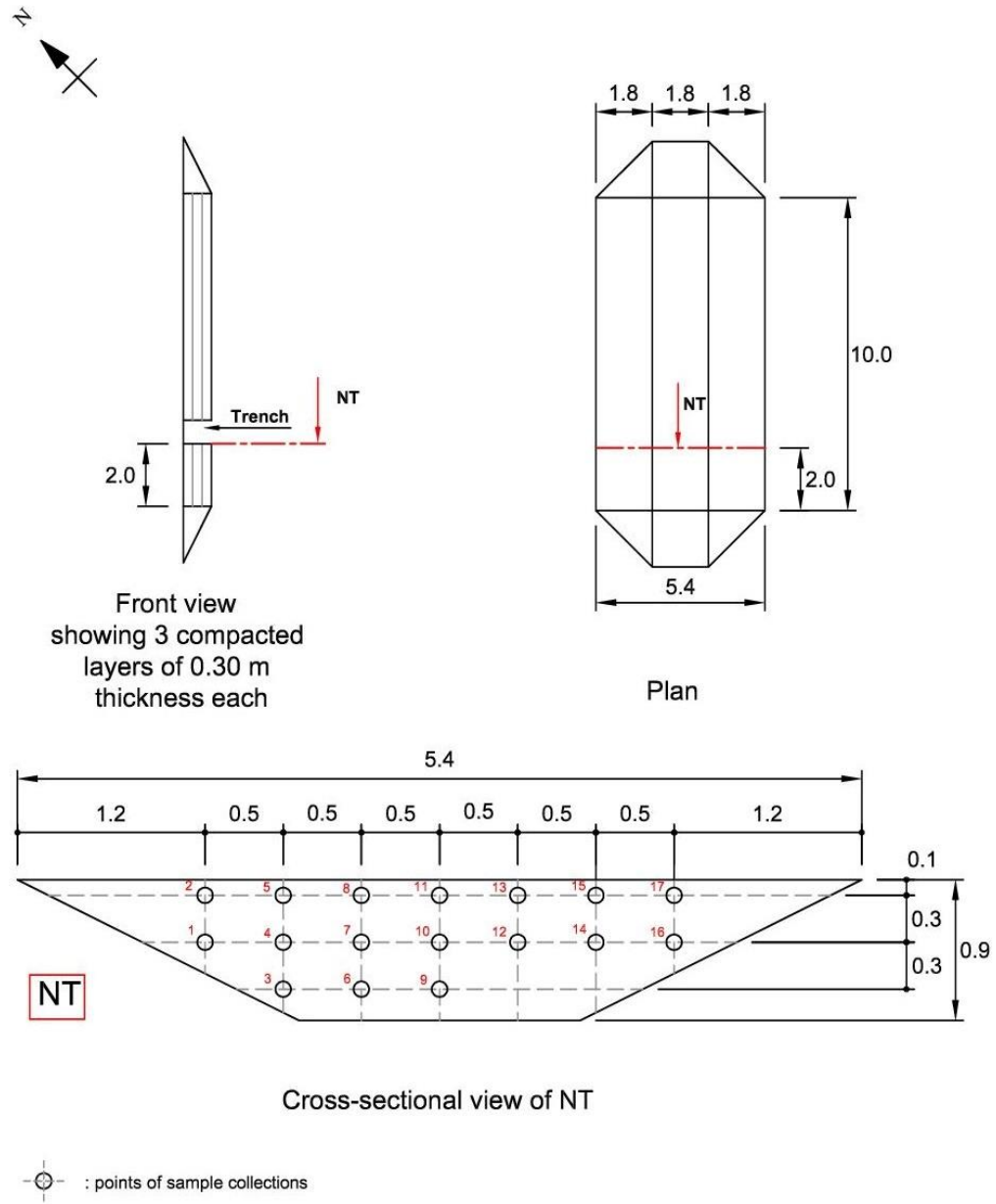


Fig. 3-2 Plan view, Front view along with Cross-sectional view of the excavated trench made for sample collections from the Untreated embankment (All units in meter)

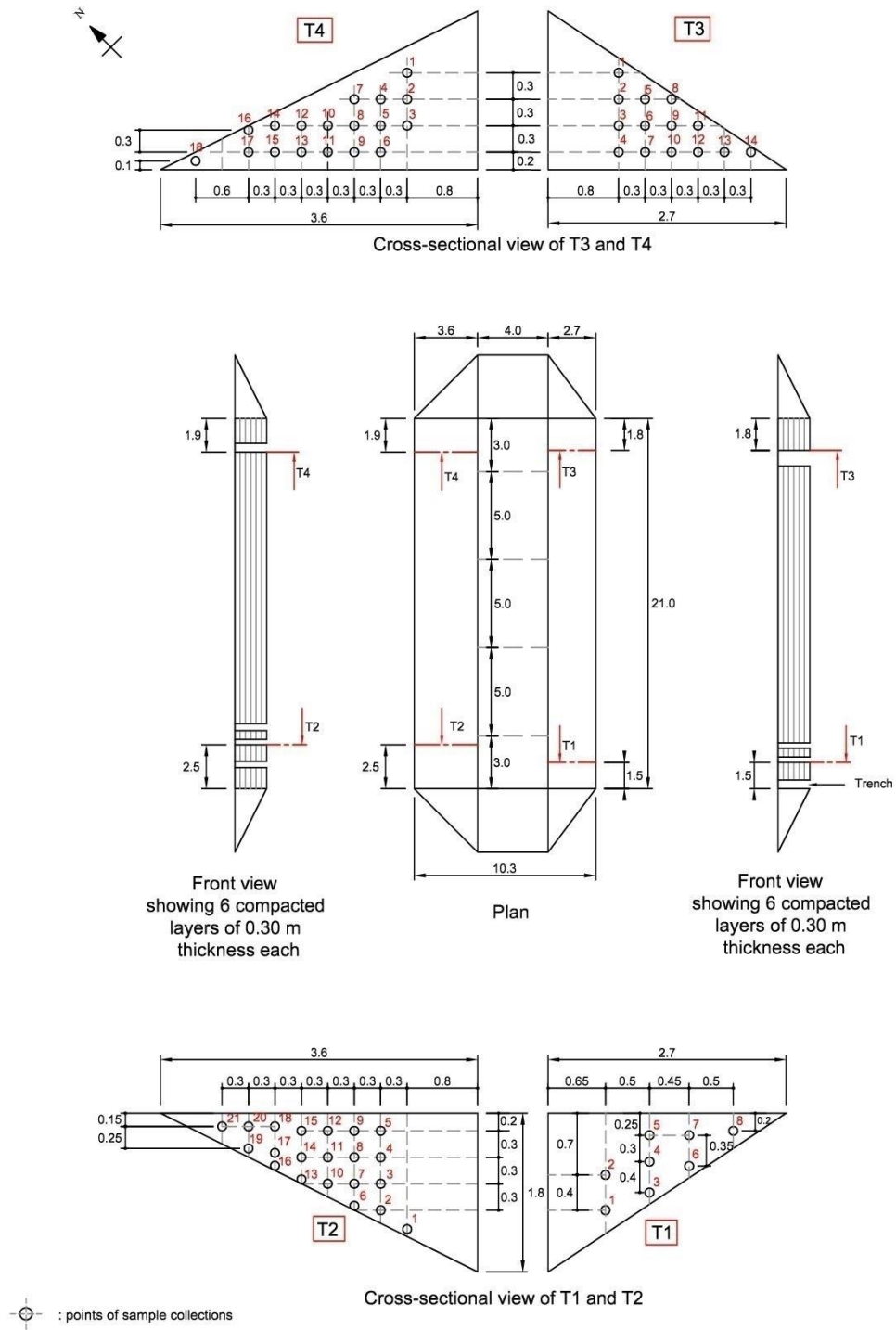


Fig. 3-3 Plan view, Front view along with Cross-sectional view of the excavated trenches made for sample collections from the lime-treated embankment (All units in meter)

3.2 Laboratory Tests

For strength measurement, two compacted cubic blocks were sampled from point T1-1 and T2-4, located at a depth of 0.30 m and 0.75 m normal to the slope, respectively (Fig. 3-3). These blocks were later trimmed at the laboratory using a cutting machine to obtain specimens having dimensions of length (l) and diameter (d) with an l/d ratio of 2 and 1. The 'l' and 'd' of specimens corresponding to l/d ratio of 2 were 0.08 m and 0.04 m, respectively, and while it was 0.05 m for both 'l' and 'd' for specimens corresponding to l/d ratio of 1. Samples of dimension l/d = 2 were obtained as ASTM D 2166 (ASTM, 2006) recommends the standard size of specimens to be within l/d ratio of 2 and 2.5 for the UCS test. Additional samples of l/d = 1 were trimmed.

The physicochemical behavior was investigated by measuring the water content, suction, and pH of the collected samples. Specimens sampled throughout the core of the trenches (Fig. 3-2 and Fig. 3-3) were subjected to all three tests. At the same time, the upper-layer-sampled specimens were subjected to water content and pH measurements.

The Specific Surface Area (SSA) and Pore characterization of compacted freeze-dried samples were analyzed. The contribution of lime treatment on pore structure modification was investigated by a comparative analysis of pore characterizations made on four selected samples. These specimens were collected at two constant depths to avoid any possible additional stress impact: untreated specimens Nat 1, Nat 2, and lime-treated specimens T2-2, T2-3. Specimens Nat 1 and T2-2 were sampled at 0.15 m depth, whereas Nat 2 and T2-3 are located at 0.45 m depth, normal to the slope.

The distribution of moisture content, pH, and SSA of the specimens sampled from the core of the embankments are presented using contour plots obtained by using the mapping software: Surfer 13.

Table 3-1 summarizes the complete testing programs with the corresponding identifications and numbers of specimens.

Table 3-1 Test programs with samples identifications and numbers

Sample type	Test name	No. of samples	Sample name
Laboratory (Lab.) specimens	UCS	3	Lab.-28days-20°C (l/d=2), Lab.-90days-20°C (l/d=2), Lab.-90days-40°C (l/d=1)
In-situ (upper layer-sampled) specimens	Water content, pH	13 each	T1 and T2
	UCS	4	T1-1 (l/d=2 ; 0.30 m), T2-4 (l/d=2 ; 0.75 m), T1-1 (l/d=1 ; 0.30 m), T2-4 (l/d=1 ; 0.75 m)
	SEM	2	Nat 2 (0.45 m), T1-1 (0.30 m)
In-situ (core-sampled) specimens	Water content, pH, SSA	78 each	All specimens shown in cross-sections of Fig. 2 & 3
	PSD by MIP	4	Nat 1 (0.15 m), Nat 2 (0.45 m), T2-2 (0.15 m), T2-3 (0.45 m)
	PSD by BJH	17	Nat 1 (0.15 m), Nat 2 (0.45 m), T1-1 (0.30 m), T2-2 (0.15 m), T2-3 (0.45 m), T2-4 (0.75 m), T1-2, T1-3, T1-6, T1-7, T2-13, T3-7, T3-9, T3-14, T4-8, T4-11, T4-12

3.3 Results

3.3.1 Unconfined Compressive Strength.

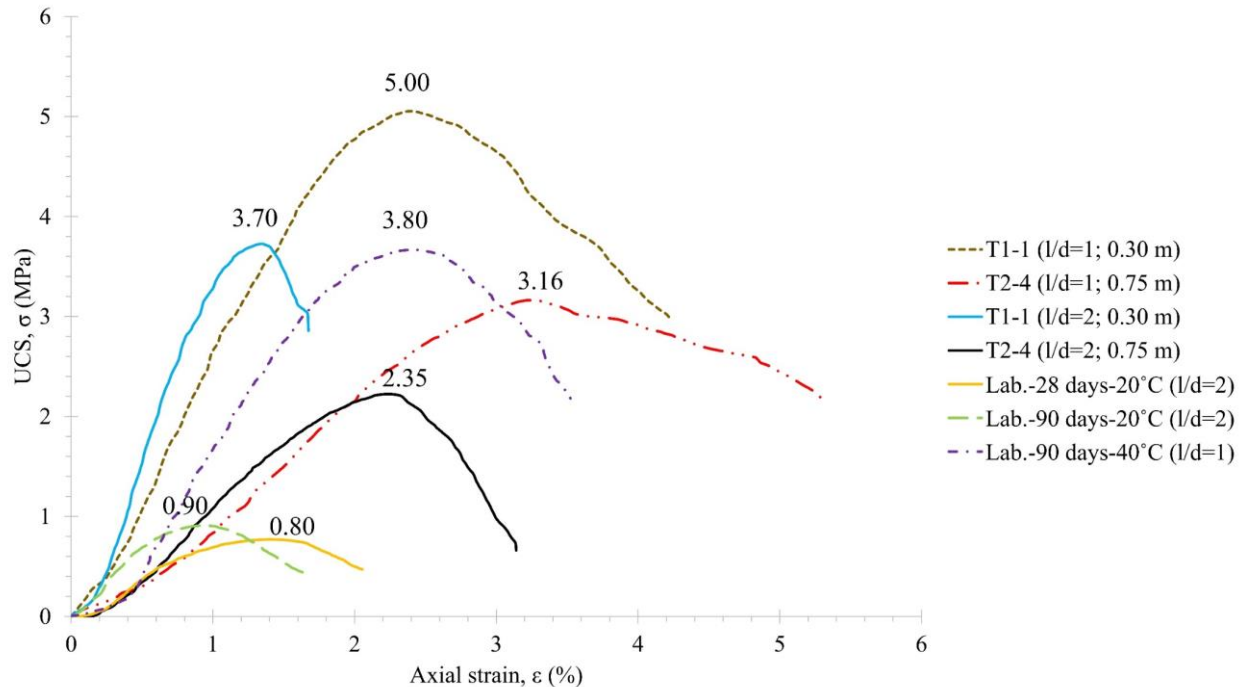


Fig. 3-4 UCS measured from the field- and laboratory-cured specimens.

The UCS values of the four trimmed core-sampled specimens from T1-1 (0.30 m) and T2-4 (0.75 m), as mentioned in section 3.2, are presented in Fig. 3-4. Specimens from T1-1 show UCS values of 3.70 MPa ($l/d = 2$) and 5.00 MPa ($l/d = 1$). Specimens from T2-4 show UCS values of 2.35 MPa ($l/d = 2$) and 3.16 MPa ($l/d = 1$). The corresponding water content of these specimens during the UCS test was measured to be around 11.0 %.

The UCS measured in the in-situ specimens was compared with three laboratory-cured samples prepared with similar soil and the same lime content and water content as the field specimens. Two laboratory compacted specimens of dimension having l/d ratio of 2 were cured for 28- and 90-days at about 20°C using a desiccator to regulate a controlled temperature and relative humidity. The 28-day curing was considered as a reference short curing period, whereas 90-day was the long curing period at a laboratory scale. Since no laboratory study was made with specimens subjected to 7 years of curing, a third laboratory compacted sample was subjected to accelerated curing (at 40°C) for 90 days. Lemaire et al. 2013 and Zhang et al. 2020 have demonstrated that the increase in temperature accelerates the soil-water-lime chemical reactions resulting in a rapid rise of UCS level in the lime-treated soil.

Fig. 3-4 shows that the UCS measured for 28- and 90-days laboratory cured specimens at 20°C (of dimension $l/d = 2$) were 0.80 and 0.90 MPa, respectively. While the UCS measured for the accelerated cured specimens (of size $l/d = 1$) was 3.80 MPa.

3.3.2 SEM observations.

Fig. 3-5 presents the SEM images showing the fabric structures of Nat 2 (untreated specimen sampled at 0.45 m depth from the slope) and T1-1 (lime-treated specimen sampled at 0.30 m depth from the slope) freeze-dried and gold-coated specimens. At a magnification of 1.00k, macropores and aggregates were observed in Nat 2 (Fig. 3-5 (a)), while in T1-1, the aggregates, minerals, and pores were found to be covered by a gel layer (Fig. 3-5 (b)).

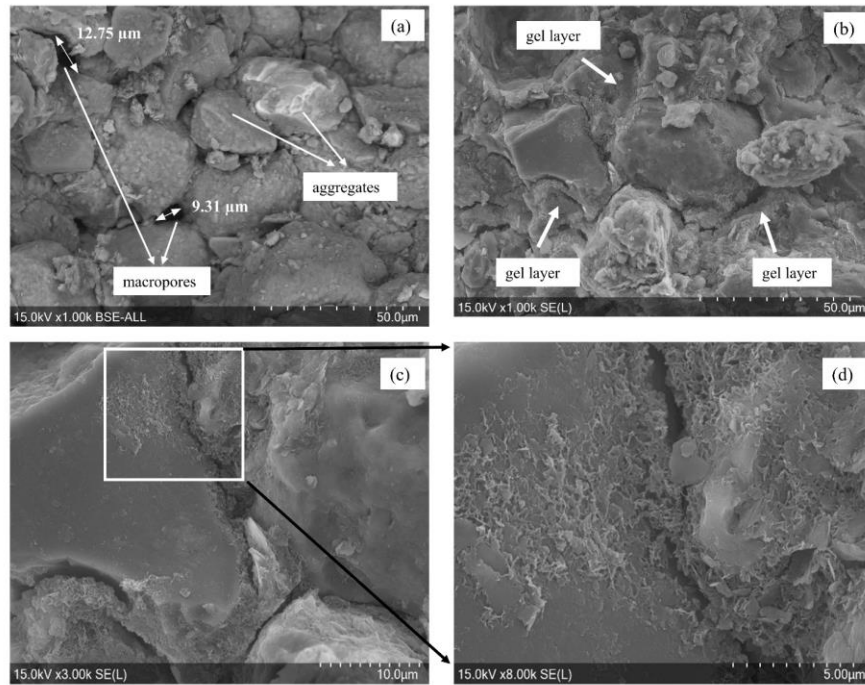


Fig. 3-5 SEM images of specimens Nat 2 (0.45 m) (a) and T1-1 (0.30 m) (b-d) at different magnifications sampled from the core of the embankments.

At higher magnifications (Fig. 3-5(c & d)), the cementitious bonding was observed between minerals and soil aggregates in T1-1, which is as reported in prior literature (Di Sante, 2019; Jha and Sivapullaiah, 2019; Lemaire et al., 2013).

3.3.3. Physicochemical properties

3.3.3.1. Distribution of water content

Fig. 3-6 presents the distribution of water content throughout the core of the untreated and lime-treated embankments measured during deconstruction.

In the core of the untreated embankment, the water content was measured to be minimum at the surface, i.e., 11.8 %, and it gradually increased with depths reaching 15.4 % at the subgrade (Fig. 3-6(a)). While throughout the core of the lime-treated embankment, the water content measured was observed to be unevenly distributed in the range 17-19.3 % (Fig. 3-6(b-e)).

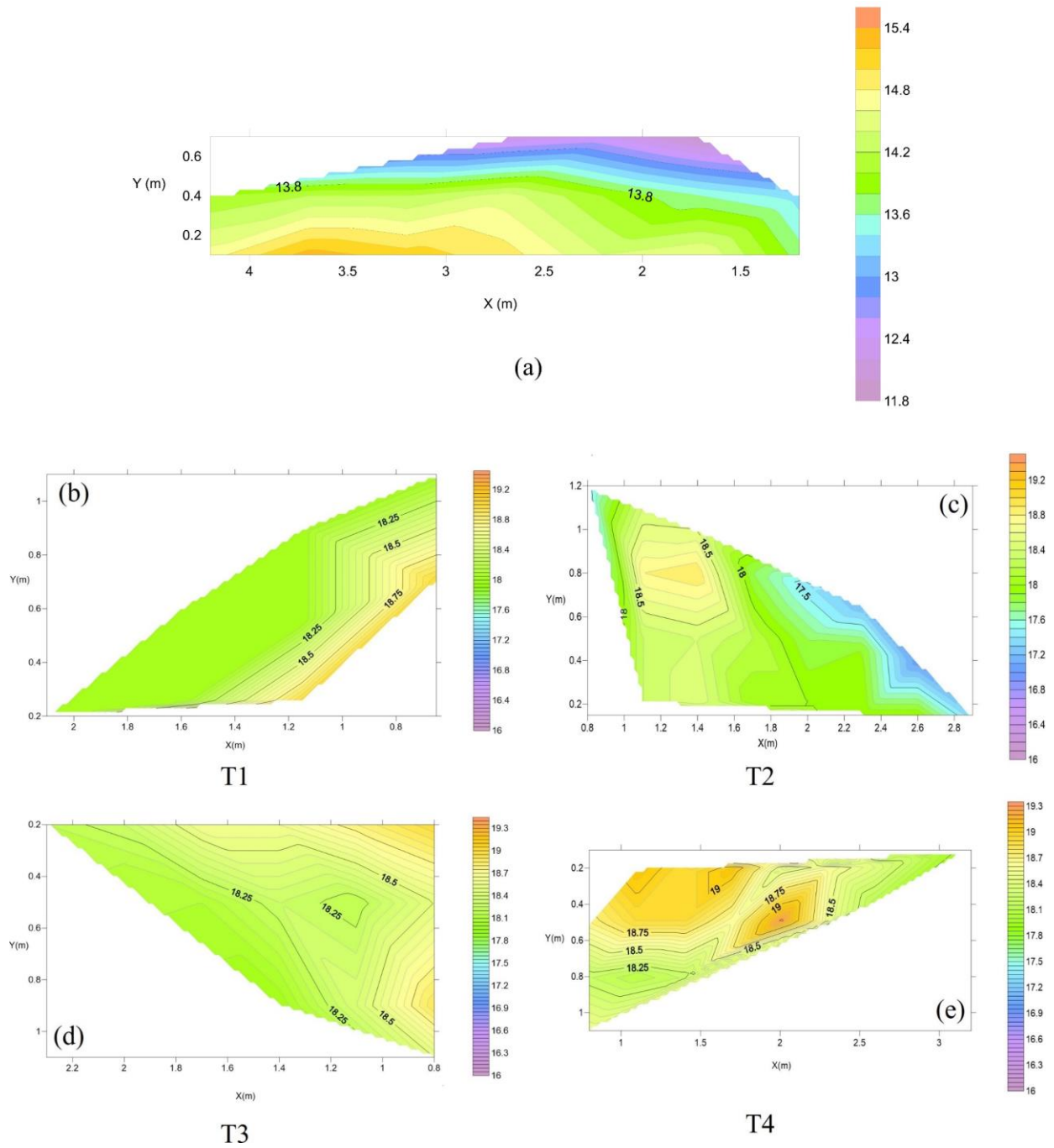


Fig. 3-6 Contour plots showing the distributions of water content (%) in the untreated (a) and the cross-sections T1 (b), T2 (c), T3 (d), and T4 (e) of the lime-treated embankments measured during deconstruction.

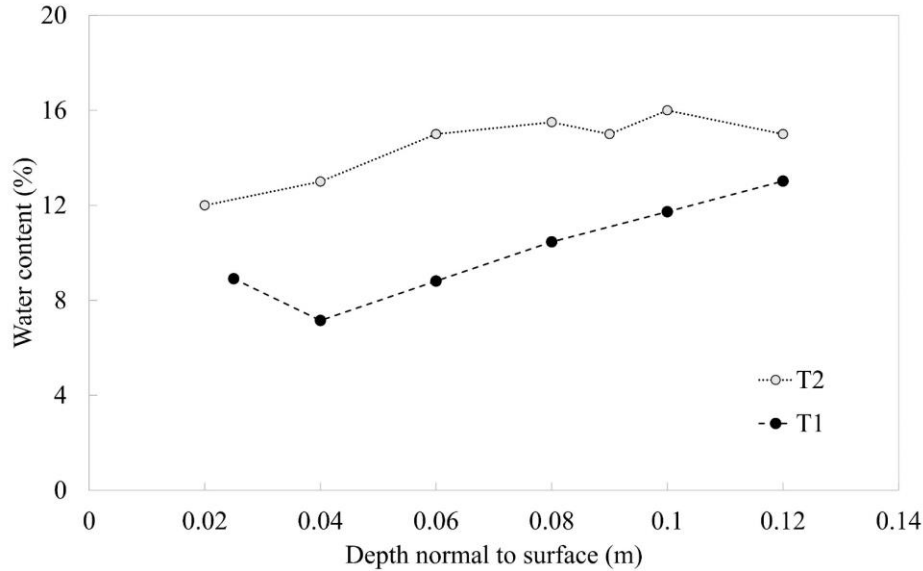


Fig. 3-7 Water content (%) measured on specimens sampled from the upper layer of the lime-treated embankment during deconstruction.

Fig. 3-7 presents the water content measured on the upper layer-sampled specimens of the lime-treated embankment from the cross-sections T1 and T2 up to a depth of 0.12 m normal to the surface. The minimum water content observed in T1 was 7.0 %, while it was 12.0 % for T2. The water content then gradually increased with depth from the surface and reached a maximum value of 15 % for T2 and 13 % for T1.

3.3.3.2. Measurement of suction

The suction measured for all the untreated and the lime-treated core-sampled specimens is presented in Table 3-2. Due to the presence of 78 samples, measurement of suction was done sequentially, one after the other. This led to a slight variation between the water content measured during suction measurement and the one measured during deconstruction, as seen in Table 3-2. The suction range measured for the untreated specimens was 0.19-1.14 MPa, which corresponds to a water content range of 9.89-11.71 %. While for the lime-treated soil, the suction range measured was 0.17-2.71 MPa, corresponding to a water content range of 15.8-17.9 %.

Table 3-2 Suction measured on untreated and lime-treated core-sampled specimens.

Sample	Numbers	1	2	3	4	5	6	7	8	9	10	11	12	13	14	15	16	17	18	19	20	21	
Untreated	WC (DC) ¹ (%)	13.3	13.7	11.9	13.6	14.6	12.4	14.0	14.4	12.2	14.5	14.9	14.2	15.1	14.2	15.3	14.0	14.7					
	WC (SM) ² (%)	9.89	11.2	9.73	10.8	12.9	9.71	11.9	11.6	9.38	11.7	11.4	12.7	12.6	12.3	12.3	11.5	12.1					
	Suction (MPa)	1.14	0.73	0.60	0.88	0.40	0.80	0.57	0.65	1.01	0.19	0.46	0.21	0.61	0.45	0.66	0.39	0.31					
T1	WC (DC) (%)	18.2	19.0	18.1	18.2	18.7	17.9	18.2	18.2														
	WC (SM) (%)	17.0	18.0	17.0	17.0	18.0	16.3	17.3	17.2														
	Suction (MPa)	1.15	0.80	1.29	0.76	0.72	1.47	0.78	0.71														
T2	WC (DC) (%)	17.4	18.4	18.8	18.3	18.3	18.5	18.9	18.4	18.5	17.8	18.2	18.0	17.4	17.8	18.0	17.2	17.9	18.0	18.0	17.0	17.3	
	WC (SM) (%)	14.1	16.0	15.2	16.2	18.2	16.4	15.2	16.3	17.2	17.0	16.0	15.4	16.4	17.0	17.5	16.8	16.4	16.6	16.3	16.0	16.4	
	Suction (MPa)	1.51	0.86	0.89	0.34	0.40	0.55	0.95	0.83	0.93	0.80	1.29	1.75	1.10	0.83	0.80	1.27	1.29	1.03	1.39	1.61	1.13	
T3	WC (DC) (%)	18.5	18.9	18.5	19.0	18.4	18.2	18.8	18.0	18.3	18.6	18.1	18.6	18.3	18.2								
	WC (SM) (%)	17.9	17.6	17.2	17.7	18.2	18.1	17.9	17.2	17.1	18.2	17.8	17.9	18.2	17.2								
	Suction (MPa)	0.42	0.63	0.51	0.71	0.56	0.41	0.53	0.71	0.68	0.18	0.40	0.17	0.35	0.85								
T4	WC (DC) (%)	18.5	18.2	18.7	18.1	18.9	19.1	18.2	18.9	18.9	18.6	19.1	19.3	18.4	18.5	18.6	18.1	18.4	17.9				
	WC (SM) (%)	17.9	14.5	18.0	17.3	17.6	16.6	16.9	17.1	15.3	16.5	16.6	18.5	14.5	15.8	17.2	16.1	17.5	16.9				
	Suction (MPa)	0.97	0.30	0.50	0.95	0.87	1.14	0.90	1.31	1.40	1.77	1.46	0.70	2.04	2.71	1.03	1.76	0.98	1.63				

¹WC(DC): Water content measured during the deconstruction of embankments.

²WC(SM): Water content measured during the suction measurement.

3.3.3.3. Distribution of soil pH

Fig. 3-8 presents the distribution of soil pH throughout the core of the untreated and the lime-treated embankments measured during deconstruction.

The pH value of the untreated embankment was between 8.3 to 8.8 (Fig. 3-8(a)). In the lime-treated embankment, the measured pH value ranges between 11.08 and 11.66 (Fig. Fig. 3-8(b-e)).

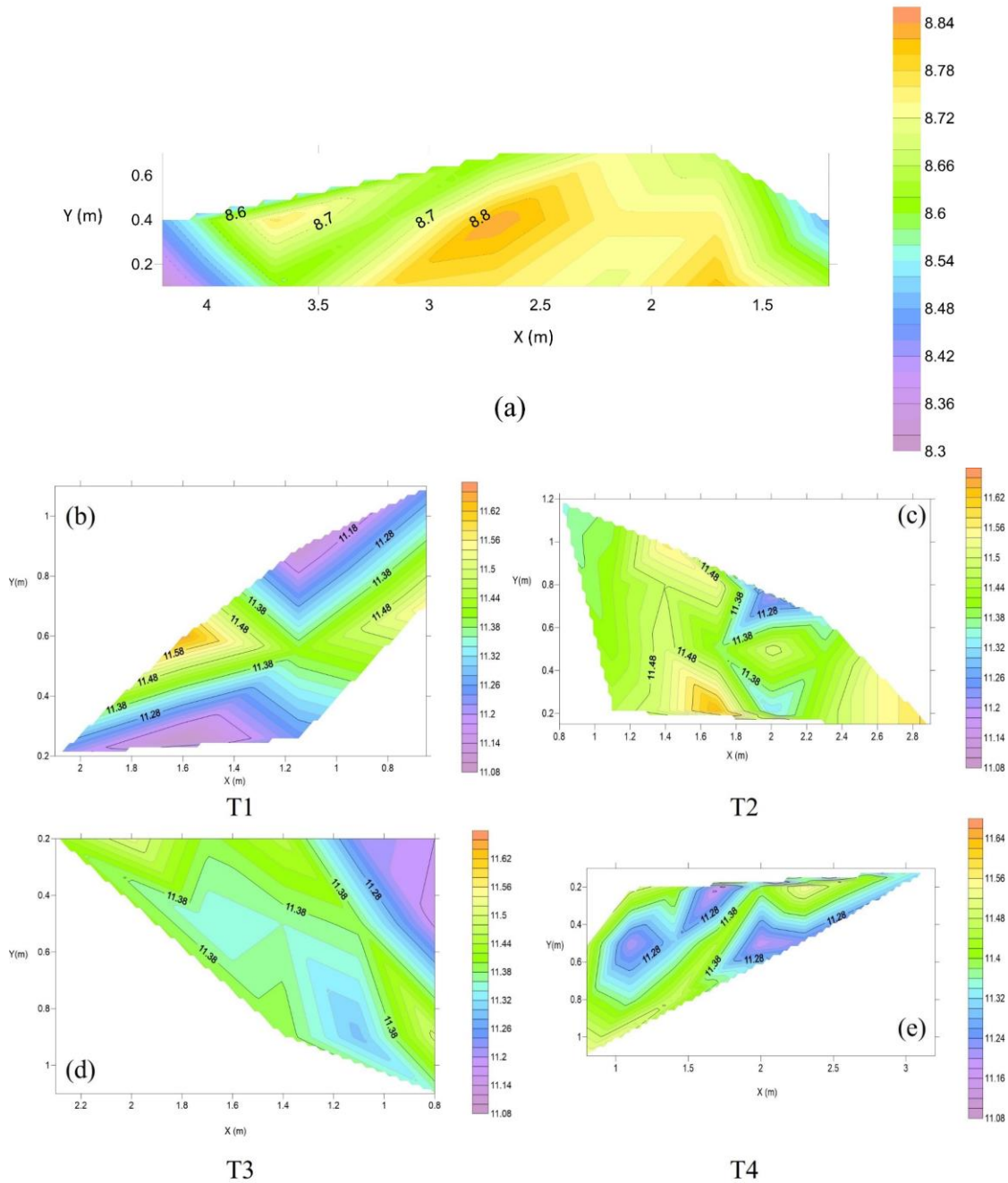


Fig. 3-8 Contour plot showing the distribution of pH in the untreated (a) and the cross-sections T1 (b), T2 (c), T3 (d), and T4 (e) of the lime-treated embankments measured during deconstruction.

The pH measured from the specimens sampled at the upper layer (up to 0.12 m depth from the surface) of T1 and T2 was observed to be between 8.0 and 9.0 (Fig. 3-9). The trend of pH distribution in the upper layer of T1 and T2 appears to be almost similar.

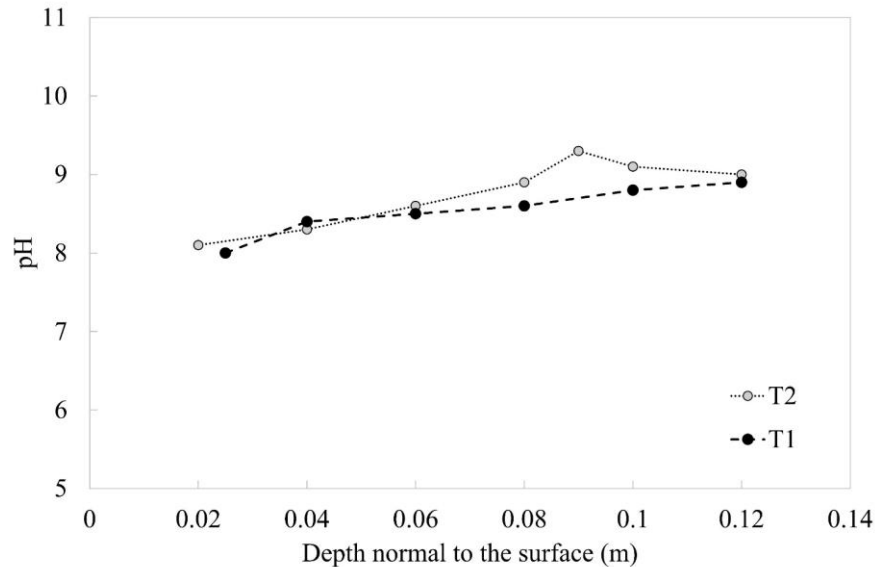


Fig. 3-9 pH measured on specimens sampled from the upper layer of the lime-treated embankment during deconstruction.

3.3.4. Pore size distributions.

Fig. 3-10(a-h) presents the PSD and cumulative pore volume of the untreated (Nat 1 and Nat 2) and the lime-treated specimens (T2-2 and T2-3) core-sampled at two different depths using the MIP test and BJH method.

On investigating the pore structure of the untreated specimens by MIP, Nat 1 (0.15 m) and Nat 2 (0.45 m), bimodal and unimodal PSD were observed, respectively (Fig. 3-10(a)). Nat 1 shows the higher intensity of macropores diameter of around 10^4 and 10^5 Å, while Nat 2 shows the same around pore diameter 10^4 Å. The cumulative pore volume measured for Nat 1 was about 19 % higher than Nat 2 (Fig. 3-10(b)). On observing the PSD and cumulative pore volume (in the range of pore diameter 20-250 Å) of the same untreated specimens by BJH, no significant presence of pores was observed in the mesopore range of pore diameter 50-500 Å (Fig. 3-10(e & f)). Moreover, a similar narrow peak was seen at the pore diameter of 40 Å for both Nat 1 and Nat 2 (Fig. 3-10(e)).

For the lime-treated specimens, the MIP results of both samples T2-2 (0.15 m) and T2-3 (0.45 m) show a broad unimodal peak at 625 Å with the development of smaller pores lower than pore diameter of 3000 Å (Fig. 3-10(c)). The trend of PSD remains the same for T2-2 and T2-3. However, T2-2 shows 20 % lower total pore volumes than T2-3 (Fig. 3-10(d)). While analyzing the pore structure of these specimens by BJH, the trend of the PSD in the mesopore range of pore diameter 40-500 Å remains the same for both the lime-treated samples Fig. 3-10(g). Both the specimens show a significant presence of mesopores of pore diameter in the range 50-500 Å. Specimen T2-2 shows a 27 % lower cumulative pore volume in the

mesopore range of pore diameter 20-250 Å than T2-3 (Fig. 3-10(h)). Additionally, a similar narrow peak at the pore diameter of 40 Å was observed for both T2-2 and T2-3 (Fig. 3-10(g)).

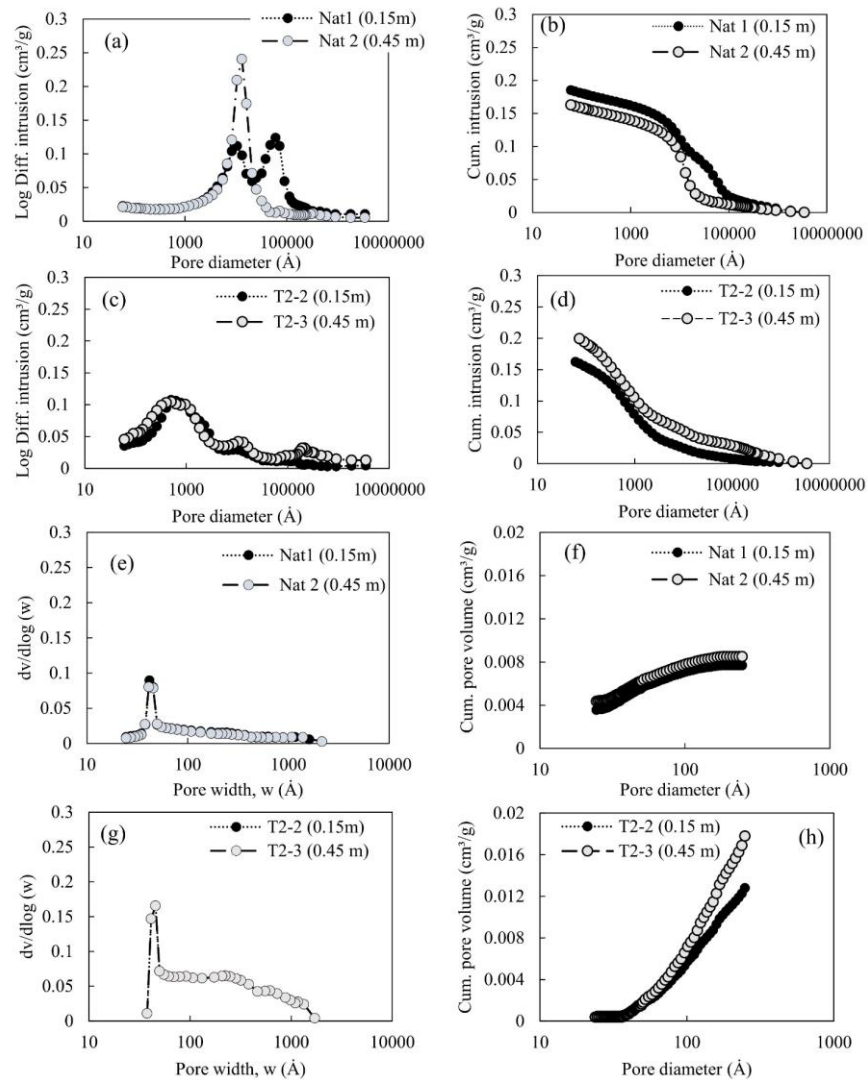


Fig. 3-10 PSD and Cumulative (Cum.) pore volume observed between untreated (Nat & Nat 2) and lime-treated specimens (T2-2 & T2-3) at a depth of 0.15 m & 0.45 m normal to the slope by MIP (a-d) & BJH (e-h) methods.

3.3.5. Distribution of SSA.

Fig. 3-11(a) shows the distribution of SSA throughout the core of the untreated embankment, which remains almost similar.

The SSA measured throughout the core of the lime-treated embankment appears to be unevenly distributed in all the cross-sections presented in Fig. 3-11(b-e). The maximum range of SSA measured was between 40 m²/g and 45 m²/g, which was observed in few specimens sampled from T1 (Fig. 3-11(b)), while other specimens show SSA values within 11 m²/g and 39 m²/g (Fig. 3-11(b-e)).

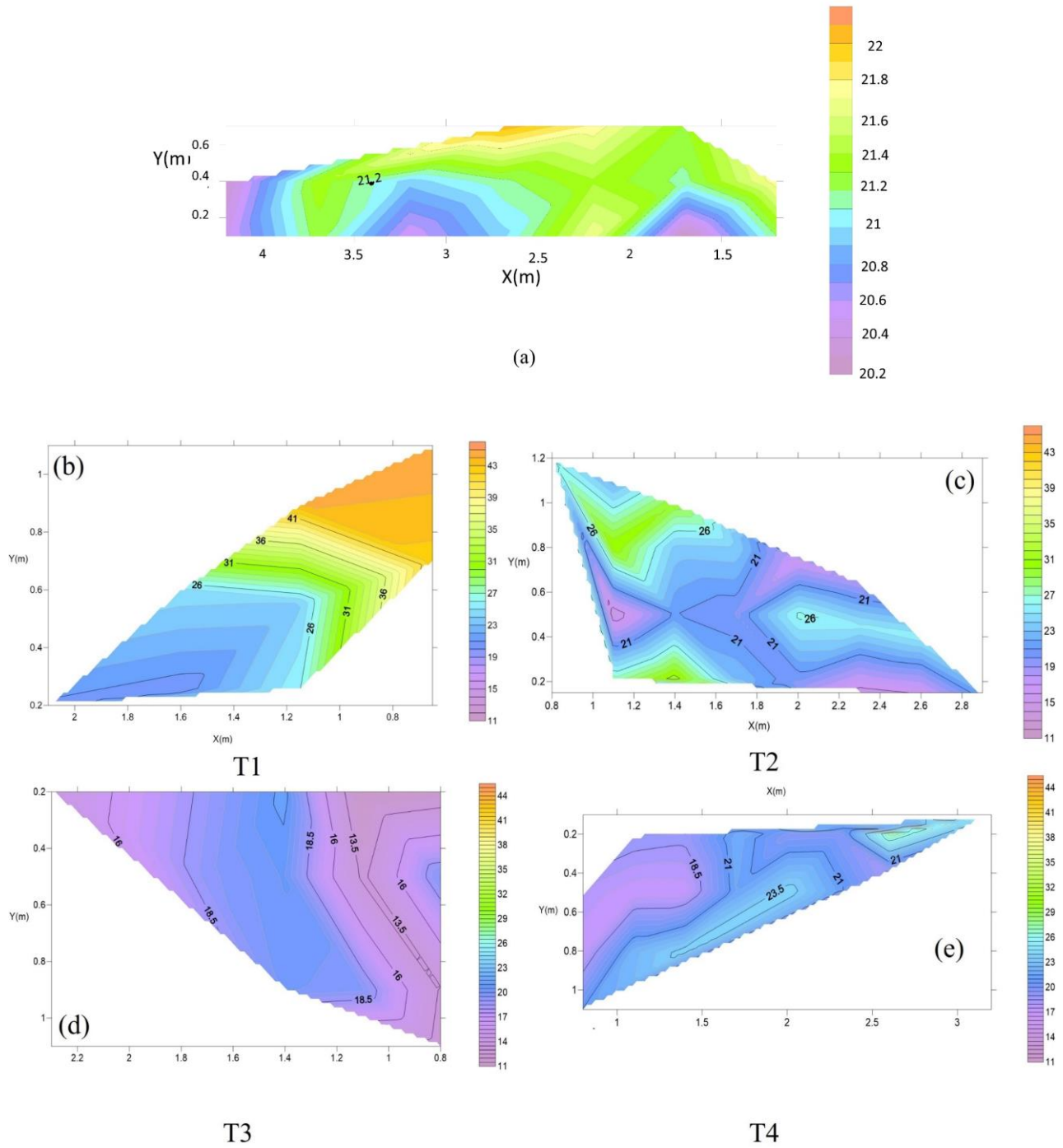


Fig. 3-11 Contour plot showing the distribution of SSA (m^2/g) in the untreated (a), and cross-sections T1 (b), T2 (c), T3 (d), and T4 (e) of the lime-treated embankments during deconstruction

3.4 Discussions.

3.4.1 Evaluation of the UCS measured from the in-situ cured lime-treated specimens.

Since specimens tested for the UCS had two different l/d ratios, a comparison between two samples of different ratios is made by applying a correction factor. According to ASTM-C42-77 (ASTM, 1978), a correction factor of 0.87 should be applied to the UCS measured using specimens with l/d = 1 to obtain the corresponding UCS of a similar sample having l/d = 2. Thus, corrected UCS values of 4.35 (5.00×0.87) and 2.74 (3.16×0.87) MPa (Fig. 3-4) were obtained for T1-1 and T2-4, respectively. Expectedly, these corrected values are nearly equal to the UCS of specimens (T1-1 & T2-4) having l/d = 2 (Fig. 3-4). Thus, considering different depths of sampling and different dimensions of the specimens, the UCS results can be assumed to be repeatable.

At the laboratory scale, the UCS measured from the accelerated cured specimen (Fig. 3-4) was corrected to 3.31 (3.80×0.87) MPa using the correction factor. The UCS of the in-situ specimens (Fig. 3-4) was observed to be about 2-4 times higher than what was measured after 28- and 90-days laboratory curing at 20°C. This highlights the contribution of lime treatment in increasing the UCS of the soil after long-term curing.

The average of the UCS value measured for the four in-situ cured specimens was 3.29 (± 0.45) MPa. This average UCS value was found to be of comparable order to the UCS of the laboratory accelerated cured specimen of dimension having l/d = 2 (3.31 MPa). This implies that such UCS levels can be expected after long-term curing. An inspection of the SEM images (Fig. 3-5(b-d)) reveals that such evolution of UCS in the in-situ samples can be attributed to the formation of cementitious bonds as a result of pozzolanic reactions.

Another factor that can influence the in-situ measured UCS is the loss in water content. The water content measured in T1-1 and T2-4 during the UCS test was found to be 7 % lower than what was measured during the deconstruction period ($\approx 18\%$) (Fig. 3-6(b & c)). This loss of water occurred due to the complications faced at the time of the trimming of the block-sampled specimens in the laboratory, as mentioned in section 3.2. One might argue that this loss of water might have resulted in a higher UCS level than expected. However, the evolution of a comparable level of UCS in the laboratory accelerated cured specimens, the maintenance of pH greater than 11, and the formation of cementitious bonding support the fact that the observed level of UCS was unlikely to have been influenced by the loss of water.

3.4.2 Contribution of mesopores generation towards strength evolution in lime-treated soil

The UCS of specimens T1-1 and T2-4 differs by 2 MPa (Fig. 3-4) even after they show similar water content during deconstruction ($\approx 18\%$) and UCS test (11 %). Also, the pH measured during deconstruction was of the same level (Fig. 3-8(b & c)). Thus, it can be derived that the observed difference in the UCS is not due to the difference in water content or pH. However, the suction measured for T1-1 corresponding to a water content of 17 % was 1.15 MPa, while it was 0.34 MPa for T2-4 at a water content of 16 % (Table 3-2). This difference in suction level might be due to differences in microstructural-development between T1-1 and T2-4 under the lime effect.

Lime treatment generates smaller pores (Cuisinier et al., 2011), which was shown to contribute to the rise in cohesion and hence strength (Verbrugge et al., 2011). In this aspect, the difference in smaller pores evolution between T1-1 and T2-4 was investigated by BJH method, as BJH method was observed to measure ranges of pores relatively lower than the one measured by MIP test in Fig. 3-10.

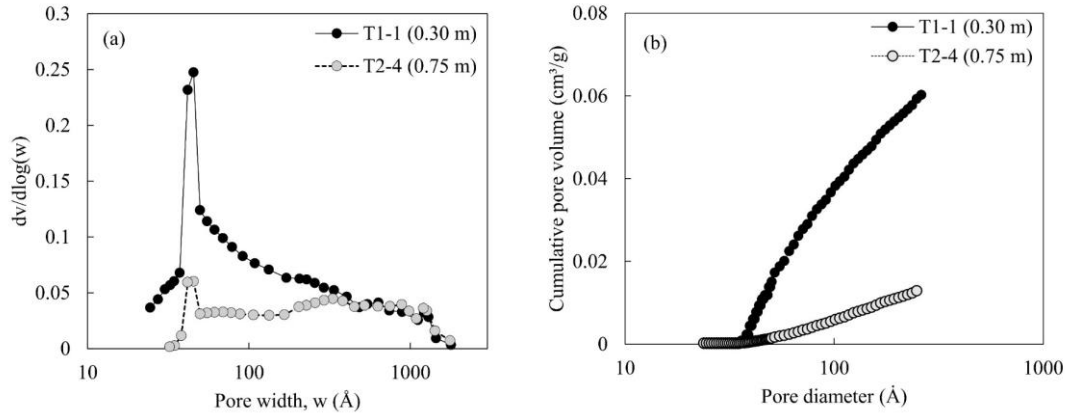


Fig. 3-12 Evolution of mesopores distribution (a) and cumulative pore volume (b) between T1-1 & T2-4 by BJH method.

Fig. 3-12 shows the mesopores distribution of T1-1 and T2-4. In Fig. 3-12(a), a narrow peak at a pore diameter of 40 Å was observed, which is five times higher in T1-1 than in T2-4. Moreover, a relatively large number of mesopores of pore diameter 50-500 Å was found in T1-1 compared to T2-4. Cumulatively, specimen T1-1 shows about 5.5 times higher presence of pore volume in the mesopores range of pore diameter 25-250 Å than T2-4 (Fig. 3-12(b)).

Thus, this higher number of mesopores development in T1-1 has led to the increased suction and consequently resulted in greater strength in T1-1 than in T2-4.

3.4.3 Long-term effect of lime treatment on the water content and pH distribution at the core of the embankments.

The average water content measured at the end of construction was 17.0 % and 19.4 % in the untreated and the lime-treated embankment, respectively. Thus, approximately a 5 % loss in water content was observed from the end of construction up to a depth of about 0.35 m normal to the surface of the untreated embankment (Fig. 3-6(a)). This loss of water gradually decreases with depth. This was expected in the untreated embankment. The maximum loss of water in the core of the lime-treated embankment was about 2 % from the end of construction, comparatively lower than the untreated embankment.

Additionally, unlike the untreated embankment, the overall distribution of water content does not vary significantly with depth in the lime-treated embankment (Fig. 3-6(b-e)). Most of the core-sampled specimens from the lime-treated embankment show water content ranging from 18.0 to 19.3 % (Fig. 3-6(b-e)). Thus, this distribution can be said to be homogeneous. This can be attributed to the proper mixing and compaction process implemented during the construction time, as reported by Makki-Szymkiewicz et al. (2015). Thus, the presence of this homogeneous water content throughout the embankment and the lesser reduction in water content from the end of construction than the untreated embankment highlights the long-term water retention capacity of the lime-treated soil.

Lime treatment increases the pH of the natural soil due to the release of OH⁻ ions in the soil-water-lime medium (Little, 1995). On evaluating the pH measured during deconstruction, the average pH measured in the untreated embankment was 8.5 (Fig. 3-8(a)), which was found to be almost equivalent to the pH value of the present silty soil. However, all the lime-treated soil show pH greater than 11 (Fig. 3-8(b-e)) and lower than 12.3, which corresponds to the pH at Lime Modification Optimum (LMO) of the soil. This decrease in pH can be attributed to the consumption of lime during the curing time, as demonstrated

by De Bel et al. (2013). Besides, the difference measured in the pH level between the untreated and lime-treated soil evidences the presence of pozzolanic products within the core of the lime-treated embankment.

Like the homogenous distribution of water content observed throughout the core of the lime-treated embankment, the pH, too, was found to be uniformly distributed throughout, ranging from 11.08 to 11.66 (Fig. 3-8(b-e)). This can also be attributed to proper mixing, as mentioned previously.

3.4.4 Effect of lime treatment on the evolution of suction at the core of the embankments.

Within the range of suction measured for the untreated embankment (0.19 MPa-1.14 MPa), a total variation of around 1.00 MPa in suction corresponds to a 2 % (9.89 %-11.71 %) variation in water content (Table 3-2). At the same time, this variation is around 2.50 MPa (0.17 MPa-2.71 MPa) for the lime-treated soil corresponding to the same percentage difference in the water content (15.80 %-17.90 %). Thus, the maximum suction measured for the lime-treated soil was about 1.57 MPa higher than the untreated soil, although the corresponding water content in the lime-treated soil was about two times higher than the untreated soil. The average minimum suction measured for the untreated specimens approximately corresponds to the average maximum measured water content and vice versa (Table 3-2). This behaviour of suction variation with water content was expected in the untreated specimens. While in the lime-treated samples, the variation of suction was less affected by the difference in the water content level.

Makki-Szymkiewicz et al. (2015) reported a suction level of 0.051MPa to 0.084 MPa at about an average water content of 19.4 % in specimens collected up to 1 year from the end of construction in the same lime-treated embankment. Thus, the present measured suction range (0.17 MPa-2.71 MPa) in the lime-treated specimens increased by about 2 to 30 times with a maximum of 3 % difference in the level of water content (15.80-17.90 %) during the additional six years curing period. This can be attributed to the modification of the lime-treated soil microstructure illustrated by an additional generation of smaller pores ($< 3000 \text{ \AA}$) (Fig. 3-10(c)) in the present specimen compared to the MIP result reported by Makki-Szymkiewicz et al. (2015) for the six months in-situ cured specimen.

Besides, the present variation of suction with respect to water content (Table 3-2) was also compared with the water retention plot provided by Nguyen et al. (2015) for the same soil and are presented in Fig. 3-13. Nguyen et al. (2015) showed the evolution of suction with respect to volumetric water content for 28 days (28d) and 90 days (90d) laboratory cured specimens treated with 2 % and 4 % quicklime.

Fig. 3-13 shows that the volumetric water content corresponding to the suction range of about 0.1 - 5.0 MPa was slightly higher for 90 days cured specimens compared to the corresponding 28 days cured specimens. Similar evolution of volumetric water content was observed in the present untreated soil corresponding to the suction range of 0.19-1.14 MPa. However, the volumetric water content in the 7-year cured specimens was about 50 % higher compared to all the specimens from Nguyen et al. (2015), corresponding to a similar range of suction (0.17-2.71 MPa).

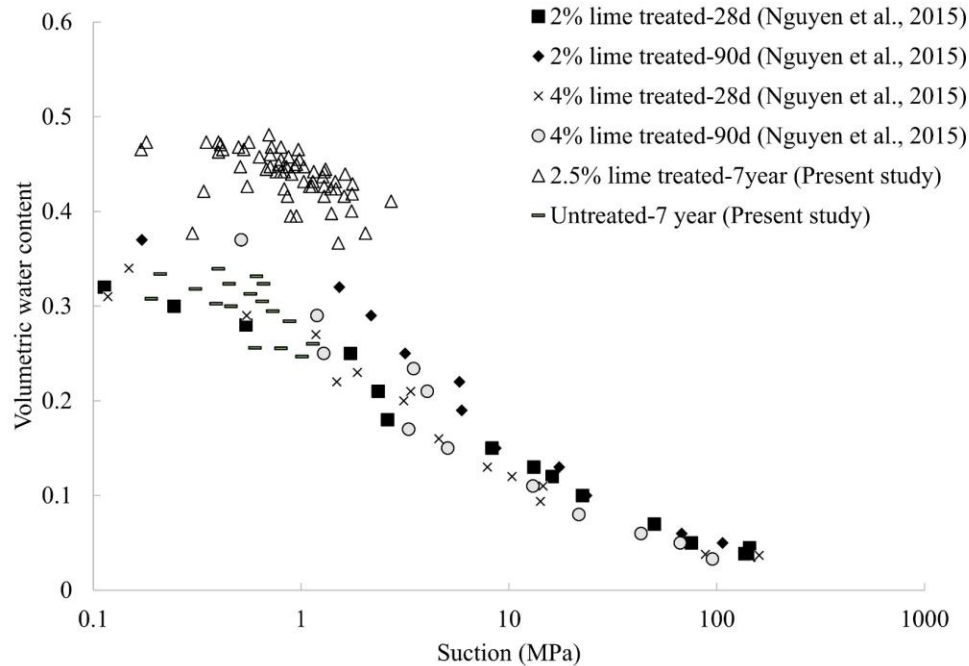


Fig. 3-13 Water retention plot obtained from the present soil compared to the one obtained from Nguyen et al. (2015).

Thus, based on the above discussion, it can be concluded that the observed long-term water retention capacity of the present lime-treated soil was due to this increased suction because of long-term pozzolanic reactions. Literature, based on laboratory studies, has demonstrated how lime treatment improves the water retention capacity of soil with the increase in curing time due to the modification of soil microstructure resulting from the generation of cementitious compounds (Russo, 2005; Wang et al., 2016).

Thus, the overall suction variation in the untreated soil follows the variation in the water content level inversely. However, in the lime-treated soil, the evolution of suction was due to the development of smaller pores as a result of pozzolanic reactions and was less affected by the variation in the water content level.

3.4.5 Effectiveness of lime treatment on the upper layer of the embankment submitted to atmospheric exposure.

The minimum water content measured in the upper-layer specimens of T1 and T2 was 7 % and 12 %, respectively (Fig. 3-7). This was about 12 % and 7 % less than the maximum water content measured in the core of T1 and T2, respectively (Fig. 3-6(b & c)). The increase in loss of water as one moves from the core towards the upper layer emphasizes the effect of soil-atmosphere interaction. Besides, the development of vegetation roots (as observed during deconstruction) also contributes towards this water loss. Bicalho et al. (2018) and Rosone et al. (2018) reported a similar impact of soil-atmosphere interaction on the upper surface of an in-situ cured lime-treated embankment. They showed a significant loss of water from the surface to a depth of 0.45-0.75 m of the embankment. Thus, the present study shows that the influence of soil-atmosphere interaction is significant up to a depth of 0.12 m normal to the surface of the lime-treated embankment.

In addition to the loss of water, a maximum reduction in pH for T1 and T2 was observed to vary from 11.66 (Fig. 3-8(b & c)) in the core to 8 in the upper layer (Fig. 3-9). This might be a consequence of carbonation (Xu et al., 2020) or dissolution of lime by leaching (Deneele et al., 2016; Khattab et al., 2007) under the long-term exposure of soil to the atmosphere. In the upper layer, the average pH for T1 and T2 gradually increases from around 8 near the surface to 9 corresponding to the depth of 0.12 m. This indicates that the atmospheric effects are minimized with depth.

Thus, it can be concluded that although the effect of lime treatment remains within the core of the lime-treated embankment, it was lost up to a depth of 0.12 m normal to the surface.

3.4.6. Evaluation of pore structures measured between the untreated and the lime-treated soil.

Unlike the MIP results of the untreated soil (Fig. 3-10(a)), no significant macropores were found at a pore diameter of 10^4 Å and 10^5 Å in the lime-treated specimens (Fig. 3-10(c)). Instead, both samples T2-2 and T2-3 show the presence of smaller pores of diameter lower than 3000 Å (Fig. 3-10(c)). Such smaller pores formation due to lime treatment was also reported by Cuisinier et al. (2011). Additionally, in the lime-treated soil, as per the BJH results, the observed development of mesopores in the range of pore diameter 50 Å to 500 Å (Fig. 3-10(g)) was more significant than that in the untreated soil (Fig. 3-10(e)). The narrow peak developed at the pore width of 40 Å for the lime-treated specimens (Fig. 3-10(g)) was about 1.8 times higher than what was observed in the untreated samples (Fig. 3-10(e)). In the untreated specimens, this observed peak can be due to the presence of clay porosity (Bin et al., 2007; De Bel et al., 2013). The increase in this peak for the lime-treated samples might be due to the combined presence of clay porosity and cementitious bonding because of pozzolanic reactions.

The overall development of smaller pores in the lime-treated soil is attributed to the development of pozzolanic products (C-S-H, C-A-S-H, C-A-H, *etc.*), and not due to carbonation, as both T2-2 and T2-3 exhibit pH greater than 11 (Fig. 3-8(c)), while carbonation reactions lead to a decrease in pH below 9 (Xu et al., 2020). Besides, the observed increase in smaller pores in the present 7-year cured specimens when compared to that reported by Makki-Szymkiewicz et al. (2015) (as explained in section 3.4.4) underscores the contribution of the pozzolanic reactions towards the development of smaller pores in the long-term.

Specimen Nat 1 (0.15 m) shows a higher number of macropores of pore width 10^5 Å and 19 % greater cumulative pore volume than Nat 2 (0.45 m), as reported in section 3.3.4. This indicates that the untreated specimen collected at a lower depth (0.15 m) exhibits more macropores than the one sampled from a greater depth (0.45 m). Samples Nat 1 and Nat 2 were located within the 2nd and the 3rd layer of compaction normal to the surface of the trench, respectively, in the untreated embankment (Fig. 3-2). Thus, during the construction of the untreated embankment, the compaction effort achieved by Nat 2 in the 3rd layer was higher than the one obtained by Nat 1 in the 2nd layer. Lipiec et al. (2012) and Mossadeghi-Björklund et al. (2019) have demonstrated how an increase in compaction effort leads to a decrease in the diameter of macropores with depths from the surface of the pavement. Thus, the presence of more macropores in Nat 1 than Nat 2 can be partly due to this difference in the compaction effort achieved with respect to depth during construction. In the lime-treated embankment, specimen T2-2, located at 0.30 m above T2-3 (Fig. 3-3), shows a 27 % lower pore volume than T2-3 as per the BJH results (Fig. 3-10(h)). However, specimen T1-1 located 0.45 m above T2-4, shows 5.5 times greater pores volume in the same pore range (Fig. 3-12(b)).

Thus, it can be said that the presence of macropores in the untreated specimens are affected by the sampling-depth of the embankment, while the formation of mesopores in the lime-treated samples under the lime effect remains less affected by the same.

3.4.7. Comparison between the volume of mesopores measured by MIP and BJH.

The discussions in the preceding section show how lime treatment brings about the formation of pores smaller than 3000 Å in diameter, including mesopores. On comparing this formation of smaller pores detected using MIP (Fig. 3-10(c)) and BJH (Fig. 3-10(g)), it was observed that BJH results give a more precise distribution of intensities showing a narrow peak at 40 Å and a broad peak at 50-500 Å. This was missing in MIP results for the same specimens. Based on this observation, Table 3-3 is presented to show the percentage difference of cumulative pore volume in the mesopore range that can be accessed by both MIP and BJH methods. It includes specimens T2-2 and T2-3 in the pore range of mesopore diameter 60-250 Å (i.e., the intersection of the ranges accessible through MIP and BJH). Table 3-3 shows that the cumulative pore volume measured by BJH for T2-2 and T2-3, in the mesopore range (60-250 Å) was about 3.5 and 3.2 times higher than that measured by MIP, respectively.

Table 3-3 Difference in pore volume measured in the mesopore range of pore diameter 60-250 Å by MIP and BJH methods.

Sample name	Total V_{cum}^1 measured by MIP (60-3.5 × 10 ⁶ Å) (cm ³ /g)	Total V_{cum} measured by BJH (25-250 Å) (cm ³ /g)	V_{cum} measured by MIP (60-250 Å) (cm ³ /g)	V_{cum} measured by BJH (60-250 Å) (cm ³ /g)	Calculated V_{cum} (60-250 Å) as a percentage of total measured by MIP (%)	Calculated V_{cum} (60-250 Å) as a percentage of total measured by BJH (%)
T2-2 (0.15 m)	0.160	0.013	0.029	0.010	17.8	81.0
T2-3 (0.45 m)	0.200	0.018	0.040	0.015	19.8	84.0

¹ V_{cum} : cumulative pore volume.

These results, thus, show the effectiveness of the BJH method in quantifying the mesopores formed under long-term lime effect.

3.4.8 Long-term effect of lime treatment on the SSA.

Lime treatment is known to decrease the SSA of highly expansive soil based on laboratory investigations (Bhuvaneshwari et al., 2014; Cherian and Arnepalli, 2015). So far, the long-term effect of lime treatment on the SSA of lime-treated low plastic soil, such as silty soil, remains less investigated.

De Bel et al. (2013) conducted SSA by BET of the present MLD soil and stated that 3 % quick lime-treated MLD soil shows a decrease in SSA from 23.0 m²/g to 13.3 m²/g after 7 days of curing. At the same time, this SSA value rises to 21.6 m²/g after 400 days of curing at a laboratory scale. The former behaviour was attributed to the flocculation effect, while the latter to the formation of pozzolanic products (C-S-H and C-A-H). Considering this, it can be derived that the uneven distribution of SSA, as reported in Fig. 3-11(b-e), could be linked to the development of cementitious compounds in the different specimens sampled at varying depths throughout the lime-treated embankment. As the evolution of cementitious compounds leads to the formation of mesopores, the correlation between the range of mesopores generation and the evolution of SSA was evaluated by BJH.

Using BJH data, the percentage of cumulative pore volume present in the pore diameter range 25-250 Å was evaluated for specimens showing the maximum (T1-1 = 45 m²/g), the intermediate (T1-6 = 25

m^2/g), and the minimum (T3-7 = 11 m^2/g) SSA values. Fig. 3-14(a) presents the percentage of pore volume for specimens over the range of pore diameter 25-250 Å at 25 Å intervals. It was observed that T1-1 shows about 11 % and 30 % higher pore volume in the range of pore diameter 25-75 Å than T1-6 and T3-7, respectively. T1-6 shows about 19 % higher pore volume in the same pore range than T3-7. For the remaining range of pore diameter (75-250 Å), the pore volume was observed to increase for T3-7, while it decreased more for T1-1 than T1-6. This indicates that the specimen with maximum SSA shows the presence of more pores of pore diameter 25-75 Å and vice versa.

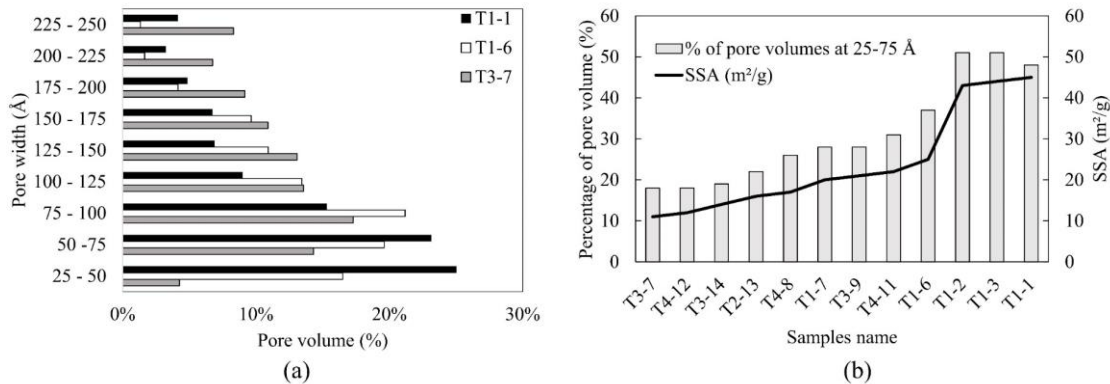


Fig. 3-14 Evolution of SSA with respect to the presence of pore volume in the mesopore range of pore diameter 25-75 Å.

Based on this observation, the SSA of a few selected lime-treated specimens was plotted with respect to the evolution of pore volume in the range of pore diameter 25-75 Å (Fig. 3-14(b)). An increase in the trend of pore volume was observed with the gradual rise in SSA. It can thus be derived that there exists an apparent correlation between the two quantities.

3.5 Conclusions.

The long-term effect of lime treatment on a silty soil embankment was evaluated in terms of mechanical, physicochemical, and microstructural properties after 7 years of atmospheric exposure in a wet climate. The evaluation was made by undergoing laboratory investigations using several specimens gathered in the upper layer as well as throughout the core of the embankment. Based on the investigations, the following conclusions are derived:

- 1) An average UCS level of 3.29 MPa was obtained from the in-situ cured lime-treated specimens. Comparison of this UCS level with the UCS obtained from the accelerated-cured sample (at 40°C after 90 days) at laboratory scale confirms that such UCS level can be expected from the in-situ cured specimens after 7 years of curing.
- 2) SEM images evidenced the presence of cementitious bonding formed because of pozzolanic reactions under the lime effect in the core-sampled specimens of the lime-treated embankment.
- 3) The lime effect persists throughout the core of the lime-treated embankment as the pH measurement was greater than 11 despite 7 years of curing in a region that receives significant rainfall throughout the year.

4) A maximum loss of 12 % and 18 % in the water content and pH, respectively, was observed in the upper layer-sampled specimens compared to the core-sampled specimens. This shows that the effect of lime was lost in the upper layer of the lime-treated embankment due to long-term exposure of the soil to the atmosphere and due to the development of vegetation roots.

5) The relevance of the combined MIP- and BJH-pore structure analysis is shown by their efficiency in representing the complete range of macropores and mesopores affected by lime-treatment. MIP highlights the reduction in macropores (10^4 - 10^5 Å) and an increase in the number of smaller pores (< 3000 Å) in the lime-treated soil when compared to the untreated soil. Simultaneously, BJH shows the formation of mesopores (50-500 Å) in the lime-treated specimens, which was missing in the untreated soil. BJH method happens to define the evolution of mesopores under the lime effect more precisely than MIP.

6) The formation of smaller pores enhances the evolution of suction in the lime-treated core-sampled soil when compared to the untreated soil. This has led to a lower reduction in the water content during this 7-year curing period, and the distribution of water content remains less affected by depth. Thus, lime treatment improves the long-term water retention capacity of the soil.

7) The formation of mesopores in lime-treated specimens was less affected by the depth of sampling in the lime-treated embankment. These mesopores contribute to the evolution of strength and SSA. An increase in mesopores results in increased strength, while the SSA was found to be correlated to the presence of mesopores in the range of pore diameter 25-75 Å.

Thus, the study presented in this chapter confirms the long-term persistence of the effect of lime within the core of a lime-treated silty soil embankment even after its exposure to a damp climate for 7 years. Based on the physicochemical and microstructural observations, a good and persistent mechanical performance was evidenced to be achieved at a lime content of 2.5 %.

Chapter 4

EFFECT OF KNEADING ACTION ON THE COMPRESSIVE STRENGTH AND MICROSTRUCTURE EVOLUTION OF LIME-TREATED SILTY SOIL (PROPOSAL 2).

Das, G., Razakamanantsoa, A., Herrier, G., & Deneele, D. (2021). Compressive strength and microstructure evolution of lime-treated silty soil subjected to kneading action. *Transportation Geotechnics*. <https://doi.org/10.1016/j.trgeo.2021.100568>

General

Chapter 1 highlights the importance of compaction conditions on the long-term performances of the lime-treated soil through laboratory investigations. Besides, the preceding chapter emphasized the fact that due to the conduction of controlled mixing and compaction conditions during the construction of the embankment, a uniform distribution of pH and water content has resulted throughout the core of the embankment which has led to a significant evolution in compressive strength. Thus, the long-term hydromechanical performance can be said to be associated with the compaction conditions implemented during the construction of such structures.

The studied embankment presented in Chapter 3 was compacted by a padfoot roller, which produces rolling and kneading action by the sheep foot present on the drum surface of the roller. The effect of roller compaction was detailed by Lekarp et al. (2000), and recently its implementation was shown in le Vern et al. (2020). However, the effect of kneading action has not been well investigated. Clegg (1964) urged the importance of implementing kneading compaction at a laboratory scale to produce realistic laboratory compacted fine-grained specimens by showing a similar generation of soil structure and residual interparticle stresses with the in-situ soil. Kouassi et al. (2000) confirmed that soil properties, including the dry density and elastic stiffness obtained under kneading effect at a laboratory scale, were close to those obtained in the in-situ compacted soil. Cuisinier et al. (2011) and Herrier et al. (2012) highlighted that the magnitude of k obtained from kneaded lime-treated silty soil was lower compared to the soil compacted statically.

However, apart from these studies, the effect of kneading compaction on mechanical behavior is less investigated. The consideration of compaction energy is not available in the previous studies, which is essential to analyze the soil mechanical behavior. Moreover, since compaction condition was shown to play an important role in the long-term evolution of lime-treated soil thus, the contribution of the kneading effect to the mechanical behavior must be evaluated.

In this context, the present chapter investigates how the kneading mechanism contributes to the mechanical performance and microstructural modifications of lime-treated soil at a laboratory scale. The first section of the study highlights the compressive strength of kneaded soil by comparing the same with soil compacted by a reference standard method (standard static compaction). The second section describes the contribution of kneading compaction at microstructure levels and its correlation with the strength evolution. Finally, comments are made regarding the relevancy attained in results between the laboratory-produced and field sampled specimens, both kneaded.

4.1 Materials.

MLD soil and quicklime, as reported in Chapter 2 was used in this study. Three different lime contents were used, lime content equal to LMO (=1%), 2.5%, and 4%. This is because soil treated at LMO was shown to have limited contributions towards the long-term performances of lime treated soil, as evident in Chapter 1.

4.1.1 Sample preparations.

Soil mixtures for both the kneading and static compaction were prepared at OMC (Table 2-4) and the wet of OMC, *i.e.*, at WMC ($= 1.1 \times \text{OMC}$) using different lime contents. The initial compaction characteristics of the soil mixture subjected to both types of compactions were kept constant.

Cylindrical specimens of dimensions having a length of 0.10m and a diameter of 0.05m, prepared by both kneading and static compactions were used in this study.

A total of 72 specimens, including duplicates for each soil configuration, were prepared for strength and microstructural investigations by both compaction methods (Table 4-1).

Table 4-1 Types and number of specimens prepared by static-and kneading-compactions.

Compaction modes	Curing conditions		Compaction moisture content	Lime contents	Number of specimens (including duplicates)	
	Curing time (days)	Curing temperature (°C)				
Static	28	20	OMC	1%, 2.5%, 4%	6	
			WMC		6	
	90	20	OMC	1%, 2.5%, 4%	6	
			WMC		6	
	180	40	OMC	1%, 2.5%, 4%	6	
			WMC		6	
	Kneading	28	20	OMC	1%, 2.5%, 4%	6
				WMC		6
90		20	OMC	1%, 2.5%, 4%	6	
			WMC		6	
180		40	OMC	1%, 2.5%, 4%	6	
			WMC		6	

Forty-eight of the total specimens were cured for 28- and 90-days at a laboratory temperature of about 20°C using desiccators. The remaining were cured for 180 days at 40°C, *i.e.*, under accelerated curing using a climatic chamber (Table 4-1). After curing, specimens prepared for microstructural analysis were freeze-dried and then stored in vacuum bags until further analysis.

The following nomenclature is used for specimen's identification: lime content (1/2.5/4)-Static compaction method/Kneading compaction method (S/K)-compaction moisture content (OMC/WMC)-curing time (28/90/180) days. For example, 1-K-OMC-28 means 1% lime-treated soil subjected to kneading compaction (K) at OMC and then cured for 28 days.

4.2 Laboratory tests.

After curing, specimens were subjected to UCS test.

Pore characterization was made by MIP test and BJH method on freeze-dried specimens. The motive behind operating both these methods was to investigate the influence of lime treatment on pore structure modifications more elaboratively, as confirmed in the study presented in Chapter 3.

Calcium distribution evolution considering the Ca-mapping was shown to be a useful approach to observe the distribution of lime in lime-treated soil by Lemaire et al. (2013). In this aspect, the μ -XRF images are recorded for lime-treated kneading and statically compacted specimens to assess the effect of compaction on the lime-dispersion.

The observed distribution of calcium was then quantitatively analyzed by using imaging software NIS-Elements Basic Research 3.1.

4.3 Results.

4.3.1 UCS of kneading compacted specimens.

Fig. 4-1 presents the trend of strength evolution in the lime-treated kneading compacted specimens subjected to different curing periods and temperatures. The presentation was made in terms of the average stress-strain obtained from duplicates of each soil configuration. The UCS value, representing the peak of the stress-strain curve, is presented in Table 4-2.

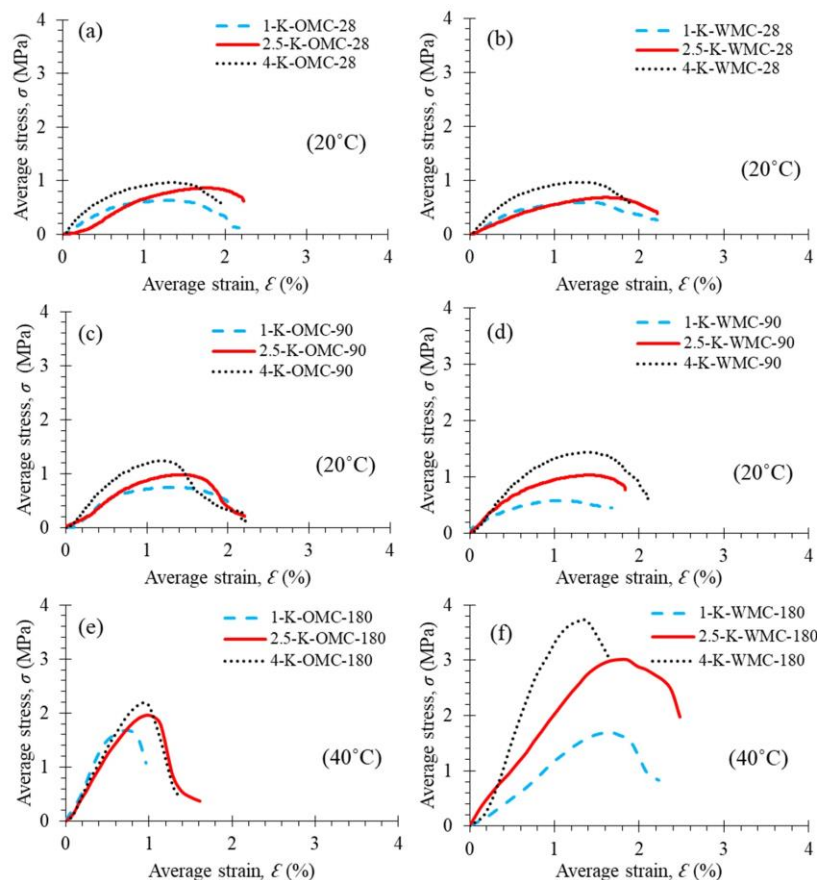


Fig. 4-1 Strength evolution of 1%, 2.5% and 4% lime-treated kneading compacted specimens at OMC-28 days (a), WMC-28 days (b), OMC-90 days (c), WMC-90 days (d), OMC-180 days (e), and WMC-180 days (f).

Table 4-2 UCS measured in lime-treated kneaded soil subjected to different curing time and temperatures.

Lime content (%)	Curing time (days)	Curing temperature (°C)	OMC-compacted specimens	WMC-compacted specimens
			UCS (MPa)	UCS (MPa)
1	28	20	0.60	0.60
	90	20	0.75	0.60
	180	40	1.70	1.70
2.5	28	20	0.86	0.70
	90	20	1.00	1.03
	180	40	1.95	3.00
4	28	20	0.96	1.20
	90	20	1.23	1.43
	180	40	2.20	3.70

The UCS of the lime-treated kneading compacted soil increased with the increase in lime content and curing time, as seen in Table 4-2 and Fig. 4-1. This increase in UCS was significantly higher for the accelerated cured specimens after 180 days of curing compared to the increase in UCS from 28 to 90 days of curing at 20°C.

Besides, the evolution of UCS was relatively higher in the WMC-compacted specimens than the corresponding OMC-compacted specimens treated with lime content higher than the LMO. The UCS measured was about 3% and 16% higher for 2.5% and 4% lime-treated specimens, respectively, for the 90-days cured WMC-compacted specimens (Fig. 4-1d). Similarly, the UCS was about 50% and 70% higher for the 2.5% and 4% lime-treated accelerated cured specimens, respectively, compacted at WMC (Fig. 4-1f).

4.3.2. Comparison of UCS evolution.

The UCS measured from the kneaded soil, were plotted against the respective values obtained from the standard statically compacted specimens in Fig. 4-2. Comparisons are made between specimens prepared at the same compaction water content, lime content and subjected to similar curing conditions.

According to Fig. 4-2a-d, almost an equivalent UCS level was observed for all the 1% lime-treated compacted specimens, subjected to 28- and 90-days of curing at 20°C. However, this UCS was about 30% higher in kneaded specimens subjected to accelerated curing (Fig. 4-2e & f).

For the 2.5% lime-treated OMC-compacted specimens, the UCS level was similar for the 28- and 90-days cured specimens (Fig. 4-2a & c) and increased by about 45% in the accelerated kneaded specimen (Fig. 4-2e). For the corresponding WMC-compacted specimens, this UCS level remains almost the same after 28 days of curing (Fig. 4-2b); increased slightly in the kneaded soil after 90 days of curing (Fig. 4-2d) and increased by about 50% for the accelerated kneaded specimen (Fig. 4-2f).

At 4% lime treatment, all the kneaded specimens show about 6-40% greater UCS values.

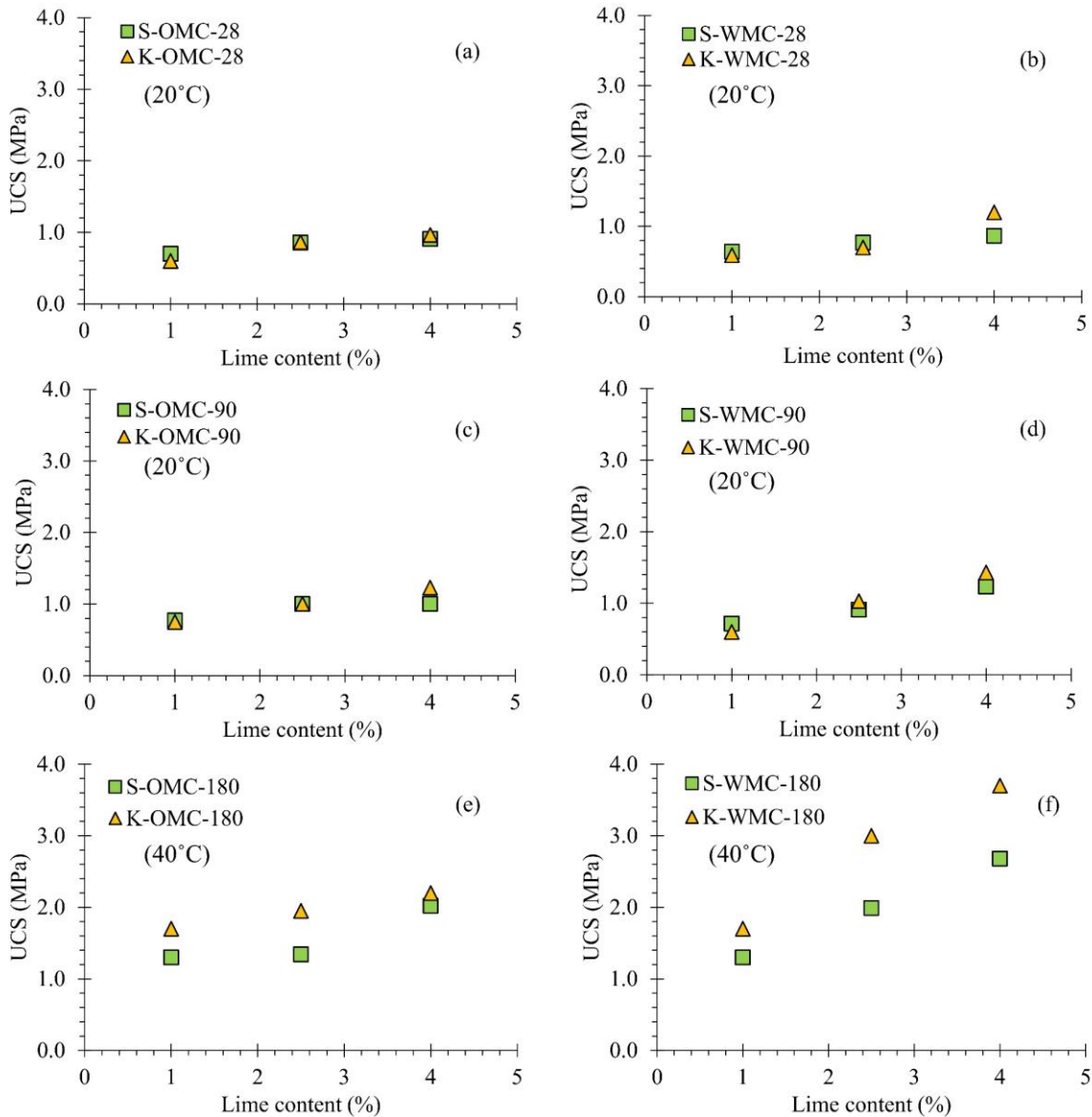


Fig. 4-2 UCS measured from 1%, 2.5% and 4% lime-treated specimens subjected to static and kneading compactions at OMC-28 days (a), WMC-28 days (b), OMC-90 days (c), WMC-90 days (d), OMC-180 days (e), and WMC-180 days (f).

4.3.3 Comparison of microstructural modifications.

4.3.3.1. Pore size distribution by MIP

Fig. 4-3 presents the pore size modification brought by lime treatment in the untreated statically compacted specimens by MIP analysis. As expected, a significant decrease in the pores present at 10^5 and 10^4 Å and evolution of pores lower than 3000 Å was brought on lime additions. Such evolution was also reported by Cuisinier et al. (2011). Besides, the evolution of pores lower than 3000 Å was enhanced with increased lime contents due to the increased formation of cementitious compounds (Cuisinier et al., 2011; Le Runigo et al., 2009, 2011).

The evolution of pore structures in the lime-treated soil compacted by kneading- and static-compactions at different lime contents were compared in Fig. 4-4. The comparison was presented in terms of PSD for the OMC- and WMC-compacted 28 days cured and WMC-compacted 90 days cured specimens.

A small number of macropores of pore diameter 10^5 Å were observed in all three different lime-treated kneaded specimens compacted at both OMC and WMC (Fig. 4-4a, b & e). On the other hand, for the statically compacted specimens, an increase in the intensity of macropores of pore diameter 10^5 Å was observed with the increased lime content (Fig. 4-4c, d & f).

Besides, almost a similar decrease in the presence of macropores of diameter 10^4 Å and increased intensity of pores of diameter lower than 3000 Å was observed in both types of compacted specimens, with increase lime content and curing time (Fig. 4-4a-f).

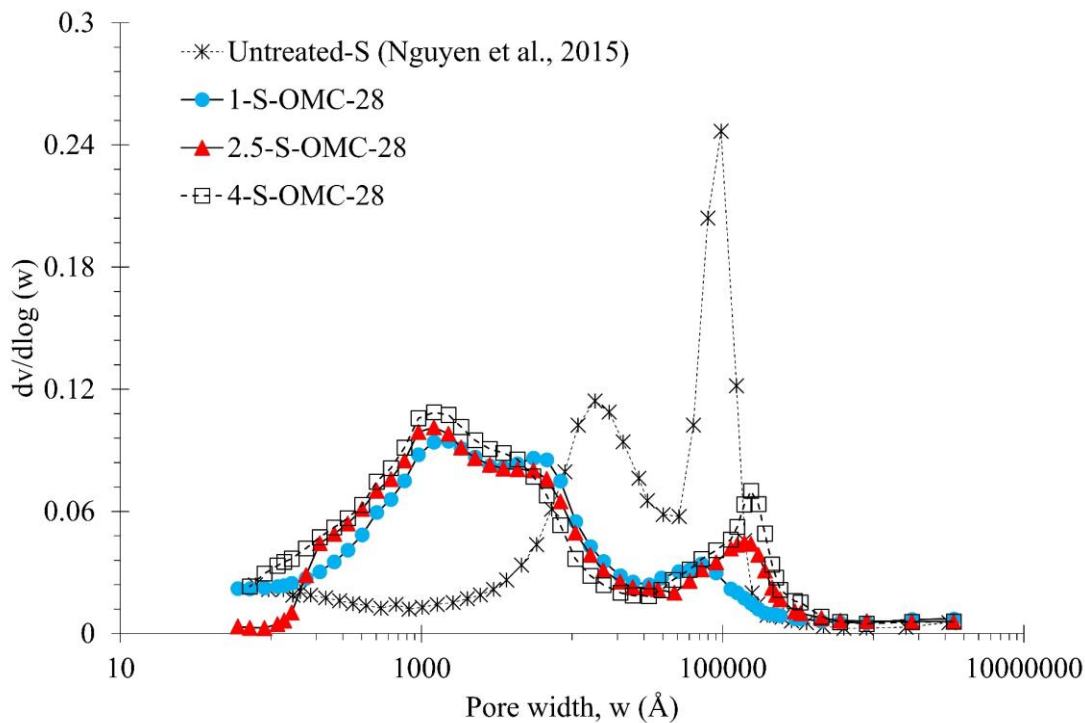


Fig. 4-3 Evolution of pore structure after addition of 1%, 2.5%, and 4% lime in the untreated statically compacted specimens at OMC and after 28 days of curing.

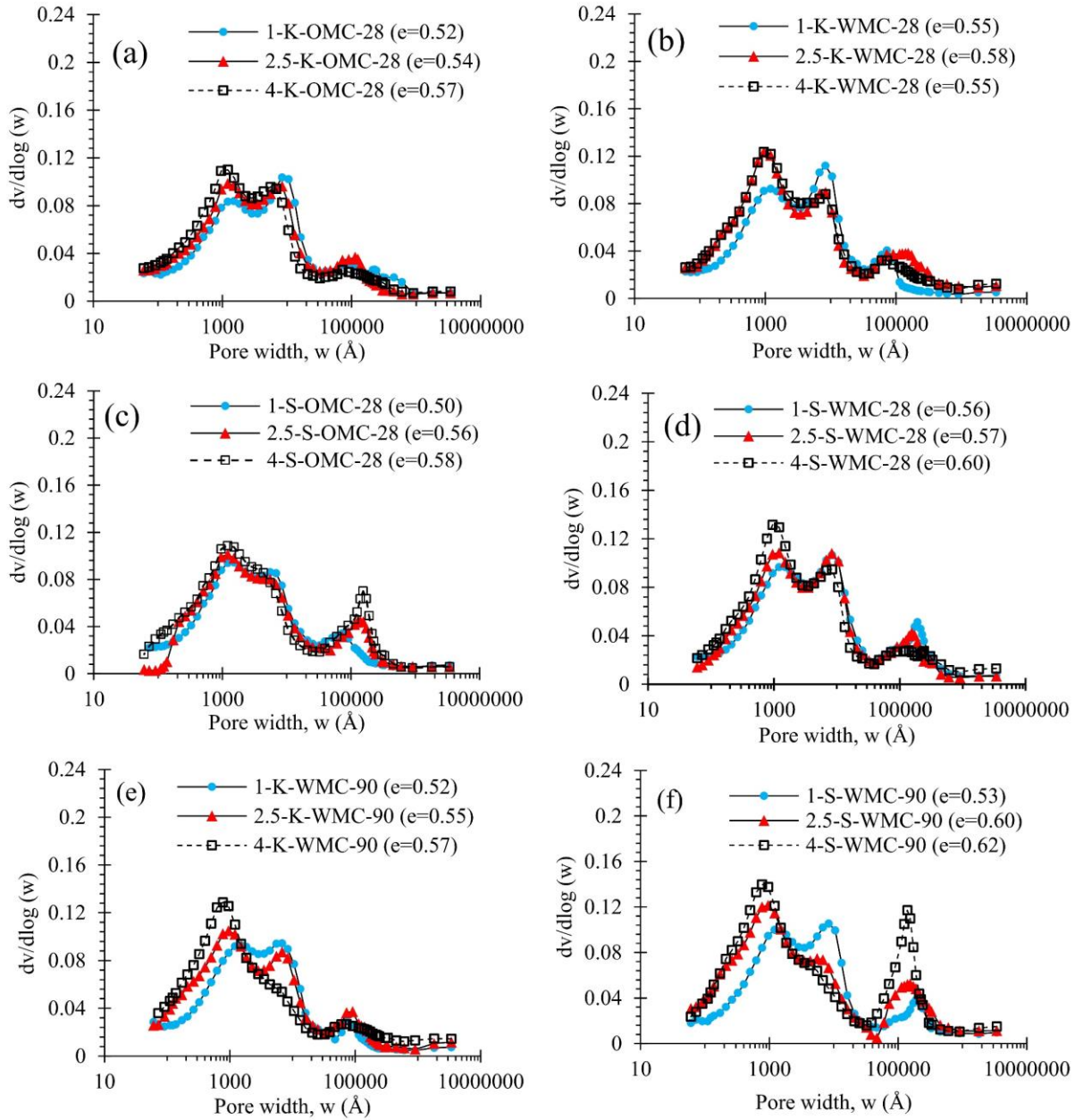


Fig. 4-4 Analysis of pore structure by MIP for 1%, 2.5% and 4% lime-treated specimens compacted by kneading and static compaction at OMC, and WMC and after 28 days (a-d) and 90 days (e, f) of curing at 20°C.

4.3.3.2. Pore size distribution by BJH.

Fig. 4-5 and Fig. 4-6 presents the pore structure analysis by the BJH method in terms of the generation of isotherms and cumulative pore volume evolutions, respectively, in the lime-treated kneading and statically compacted specimens.

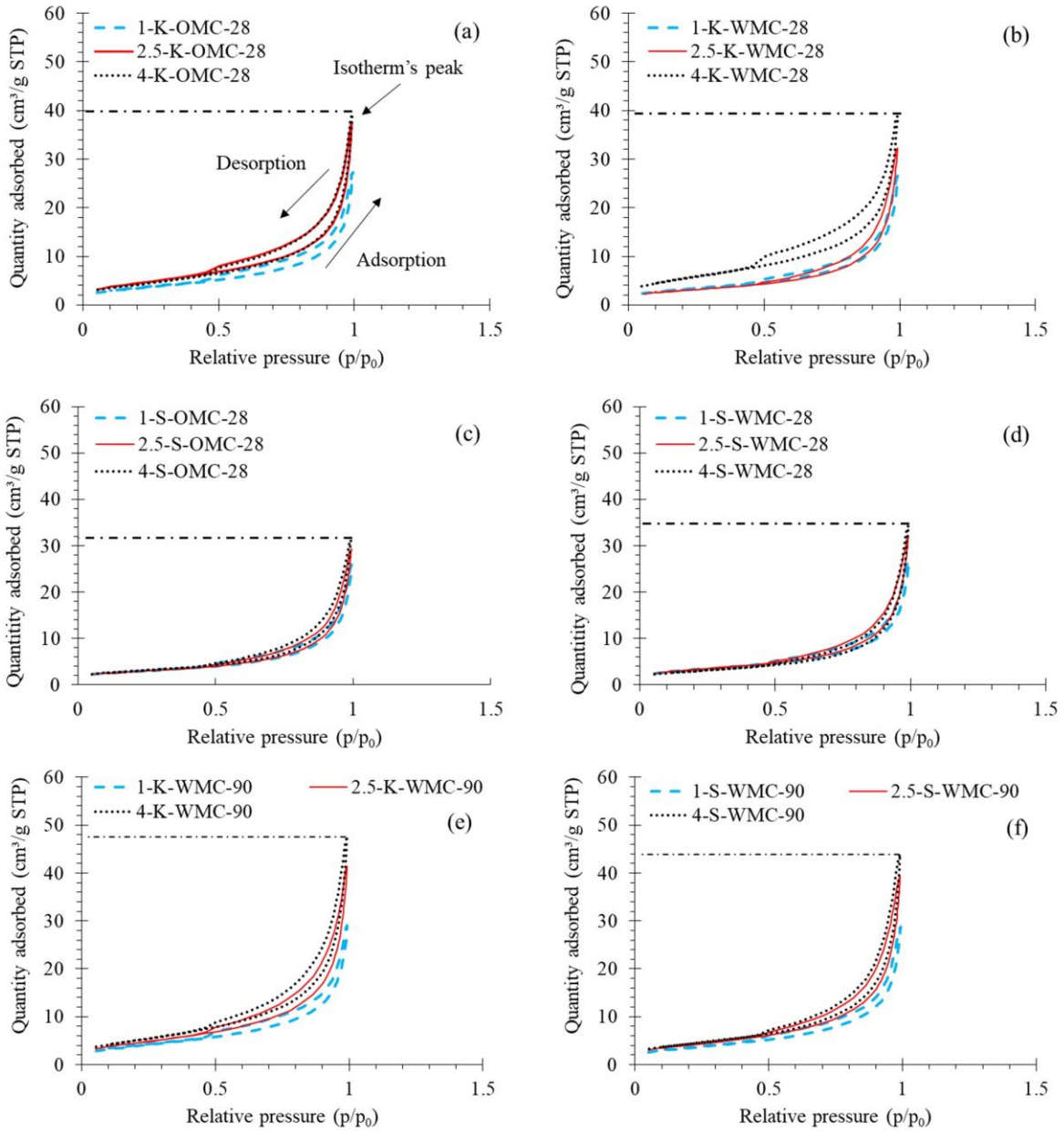


Fig. 4-5 Evolution of isotherms in 1%, 2.5%, and 4% lime-treated OMC, and WMC kneading and statically compacted specimens after 28 days (a-d) and 90 days (e, f) of curing at 20°C.

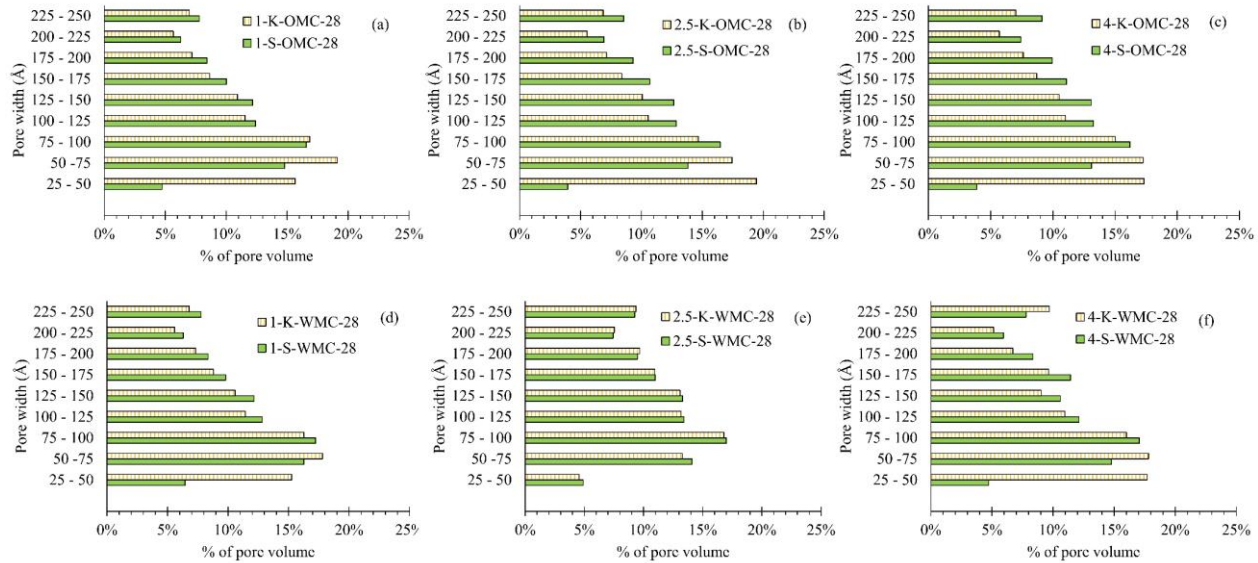


Fig. 4-6 Percentage of cumulative mesopores volume measured in 1%, 2.5%, and 4% lime-treated OMC, and WMC kneading and statically compacted specimens after 28 days (a-f) and 90 days (g-i) of curing at 20°C.

The peak of the isotherms, as seen in Fig. 4-5a, represents the total nitrogen adsorption capacity of the soil (Sotomayor et al., 2018). In the analysis made with the present soil, the PSD analyzed by the BJH method was found to be in the range of pore diameter of about 20-2000 Å. Thus, the higher is the peak of the isotherm, the greater is the presence of pores of diameter 20-2000 Å in the soil.

Fig. 4-5 shows that the peak of the isotherm rises with increased lime content. However, this rise was relatively more significant in the 4% lime-treated kneaded soil (Fig. 4-5a, b & e) than the corresponding rise in statically compacted soil (Fig. 4-5c, d & f).

The hysteresis developed in the isotherm was relatively distinctive in the 4% lime-treated 28 days cured kneaded soil (Fig. 4-5a & b). This hysteresis was demonstrated to be associated with the delay in capillary condensation and evaporation that occurs in the mesopores by McGregor et al. (2014) and Collet et al. (2008). Thus, an enhanced hysteresis indicates the presence of a greater volume of mesopores (Zielinski and Kettle, 2013).

The cumulative mesopore volume measured in the lime-treated compacted soil was in the range of mesopore diameter 25-250 Å. The variation of these mesopore volumes is presented in terms of the percentage of mesopore volume for a different interval of mesopore range (Fig. 4-6). It was observed that almost all the statically compacted soil exhibited a greater percentage of mesopore volume in the range of pore diameter of 100-250 Å. At the same time, the percentage of pore volume was relatively higher in the kneaded soil in the mesopore range of pore diameter lower than 100 Å, i.e., 25-75 Å.

4.3.3.3. μ -XRF images

Fig. 4-7 presents the distribution of calcium within the lime-treated soil matrix compacted at OMC and after 28 days of curing. The calcium distribution is represented by the blue region, while soil by the black region. The quantitative analysis of this calcium distribution is presented in Table 4-3.

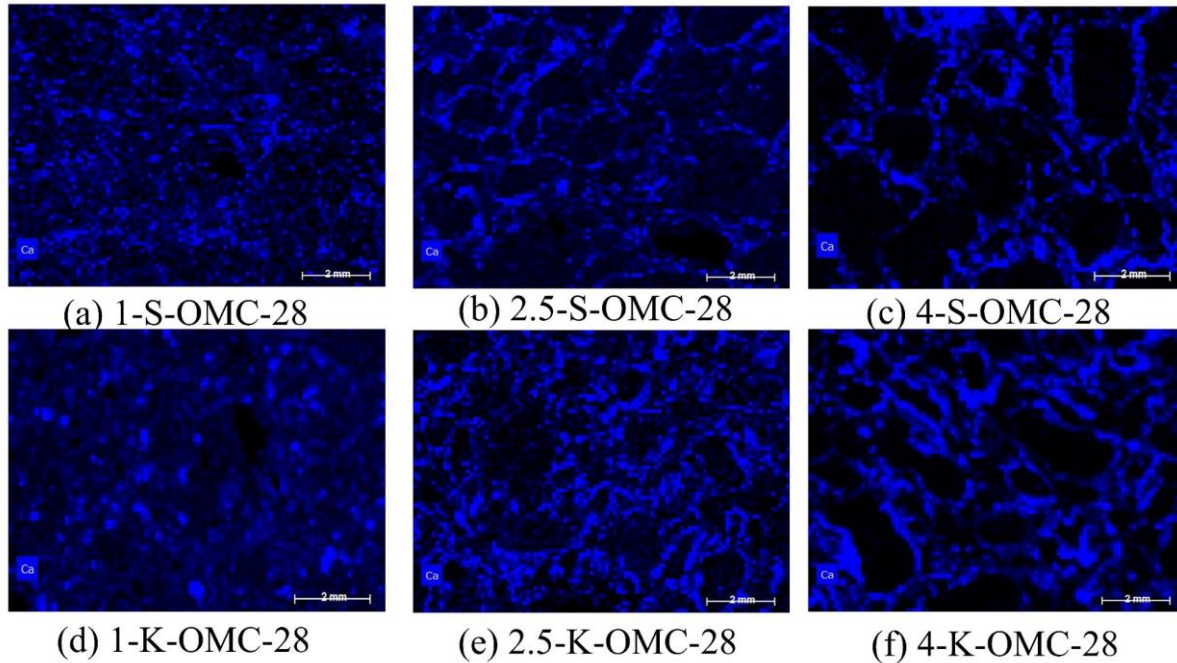


Fig. 4-7 μ -XRF image highlighting calcium distributions in 1%, 2.5%, and 4% lime-treated static (a, b, & c) and kneading compacted (d, e, & f) specimens prepared at OMC after 28 days of curing time at 20°C.

Table 4-3 Percentage distribution of Calcium (Ca) within the polished surface area of the kneading- and statically-compacted specimens.

		28 days cured specimens	
		Kneading compacted	Statically compacted
Lime%-W.C ¹	TSA ² ($\times 10^{-12}$) (m ²)	% of T.S.A covered by Ca	% of T.S.A covered by Ca
1-OMC	6.0	17.2	13.3
2.5-OMC	7.0	25.4	17.0
4-OMC	6.0	24.4	17.0

¹W.C: compaction moisture content

²T.S.A: Total Surface Area

Table 4-3 highlights that, for a constant surface area, the percentage of calcium distribution was about 4 to 8% higher in the lime-treated kneaded specimens than the corresponding statically compacted specimens.

4.4 Discussions.

As expected, kneading compacted soil showed a rise in UCS with increased curing time and lime content (Fig. 4-1). The significant UCS evolution for the accelerated cured specimens can be attributed to the acceleration of pozzolanic-reactions, as demonstrated by Lemaire et al. (2013) and Verbrugge et al. (2011) (Fig. 4-1e & f). At the same time, for soil treated with 2.5% and 4% lime, the UCS obtained was relatively higher for the WMC-compacted 90 days cured specimens when compared to the corresponding OMC-

compacted specimens (Fig. 4-1c & d). This increase in UCS was more significant for all the accelerated cured WMC-compacted specimens (Fig. 4-1e & f). Thus, kneaded soil, treated at lime content higher than LMO, cured for a longer time, and under accelerated condition, shows enhanced UCS in WMC-compacted specimens when compared to OMC-compacted specimens. However, the literature has shown that lime-treated soil compacted at WMC, which is much higher than the OMC and cured for a shorter period, resulted in lower UCS than OMC-compacted soil due to the loss in soil grain-to-grain contact with increased water content (Ajayi, 2012; Consoli et al., 2014; Le Runigo et al., 2011; Yin et al., 2018). In the present case, the soil treated at WMC is only 1.1 times higher than OMC and cured for a longer time and under accelerated conditions. Thus, the generation of enhanced UCS in the WMC-compacted specimens indicates an appropriate availability of water in the soil matrix, which might have regulated a steady consumption of water by quicklime for the formation of cementitious compounds with increased curing time and under accelerated conditions. Thus, compacting lime-treated soil at WMC slightly higher than OMC is beneficial for long-term evolution of UCS.

On comparing the dispersion of calcium measured from the polished surface area of the compacted specimens in Fig. 4-7, it was observed that this dispersion was enhanced under kneading compaction. The percentage of the polished area covered by calcium was about 8% higher in the 2.5%, and 4% lime-treated OMC kneaded specimens compared to the corresponding statically compacted specimens (Table 4-3). The observed calcium can either be the calcium from the available lime or the cementitious compounds developed because of pozzolanic-reactions. This provides evidence that kneading action enhances lime-dispersion. This feature of enhanced lime dispersion, accompanied by water availability, would contribute to the enhanced pozzolanic-reactions, particularly in the long-term. Thus, kneading compaction acts in favour of pozzolanic-reaction, which consequently leads to better development of cementitious compounds. This can be attributed to the relatively greater generation of mesopores of diameter 20-2000 Å as indicated by the enhanced isotherm peak, by the hysteresis developed (Fig. 4-5), and by the presence of a greater percentage of mesopore volume in the pore range 25-75 Å (Fig. 4-6). Increased development of cementitious compounds can increase the overall stiffness of the kneaded soil. This explains the relatively greater UCS obtained in all the 4% lime-treated kneaded soil (Fig. 4-2), in the 2.5% lime-treated 90 days cured kneaded soil, compacted at WMC (Fig. 4-2d), and in all the lime-treated accelerated cured kneaded soil (Fig. 4-2e & f).

Kneading effect was shown to bring more significant deformation in the natural soil aggregates compared to statically compacted specimens by Mitchell and McConnell (1965). Thus, upon kneading compaction of the lime-treated soil at OMC/WMC, a greater aggregate deformation accompanied by enhanced lime-dispersion occurred in comparison to the one that was statically compacted. Such a phenomenon lowered the availability of macropores of diameter 10^5 Å (Fig. 4-4a, b & e) and enhanced the mesopores evolutions (Fig. 4-5 & Fig. 4-6) in the kneaded soil. At the same time, macropores of diameter 10^5 Å increased with lime content in the statically compacted specimens (Fig. 4-4c, d & f), which was due to the formation of greater inter-aggregate pores at higher lime content, as reported by Tran et al. (2014) and Wang et al. (2017). The same specimens after curing and on being subjected to UCS showed failure due to consumption of water for cementitious compounds formation. However, owing to the above-mentioned differences produced in soil structure due to the difference in the effect of compactions, kneaded soil showed a higher ductile failure characteristic during UCS test, as evidenced by the differences in the crack development observed between the lime-treated kneading and statically compacted specimens in Fig. 4-8. The diagonal and vertical crack developed in the kneaded and statically compacted specimens (Fig. 4-8a & b) represents the shear and tensile crack, respectively, as reported by Kichou Z (2015).

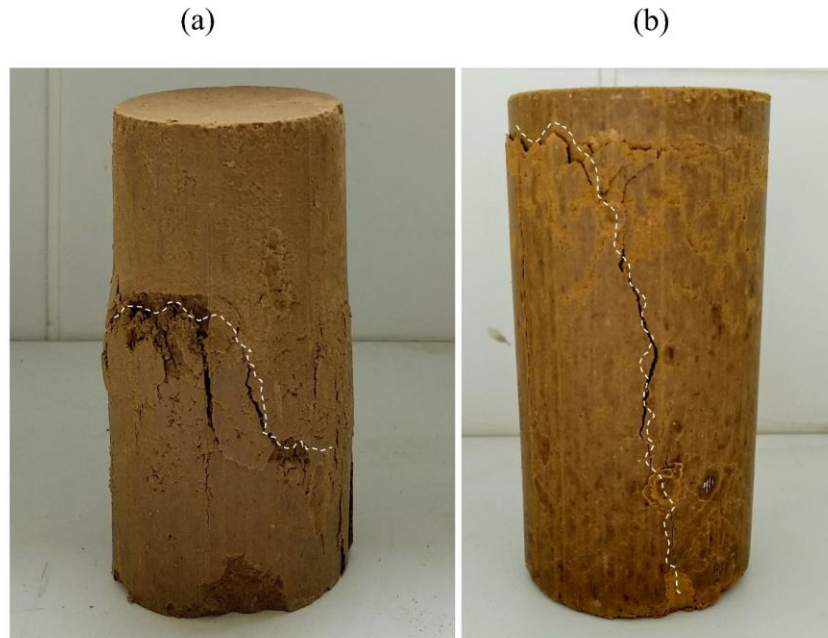


Fig. 4-8 Diagonal Crack in kneading compacted (a), and vertical crack in statically compacted (b) specimens after UCS test at 1% lime treatment, compacted at OMC and after 28 days curing.

Based on the initial findings, the difference in the effect of compaction on aggregates deformation and lime-dispersion in specimens subjected to kneading and static compaction is explained through the schematic diagram presented in Fig. 4-9.

The present 2.5% lime-treated and WMC-compacted silty soil was used in the construction of an embankment using a vibrating padfoot roller that produces kneading action during compaction (Consoli et al., 2014; Makki-Szymkiewicz et al., 2015). The process of construction was as per GTS Technical Guide for soil treatment (2000). After 7 years of atmospheric curing, the embankment was deconstructed, and the UCS of four core-sampled embankment's specimens, namely, T1-1 & T2-4 of length (l)/diameter(d) ratio of both 1 and 2 was evaluated, and the average UCS of these specimens was reported to be $3.29 (\pm 0.45)$ MPa (as presented in Chapter 3). The obtained in-situ UCS was also shown to be repeatable using the correction factor recommended by ASTM-C42-77 (ASTM 1978). The average UCS of in-situ extracted samples was shown to be comparable with a 90-day laboratory accelerated-cured specimen of similar configuration and of the dimension of $l/d=1$. The UCS obtained from in-situ and laboratory accelerated cured specimen that has been reported in Chapter 3 are compared with the trend of UCS obtained with the present accelerated kneaded soil in Fig. 4-10a & b.

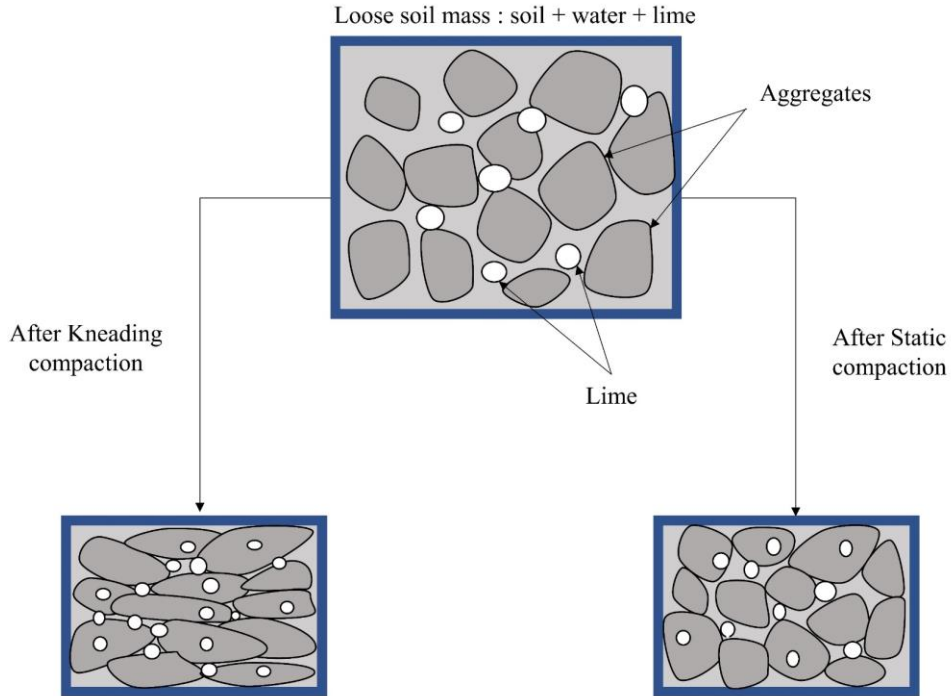


Fig. 4-9 Schematic diagram showing the difference in the effect of kneading and static compaction on aggregates deformation and lime-dispersion.

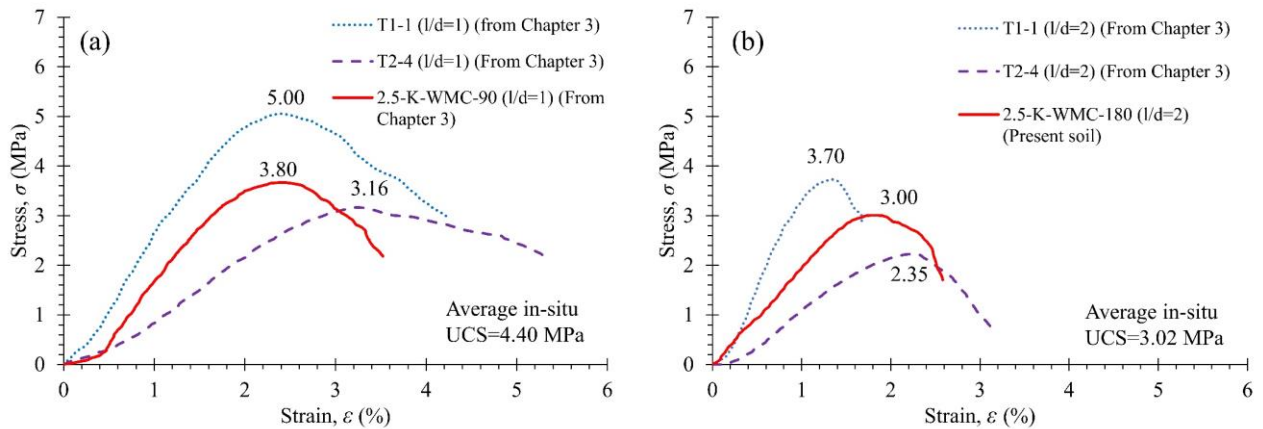


Fig. 4-10 Comparative evolution of UCS in in-situ core sampled and laboratory-accelerated cured soil of dimension of l/d ratio of 1 (a) and 2 (b).

Fig. 4-10a & b presents the comparative trend in UCS evolution in the in-situ and laboratory kneaded specimen of dimension $l/d=1$ and $l/d=2$, respectively. The average of the in-situ UCS values, if compared with the UCS of the corresponding 2.5% lime-treated accelerated cured laboratory kneaded soil, was found to be of a similar level for both dimensions. The difference in UCS observed between the laboratory 90- and 180-days accelerated cured kneaded specimens was due to the difference in dimension which is in accordance with ASTM-C42-77 (ASTM, 1978). Besides, Chapter 3 reported that the difference

in UCS of the two in-situ cured core-sampled specimens was linked with the intensities of mesopores evolution by BJH. The mesopore evolution of the present accelerated cured soil was compared with the one obtained from the in-situ cured core sampled kneaded specimens and are presented in Fig. 4-11.

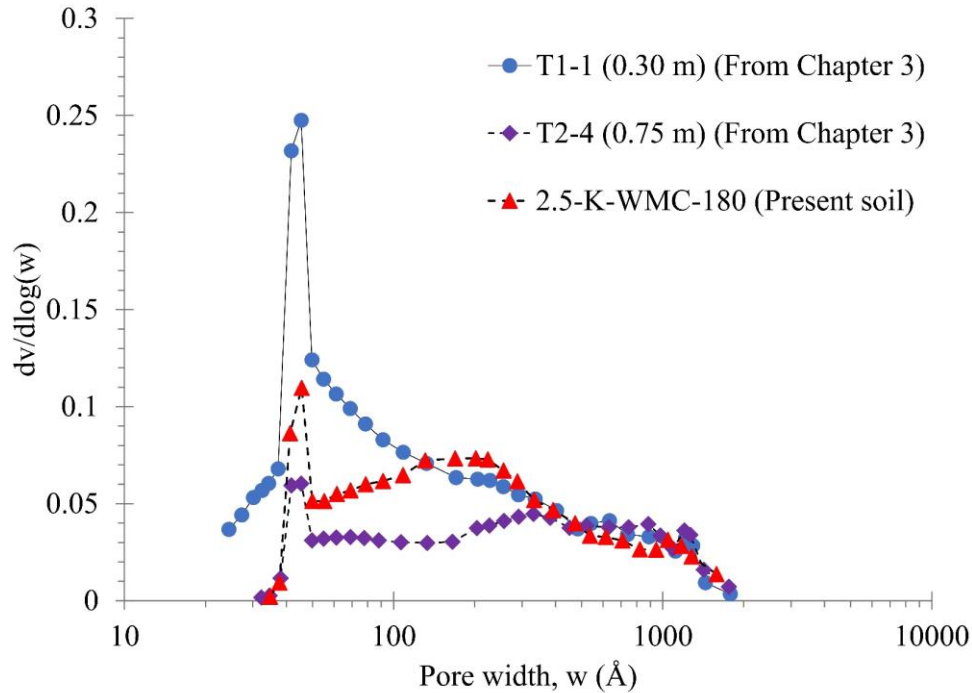


Fig. 4-11 Comparison of PSD obtained by BJH in 2.5% lime-treated kneaded specimens obtained between laboratory accelerated cured specimen and 7 years in-situ atmospherically cured specimens.

Fig. 4-11 shows that the present accelerated cured kneaded specimen exhibits intensities of mesopores greater than T2-4 and less than T1-1. Thus, the trend observed in the evolution of mesopores between the accelerated-cured and in-situ cured soil, both kneaded, corresponds well with the level of UCS measured. This confirms the fact that the soil cured under laboratory-accelerated condition and the soil sampled after 7 years of environmental exposure, both submitted to kneading action, exhibit a similar level of UCS. This shows evidence of the relevancy of the accelerated condition in the laboratory to access to the long-term UCS level similar to the sample submitted to field condition.

Additionally, Chapter 3 reported a uniform distribution of pH above 11 and water content throughout the lime-treated embankment after 7 years of atmospheric curing. This evolution was due to the controlled mixing and compaction condition conducted during the construction of the embankment by Makki-Szymkiewicz et al. (2015) and Charles et al. (2012), which again involves the kneading action due to the use of padfoot rollers. Considering the enhanced dispersive action created by kneading compaction in Fig. 4-7, a uniform evolution of lime and lime components might have resulted throughout the embankment, thus giving all pH values of the sampled specimens above 11 and a homogeneous water content.

Fig. 4-3 & Fig. 4-4 showed that lime treatment has led to the generation of pores lower than the pore diameter of 3000 Å, and such generation was shown to increase soil cohesion and enhance UCS by Verbrugge et al. (2011). However, pores diameter lower than 3000 Å includes a part of macropores, total

mesopores, and micropores as per IUPAC (1994). In the present soil, BJH measured the evolution of pores under the lime effect in the range 20-2000 Å (Fig. 4-5), which includes macropores and mesopores, and the cumulative pore volume in the range 25-250 Å that includes only mesopores (Fig. 4-6). Hence, to identify the contribution of different classes of pores to the UCS evolution, a regression equation was developed.

The proposed equation (Equation 4-1) considers compacted specimens cured at 20°C. The input data of the proposed equation involves the isotherm peak which indicates the total volume of nitrogen injected in pores of diameter 20-2000 Å, and the cumulative pore volume measured in the mesopore range 25-250 Å. The input data is provided in Table 4-4.

$$\text{UCS} = -0.034 + 0.015 \times (\text{pores of diameter 20-2000 Å}) + 27.7 \times (\text{mesopores of diameter 25-250 Å})$$

(Equation 4-1)

Table 4-4 Isotherm peak and cumulative pore volume measured in lime-treated soil.

Samples name	Isotherm peak (cm ³ /g)	^I V _{cum} in pore range (25-250 Å) (cm ³ /g)	UCS (MPa)	Samples name	Isotherm peak (cm ³ /g)	V _{cum} in pore range (25-250 Å) (cm ³ /g)	UCS (MPa)
1-K-OMC-28	27.3	0.008	0.60	1-S-OMC-28	26.0	0.011	0.70
2.5-K-OMC-28	37.6	0.015	0.86	2.5-S-OMC-28	29.3	0.013	0.86
4-K-OMC-28	39.3	0.018	1.00	4-S-OMC-28	31.3	0.014	0.90
1-K-WMC-28	26.6	0.010	0.60	1-S-WMC-28	27.0	0.010	0.64
2.5-K-WMC-28	32.2	0.012	0.68	2.5-S-WMC-28	32.0	0.012	0.77
4-K-WMC-28	38.9	0.014	0.96	4-S-WMC-28	34.4	0.012	0.87
1-K-OMC-90	31.4	0.011	0.75	1-S-OMC-90	28.8	0.010	0.77
2.5-K-OMC-90	39.3	0.015	0.98	2.5-S-OMC-90	42.5	0.016	1.00
4-K-OMC-90	46.8	0.020	1.23	4-S-OMC-90	43.0	0.019	1.00
1-K-WMC-90	29.0	0.009	0.60	1-S-WMC-90	28.8	0.011	0.72
2.5-K-WMC-90	41.4	0.017	1.03	2.5-S-WMC-90	39.3	0.016	0.91
4-K-WMC-90	47.7	0.020	1.43	4-S-WMC-90	43.8	0.018	1.23

Equation 4-1 demonstrates accurately ($R^2 = 0.90$) that the mesopore range 25-250 Å makes the maximum contribution to the rise in UCS in the range of pores lower than 2000 Å developed under the lime effect. This indicates how lime treatment brings greater development of mesopores due to the cementitious bonding formed because of pozzolanic-reactions and how this contributes towards the strength evolution.

4.5 Conclusions

The effect of the kneading mechanism on the UCS evolution and microstructural properties of lime-treated silty soil was investigated. Based on the studies, the following findings are derived:

1. Lime-treated kneaded soil, particularly compacted at WMC, prepared at lime content higher than LMO and subjected to longer and accelerated curing, showed enhanced evolution of UCS. With appropriate

availability of water in the soil matrix, a steady consumption of water by quicklime was regulated for the formation of cementitious bonding with increased curing time and under accelerated conditions.

2. The kneading action caused relatively greater deformation of large aggregates and decreased the macropores of diameter 10^5 \AA , compared to the corresponding statically compacted soil.

3. Kneading compaction enhanced better dispersion of lime during compaction. When accompanied by the available water, such configuration works in favour of long-term pozzolanic-reactions. This resulted in up to about 50% greater UCS in the kneaded soil than the statically compacted soil prepared at lime content greater than LMO, compacted at WMC, and subjected to longer and accelerated curing.

4. The UCS obtained from the laboratory accelerated kneaded soil was of a similar level as the average UCS obtained from in-situ specimens sampled from the 7-year atmospherically cured embankment. The mesopores generation showed a positive trend with respect to the evolution of UCS between the laboratory-accelerated cured, and in-situ cured sampled soil.

5. Increased lime content and curing time resulted in increased isotherm peak, which indicated the greater generation of pores in the range of pore diameter 20-2000 \AA . Among the pore ranges produced under the lime effect, the contribution of mesopores in the pore range 25-250 \AA towards the evolution of UCS was shown to be most significant, as highlighted by a regression equation relating UCS with pore size.

Thus, the above findings are part of a holistic investigation into the mechanical behaviour and microstructural modification of lime-treated silty soil subjected to kneading action. The kneading action caused compressive strength gain, particularly in the long-term and for WMC-compacted soil. These results were evidenced by UCS, and microstructure evaluated from 7 years in-situ cured core-sampled soil. Further studies are required to be conducted to understand the hydraulic characteristics of lime-treated soil subjected to the kneading effect. These studies are presented in the following Chapter 5.

Chapter 5

INFLUENCE OF PORE FLUID-SOIL STRUCTURE INTERACTIONS ON COMPACTED LIME-TREATED SILTY SOIL (PROPOSAL 3).

Das, G., Razakamanantsoa, A., Herrier, G., & Deneele, D., 2021. Influence of pore fluid-soil structure interactions on compacted lime-treated silty soil. *Engineering Geology*. <https://doi.org/10.1016/j.enggeo.2021.106496>.

General.

Chapter 4 evidences the importance of the kneading mechanism towards the long-term strength evolution of lime-treated soil. Such an observation makes it essential to assess the influence of the kneading mechanism on the hydraulic conductivity evolution of lime-treated soil as well, since the durability of an earth structure is governed by the hydromechanical performances. Besides, compaction conditions were shown to bring major changes on the magnitude of the hydraulic conductivity of lime-treated soil in Chapter 1.

In addition to the availability of limited investigations regarding the kneading effect on hydraulic conductivity of lime-treated soil, the effect of the chemistry of pore water solution during its percolation through lime-treated compacted soil also remained less investigated. Since lime-treated soil is susceptible to increase leaching, which can decrease or slow down the improvement brought by lime treatment as reported in Chapter 1, hence, the leaching mechanism of lime-treated soil should be evaluated by considering the chemistry of the porewater to which the selected soil is subjected. The effect of the chemistry of pore fluid such as leachates on the hydraulic behavior of natural clay in the context of liner material used in underground nuclear disposal repository was widely investigated. Several studies have shown how the aggressive effect of leachates induces cracks in clay-liner and causes an increased hydraulic conductivity during the soil-leachate interactions (He et al., 2015; Sunil et al., 2008; Vaverková et al., 2020). Currently, demineralized water (DW) is used as a conventional permeant solution in most of the existing studies to investigate the hydraulic and leaching behaviors of lime-treated soil, whereas in the field, water from natural sources influences such behaviors. Thus, it is essential to consider the interactions of pore solution chemistry with the lime-treated soil while investigating the soil hydromechanical evolution.

In this context, the present chapter investigates the influence of compaction modes and pore solution chemistry on the hydromechanical performances of lime-treated silty soil. The compaction modes involved static and kneading compactions, and DW and a low ionic strength solution were used as pore solutions. The investigation includes evaluating the hydraulic conductivity and mechanical performances based on the leaching mechanism and microstructural modifications.

5.1 Materials.

MLD soil and quicklime, as reported in Chapter 2 was used in this study. Three different lime contents were used, lime content equal to LMO (=1%), 2.5%, and 4%. Two permeant solutions were chosen demineralized water (DW), and DW+10⁻³M NaCl. 10⁻³M NaCl has been used previously by Razakamanantsoa et al. (2012) and Sato et al. (2017) as a reference fluid to highlight the negative effect of leachates on Bentonites in the

context of landfill. The pH and Electric Conductivity (EC) of the DW and DW+10⁻³ M NaCl, latter regarded as Low-mineralized Water (LW) is presented in Table 5-1.

Table 5-1 The pH and Electric Conductivity of solutions.

Permeant solutions	pH	Electric Conductivity ($\mu\text{S}/\text{cm}$)
DW	7.4	4.0
LW	6.5	172.0

5.1.1 Sample preparations.

Cylindrical specimens of dimensions 0.05 m in height and 0.05 m diameter were prepared by Static (S) and Kneading (K) compaction methods at OMC and maximum dry density as mentioned in Table 2-4.

A total of 18 specimens was prepared, 9 specimens corresponding to each compaction method. After compaction, specimens were wrapped in plastic film and cured for 28-days at a laboratory temperature of 20 ± 1 °C.

5.2 Laboratory tests.

5.2.1 Hydraulic conductivity test.

At the end of curing time, specimens were subjected to a hydraulic conductivity test using a flexible wall permeameter by a constant hydraulic head. Details regarding the operation of the permeability setup are provided in section 2.2.6 of Chapter 2.

A total of 12 setups for hydraulic conductivity tests were designed, of which 6 setups consist of specimens submitted to DW, and the remaining were submitted to LW.

5.2.1.1. Hydraulic conductivity test protocol.

During the hydraulic conductivity test, a confining pressure of 88 ± 2 kPa was applied for at least 24-48 hours before the application of hydraulic head pressure to ensure the homogeneity of the stress distribution. The hydraulic head applied was 170 ± 5 cm. Thus, the applied confining stress was about 5 times higher than the hydraulic head pressure. This was done (i) to maintain the structure of the compacted specimen against any microstructure change due to the hydraulic head, and (ii) to avoid any preferential flow between the soil and the membrane (Ranaivomanana et al., 2017).

The hydraulic conductivity test was carried out in two phases: saturation and percolation. The saturation phase involves the wetting of specimens until full saturation, and the percolation phase involves the renewal of the entire porewater in the specimens. During the saturation phase, the outlet of the permeability setup was kept closed until a volume of influents corresponding to 1 Pore Volume Flow (PVF) of each specimen enter the specimens. One PVF is defined as the volume of pore water required to fill and renew the total volume of pore water and void initially present in the soil once (Katsumi et al., 2008). This level of PVF was selected to ensure about 90-95% saturation of the specimens before initiating the percolation phase. Mathematically, 1 PVF is the product of the volume of soil solids, V_s , and the void ratio, e of a given specimen. Then the accumulated volume of flow passing through the soil is denoted in terms of PVF by dividing the total flow by the volume corresponding to 1 PVF.

The concept of PVF was proposed to consider the duration of contact between the permeant solution and the lime-treated soil. Longer contact between soil and the permeant solution might be favorable to the development of dissolution or precipitation mechanism inside the soil structure. Thus, the PVF can be called an important index to assess the durability of the lime treatment. PVF was less often used for hydraulic performance studies related to lime-treated soil. However, it was widely implemented in the literature related to the hydraulic performance of Bentonite used in waste storage management (Katsumi et al., 2008; Shackelford et al., 2000).

The hydraulic conductivity measurements were stopped in accordance with the following termination criteria: (i) after 40 PVF was reached; and (ii) the last 5 values of EC measured during percolation became almost stable.

5.2.1.2 Calcium analysis.

During the percolation phase, effluents were collected at different PVF. The effluents were then subjected to Inductively Coupled Plasma Optical Emission Spectrometry (ICP-OES) analysis for determining the elementary concentrations of Calcium (Ca). The analysis of Ca concentration was made to investigate the difference in the concentration of Ca leached from the lime-treated soil under the influence of DW and LW.

5.2.2 Unconfined compressive strength (UCS) test.

Specimens after 28 days of curing and at the end of the percolation phase were subjected to compressive strength analysis.

5.2.3 Pore structure determination.

Soil specimens sampled from 28 days cured soil and from specimens at the end of hydraulic conductivity test were freeze-dried and then subjected to Mercury Intrusion Porosimetry (MIP) test.

In this study, pore classifications were made as per the International Union of Pure and Applied Chemistry (IUPAC) (Rouquerol et al., 1994).

Following nomenclature is used for specimen's identification: type of specimen (untreated, 1%/2.5%/4% lime-treated)-compaction mode (S/K)-type of permeant solutions (DW/LW). For example, 1%-S-DW represents 1% lime-treated statically compacted soil submitted to DW percolation.

5.3 Results.

5.3.1 Comparative evaluation of UCS in the lime-treated unleached and leached soil.

The UCS obtained from the lime-treated 28 days cured specimens (unleached) were compared with the UCS obtained from the lime-treated leached soil at the end of the hydraulic conductivity test (Fig. 5-1).

Fig. 5-1a show that 1% lime-treated statically compacted specimens lost about 60% of the initial UCS on being leached by DW and LW. On the other hand, no significant change in the UCS was observed in the 2.5% lime-treated leached specimens. However, the UCS increased by about 57% for the 4% lime-treated leached specimens.

The UCS of 1% lime-treated kneaded specimens leached by DW decreased by about 60% (Fig. 5-1b). The UCS measurement of the corresponding LW submitted soil was not possible as the specimen broke at the end of the hydraulic conductivity test. About 40% of the initial UCS was lost in the 2.5% lime-

treated DW leached kneaded specimen, whereas this decrease in UCS was about 20% in the corresponding LW leached specimen. The UCS for 4% lime-treated leached specimens increased by about 36%.

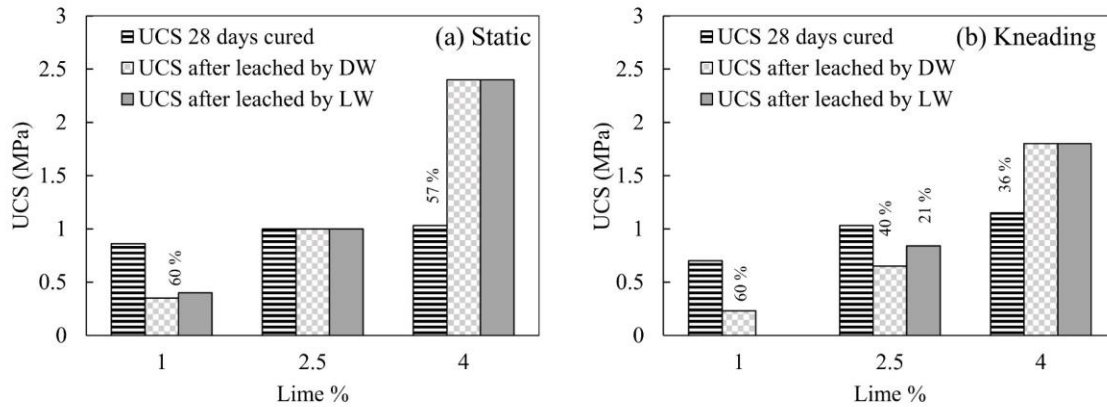


Fig. 5-1 Comparative evolution in UCS obtained in the 28 days cured and leached statically (a) and Kneading (b) compacted specimens.

5.3.2 Comparative evolution of Pore size distribution.

5.3.2.1 In 28-days cured lime-treated specimens.

The Pore Size Distribution (PSD) of the statically and kneading compacted lime-treated 28-days cured specimens is summarized in Fig. 5-2.

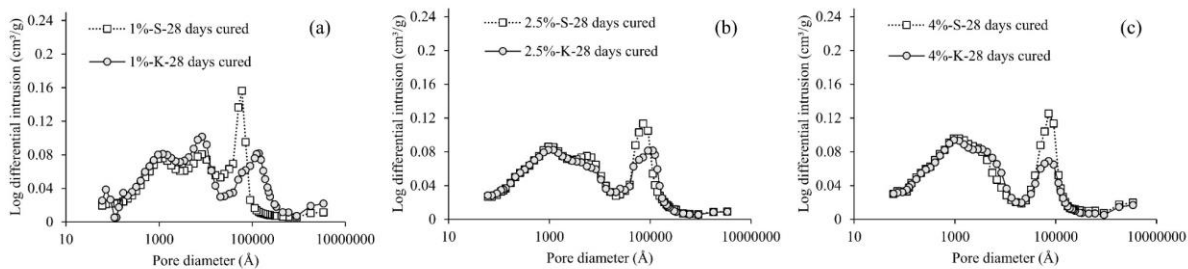


Fig. 5-2 Comparative evolution of PSD in the 1% (a), 2.5% (b), and 4% (c) lime-treated statically and Kneading compacted 28-days cured specimens.

In Fig. 5-2, three different peaks were observed at pore diameter 10^3 , 10^4 , and 10^5 Å. The total pores of diameter 10^3 Å were minimum in 1% lime-treated soil (Fig. 5-2a), slightly higher in 2.5% lime-treated soil (Fig. 5-2b), and maximum in 4% lime-treated soil (Fig. 5-2c). At the same time, pores of diameter 10^4 Å were minimum in 4% lime-treated soil and maximum in 1% lime-treated soil. This difference in the evolution of pores is attributed to the lime content used. At higher lime content, the evolution of cementitious compounds was enhanced (Lemaire et al., 2013; Little, 1987; Verbrugge et al., 2011), and hence more pores

of diameter 10^3 \AA were developed. The trend of pore evolution of diameters 10^3 and 10^4 \AA remained at a similar level in both types of compacted soil.

However, the presence of the macropores of diameter 10^5 \AA was comparatively significant in all the statically compacted specimens than the corresponding kneaded soil.

5.3.2.2. In unleached and leached lime-treated specimens.

At the end of the hydraulic conductivity test, the evolution of PSD in the two types of compacted soil after being leached by DW and LW was compared with the unleached specimens in Fig. 5-3.

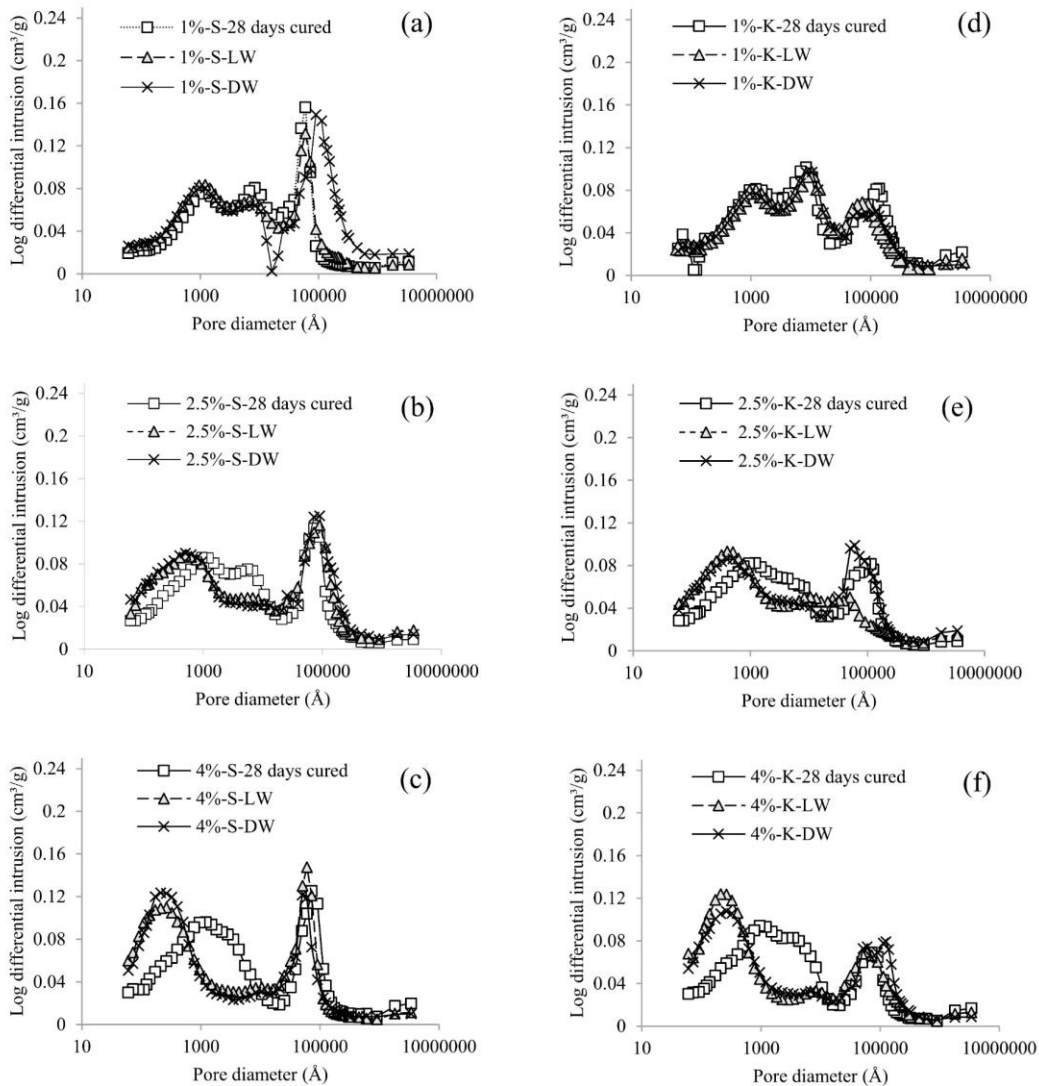


Fig. 5-3 Comparative evolution of PSD between 1%, 2.5%, and 4% lime-treated unleached and leached statically compacted (a-c) and kneading compacted specimens (d-f).

A decrease in the pores of diameter 10^4 \AA and generation of pores of diameter lower than 10^3 \AA in the 2.5% and 4% lime-treated leached specimens was observed compared to the unleached specimens (Fig. 5-3b, c, e & f). This generation of pores lower than 10^3 \AA was relatively significant in the 4% lime-treated soil.

However, the macropores of diameter 10^5 \AA increased in the 1% lime-treated statically compacted specimen after being leached by DW (Fig. 5-3a). At the same time, no significant change occurred in the corresponding LW leached specimen compared to the unleached specimen. In the 2.5% and 4% lime-treated soil, the evolution of macropores of diameter 10^5 \AA remained constant after being leached by both DW and LW (Fig. 5-3b & c).

In the kneaded specimens, a constant evolution of the macropores of diameter 10^5 \AA was observed in the leached and unleached 1% lime-treated specimens (Fig. 5-3d). On the other hand, 2.5% lime-treated specimens showed an increase in the macropores of diameter 10^5 \AA after being leached by DW. Whereas in the corresponding LW submitted specimen, the macropores of diameter 10^5 \AA decreased than the unleached soil (Fig. 5-3e). In the 4% lime-treated soil, macropores of diameter 10^5 \AA increased slightly in the DW leached specimen, while this macropore feature remained almost constant in the corresponding LW leached specimen (Fig. 5-3f).

5.3.3 Hydraulic conductivity measurements in untreated and lime-treated soil.

The analysis of the hydraulic conductivity was conducted after verifying the level of saturation in the lime-treated soil after 28 days of curing and at the end of the hydraulic conductivity test, *i.e.*, after the renewal of 40 PVF. The measured degree of saturation, S_r is summarized in Table 5-2.

Table 5-2 S_r measured in the lime-treated soil at the end of curing time and at the end of hydraulic test.

	S_r (%) of statically compacted soil			S_r (%) of kneaded soil		
	1% lime-treated	2.5% lime-treated	4% lime-treated	1% lime-treated	2.5% lime-treated	4% lime-treated
After 28 days of curing	74.6	78.5	74.4	74.4	69.3	71.7
After 40 PVF was renewed in DW submitted soil	98.2	100	99.8	100	90.2	98.8
After 40 PVF was renewed in LW submitted soil	100	99.4	100	–	100	98.8

The S_r of all the lime-treated leached specimens was greater than 90%, which indicates that the hydraulic conductivity measurement was conducted in saturated specimens. It is worth noting that in-situ lime-treated soil may rarely reach a similar saturation level as the one obtained herein (Table 5-2) before the percolation happens.

The evolution in the k of the lime-treated and the untreated soil is presented in Fig. 5-4 with respect to the PVF measured during the hydraulic conductivity test.

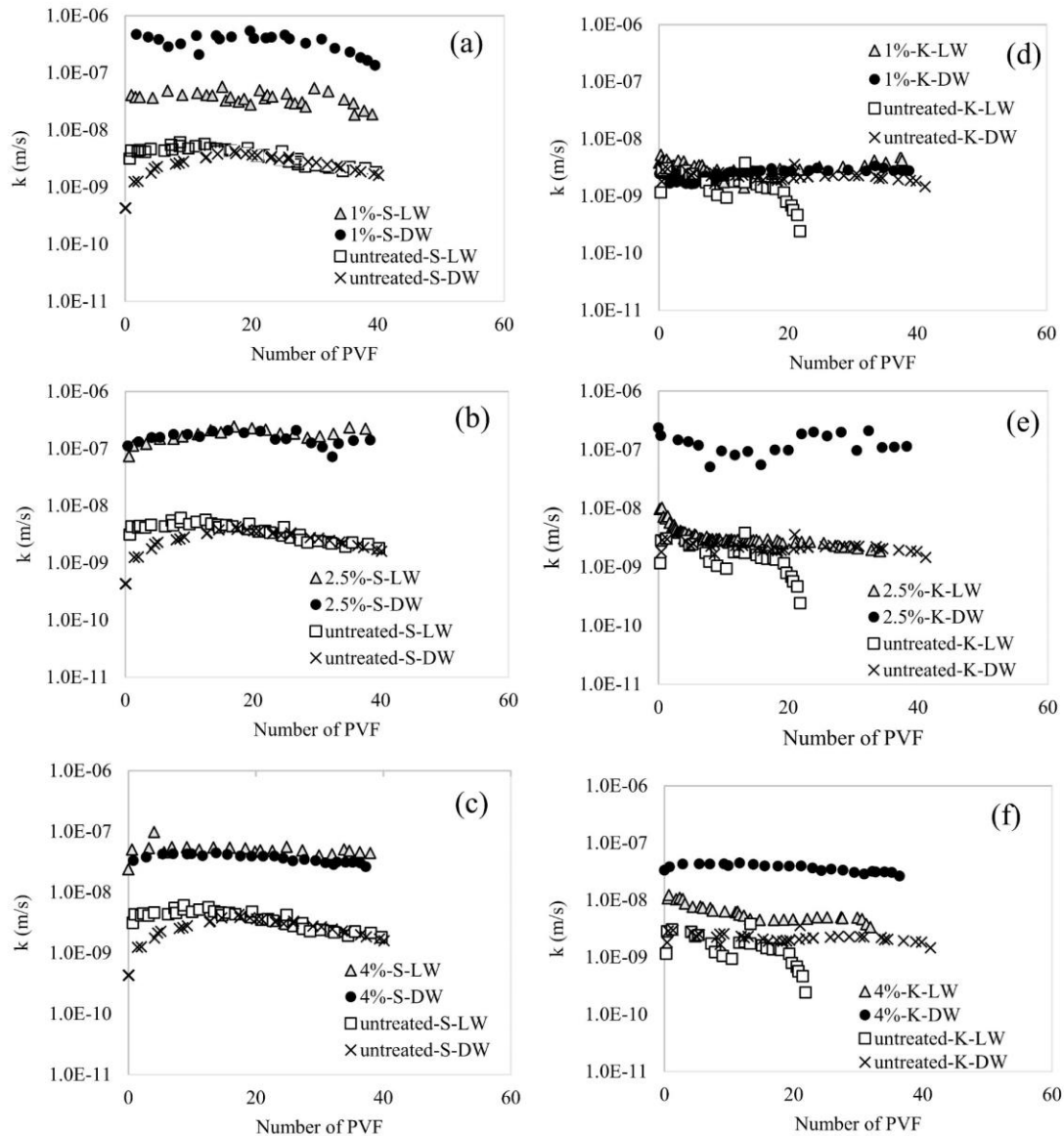


Fig. 5-4 Evolution in hydraulic conductivity of untreated and 1%, 2.5%, and 4% lime-treated DW and LW submitted statically (a-c), and kneading (d-f) compacted specimens.

Table 5-3 Duration of percolation phase in the lime-treated soil to renew 40 PVF of solutions.

	Duration taken by statically compacted soil (days)				Duration taken by kneaded soil (days)			
	untreated	1% lime-treated	2.5% lime-treated	4% lime-treated	untreated	1% lime-treated	2.5% lime-treated	4% lime-treated
DW submitted soil	77	0.7	1.5	5	87	70	4	6
LW submitted soil	55	6	1.5	5	93	65	75	40

The duration taken by each specimen of the present dimensions to renew the volume of solution that corresponds to 40 PVF is provided in Table 5-3.

Fig. 5-4a shows that the magnitude of k in the untreated statically compacted specimens, submitted to both types of solutions, remained within the range of 10^{-8} to 10^{-9} m/s. This k then increased by about two and one orders of magnitude in the 1% lime-treated DW and LW submitted soil, respectively. The duration taken by the LW submitted soil to renew 40 PVF was about 5 days higher than the corresponding DW submitted soil (Table 5-3). However, it took about 49 to 76 more days to circulate a similar volume of solutions through the untreated soil.

In the 2.5% and 4% lime-treated statically compacted soil, the k was in between 10^{-7} to 10^{-8} m/s for both DW and LW submitted soil. Thus, k was about one order of magnitude higher than the untreated soil (Fig. 5-4b & c). The total duration corresponding to the percolation of 40 PVF was only 1.5 and 5 days for the 2.5% and 4% lime-treated soil, respectively, which was much lower than the duration taken by the corresponding untreated soil (Table 5-3).

For the lime-treated kneading compacted soil, the level of k measured for the untreated soil was in the range of 10^{-8} to 10^{-9} m/s (Fig. 5-4d). In the untreated LW submitted soil, the level of k further decreased after about 20 PVF. This decrease is attributed to the grain rearrangement within the soil matrix during the percolation phase (Young, 2012). However, the obtained level of k in the 1% lime-treated kneaded specimens submitted to DW and LW remained almost at a similar level as the untreated soil (Fig. 5-4d). At the same time, the k increased by an order of magnitude in the 2.5% and 4% lime-treated kneaded specimen submitted to DW, whereas it remained constant for the corresponding LW submitted specimen (Fig. 5-4e & f). 2.5% and 4% lime-treated kneaded soil took 75 and 40 days, respectively, to renew 40 PVF, whereas the corresponding DW submitted soil took only 4-6 days to circulate the similar volume of solutions (Table 5-3). However, the duration of the percolation phase was relatively higher in the untreated kneaded soil than in the lime-treated kneaded soil.

Based on the evolution of k obtained for each specimen in Fig. 5-4, Table 5-4 presents the estimated hydraulic life expectancy of an in-situ lime-treated earth structure of a unit reference height if built with the present soil configuration. The duration of life expectancy was expressed both in years and days (Column D) and was calculated by dividing the reference unit height of the structure by the average of the last 10 values of k measured in each specimen (Fig. 5-4).

As per Table 5-4, the estimated hydraulic life expectancy was 14.5 years for 2.5% lime-treated kneaded soil percolated by LW (Column D), while it was just 1.1 years for the corresponding DW percolated soil. For 4% lime-treated kneaded soil, the life expectancy was 6 years higher for LW- compared to the DW-percolated soil. The difference in life expectancy based on the types of solution percolated was less significant for the 1% lime-treated kneaded soil. In the statically compacted soil, the difference in life expectancy for soil treated with 2.5% and 4% lime and percolated by both types of the solution was less significant. However, the hydraulic life expectancy of 1% lime-treated soil percolated by LW was 0.9 years higher than the corresponding DW percolated soil. It is worth noting that the above-estimated life expectancy did not consider the soil structure-pore fluid interactions during percolation. The obtained duration represents the duration taken by a given pore fluid to reach the bottom of a unit height structure if percolated from the top, considering k as the flow velocity.

All tested specimens renewed 40 PVF over a measured duration (Table 5-3). This duration was used to calculate the required duration to renew 40 PVF in a unit height hydraulic structure (Table 5-4), Column E). These obtained durations were further expressed in percentage with respect to the percentage of the total life expectancy estimated for the structure of unit height (*i.e.*, Column E/Column D) in Fig. 5-5.

Table 5-4 Estimated life expectancy of a unit height in-situ earth structure, if built with the present soil configurations.

A	B	C	D	E
Compaction modes	Specimen's configuration	Average k (m/s)	Estimated life expectancy for a unit height structure (years (days))	Required duration to reach 40 PVF in a unit height structure (days)
Statically compacted	1-S-OMC-28-DW	2.97E-07	0.1 (39.0)	16
	1-S-OMC-28-LW	3.30E-08	1.0 (350.6)	120
	2.5-S-OMC-28-DW	1.71E-07	0.2 (67.7)	32
	2.5-S-OMC-28-LW	2.01E-07	0.2 (57.7)	32
	4-S-OMC-28-DW	4.56E-08	1.0 (254)	100
	4-S-OMC-28-LW	4.73E-08	0.7 (244.7)	100
Kneading compacted	1-K-OMC-28-DW	2.91E-09	10.9 (3983.5)	1400
	1-K-OMC-28-LW	3.56E-09	8.9 (3249.4)	1300
	2.5-K-OMC-28-DW	1.49E-07	0.2 (77.7)	80
	2.5-K-OMC-28-LW	2.18E-09	14.5 (5297.0)	1500
	4-K-OMC-28-DW	3.00E-08	1.1 (385.8)	120
	4-K-OMC-28-LW	4.54E-09	7.0 (2548.3)	800

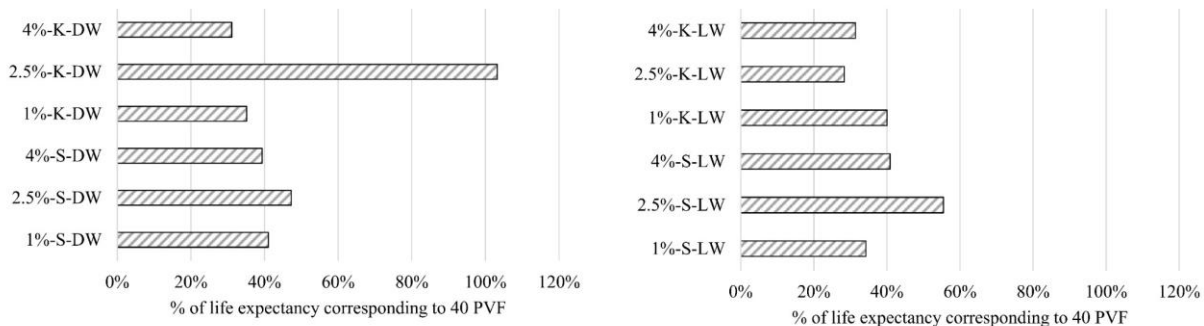


Fig. 5-5 Percentage of life expectancy that can be reached in a unit height earth structure if subjected to 40 PVF of DW (a) and LW (b) in kneading-and statically-compacted soil.

According to Fig. 5-5a, the estimated lifetime of the 2.5% lime-treated kneaded soil structure, if percolated by 40 PVF of DW, already reached its expected life values. The corresponding kneaded specimen on being submitted to 40 PVF of LW reached only 28% of its total life expectancy (Fig. 5-5b). Besides, the renewal of 40 PVF has reached about 30 to 50% of the total estimated life of the structure, built with the remaining configuration. The above evaluation of hydraulic performance was in terms of PVF, which presents the advantage of considering the pore fluid-soil structure interactions. Based on this evaluation, it was shown that the total life expectancy was yet to be reached even after the renewal of 40 PVF (Fig. 5-5). Thus, such an assessment helps to investigate the life scale of in-situ earth structures at laboratory scale.

However, it is worth noting that the above estimation of life expectancy was based on the hydraulic performances and did not consider the mechanical performances of the compacted soil.

5.3.4 Evolution of calcium concentrations in the effluents of untreated and lime-treated soils.

Fig. 5-6 presents the calcium concentration, Ca (mg/l) measured in the effluents collected at different PVF from the untreated and the lime-treated statically and kneaded specimens during the percolation phase.

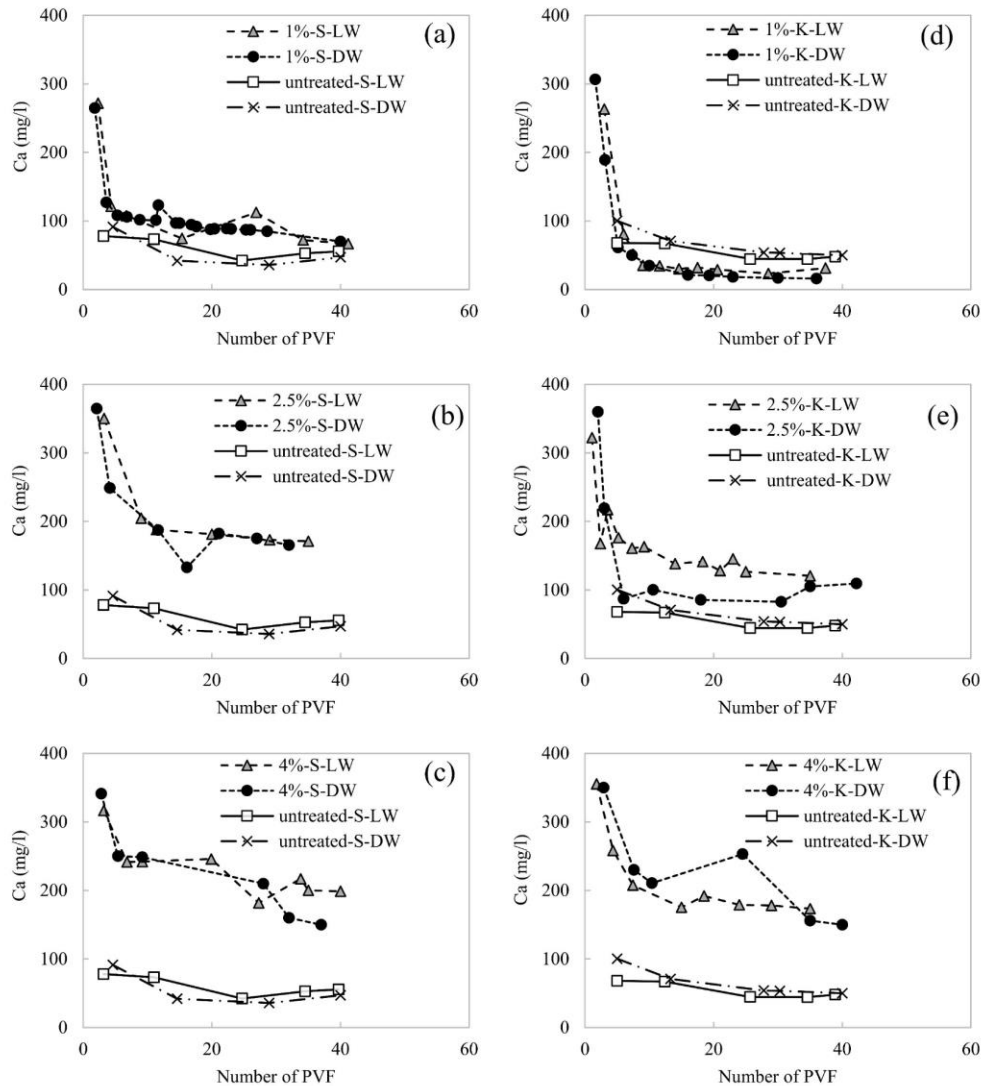


Fig. 5-6 Concentration of Ca leached from the untreated and 1%, 2.5%, and 4% lime-treated DW & LW submitted statically (a-c) and kneading (d-f) compacted specimens.

Permeant solution flows mostly through the widest connecting pore available in soil (Hunt and Sahimi, 2017). Hence, the leaching mechanism in a saturated lime-treated soil (Table 5-2) is more likely to be pronounced on the available minerals around the inter-aggregate pores constituting the flow-path compared to the intra-aggregate pores.

In the 1% lime-treated statically compacted soil, most of the *Ca* coming from the added lime and available particularly around the flow-path was lost on renewal of 10 PVF of DW and LW (Fig. 5-6a). Further renewal of solution triggered a release of soluble *Ca* from the soil. In the 2.5% and 4% lime-treated specimens, a sharp concentration of *Ca* was leached up to about 10 PVF, and the rate of leaching then slowed down. However, the overall trend of *Ca* leaching for the treated soil remained much above the trend obtained from the untreated soil, thus, indicating that the loss of *Ca* was either from the cementitious compounds or residual lime available, particularly around the flow path (Fig. 5-6b & c).

For the kneading compacted soil, *Ca* available around the flow-path in the form of cementitious compounds or residual lime was lost completely at about 5-7 PVF from the 1% lime-treated soil (Fig. 5-6d). Then a concentration of soluble *Ca* was leached from the soil. 2.5% lime-treated DW submitted specimen leached a significant *Ca* concentration, particularly coming from the lime added during the renewal of 40 PVF of DW. Besides, a part of soluble *Ca* was also lost from the soil (Fig. 5-6e). At the same time, the trend observed in the loss of *Ca* concentration in the corresponding LW submitted soil remained above the DW submitted soil, thus, indicating a part of *Ca* was lost only from the added lime (Fig. 5-6e).

For the 4% lime-treated kneaded soil, the evolution in the loss of *Ca* for the DW and LW submitted specimens remained at about a similar level (Fig. 5-6f). The leached *Ca* comes from the added lime.

Besides, 2.5% and 4% lime-treated DW submitted kneaded soil leached a significant *Ca* concentration in just 4 and 6 days of percolation phase, respectively, whereas it took 75 and 40 days for the corresponding LW submitted soil to leach the equivalent *Ca* concentration (Table 5-3).

5.4 Discussions.

5.4.1 Influence of pore fluid-soil structure interaction on the UCS evolution of lime-treated soil.

Soil treated at LMO was shown to have a limited contribution towards the development of cementitious compounds (le Runigo et al., 2011). Hence, 1% lime-treated soil can be considered insufficient to maintain its strength and lost almost 60% of its initial UCS, irrespective of the compaction modes and the pore solutions the specimens were submitted to (Fig. 5-1).

The evolution of compressive strength in lime-treated soil enhances with the development of cementitious bonding, which depends on the lime content used (higher than the LMO), water content, and curing time (Lemaire et al., 2013; Little, 1995; Verbrugge et al., 2011). Thus, in the 2.5% and 4% lime-treated soil, due to the constant contact of the compacted soil structure with the pore solution, particularly during the saturation phase, a significant evolution of cementitious compounds occurred. This was confirmed by the decrease in pores of diameter 10^4 \AA and increased formation of pores of diameter lower than 10^3 \AA in both types of 2.5% and 4% lime-treated compacted soil (Fig. 5-3b-c, e-f). As expected, the evolution of pore lower than 10^3 \AA was more pronounced in 4% lime-treated soil due to the greater availability of lime. As a result, the UCS in 4% lime-treated soil increased by 57% and 36% in the statically and kneaded specimens, respectively, at the end of the hydraulic conductivity test compared to the 28 days cured specimens (Fig. 5-1a & b). The UCS remained unaffected in the 2.5% lime-treated statically compacted soil (Fig. 5-1a); however, it decreased in the corresponding kneaded soil.

The decrease in UCS of the kneaded soil was about 20% higher in the DW submitted soil than the LW submitted soil (Fig. 5-1b). This relatively greater decrease in UCS indicates the pronounced influence of pore solution chemistry on the kneaded soil structure. This phenomenon is detailed in the later sections, which involve the mechanism of hydraulic conductivity and leaching as a result of the coupled influence of soil structures and pore solutions.

5.4.2 Influence of pore fluid-soil structure interaction on the hydraulic behavior of lime-treated soil.

The observed hydraulic performances in the lime-treated soil appear to be in accordance with the microstructural modifications brought about by a coupled effect produced between the compacted soil structure and the chemistry of the solutions.

5.4.2.1 Influence of soil structure on the hydraulic conductivity evolution.

As pore fluid through a compacted soil matrix follows the pore geometry constituted by the widest connecting pores (Hunt and Sahimi, 2017). Besides, previous studies have demonstrated that lime treatment increases the size of inter-aggregates pores due to flocculation, and as a result, increases the magnitude of hydraulic conductivity compared to the untreated soil (Nguyen et al., 2015; Tran et al., 2014). This explains the increased k from about 10^{-9} m/s to somewhere in between 10^{-6} and 10^{-8} m/s in all the lime-treated statically compacted specimens (Fig. 5-4a-c).

However, according to Fig. 4-9, under kneading action, large inter-aggregates formed due to lime treatment were relatively deformed and consequently the macropores were reduced. Fig. 5-2 shows the presence of a relatively lower number of macropores of diameter 10^5 Å in all the lime-treated kneaded soil compared to the corresponding statically compacted soil. Thus, the evolution of k remained constant, *i.e.*, in between 10^{-8} to 10^{-9} m/s in the 1% lime-treated kneaded soil submitted to both types of solutions, and 2.5% and 4% lime-treated kneaded specimens submitted to LW (Fig. 5-4d-f).

However, the magnitude of k for the 2.5% and 4% lime-treated DW submitted soil was between 10^{-7} and 10^{-8} m/s, which was one order of magnitude higher than the corresponding untreated and LW submitted soil (Fig. 5-4e & f). This difference in k was because of the effect of pore solution chemistry, which is explained in the later section.

5.4.2.2 Influence of soil structure on flow characteristics.

From the preceding discussion, the evolution of the macropores of diameter 10^5 Å occurs to be different under static and kneading actions. Hence it will be interesting to evaluate the flow path of the permeant solutions through both types of compacted structures, which is measured by hydraulic tortuosity.

The hydraulic tortuosity, T is defined as the parameter that characterizes the heterogeneity in the flow path of the solution in a porous media (Srisutthiyakorn and Mavko, 2016). In this study, T was calculated using the Kozeny-Carman equation (Equation 5-1), which considers T as a function of the pore geometry (Allen and Sun, 2017). Results of T calculated for the static and kneading compacted specimens are summarized in Table 5-5.

$$T = \sqrt{\frac{\phi^3}{c k S^2}} \quad (\text{Equation 5-1})$$

In Equation 5-1, k is the coefficient of permeability in m/s, ϕ is the porosity calculated from each specimen, c is the Kozeny constant assumed to be equal to 200 for calculation convenience, and S is the specific surface area in m^2/g measured with BET. The value of c was considered based on the plot provided by Allen and Sun, (2017), where c was shown to be a function of the porosity of the soil.

Table 5-5 Tortuosity calculated from statically and kneading compacted specimens

Specimen ID	k (m/s)	ϕ	S (m ² /g)	T	Specimen ID	k (m/s)	ϕ	S (m ² /g)	T
1%-S-DW	2.97E-07	0.38	13.16	2.32	1%-K-DW	2.91E-09	0.37	11.75	24.84
1%-S-LW	3.30E-08	0.35	12.02	6.81	1%-K-LW	3.56E-09	0.37	11.62	23.34
2.5%-S-DW	1.71E-07	0.38	19.78	2.04	2.5%-K-DW	1.49E-07	0.38	18.56	2.27
2.5%-S-LW	2.01E-07	0.39	18.42	2.08	2.5%-K-LW	2.18E-09	0.38	18.56	19.46
4%-S-DW	4.56E-08	0.38	22.93	3.36	4%-K-DW	3.00E-08	0.37	22.10	4.12
4%-S-LW	4.73E-08	0.37	23.73	3.12	4%-K-LW	4.54E-09	0.39	20.60	12.34

According to Table 5-5, almost all the statically compacted specimens showed a comparatively lower value of T than the corresponding kneaded specimens. Thus, the consequence of kneading action on lowering the macropores by deforming the flocculated particles was reflected in the greater value of T obtained in the kneaded soil. Hence, it can be said that the kneaded soil structure experiences an intimate and longer contact with the permeant solution, and the pore fluid within the kneaded soil structure has greater accessibility towards the available lime. Such intimacy is favorable for the development of pozzolanic reaction, and consequently, a significant formation of cementitious compounds can occur in the pores. This benefit of kneading action was confirmed by the observed decrease in macropores of diameter 10^5 \AA in the 2.5% lime-treated LW submitted kneaded soil compared to the unleached soil (Fig. 5-3e). As a result, the estimated hydraulic life expectancy and the duration to renew 40 PVF of LW through a unit height in-situ kneaded structure was relatively longer (Table 5-4).

Based on the above discussion, Fig. 5-7 presents a synthetic schematic diagram that elaborates the flow paths within the lime-treated statically and kneading compacted soil.

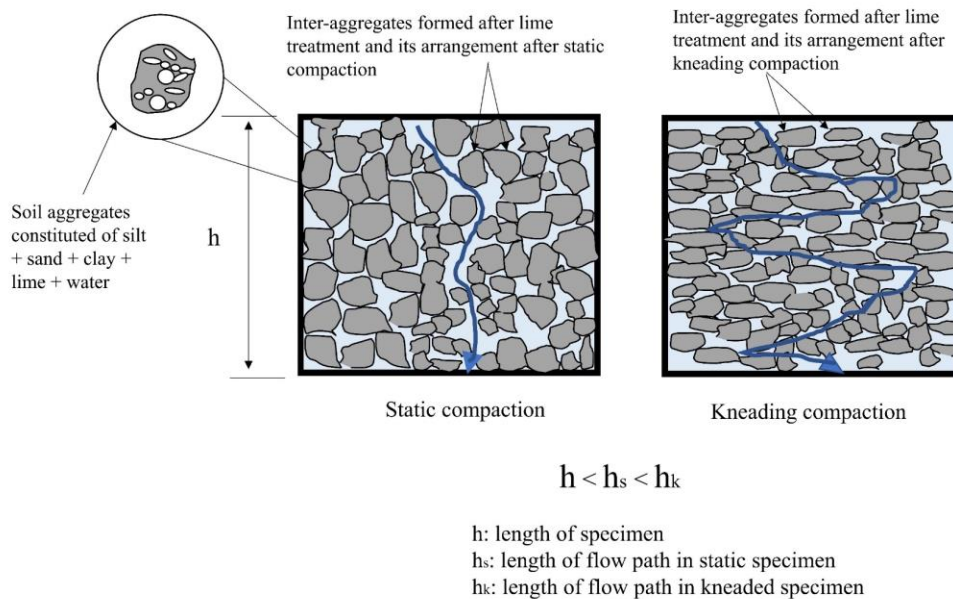


Fig. 5-7 Schematic diagram showing differences in lime-treated compacted soil matrices after being subjected to static and kneading compactions and the expected flow paths of permeant solution during hydraulic test.

5.4.2.3 Influence of pore solution chemistry on flow characteristics and leaching mechanism.

The mechanism of leaching was defined by the chemistry of the pore solutions the specimens were submitted to. As evident from Fig. 5-6e & f and Table 5-3, the leaching of *Ca* was comparatively higher and accelerated in the DW submitted kneaded specimens compared to the corresponding LW submitted specimens. As described earlier, due to the constant contact of soil-lime with the pore solution during the saturation phase of the hydraulic conductivity test, a significant formation of cementitious bonding occurred in the inter-and intra-aggregate pores. Once the percolation phase was initiated, the renewal of the pore solution occurred. Since DW is devoid of ions and has a low EC (Table 5-1), it dissolves a relatively greater concentration of *Ca* from the cementitious compounds, particularly present around the flow path, and soluble *Ca* from the soil. The dissolution of cementitious compounds from the macropores, thus, in turn, increased the magnitude of *k* (Fig. 5-4e & f). As a result, 40 PVF of DW was percolated through the 2.5% and 4% lime-treated kneaded soil only in 4 and 6 days, respectively. At the same time, the corresponding 2.5% and 4% lime-treated LW submitted specimens took 75 and 40 days, respectively, to percolate a similar volume of LW (Table 5-3). The above phenomenon also explains the relatively greater UCS reduction observed in the DW submitted kneaded specimen (Fig. 5-1b).

However, the above influence of pore solution chemistry in the leaching mechanism inducing a modification in the flow-path remained less pronounced in the 1% lime-treated kneaded specimen. As soil treated at LMO has limited contribution towards the development of cementitious compounds thus, almost all *Ca* from the added lime was leached, and consequently, a significant concentration of soluble *Ca* was leached from the soil (Fig. 5-6d). Besides, under the application of a constant load during kneading compaction, the flocculated particles in 1% lime-treated specimens tend to deform more than 2.5% and 4% lime-treated soil as the addition of lime creates stronger flocculated particles. Thus, the evolution of *k* in the 1% lime-treated remained at a similar level as the untreated kneaded soil (Fig. 5-4d).

Although the impact of pore solution chemistry on the mechanical and hydraulic evolution was pronounced in the kneaded soil, it remained less significant in the statically compacted soil. Due to the presence of relatively more macropores (Fig. 5-2), statically compacted soil can be said to have undergone preferential flow, which was reflected in the relatively lower value of *T* (Table 5-5). In the process of preferential flow, the pore solution-soil structure interaction remained less significant, and thus the leaching mechanism remained at a similar level irrespective of the types of pore solutions the specimens were submitted to (Fig. 5-6a-c). This explains the evolution of a similar level of *k* in the 2.5% and 4% lime-treated statically compacted soil regardless of the types of pore solution they were submitted to (Fig. 5-4b & c). It also explains the difference in UCS observed between the statically and kneading compacted soil (Fig. 5-1).

However, the *k* increased by 10 times in the 1% lime-treated DW submitted soil compared to the LW submitted soil (Fig. 5-4a). As the leaching mechanism in 1% lime-treated statically compacted soil remained at a similar level (Fig. 5-6a), and 1% lime-treated soil has limited contribution towards the deposition of cementitious compounds around the flow path. Hence, the observed increased in *k* in the DW submitted soil was due to the partial disintegration of inter-aggregates around the flow path, which increased the macropores of diameter 10^5 \AA (Fig. 5-3a).

5.4.2.4 Comparison of hydraulic evolution in laboratory and in-situ cured soil.

The hydraulic evolution and the estimated hydraulic life expectancy of 2.5% lime-treated LW-percolated kneaded soil (Table 5-4) were compared with atmospherically cured specimens. In-situ specimens were sampled from a 7-years atmospherically cured embankment built with the same soil configuration, as

reported in Chapter 3. The embankment was previously studied by Makki-Szymkiewicz et al. (2015), who reported a k of $2.00\text{E-}09$ m/s after 6 months of atmospheric curing. Later the hydraulic conductivity was evaluated after 7 years of atmospheric curing by subjecting the sampled-soil to LW at the laboratory and was found to be $9.18\text{E-}10$ m/s. The estimated hydraulic life expectancy and the evolution of k in the laboratory and the in-situ cured specimens are compared and are presented in Table 5-6.

Table 5-6 Comparison of k and life expectancy obtained for in-situ and laboratory cured 2.5% lime-treated kneaded soil, percolated by LW.

Type of specimens	Duration of curing	k (m/s)	Life expectancy (years)
Laboratory-cured	28 days	$2.18\text{E-}09$	14.5
	6 months	$2.00\text{E-}09$	15.9
In-situ cured	7 years	$9.18\text{E-}10$	34.5

Table 5-6 shows that the obtained values of k and hydraulic life expectancy evolved in a positive manner. The k decreased, and the hydraulic life expectancy increased with curing time. The decrease in k was due to evolution of cementitious compounds, which increased the mesopores by decreasing the available macropores, as reported in Chapter 3. The increased mesopores positively contribute to an increase in UCS, which has led to an average UCS of 3.29 MPa in the 7 years atmospherically cured soil, as reported in Chapter 3.

Thus, in addition to the positive evolution of k with increased curing time, an enhanced mechanical behavior can also be expected with time. Such an evolution can contribute to the increased hydromechanical life expectancy of the structure. This underlines the relevance of kneading compaction and the use of LW to evaluate the long-term hydromechanical performance of lime-treated soil.

5.5 Conclusions.

The study presented in this chapter investigates the hydromechanical evolution in lime-treated soil based on the leaching mechanism, and microstructural modifications brought about by a coupled pore solutions-soil structure interaction. Based on the analysis, the following conclusions are derived:

1) The evolution of UCS in the lime-treated leached specimens was impacted by combined influence created by (i) the availability of lime, (ii) the quality of the interaction of the pore fluid with the soil-lime component and, (iii) the impact of compaction mechanism on the extent of deformation of larger-sized flocculated particles. Thus, the UCS increased by 57% and 36% in the leached 4% lime-treated statically compacted and kneaded specimens, respectively, compared to the unleached specimens. The UCS remained unchanged in the 2.5% lime-treated statically compacted specimen, while it decreased by 21% and 40% in the 2.5% lime-treated kneaded soil, percolated by LW and DW, respectively.

2) Evaluation of hydraulic conductivity in terms of PVF helps to determine the percentage of life expectancy that can be reached in an in-situ hydraulic structure by considering the pore fluid-soil structure interactions. The renewal of 40 PVF corresponds to the deterioration of about 30 to 50% of the total estimated life of the lime-treated structure, built with the present soil configurations.

3) Kneading action reduced the presence of macropores of diameter 10^5 \AA in the compacted soil structure. A lower macropore reduces the magnitude of k . Thus, the magnitude of k was 10^{-8} to 10^{-9} m/s in the LW submitted kneaded soil while it was 10^{-6} to 10^{-8} m/s in the corresponding statically compacted soil.

4) Higher hydraulic tortuosity obtained in the kneaded soil demonstrated the longer contact duration between the pore solution and the soil and lime component. This feature favored the development of cementitious compounds and lowered the macropores of diameter 10^5 \AA in the 2.5% lime-treated LW submitted kneaded soil, which is favorable for the long-term performance of lime-treated earth structure.

5) The chemistry of pore fluid showed a significant modification in the hydromechanical evolution of lime-treated soil based on its accessibility to the soil and lime component. DW, being relatively more aggressive than LW, dissolved a greater concentration of Ca from the cementitious compounds, thus resulting in an increase in the k of 2.5% and 4% lime-treated kneaded soil. This influence of DW on the leaching mechanism and the hydraulic conductivity evolution remained less pronounced in the statically compacted soil due to the limited accessibility of pore fluid to the soil components.

6) The hydromechanical behavior of lime-treated kneaded soil evolved with curing time, which in turn increased the life expectancy of an in-situ earth structure. The hydraulic evolution and the life expectancy of 28 days laboratory cured 2.5% lime-treated kneaded soil, percolated by LW was $2.18\text{E-}09$ m/s and 14.5 years, respectively. After 7 years of atmospheric curing, the hydraulic evolution and the life expectancy evolved to $9.18\text{E-}10$ m/s and 34.5 years, respectively. This is due to evolution of cementitious compounds, which also increased the UCS to 3.29 MPa. This underlines the relevance of the use of kneaded soil and LW to evaluate the long-term hydromechanical performance of the lime-treated in-situ structure.

7) Soil treated at LMO (1%) has limited contribution towards the development of cementitious compounds. Thus, the influence of pore solution-soil structure interaction remained less significant in the hydraulic, leaching, and compressive strength evolution of the 1% lime-treated soil. Significant modifications in these properties can be observed in soil treated with lime content of 2.5% and 4%.

Thus, the above findings showed that the hydromechanical evolution in lime-treated soil is governed by the mechanism created during the pore fluid-soil structure interactions. The duration of the pore fluid-soil structure interaction is defined by the compaction mechanism implemented, and the extent of influence is determined by the pore solution chemistry, and the lime content added. Implementation of kneading compaction accompanied with 10^{-3} M of NaCl concentration, a low ionic strength solution brings a significant modification in the hydromechanical performance. Thus, the selected compaction procedure and the permeant solution in the laboratory scale must be representative of the compaction mechanism and pore water that the structure is likely to be subjected to in the field. This will help to have a close prediction of the long-term hydromechanical performance of in-situ lime-treated structures. Such a prediction can contribute effectively to the efficient management of construction resources. Besides, to have a considerable modification in the hydromechanical performance, the addition of lime content higher than LMO is essential.

Chapter 6

INFLUENCE OF DIFFERENT WETTING-DRYING CYCLES TESTING CONDITIONS ON THE PHYSICOCHEMICAL AND MICROSTRUCTURE EVOLUTION OF LIME-TREATED SOIL (PROPOSAL 4).

General.

Chapter 3 to Chapter 5 showed the importance of reproducing a laboratory implementation mechanism that represents a situation closer to the field for attaining accurate hydromechanical performances of lime-treated soil.

The improvement brought in lime-treated soil needs to be maintained for the structure in order to attain long-term durability. However, on exposure of lime-treated soil to an open atmospheric environment, the soil is subjected to successive alteration of seasonal temperatures as well as fluctuations of water level. Under such circumstances, the long-term performances of the lime-treated soil are still a concern. Such a concern varies with the climate of the specific regions on which the structure is located or constructed. Some field investigations conducted with lime-stabilized roads evidenced that a significant alteration in climatic conditions can negatively impact the performance of lime-treated soil (Cuisinier and Deneele 2008; Kelley 1977). Additionally, several laboratory studies are available that delineated the severity of wetting and drying (W-D) cycles, as well as freeze/thaw cycles on degrading the improved hydromechanical behavior of lime-treated soil (Chittoori et al. 2018; Cuisinier et al. 2020; Nabil et al. 2020). The effect of W-D cycles in the field is explained below.

In the field, the slope of the lime-treated hydraulic earthen structure built near water bodies often suffers W-D cycles due to several fluctuations in water level (Chen et al., 2018; Jia et al., 2009; Johansson and Edeskär, 2014; Xiong et al., 2019). During heavy rainy periods, due to the rise in water level in water bodies, the slope towards the base of the hydraulic structure may remain underwater for several weeks to months. Such a situation can increase the available saturation level of the soil. On the other hand, during severe drought periods, a drastic decrease in the water level might occur, thus exposing the same base level to severe drying for several months to years, which in turn can decrease the saturation level. Such a fluctuation in the saturation level can modify the mechanical resistivity of the lime-treated soil and might impact the service life of the structure. Though assessment of the durability of lime-treated soil subjected to W-D cycles was extensively studied, of which most of the studies were made following the testing condition provided in ASTM D559 standard (ASTM 2015). However, how well this technique represents the above in-situ W-D situation is less investigated. Chapter 1 has detailed the ASTM procedure and how its implementation does not represent the field situation.

In this context, this chapter focuses on analyzing the physicochemical and microstructure mechanism contributing to the evolution of UCS in compacted lime-treated cured specimens subjected to different W-D cycles testing conditions. Two laboratory testing conditions were proposed to represent the W-D cycles lime-treated soil may experience in the field. The results obtained were compared with the respective results obtained using the reference ASTM standard. The first part of the study focuses on comparing the UCS evolution and volume variation of the specimens. Later, the physicochemical and microstructure characteristics are presented. In the end, the mechanism correlating the physicochemical and microstructure properties with the UCS evolution is explained.

6.1 Materials.

MLD soil and quicklime presented in Chapter 2 were used for this study. Lime content, 1.5% higher than LMO, i.e., equal to 2.5%, was used as soil treated at LMO was shown to have limited contributions towards long-term pozzolanic reactions in Chapter 5.

6.2 Sample preparations.

The silt was mixed with distilled water at a water content of $1.1 \times \text{OMC}$, i.e., specimens were prepared at the wet of optimum (WMC). This is because a compaction moisture content similar to the one reported in Chapter 3 was used, which involves the performance of an in-situ embankment built with the present soil configuration.

Cylindrical specimens of dimensions 0.10 m in height and 0.05 m diameter were prepared by the static compaction method at WMC. A total of 2 untreated and 14 lime-treated specimens were prepared. After compaction, specimens were wrapped in plastic film and then subjected to long-term curing of 10 months at a laboratory temperature of 20 ± 1 °C, since curing is an important parameter that enhances the improvement in lime-treated soil as reported in Chapter 1.

6.3 Testing conditions for Wetting and drying cycles.

The W-D cycles were imposed as per the ASTM standard and using two laboratory-developed testing conditions. The testing condition implemented as per the procedure demonstrated in ASTM D559 is denoted as AP. The second and third testing conditions were proposed to represent the situation a soil might experience in the field during rainy and drought seasons, respectively.

Alteration of W-D cycles brings an increase and then decrease of the soil-saturation level, respectively. During rainy periods, when the slope towards the base of the hydraulic earthen structure remains under water for a long time, the soil can be assumed to have attained a maximum saturation level of 85-90%. Again, due to the greater frequency of precipitation during the rainy season, the soil can be assumed to have reached a saturation level not less than 65-70% during the drying period, when the water level in the water bodies decreases for a certain period. Similarly, the soil was assumed to dry up to a saturation level of 25-30% during the drought season and considering the slightest rainfall that can probably happen during the drought period; the soil was supposed to reach a maximum saturation level of only 65-70%. For the present lime-treated soil, the duration required to attain the above-assumed saturation level during rainy and drought periods was measured in the laboratory, during which the temperature and relative humidity varied from 22.1-25.2°C and RH of 34.3-52.8%, respectively. The obtained wetting and drying duration were then used to undergo successive W-D and drying-wetting cycles to represent the rainy and drought situations, respectively. The testing conditions and the duration required to attain the assumed levels of saturation are provided in Table 6-1. The second and the third testing conditions, which represent the rainy periods and drought periods, respectively, are regarded as RP and DP, respectively, in the following study. It is worth noting that specimens subjected to AP and RP experience alternate W-D cycles, whereas specimens subjected to DP experience alternate drying and wetting (D-W) cycles.

Table 6-1 Presentation of testing conditions

Designation	Testing conditions			Sequence of cycles	Number of specimens
	Wetting hours	Drying hours	Temperature (°C)		
AP (ASTM standard)	5	43	71	Wetting then drying (W-D)	4
RP (to represent in-situ rainy situation)	7	17	22.1-25.2	Wetting then drying (W-D)	4
DP (to represent in-situ drought situation)	2	70	22.1-25.2	Drying then wetting (D-W)	4

The RP and DPs were conducted by a laboratory proposed device, which involves successive wetting of the specimens by soaking in water for the proposed time and then drying the same by allowing the water to move out after completion of the wetting duration. A part of the water after each wetting, *i.e.*, the effluent, was stored for chemical analysis. A total of 17 wetting-drying and drying wetting (W-D/D-W) cycles were operated using the three testing conditions. The mass and volume of the specimens subjected to all three conditions were recorded at the end of each cycle. To establish the homogeneity of the specimens, they were periodically turned during the alternate cycles.

Of the 14 lime-treated specimens prepared and cured, three sets of 4 specimens were subjected to the three testing conditions, and the remaining 2 were used to evaluate the initial state of the specimen after 10 months of curing.

6.4 Laboratory Experiments.

10 months cured specimen, *i.e.*, the initial specimen, and the specimens subjected to 5th, 9th, 13th, and 17th alternate W-D/D-W cycles in each of the three testing conditions were subjected to UCS test.

The water content of each UCS-subjected specimen was measured and was used to estimate the water content corresponding to the remaining cycles. The suction of the UCS subjected specimen was determined. The pH of the UCS subjected specimens was also measured. To have more reliable results, at least an average of the three values of preceding properties was reported.

The Electric Conductivity (EC) of the effluents collected after each wetting was determined. A part of the collected effluent corresponding to a certain number of wetting cycles was subjected to Inductively Coupled Plasma Optical Emission Spectrometry (ICP OES) analysis. This was done to determine the elementary concentrations of Calcium (*Ca*) that have been leached from the lime-treated soil subjected to W-D/D-W cycles.

Pore Size Distribution (PSD) was analyzed by MIP test and BJH method. Since MIP was known to investigate macropores and BJH, the mesopores more elaboratively, as shown in Chapter 3, hence both the methods are used herein. The analysis was made on the freeze-dried samples gathered from the core of the 10 months cured specimen and the specimens subjected to the UCS test.

The discussion of pore structure is presented as per the International Union of Pure and Applied Chemistry (IUPAC) (Rouquerol et al. 1994).

6.5 Results.

6.5.1 W-D/D-W cycle influence on UCS evolution.

At the very first wetting performed as per the three testing conditions, the untreated silty soil was destroyed without the possibility of undergoing UCS and any further tests.

The UCS evolution of the lime-treated soil subjected to 17 W-D/D-W cycles as per the 3 testing conditions is presented in Fig. 6-1.

The UCS of the initial specimen after 10 months of curing was 1.26 MPa. This UCS increased to 3.40 MPa after the lime-treated soil underwent 5 cycles of W-D cycles as per the AP. Further increase in W-D cycles decreased the UCS to about 3.26 MPa, 2.28 MPa, and 1.57 MPa after the 9th, 13th, and 17th W-D cycles, respectively. For the RP-subjected soil, the UCS increased by about 0.40 MPa after the 9th W-D cycle compared to the initial soil. However, the overall evolution of UCS throughout the 17 W-D cycles remained almost similar compared to the initial specimen. The UCS of the DP-subjected soil showed a gradual decrease up to the 13th D-W cycle, and then after the 13th and 17th D-W cycles, the obtained UCS was almost similar (Fig. 6-1).

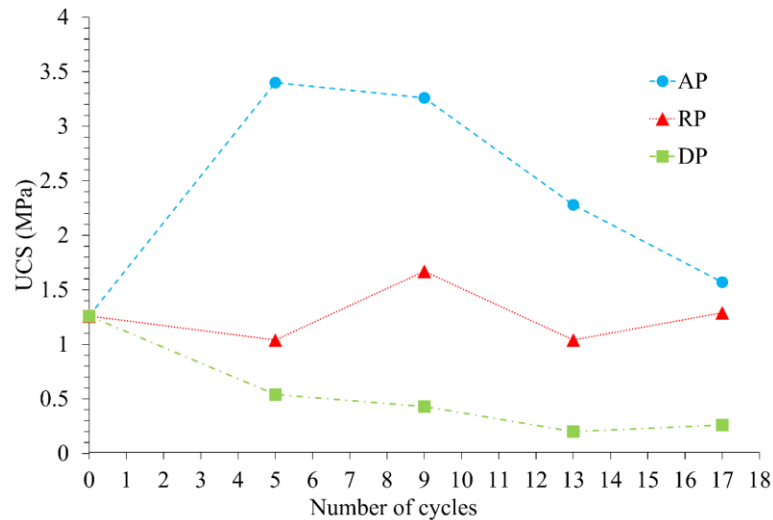


Fig. 6-1 UCS evolution in the lime-treated specimens subjected to W-D/D-W cycles as per AP, RP, and DP testing conditions.

6.5.2 W-D/D-W cycle influence on volume variations.

The change in volume of the specimens during W-D/D-W cycles are presented as a percentage increase or decrease in volume of respective specimens compared to the volume of the initial specimen in Fig. 6-2(a-c). The presented percentage change in volume is the average of the volume change obtained during the 17 W-D cycles of the 4 specimens subjected to each of RP, AP, and DP.

The amplitude of average volume changes between wetting and drying phase and between 2 successive cycles during the W-D cycles remained less significant in the specimens submitted to the RP testing condition (Fig. 6-2a). A maximum increase and decrease of about 0.8% in the average volume occurred compared to the initial volume.

Compared to the initial volume of the specimen, the AP submitted specimens showed a slight increase in average volume during the 1st wetting, and then the volume decreased by about 2% after the 1st

oven-drying (Fig. 6-2b). In the successive W-D cycles from 1st to about 8th cycles, the amplitude in average volume variations between the wetting and drying phase remained almost similar, where the increase and decrease in the average volume was less than 1% and 2%, respectively, than the initial volume. The fluctuation in the average volume variation was then lowered in the following W-D cycles. However, the maximum increase in average volume during wetting remained lower by about 0.4% compared to the initial volume throughout the 17 W-D cycles.

DP-subjected soil underwent a maximum decrease in average volume during drying of about 1.5%, and the maximum increase in average volume corresponds to the initial volume from the 1st to about 7th D-W cycles. For the remaining cycles, the loss in the average volume was almost insignificant (Fig. 6-2c). The overall trend observed in the average volume variation between the AP, and the DP submitted specimens were almost the same. However, the percentage of average volume loss after each drying was comparatively higher in the AP compared to the DP-subjected soil. On the other hand, the percentage increase in average volume after each wetting was relatively higher in the DP than the AP-subjected soil.

6.5.3 W-D/D-W cycle influence on physicochemical evolution in the specimens.

The water content was measured for the 10 months cured soil and for the specimen subjected to UCS test after 5th, 9th, 13th, and 17th cycles. The water content corresponding to the remaining cycles was then estimated by using the bulk mass of the soil measured after each cycle, and the dry mass of the soil measured at the end of the 17th cycle. This method of back estimation was approved in ASTM D559. The evolution of average water contents is presented in Fig. 6-2 (d-f).

According to Fig. 6-2d, a maximum of 2% increase and decrease in the average water content occurred during the wetting and drying phases, respectively, at laboratory temperature in the RP-subjected soil throughout the 17 W-D cycles. This increase and decrease in the average water content were found to almost correspond with the average maximum and minimum saturation level set earlier for the RP testing condition. The global trend of average water content evolution between 2 successive wetting and drying cycles remained almost constant.

Similar to the RP-subjected soil, the overall trend in the variation of the average water content between the wetting and drying phases and between 2 successive cycles remained almost constant in the AP-subjected soil (Fig. 6-2e). About 1% increase in the average water content compared to the initial water content occurred during each 5 hours of wetting at laboratory temperature, however, almost a complete loss in water content occurred during each 71°C oven-drying of the AP submitted soil.

In the DP submitted soil, the increase in average water content level during each wetting remained almost at a similar level, which was equivalent to the initial water content (Fig. 6-2f). However, a mean loss in average water content of about 13% occurred during the D-W cycle compared to the initial water content. The increase in average water content attained during almost each wetting though corresponds with the average saturation level set for the DP testing condition, the average saturation level was fluctuated during the drying in certain number of cycles.

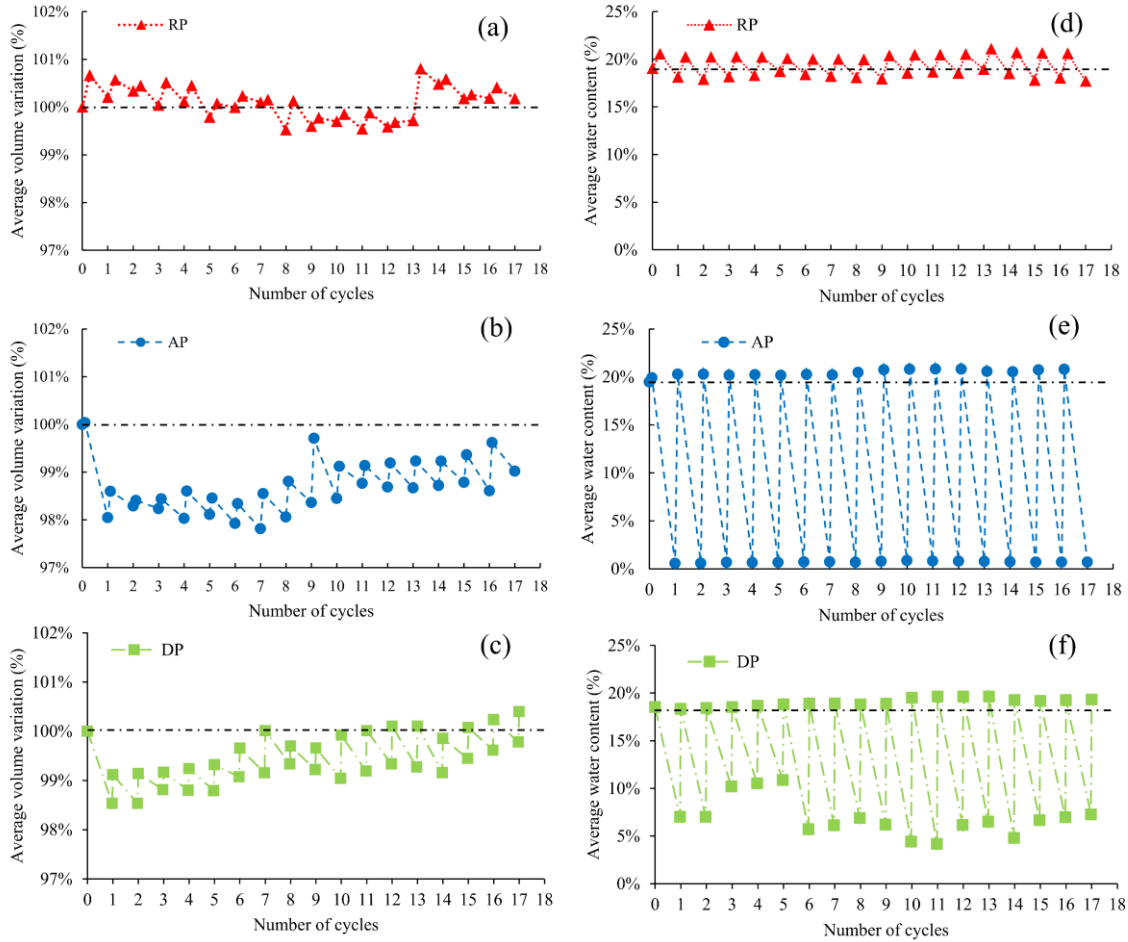


Fig. 6-2 Average volume variations (a-c), and water content variations (d-f) recorded from the specimens subjected to W-D/D-W cycles as per AP, RP, and DP testing conditions.

At the end of the UCS test, the soil suction and pH of the soil were measured and presented in Fig. 6-3 for each testing condition, with the soil suction and soil pH recorded from the initial soil.

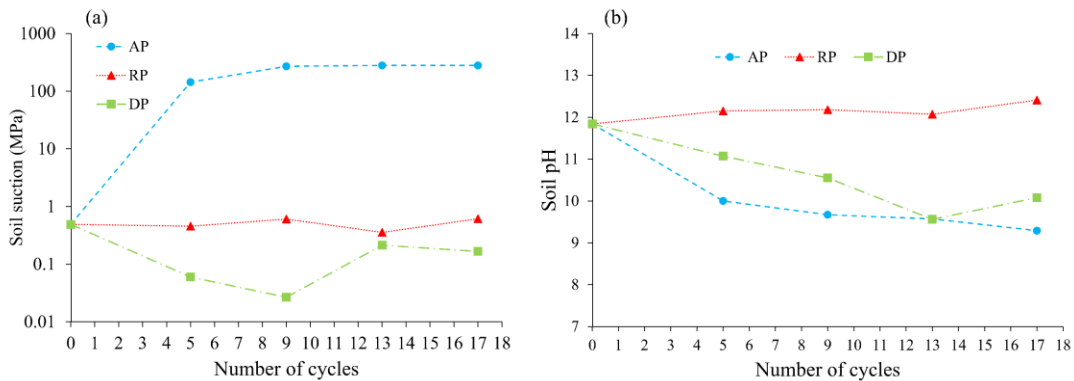


Fig. 6-3 Soil suction (a) and pH (b) measured in the initial and UCS subjected specimens during W-D/D-W cycles as per AP, RP, and DP testing conditions.

As expected, the soil suction of the AP submitted soil increased significantly in comparison to the initial suction of the soil due to almost total loss in water content (as seen in Fig. 6-2). The soil suction increased to 143.5 MPa after 5th cycle, then it increased to 270.0 MPa after 9th cycle and then remained approximately unchanged for the 13th and 17th cycles. The difference in the soil suction measured for the corresponding RP submitted soils remained less significant compared to the initial soil suction (Fig. 6-3a). The soil suction decreased for the DP-subjected soil up to 9th cycle, and then this decrease was slightly lowered after the 13th and 17th D-W cycles.

The pH measured for the initial specimen was 11.86. For the RP-subjected soil, this pH remained approximately unchanged up to 17th cycle (Fig. 6-3b). The pH of the AP-subjected soil decreased to 10 from the initial soil pH after the 5th cycle. The pH then further decreased; however, the decrease was relatively lower and remained above 9.3. Similar to the AP submitted soil, the pH of the DP submitted soil also decreased compared to the initial pH of the soil (Fig. 6-3b).

Fig. 6-4 presents the concentration of Ca and EC measured in the effluents collected during the W-D/D-W cycles conducted as per the testing conditions. The initial CaO in the untreated silty soil was estimated as 0.5%, and 2.5% of CaO was added during specimen preparation. Thus, the lime-treated soil consists of 3% CaO before curing. The Ca content in the 3% of the CaO , *i.e.*, $Ca_{initial}$ was estimated, and the release of Ca measured in the effluent, *i.e.*, $Ca_{leached}$ was then expressed as a percentage of the former in Fig. 6-4a.

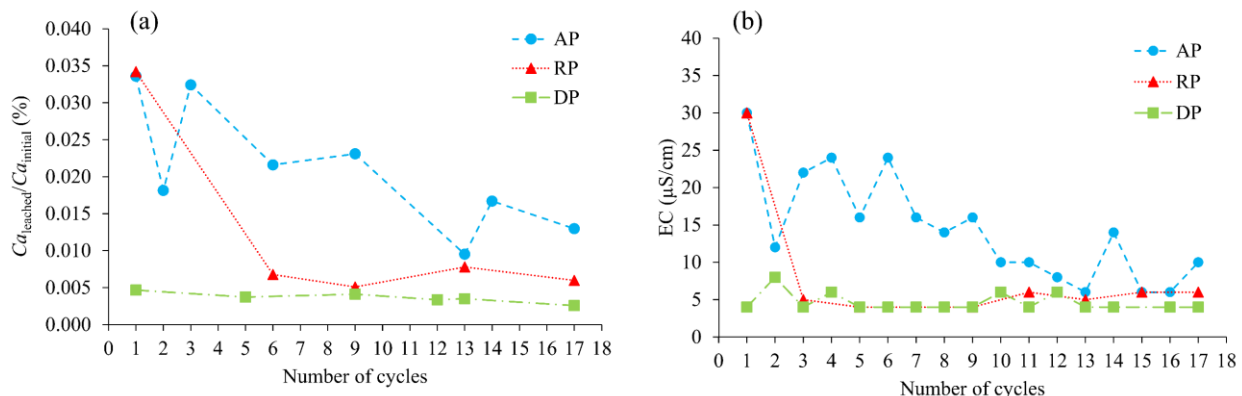


Fig. 6-4 Calcium concentration (a) and Electric Conductivity (b) measured in the effluents collected from the specimens subjected to W-D/D-W cycles as per AP, RP, and DP testing conditions.

The percentage of Ca leached from the lime treated soil was observed to be extremely low in all the specimens, regardless of the testing conditions (Fig. 6-4a). However, the loss of Ca and the magnitude of EC obtained were relatively higher in AP-subjected soil compared to the corresponding RP-subjected soil throughout the W-D cycles. The trend of the loss in Ca concentration and the measured EC decreased during the W-D cycles for the AP-subjected soil. On the other hand, this trend remained almost constant for the corresponding RP-subjected soil.

For the specimens subjected to DP testing condition, the leaching of Ca and EC measured remained relatively lower than both RP and AP-subjected specimens, and the overall evolution was almost similar throughout the D-W cycles (Fig. 6-4b).

6.5.4 W-D/D-W cycle influence on pore structure modifications.

The PSD and cumulative pore volume evolution in the lime-treated W-D/D-W cycles subjected specimens were compared with the one obtained from the untreated and the 10 months cured soil by MIP and BJH, respectively in Fig. 5.

Fig. 6-5 showed that the untreated soil exhibits greater intensities of macropores of diameter in the range of 10^4 and 10^5 Å. After lime treatment and 10 months of curing, macropores of diameter 10^5 Å evolved, a significant decrease of macropores of diameter 10^4 and 10^5 Å and an increase in pores smaller than 3000 Å occurred (Fig. 6-5(a-c)). Pores of diameter 10^5 Å was due to agglomeration of lime-treated soil, while pores smaller than 3000 Å evolved because of cementitious bonding as reported in previous studies presented in Chapter 3 to Chapter 5.

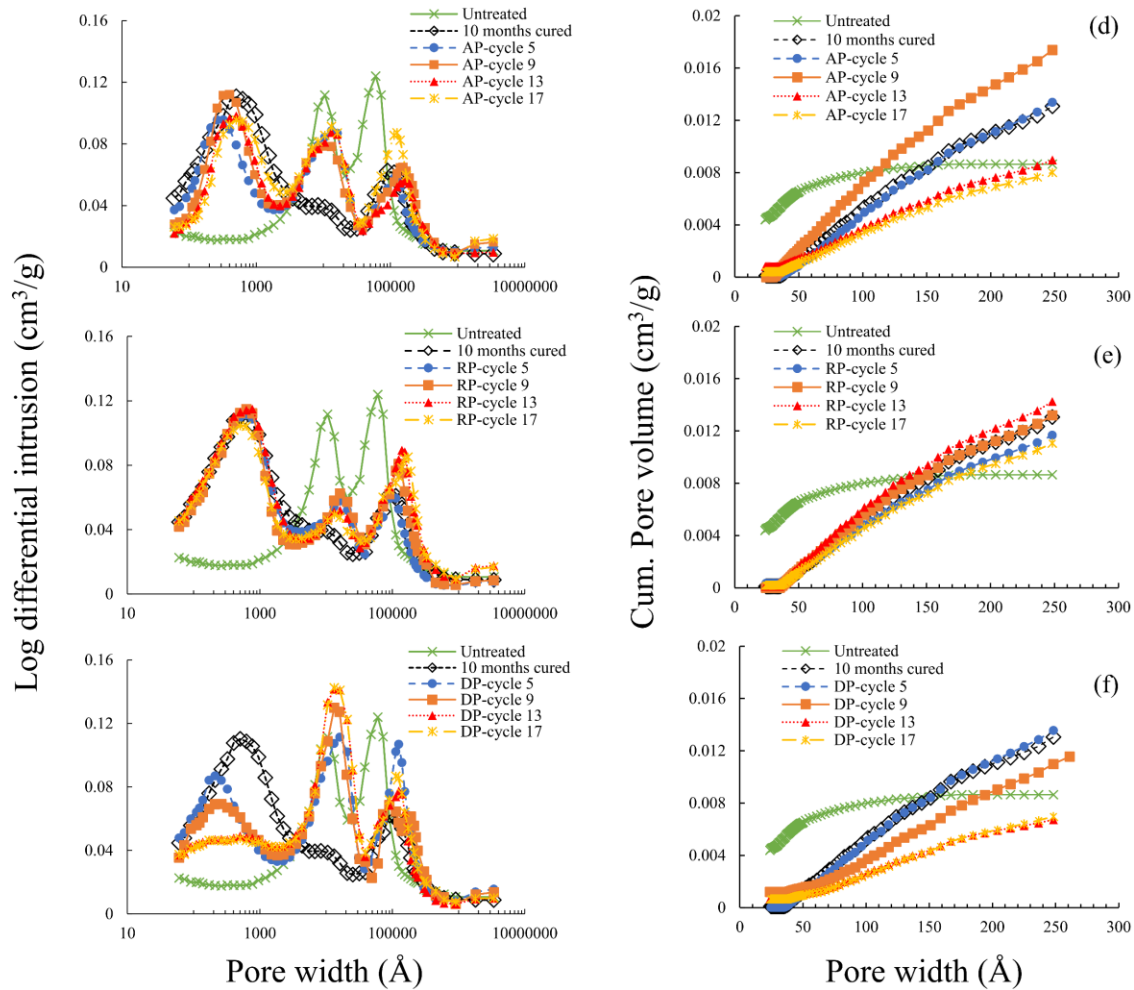


Fig. 6-5 Comparative PSD by MIP (a-c), and Cum. (cumulative) pore volume evolution by BJH (d-f) between untreated and 10 months cured lime-treated specimen with the lime-treated specimens subjected to W-D/D-W cycles as per AP, RP, and DP testing conditions.

On subjecting the 10 months cured lime-treated soil to the W-D cycles as per the AP testing condition, macropores of diameter 10^4 Å increased, and the broad pore peak developed in the 10 months

cured soil over pores smaller than 3000 Å was narrowed down during the W-D cycles (Fig. 6-5a). These features remained almost similar irrespective of the number of W-D cycles the specimens were subjected. On the other hand, 10 months cured lime-treated soil, despite being subjected to over 17 cycles of W-D as per the RP, showed no significant change in the broad pore peak developed over a pore range smaller than 3000 Å (Fig. 6-5b). A slight insignificant rise in intensities of pores of diameter 10⁴ Å occurred during the W-D cycles.

For specimens subjected to DP, pores smaller than 3000 Å were gradually decreased, and pores of diameter 10⁴ Å increased with an increased number of D-W cycles (Fig. 6-5c).

Using the BJH method, the evolution of cumulative pore volume in the pore range 24-250 Å, which comes under the mesopores range, was analyzed, and presented in Fig. 6-5(d-f).

According to Fig. 6-5(d-f), lime-treated 10 months cured soil showed a significant development of pore volume in the mesopore range 24-250 Å compared to the untreated soil.

For the AP-subjected specimens, after the 5th W-D cycles, the cumulative pore volume in the mesopore range 24-250 Å remained at a similar level with the initial 10 month cured specimen (Fig. 6-5d). However, after the 9th W-D, these cumulative pore volumes increased by about 1.3 times compared to the initial specimen. Further increase in W-D cycles, *i.e.*, after the 13th and 17th W-D cycles, has resulted in a decrease in the cumulative pore volume by about 1.5 to 1.6 times compared to the initial specimen.

Specimens that underwent W-D cycles as per the RP testing condition showed a minimal difference in the cumulative pore volume in the mesopore range 24-250 Å over the entire 17 W-D cycles compared to the initial specimen (Fig. 6-5e).

For the DP-subjected soil, the cumulative pore volume in the mesopore range 24-250 Å after the 5th D-W cycles remained at a similar level with the initial specimen (Fig. 6-5f). This feature then gradually decreased by about 1.1 times in the specimen that has suffered the 9th D-W cycles and by about 2 times in the specimen subjected to the 13th D-W cycles. The cumulative pore volume then remained almost similar for the 17th D-W subjected specimen with the 13th D-W subjected soil (Fig. 6-5f).

6.6 Discussions.

The UCS of a lime-treated soil is the resistance to deformation of the compacted soil structure under unconfined compression. This resistance is a resultant of the inter-and intra-aggregates modifications, which are influenced by the water content (Yin et al. 2018) and cementitious compounds (Lemaire et al., 2013; Little, 1995). Thus, during these W-D/D-W cycles, a significant loss or gain in water can modify the inter-aggregate structure of the compacted soil. In the present study, subjecting the lime-treated soil to oven drying at 71°C as per AP testing condition resulted in total loss of moisture content (Fig. 6-2e). This phenomenon has possibly induced a greater contact between soil particles and hence has increased the matric suction of the soil. This has resulted in a significant increase in total suction of the AP-subjected soil compared to the initial soil suction (Fig. 6-3a). Besides, the AP-subjected soil did not show significant evolution of cementitious compounds during the W-D cycle as reflected by the generation of pores smaller than 3000 Å in Fig. 5a-c. Thus, it can be derived that the high UCS developed in the AP-subjected soil was mostly contributed by the high soil suction generated (Fig. 6-1 & Fig. 6-3a). The preceding statement is supported by the less significant evolution of soil suction and UCS in the specimens with similar configuration but were subjected to air-drying. Thus, the soil suction developed in the lime-treated soil during successive W-D/D-W cycles possibly contributes towards the evolution of UCS.

The insignificant soil suction generated in the RP-subjected soil (Fig. 6-3a) during the W-D cycle compared to the initial suction is attributed to only 2% average water content loss during every 17 hours of

air-drying at 22.1-25.2°C (Fig. 6-2d). However, though the average water content loss after each air-drying was higher in the DP-subjected soil compared to the RP-subjected soil, due to longer air-drying of the DP-subjected soil (Fig. 6-2d & f), the suction evolution was comparatively lower in the former than the latter (Fig. 6-3a). This was due to the presence of higher water content in the DP-subjected soil, as the soil suction was measured after the wetting phase of the D-W cycles, while suction measurement was conducted after the drying phase of the W-D cycles in the AP- and RP-subjected soil.

The amplitude of the average volume variations between wetting and drying phases and the overall trend of average volume changes in the specimens over the 17 W-D cycles evolved based on the temperatures and durations of wetting and drying applied as per the three different testing conditions (Fig. 6-2(a-c)). However, the present silty soil does not consist of smectite as a clay mineral, which is mainly responsible for the volume change behavior of soil (Das and Bharat 2016; Gapak et al. 2017). Besides the soil was treated with 2.5% lime, which already subsided the ability of the soil to show considerable volume change (Chittoori et al. 2013, 2018). As a result, the overall trend of average volume variations was insignificant. For the RP-subjected soil, owing to the air-drying at 22.1-25.2°C, which caused a minimum loss in average water content, the amplitude of average volume change in each cycle remained almost insignificant compared to the initial volume of the specimen (Fig. 6-2a). Though DP-subjected soil was also air-dried at 22.1-25.2°C, however, due to 70 hours of drying, which was 53 hours higher than the RP-subjected soil, the amplitude of average volume change was comparatively higher (Fig. 6-2c). However, the complete evaporation of water in the AP-subjected soil caused the maximum average volume loss of the specimen during each oven-drying (Fig. 6-2b).

Durability of a hydraulic earth structure is interlinked with the ability of water to flow into the structure. Water flow level can be quantified by the velocity of wetting front developed during infiltration of water into the structure during the W-D cycles created by the in-situ water fluctuations. A greater wetting front velocity increases the dampness of the structure and causes the structure to collapse due to loss in mechanical strength (Jia et al. 2009; Johansson and Edeskär 2014). Besides, lime-treated soil is prone to leach more lime if subjected to a greater wetting front velocity (Chittoori et al. 2013; Hara et al. 2008). Thus, considering the wetting front velocity of water as an important parameter, the same was estimated herein for the specimens subjected to W-D/D-W cycles as per the different testing conditions. Using the average increase in the volume of the specimens during each wetting of the W-D/D-W cycles, the average volume flow rate of water (Q) was calculated. From the Q , the average velocity of wetting front (W_f) into the specimens was estimated as per Equation 6-1.

$$W_f = Q/A = V_i/A \times t \quad \text{(Equation 6-1)}$$

where Q is the average volume flow rate of water into the specimens in m^3/s ; V_i is the increase in the average volume of the specimens during each wetting in m^3 ; t is the duration of wetting during each cycle in s; W_f is the average wetting front velocity of water in m/s ; A is the total surface area of cylindrical specimen in m^2 . Since the flow of water into the specimen occurred from all directions during wetting hence, the total surface area of the cylindrical specimen was considered.

Table 6-2 presents the average of the estimated average W_f of water into the specimens subjected to W-D/D-W cycles as per the different testing conditions. Using the estimated average velocity of W_f , the duration required by the infiltrated water to flow to the center of an in-situ structure of reference thickness 1m was obtained (see Table 6-2).

Table 6-2 Estimated average velocity of wetting front and duration required by infiltrated water to flow to the center of a reference in-situ structure

Testing conditions	Average W_f (m/s)	Duration to reach the center of a 1m reference thickness in-situ structure (years)
AP	3×10^{-09}	05
RP	1×10^{-09}	13
DP	9×10^{-09}	02

The average W_f caused during wetting of the W-D/D-W cycles was maximum for the DP- followed by AP-, and then RP-subjected soil (Table 6-2). Correspondingly, the duration estimated for the water to invade the center of an in-situ structure was maximum for RP- followed by AP-, and then DP-subjected soil. Thus, Table 6-2 evidence that lime-treated soil exhibiting similar configuration on being subjected to W-D/D-W cycles conducted as per different testing conditions can show different W_f which can lead to a difference in the durability of the structures. However, interestingly, the W_f was higher in the DP-subjected soil compared to the AP-subjected soil, though the AP-subjected soil underwent complete evaporation of water during each drying (Fig. 6-2e). Such an evolution was noticed due to greater amplitude of average volume increase, *i.e.*, swelling during wetting in the DP-compared to the AP-subjected soil (Fig. 6-2b & c). Studies have reported that oven-drying of soil cause soil aggregation and loss in plasticity, thus, resulting in a reduction of the swelling potential of soil (Basma et al. 1994; Sunil and Deepa 2016). Thus, in the present case, it might be probably due to the preceding statement the swelling was relatively lowered in the AP-subjected soil due to oven-drying. Since the W_f was estimated based on the increase in volume during each wetting thus, it occurred to be lower in the AP- than the DP-subjected soil. Thus, oven-drying of soil may cause an underestimation of the W_f .

Specimens subjected to W-D/D-W cycles showed Ca leaching, which was significantly lower than the Ca content estimated to be present in the soil during sample preparation (Fig. 6-4a). This is attributed to the consumption of Ca by the pozzolanic reactions during the 10 months curing, thus, probably leaving a limited soluble Ca in the soil. Also, the limited contact of the soil structure with water during wetting, which mostly exposes the outer layer of the compacted soil to leach comparatively higher amount of minerals than the internal soil structure, has led to presence of such lower Ca concentration in the effluent. However, despite the fact that the RP-subjected soil was exposed to longer wetting hours than the corresponding AP-subjected soil, the leaching of Ca and EC measured was comparatively higher in the latter than the former (Fig. 6-4a & b). Such an evolution was due complete drying of the AP-subjected soil because of oven-drying, thus, making the soil more vulnerable to loss of minerals during wetting. However, due to only 2 hours of contact of the specimens with water during each wetting as per the DP testing condition, the loss in Ca and the measured EC remained relatively lower (Fig. 6-4a & b).

Additionally, according to Fig. 6-4a & b, the trend observed in the evolution of Ca and EC was almost equivalent. Fig. 6-6 presents the obtained linear trend for the Ca and EC evolution in the W-D/D-W subjected specimens. Such an observation demonstrates the important role of Ca component on controlling the EC evolution of the lime-treated soil. Thus, EC can be used as an important parameter to assess the leaching process of Ca occurring during the W-D/D-W cycles.

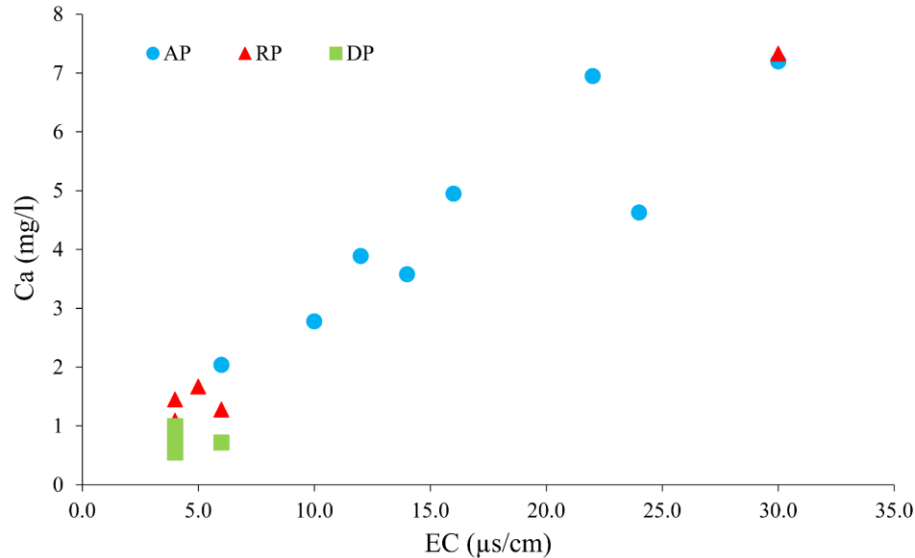


Fig. 6-6 Comparative evolution of calcium concentration and electric conductivity in the specimens subjected to W-D/D-W cycles.

The above discussion shows that specimens subjected to RP testing condition exhibited an insignificant change in soil suction (Fig. 6-3a), minimum volume and water content variations (Fig. 6-2a & d), minimum Ca loss, and EC evolution (Fig. 6-4). Thus, the soil pH remained almost unchanged compared to the initial soil pH (Fig. 6-3b), despite being subjected to 17 W-D cycles. The preceding feature favored the conservation of cementitious bonding formed in the 10 months cured soil as evidenced by the almost similar presence of smaller pores lower than 3000 \AA (Fig. 6-5b) and mesopores volume (Fig. 6-5b) in the RP-subjected soil. On the other hand, a gradual loss in soil pH up to less than 10 from initial soil pH 11.86 (Fig. 6-3b) occurred in the AP- and DP-subjected specimens. Fig. 6-5a & c showed that the significant evolution of pores smaller than 3000 \AA in the initial specimen decreased, and macropores at 10^4 \AA increased. The former feature evidenced the possible loss in cementitious bonding, which contributed to the decrease in soil pH, and the latter was probably due to soil shrinkage, thus, inducing cracks and increasing the macropores. In addition to the loss in cementitious bonding, the observed loss in soil pH in the AP and DP submitted soil can also be a consequence of a possible carbonation, as reported in previous studies (Deneele et al. 2021; Xu et al. 2020).

However, the observed decrease in pores smaller than 3000 \AA compared to the one available in the 10 months cured soil was more significant in the DP- compared to the AP-subjected soil during the D-W and W-D cycles, respectively. Owing to the subjecting of specimens to high temperature during each drying, accelerated-pozzolanic reactions were induced (Little 1995; Wang et al. 2017), which probably have resulted in the presence of more pores smaller than 3000 \AA in the AP-subjected soils. The preceding statement was evidenced by the pore structure analyzed by both MIP and BJH in Fig. 6-5a & d, where the pores smaller than 3000 \AA increased after the 9th cycle in the AP-subjected soil. Such a feature was missing in the specimens subjected to other testing conditions. Thus, such a phenomenon explains that 5 hours of wetting duration followed by oven-drying at 71°C provide sufficient water to reactivate the generation of cementitious compounds in the AP-subjected soil. Thus, such an evolution can overestimate the actual cementitious compounds that can be expected from an in-situ lime-treated soil subjected to W-D cycle.

Additionally, the gradual decrease in pores smaller than 3000 Å with increased D-W cycles in the DP-subjected soil can be attributed to only 2 hours contact of the lime-treated soil with water during each wetting (Fig. 6-5c & f). This is evident from the maintenance of cementitious compounds in the RP-subjected soil (Fig. 6-5b & e), which was subjected to 5 hours of wetting under a same testing environment (temperature and RH), as the DP-subjected soil. Thus, the duration of wetting hours implemented during the W-D/D-W cycles significantly influence the maintenance of cementitious compounds.

6.7 Conclusions.

The physicochemical properties and microstructure modification that underlines the mechanism governing the UCS evolution in lime-treated soil subjected to W-D/D-W cycles as per different testing conditions were evaluated. Following conclusions were derived based on the evaluations:

- 1) The soil suction generated in the lime-treated soil during successive W-D/D-W cycles contributes towards the UCS evolution. Lime-treated soil subjected to W-D/D-W cycles did not show any significant generation of cementitious compounds compared to the one that evolved during curing time. However, the total loss in water content during the oven-drying of the AP-subjected soil induced a greater soil-particles contact, which increased the soil suction and resulted in up to about 3 times greater UCS in the AP-subjected soil. At the same time, the corresponding UCS and suction evolution remained insignificant in the soil subjected to testing conditions that represent a situation close to the field condition.
- 2) Wetting front velocity of water in specimens during W-D/D-W cycles is an important index to estimate the duration taken by infiltrated water to invade an in-situ hydraulic structure, which is interlinked with the durability of such structure. Soil subjected to W-D/D-W cycles as per different testing conditions exhibited different wetting front velocities. DP-subjected soil showed 3 times greater wetting front velocity than the AP-subjected soil. At the same time, RP-subjected soil showed 3 times lower wetting front velocity than the AP-subjected soil.
- 3) The leaching of calcium from specimens exposed to W-D/D-W cycles is mainly regulated by the exposure of the soil structure to the water during wetting. Since such exposure was mainly limited to the external surface of the specimens thus, the overall leaching of calcium remained significantly low, regardless of the testing conditions they are subjected to.
- 4) Oven-drying of AP-subjected soil at 71°C makes the soil comparatively more prone to leach minerals during the wetting phase. Thus, the leaching of calcium and the electric conductivity measured in the effluent obtained from the AP-subjected specimens was comparatively higher than the specimens subjected to the RP testing condition.
- 5) A similar trend of *Ca* and EC evolution occurred in the lime-treated soil submitted to the W-D/D-W cycles, thus, demonstrating *Ca* as a controlling component on the EC evolution of the lime-treated soil. Thus, EC can be used as an important parameter to assess the leaching process of *Ca* occurring during the W-D/D-W cycles.
- 6) Re-wetting of lime-treated soil followed by oven-drying at 71°C during each cycle of the W-D cycles induced pozzolanic reactions, which potentially overestimates the actual cementitious compounds that can

be expected from an in-situ lime-treated soil subjected to W-D cycle. As a result, though loss of calcium and soil pH in the AP-subjected soil was comparatively higher, pores smaller than 3000 Å, which evolved due to lime treatment seems to be less affected.

7) The maintenance of cementitious compounds in lime-treated soil subjected to W-D/D-W cycles is significantly influenced by the wetting hours implemented under the same testing environment (temperature and RH). RP-subjected soil being in contact with water for 7 hours, maintained the cementitious bonding formed during the 10 months curing, while the same was gradually lost in the DP-subjected soil during the successive D-W cycles, which remained only for 2 hours in contact with water.

The results emphasized the fact that the important role of physicochemical and microstructural modifications should be considered while investigating the UCS evolution in lime-treated soil subjected to W-D/D-W cycles instigated by different testing conditions. Besides, to have a close prediction of in-situ UCS evolution in lime-treated soil, reproduction of laboratory testing conditions that makes a close representation of the field situation is essential. In addition to the present study, further studies should be made (i) to evaluate the influence of the W-D/D-W cycle on lime-treated soil that represents a situation similar to the one produced by wave effects on harbors, levees, *etc.* during boat movements, (ii) to investigate how such a difference in testing condition can affect the carbonation of the lime-treated soil. However, based on the present results, it can be said that lime-treated structure can maintain a longer durability in regions exhibiting longer rainy periods compared to the one with longer dry periods.

Chapter 7

INFLUENCE OF WETTING FLUIDS ON THE COMPRESSIVE STRENGTH, PHYSICOCHEMICAL, AND PORE-STRUCTURE EVOLUTION IN LIME-TREATED SOIL SUBJECTED TO WETTING AND DRYING CYCLES (PROPOSAL 5).

Das, G., Razakamanantsoa, A., Herrier, G., & Deneele, D. Influence of wetting fluids on the compressive strength, physicochemical, and pore-structure evolution in lime-treated silty soil subjected to wetting and drying cycles. (*Submitted to Bulletin of Engineering Geology and the Environment*).

General.

Chapter 6 showed that lime-treated soils underwent infiltration of water during the wetting phase of the W-D cycles. This infiltration of water, measured as the wetting front velocity, W_f of water, is dependent on the testing conditions of W-D cycles applied.

Considering the above phenomenon, an atmospherically exposed lime-treated structure is subjected to infiltration of water from different natural sources. This natural water can be constituted of several organic compounds or inorganics compounds or a mixture of both, which control the pH level of the water (Erlandsson et al., 2010; Stockdale et al., 2016). Thus, the chemical nature of such infiltrated water can modify the improvement of the lime-treated soil since soil pH in a lime-treated structure contributes greatly towards the maintenance of the long-term performance of the concerned structure, as shown in Chapter 3. Thus, subjecting the lime-treated soil to extreme W-D cycles accompanied by a wetting fluid of different chemical nature might impact the soil pH and can modify the long-term performance. Such a possibility remained less investigated.

In this context, the present chapter is focused on investigating the influence of different wetting fluids on the behaviors of lime-treated soil. Four different wetting fluids that are commonly used in the laboratory and that exhibit divergent nature from each other were selected. They were an organic solvent: methyl methacrylate (MMA); a low and a high salt concentration solution: 0.10 M NaCl and 0.60 M NaCl solutions; and demineralized water (DW).

MMA is used to investigate several aspects of soil geotechnical behaviors. For instance, MMA was used: (i) to reduce swelling potential in highly swellable clay soil (Massat et al., 2016; Mirzababaei et al., 2009); (ii) as a binder to improve the California Bearing Ratio strength in dune sand (Homauoni and Yasrobi, 2011) and compressive strength of cement-clay grouts (Anagnostopoulos, 2007). Interactions of salt solutions (NaCl) of different molar masses with lime-treated soil were reported in previous studies (Davoudi and Kabir, 2010; Sikora et al., 2019; Wang et al., 2018). Liu et al. (2018) demonstrated that the use of salt content from 0.5% to 1.0% enhances the UCS in lime-treated clay soil. However, increasing the salt content by more than 1.0% negatively impacts the UCS evolution. On the contrary, Karim et al. (2017) showed that the UCS of lime-fly ash treated sand increase linearly with an increase in NaCl up to 8%, which is much higher than 3.5% NaCl that corresponds to 0.60 M NaCl.

The above studies show that either the use of MMA and NaCl is limited to only clay and sand or to soil treated with binders other than lime. Besides, these investigations available are mostly limited to macroscale studies. Thus, this chapter aims to evaluate the influence of MMA and NaCl of different concentrations on silty soil treated with lime. DW was used as a reference fluid since it is commonly

employed in almost all kinds of studies associated with lime-treated soil. The first part of the study demonstrates the influence of different wetting fluids on the UCS evolution of lime-treated silty soil at the end of 5 wetting and drying cycles. Later the influence of wetting fluids on the evolution of physicochemical properties and microstructural modifications were presented.

7.1 Materials and Methodologies.

7.1.1 Soil, Lime, and fluid properties.

Similar to other studies, MLD soil and quicklime was used in this study. 2.5% quicklime was used for soil preparation. The pH and Electric Conductivity (EC) of the chosen wetting fluids are presented in Table 7-1.

Table 7-1 The pH and Electric Conductivity of wetting fluids.

Fluids	pH	Electric Conductivity ($\mu\text{S}/\text{cm}$)
MMA	5.80	0.0
0.10 M NaCl	8.41	20300.0
0.60 M NaCl	8.74	60300.0
DW	7.40	4.0

7.1.2 Sample preparations

The maximum dry density and Optimum Moisture Content (OMC) of the 2.5% lime-treated silt obtained as per ASTM D698-91 (ASTM 2012) were presented in Table 2-4.

Specimens prepared at the wet moisture content (WMC) ($=1.1 \cdot \text{OMC}$) were used in this study, since it allows maintaining a compaction moisture content similar to the in-situ study reported in Chapter 3. The process of sample preparation is similar to the one presented in section 2.2.3 of Chapter 2. Cylindrical lime-treated specimens of dimensions 0.10 m height and 0.05 m diameter were prepared by Standard static compaction at WMC.

A total of 10 specimens was prepared, which includes two duplicates for each soil configuration. After compaction, specimens were wrapped in plastic film and cured for 28-days at a laboratory temperature of 20 ± 1 °C.

7.1.3 Laboratory tests

On completion of the curing period, specimens were subjected to 5 cycles of W-D as per the procedure mentioned in ASTM D559 (ASTM 2015) using the four different fluids. According to ASTM D559 process, specimens are required to be alternately wetted for 5 hours at room temperature and then be dried for 43 hours in the oven at 71°C. Fig. 7-1 presents a picture showing the placement of the specimens in four different fluids for 1st wetting. In Fig. 7-1, 35 g NaCl corresponds to 0.60 M NaCl, referred herein.



Fig. 7-1 Lime-treated specimens placed in four different fluids for 1st wetting during the W-D cycles.

The mass and volume of each specimen after each cycle were recorded using a weighing machine and Vernier caliper, respectively. Specimens were periodically turned during the W-D cycles to ensure homogeneity.

After completion of the 5th W-D cycle, each specimen was subjected to UCS test. After UCS, the measurement of the water content of each UCS-subjected specimen was conducted. Specimens were collected after UCS test and are crushed to measure the suction and pH of the soil. The final pH of the fluids that remained in contact with the specimens up to the 5th wetting phase of the W-D cycle, *i.e.*, the effluent, was determined.

About 50 ml of the collected effluent at the end of 5th wetting cycle was subjected to Inductively Coupled Plasma Optical Emission Spectrometry (ICP-OES) analysis for determining the elementary concentrations of Calcium (*Ca*). The analysis of *Ca* concentrations was important to investigate the leaching of lime under the influence of W-D cycles and the wetting fluids.

Pore Size Distribution (PSD) was analyzed by Mercury Intrusion Porosimetry (MIP) test and Barrett-Joiner-Halenda pore (BJH) method (Barrett et al. 1951). The analysis was made on the freeze-dried samples gathered from the 28-days cured specimen and the specimens obtained at the end of 5th W-D cycle. Discussions regarding the classification of pores in this study were provided as per the classifications given by the International Union of Pure and Applied Chemistry (IUPAC) (Rouquerol et al. 1994).

7.2 Results

This section presents the UCS, physicochemical and microstructural evolution in the lime-treated specimens after being subjected to 5 W-D cycles using different wetting fluids. All the evolutions are presented with the respective results obtained with the 28 days cured soil, which was considered as the reference specimen.

7.2.1 UCS evolution at the end of W-D cycle.

Fig. 7-2 pre presents the evolution of UCS in the 5 W-D cycles subjected lime-treated soils.

The UCS of the 28-days cured reference specimen was 0.80 MPa. After 5 successive cycles of W-D, the UCS increased by about 3 times in the specimens subjected to NaCl solutions and MMA solvent. At the same time, the increase in UCS was about 2 times for the DW-subjected specimen.

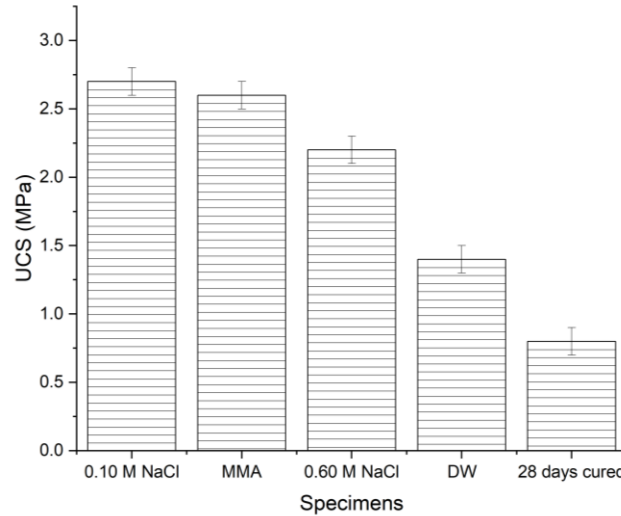


Fig. 7-2 Unconfined Compressive Strength obtained after 5 W-D cycles.

7.2.2 Physicochemical evolution at the end of W-D cycle.

The soil suction and soil pH measured at the end of 5 W-D cycles along with the reference 28 days cured soil is presented in Fig. 7-3.

The soil suction obtained in the reference 28 days cured soil was 0.49 MPa (Fig. 7-3a). After 5 W-D cycles, the soil suction measured was in the range of 290 to 320 MPa for all the specimens subjected to different wetting fluids. The corresponding water content of these specimens is presented in Table 7-2.

The pH of the reference specimen was 11.86 (Fig. 7-3b). After 5 W-D cycles, the minimum decrease in soil pH with respect to the initial soil pH was obtained for 0.60 M NaCl subjected soil, which was 11.2. The soil pH obtained for 0.10 M NaCl, and MMA subjected soil was 10.39 and 10.71, respectively. The maximum decrease in soil pH was observed for the DW-subjected soil, which was 9.77.

Table 7-2 Water content measured during suction measurement.

Specimens	Water content during suction measurement (%)
0.10 M NaCl	0.46
MMA	0.53
0.60 M NaCl	0.55
DW	0.46
28-days cured	20.1

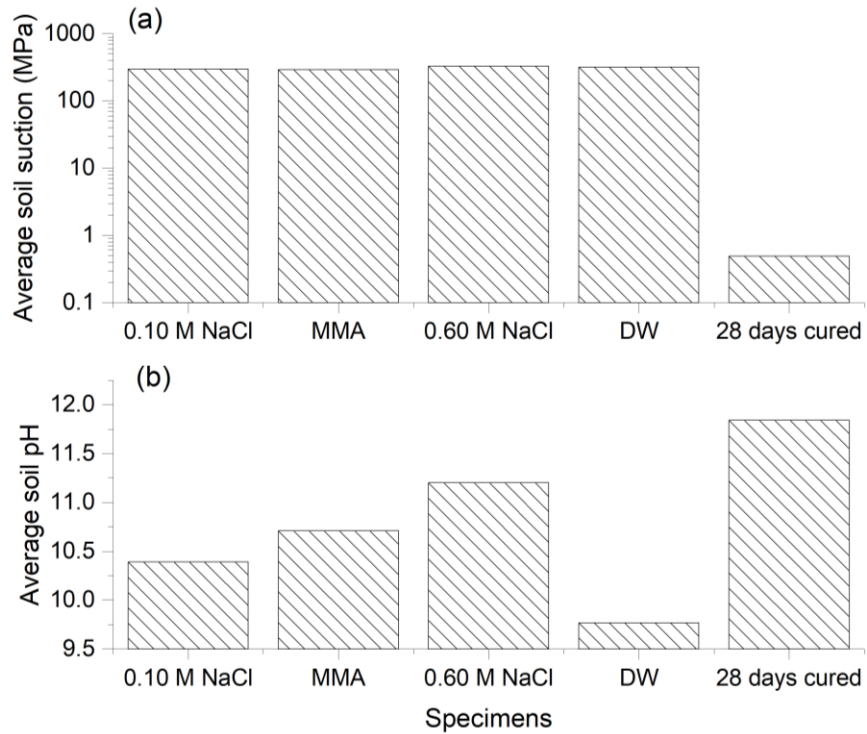


Fig. 7-3 Soil suction and soil pH measured at the end of 5 W-D cycles along with the reference 28 days cured soil.

The final pH of the effluent, measured at the end of the 5th cycle is presented in Fig. 7-4 by comparing the same with the initial pH of the respective fluids.

The final pH obtained from the effluent gathered from the MMA solvent that was in contact with the specimens till the end of 5 W-D cycles remained unchanged compared to the initial pH of the MMA solvent (Fig. 7-4). This pH increased by about 10% in the 0.10 M NaCl and 0.60 M NaCl solutions and increased by 20% in DW after being in contact with the lime-treated soil compared to the initial pH of the respective solutions.

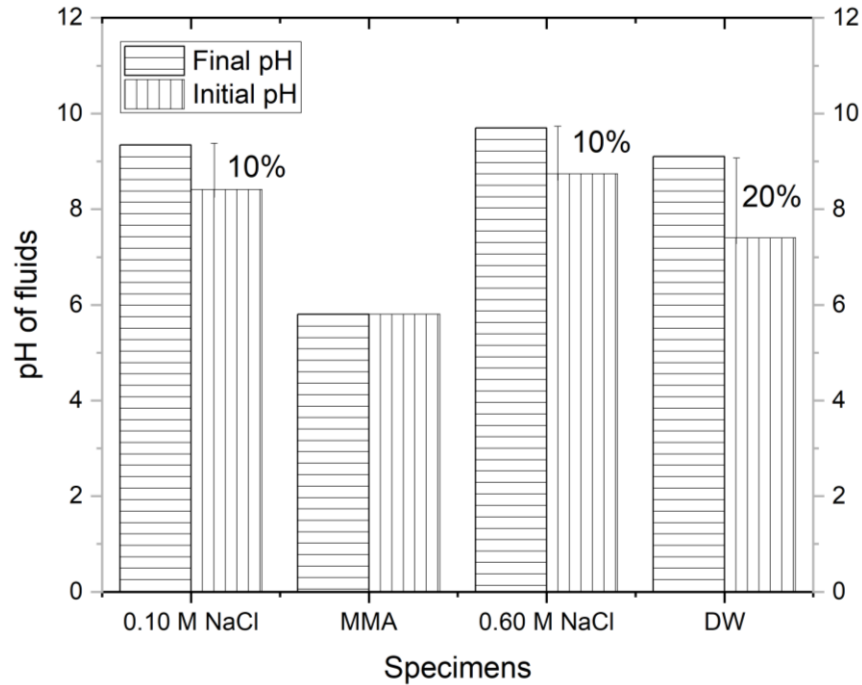


Fig. 7-4 Final pH measured in the effluents and compared with the initial pH of the respective fluids at the end of 5 W-D cycles.

Table 7-3 Cumulative (Cum.) concentration of Ca analyzed in the effluents at the end of 5 W-D cycles in the lime-treated soils.

Soil ID	Cum. Concentration of Ca (mg/l)
MMA	< 0.20
0.10 M NaCl	142.90
0.60 M NaCl	232.48
DW	49.97

Table 7-3 presents the cumulative concentration of Ca analyzed in the effluent collected at the end of 5 W-D cycles. In the effluent obtained from the specimen subjected to MMA solvent, the cumulative Ca concentration was below the limit that can be detected during the ICP-OES test, i.e., < 0.2 mg/l; hence no Ca concentration was found. The maximum cumulative Ca concentration was measured in the effluent gathered from the soil submitted to 0.60 M NaCl, followed by the one submitted to 0.10 M NaCl solution. The effluent collected from the DW subjected lime-treated soil gave the minimum value of cumulative Ca concentration, which was 49.97 mg/l.

7.2.3 Pore structure evolution at the end of W-D cycle.

The evolution of pores in all the specimens at the end of 5 W-D cycle was determined by MIP and was then compared with the untreated and the reference specimens in Fig. 7-5.

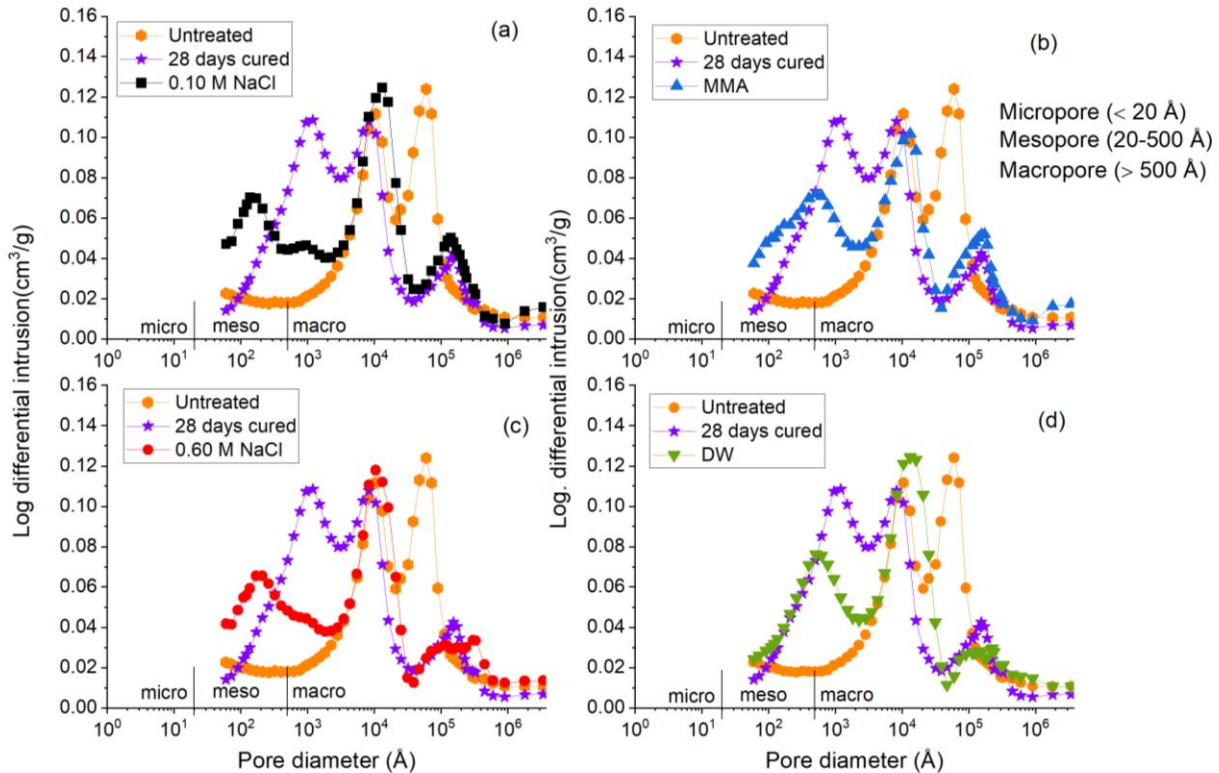


Fig. 7-5 Comparative evaluation of PSD in lime-treated specimens subjected to 0.10 M NaCl (a), MMA (b), 0.60 M NaCl (c), and DW (d) at the end of 5th W-D cycles with the with the untreated and the reference specimens by MIP.

According to Fig. 7-5, untreated compacted specimens showed bi-modal PSD with a peak at macropores diameter 10^4 and 10^5 Å. After 2.5% quicklime treatment and 28-days of curing, no significant presence of macropores greater than 3×10^4 Å was observed, and significant evolution of pores smaller than 3000 Å was observed due to the formation of cementitious bonding. Such an observation was in accordance with the studies reported in previous chapters.

Specimens subjected to 0.10 M NaCl and 0.60 M NaCl solutions showed similar evolution of pore structure at the end of 5 W-D cycles compared to the pore structure of the reference specimen (Fig. 7-5a & c). The macropore peak at 10^3 Å present initially in the reference specimen disappear, and a new mesopore peak at about 10^2 Å was observed in both the NaCl subjected soils. Similar to the NaCl subjected soils, MMA subjected soil showed the reduction of macropore peak presence at 10^3 Å and generation of mesopore peak at about 5×10^2 Å compared to the reference specimen (Fig. 7-5b).

At the same time, DW-subjected specimen showed a decrease in pores smaller than 3000 Å, which was formed due to lime treatment in the reference specimen (Fig. 7-5d).

The evolution of cumulative pore volume in the mesopore range 24-250 Å was analyzed by BJH at the end of 5 W-D cycles and is presented in Fig. 7-6 by comparing with the reference and untreated soil.

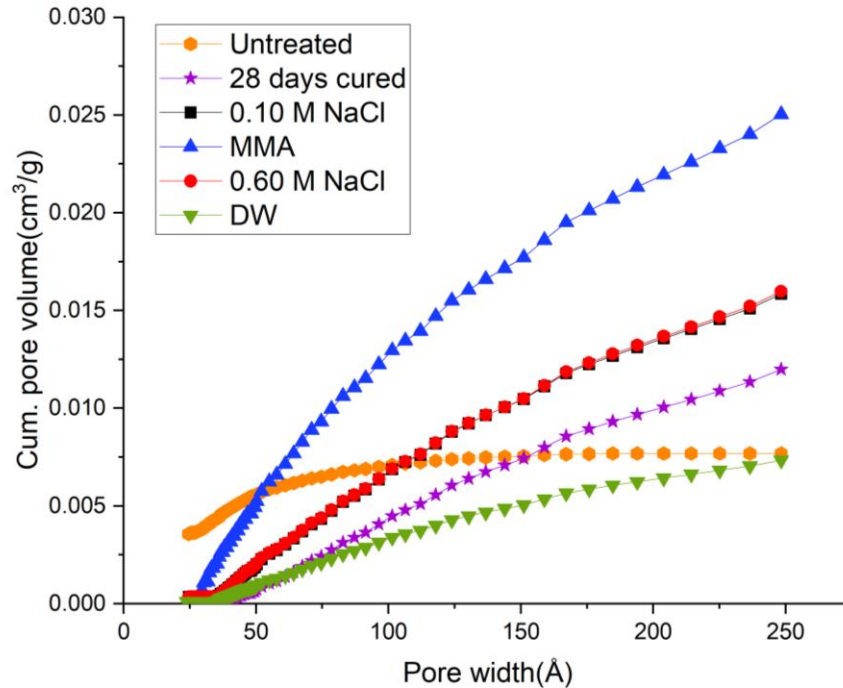


Fig. 7-6 Comparative evaluation of Cumulative (Cum.) pore volume evolution in the mesopore range 24-250 Å in specimens subjected to different fluids at the end of 5 W-D cycles with the reference and untreated soil by BJH.

Fig. 7-6 shows that compared to the reference soil, a significant cumulative pore volume in the mesopore range 24-250 Å was present in the MMA subjected soil, followed by the specimens subjected to NaCl solutions. On the contrary, the cumulative pore volume in the mesopore range 24-250 Å decreased in the DW subjected soil compared to the reference soil.

7.3 Discussions

From the results, it is evident that the UCS, chemical, and microstructural evolution of a similar configured lime-treated soil varies based on the types of wetting fluids the specimens were exposed to.

Although the specimens underwent five successive W-D cycles, the UCS evolved positively in all the lime-treated specimens compared to the reference 28 days cured soil (Fig. 7-2). This extent of UCS evolution in the specimens varied based on the wetting fluids they were subjected to; the maximum being obtained with the NaCl- and MMA-subjected soils, with a less significant difference of 0.10 to 0.50 MPa UCS values between respective soils. The evolution of UCS was comparatively lower in the DW-subjected specimen.

Similar to the UCS evolution, the extent of the average soil pH evolution at the end of 5 W-D cycles also varied with the type of wetting fluids they were subjected to (Fig. 7-3b). The average soil pH recorded with all the 5 W-D cycles subjected soils was comparatively lower than the soil pH recorded with the reference 28 days cured soil. This decrease in the average soil pH can be linked with the loss of OH⁻ ions from the soil during the wetting-drying cycles. Such a phenomenon was confirmed by the 10% and 20%

rise in final pH in the NaCl solutions and the DW, respectively (Fig. 7-4). However, the final pH of the effluent obtained from MMA-subjected soil remained constant (Fig. 7-4).

The difference in average soil pH was minimum between the 0.10 M NaCl, MMA, and 0.60 M NaCl subjected soils and the reference specimen and remained between 10.39 to 11.2 (Fig. 7-3b). However, the maximum decrease was observed in the DW subjected soil, where the pH recorded was about 9.77. This decrease explains the release of more OH⁻ ions from the DW-subjected soil, thus increasing the final pH of the effluent by 20%, as seen in Fig. 7-4.

On observing Table 7-3, the differences observed in the measured cumulative Ca concentrations between the effluents gathered from the 0.10 M NaCl-, 0.60 M NaCl- and DW-subjected specimens again emphasized the influence of the nature of the surrounding medium. The maximum cumulative Ca concentration occurred to be in the effluent obtained from the 0.60 M NaCl subjected soil, followed by 0.10 M NaCl-subjected soil and then DW subjected soil. However, similar to the constant final pH attained in the effluent obtained from the MMA-subjected soil (Fig. 7-3b), no significant cumulative Ca concentration was recorded (Table 7-3).

In addition to the changes brought in the strength and chemical properties of the lime-treated soil owing to subjection to different wetting fluids, modifications in the soil pore structure also occurred. The MIP analysis presented in Fig. 7-5 evidenced the decrease in macropore at peak 10^3 \AA and initiation of mesopore in the NaCl- and MMA-subjected soil compared to the reference soil. The significant initiation of mesopore evolution was confirmed in the BJH analysis, which provides a cumulative pore volume evolution in the mesopore range 24-250 \AA in Fig. 7-6. The maximum evolution of cumulative pore volume in the mesopore range 24-250 \AA in the MMA subjected soil indicates the certain probability of MMA interacting with the lime-treated soil components. However, such a feature was missing in the DW subjected specimen (Fig. 7-5 & Fig. 7-6). Such a difference indicates that subjecting lime-treated soil to NaCl solutions and MMA solvent favoured the mesopore evolution compared to DW. The evolution of mesopores in lime-treated soil was shown to be a benefit towards the long-term performances of lime-treated soil in the studies reported in previous chapters.

Except for the strength, chemical, and microstructural modification, it's the average soil suction that remained the same regardless of the wetting fluids the specimens were subjected to (Fig. 7-3a). Such an evolution indicates that the evolution of high soil suction in the range of 290 to 320 MPa for all the W-D cycles subjected specimens was triggered mainly by oven-drying at 71°C, which reduced the water content in the soil almost to zero (Table 7-2).

7.4 Conclusions

The influence of different wetting fluids on the UCS, physicochemical, and microstructural evolution of 2.5% quicklime treated silty soil during five successive W-D cycles were evaluated. Based on the investigation, the following conclusions are derived:

- 1) Regardless of the types of wetting fluids lime-treated soil was subjected to, the UCS evolved at the end of 5 W-D cycles compared to the reference 28 days cured soil. The extent of UCS evolution varied with the types of wetting fluids the specimens were exposed to. About 3 times higher UCS was obtained with lime-treated specimen subjected to NaCl solutions and MMA solvent with an insignificant difference of 0.10 to 0.50 MPa UCS values between respective soils. The evolution of UCS was comparatively lower in the DW-subjected specimen.

2) The average pH of the lime-treated soils decreased during the W-D cycles compared to the reference soil pH. This decrease in average soil pH was from 11.86 to 11.2 and 10.39 for the 0.60 M- and 0.10 M-NaCl-subjected soils, respectively. For MMA-subjected soil, the average soil pH decreased to 10.71. However, a comparatively greater decrease in average soil pH up to 9.77 occurred in the DW-subjected soil, thus, leading to a comparatively higher increase in the final pH of the effluent.

3) The release of calcium from the lime-treated soil occurs to be governed by the nature of wetting fluids available in the surrounding medium. Maximum calcium was released from the 0.60 M NaCl subjected specimen followed by the 0.10 M NaCl subjected specimen, and then DW subjected soil. No calcium was released in the effluent of the MMA-subjected soil during the W-D cycles.

4) Mesopore evolution in W-D cycles subjected lime-treated soil was dependent on the type of fluids the specimens were exposed to. NaCl solutions and MMA solvent subjected specimens, showed additional development of mesopores compared to the 28 days cured reference specimens. However, DW subjected specimens showed a reduction in the pores smaller than 3000 Å formed in the reference 28 days cured soil due to lime treatment.

5) The type of wetting fluids has a less significant effect on the suction evolution of the W-D cycles subjected lime-treated soils. The evolution of soil suction observed at the end of 5 W-D cycles in all specimens was high and equivalent, which is attributed to the increased soil grain-to-grain contact owing to a total loss in water content during oven-drying at 71°C.

The study highlights that the UCS, physicochemical, and microstructural evolution in the W-D cycles subjected lime-treated silty soil was significantly influenced by the type of wetting fluids the specimens were exposed to. This extent of evolution was unique for each type of wetting fluid. Such an observation indicates the necessity of considering the chemical mechanism between the wetting fluids and lime-treated soil. Future investigations should be on such chemical mechanisms. Thus, the type of fluids used while evaluating the performance of a lime-treated structure should be a close representation of the real fluids available in nature.

Chapter 8

CONCLUSIONS, CONTRIBUTIONS AND FUTURE SCOPE.

General.

The process of soil improvement by lime treatment is composed of mechanical and chemical improvements. Mechanical improvement involves the execution process, and chemical improvement involves the addition of the content of lime, water, and its reaction with the given soil type. Contribution of lime towards the enhancement of hydromechanical performances in the soil is extensively investigated at laboratory scale under controlled conditions. However, how well the laboratory and in-situ execution process as well the durability evaluation correlate needs additional investigations. This study focuses on emphasizing the importance of reproducing implementation mechanisms and durability testing conditions at laboratory scales similar to the field in order to predict the in-situ performances of lime-treated soil efficiently and effectively.

8.1 Conclusions.

The five proposals presented Table 1-5, has been successfully completed in this study. The study begins with investigating the performance of a full-scale experimental 2.5% lime-treated embankment after 7 years of atmospheric exposure from treatment. The investigation confirmed the long-term existing benefits of lime treatment in terms of compressive strength, physicochemical, and microstructure evaluation. The field investigation also highlights the importance of implementation technics, which involves kneading action developed in the soil during in-situ compaction. Thus, affect of kneading mechanism, which was less studied at laboratory scale was investigated on the hydromechanical and pore structure evolution of lime-treated soil. Again, considering the fact that a lime-treated earth structure is often exposed to uncontrolled stresses in an environment, the long-term performances of a lime-treated soil at laboratory scale was studied. This study involves subjection the soil to wetting-drying cycles testing conditions developed to represent a situation closer to the field. Following are the major conclusions derived from this study:

- Even after 7 years of damp atmospheric exposure, the effect of 2.5% quicklime persists throughout the core of the lime-treated embankment. This effect was evidenced by the availability of pH greater than 11, presence of cementitious bonding through SEM and pore structure analysis. Consequently, an enhanced water retention capacity was maintained throughout the embankment, and a UCS level of 3.29 MPa was observed in sampled specimens.
- Up to about 0.12 m depth from the surface of the 2.5% quicklime treated embankment, *i.e.*, in the sacrificial layer, the effect of lime was lost due to long-term soil-atmospheric interactions and development of vegetation roots. This was evidence by a maximum loss of 12% and 18% in the water content and pH, respectively, in the upper layer sampled soil compared to the one sampled from the core of the embankment.

- Effect of the compaction mechanism implemented during the preparation of lime-treated soil plays a vital role in long-term UCS evolution. ‘Kneading action’, *i.e.*, the compaction mechanism often practiced during compaction of in-situ fine-grained lime-treated soil, enhances lime dispersion as evidenced by μ -XRF images. Such a feature accompanied by available water contributes to long-term pozzolanic reactions, and hence UCS evolution.
- In addition to UCS, the compaction mechanism also defines the magnitude of hydraulic conductivity in lime-treated soil. Kneading action caused greater aggregate deformation than static compaction and decreased the number of macropores of diameter 10^5 \AA . As a result, the kneaded soil resulted with about 2 orders of lower magnitude of k compared to the statically compacted soil. A lower magnitude of hydraulic conductivity gives a higher hydraulic tortuosity, which demonstrates the longer pore fluid-soil structure contact during percolation in kneaded soil. Such a feature favored the development of cementitious compounds in the long-term.
- The chemistry of pore fluid percolated through a given compacted lime-treated soil significantly affects the hydromechanical evolution. A pore fluid such as demineralized water, which is a deficit of ions, can cause greater dissolution of calcium from cementitious compounds compared to the concentration of calcium that can be dissolved under the impact of a low-ionic strength solution.
- Evaluation of hydraulic conductivity in lime-treated compacted soil should be made in terms of the number of PVF rather than the percolation time. The life expectancy of a lime-treated soil structure is governed by its hydromechanical performances, which is dependent on the pore fluid-soil structure interactions, which is considered during interpretation of k in terms of the number of PVF.
- Soil treated at LMO has limited contribution towards the long-term hydromechanical performances of lime-treated soils.
- The testing conditions implemented during the evaluation of W-D cycles' effect on lime-treated soil significantly govern the physicochemical, microstructural, and UCS evolution in lime-treated compacted soil. Oven-drying lime-treated compacted soil at 71°C (elevated temperature) caused significant suction development. This has led to an overestimated UCS value compared to the one obtained with similar specimens subjected to air-drying, though the cementitious bonding evolution was lower in the oven-dried than the air-dried soils.
- In addition to the temperature influence, the nature of wetting fluids that interact with lime-treated compacted soil during W-D cycles significantly affects the physicochemical, microstructural, and UCS evolution. The evolution in UCS, average soil pH, leaching of calcium, and evolution of pores smaller than 3000 \AA is uniquely defined by the type of fluid the specimens were exposed to. However, the soil suction remained less effected by the nature of the wetting fluids.

Thus, the study concludes that the selected compaction procedure and the permeant solution in the laboratory scale must be representative of the compaction mechanism and pore water that the structure is likely to be subjected to in the field. This will help to have a close prediction of the long-term hydromechanical performance of in-situ lime-treated structures. Besides, reproduction of laboratory testing

conditions that makes a close representation of the field situation is essential during the evaluation of W-D cycles' impact on lime-treated soil.

8.2 Contributions.

Major scientific contributions from this study are:

- Reproduction of compaction mechanism and permeant fluids at laboratory scale, which mimic a closer representation of the field in-situ compaction and pore fluids exposure is of vital importance while evaluating the hydromechanical performances in lime-treated fine-grained soil.
- Reproduction of wetting and drying testing conditions which considers the temperature and nature of wetting fluid effects is essential to evaluate the long-term performances of lime-treated soil. Such an effect brings significant changes in the soil physicochemical and microstructure properties, which brings a major change in the soil strength evolution.

Laboratory contributions from this study are:

- A compaction device was proposed to implement the field kneading action at laboratory scale and validated using field results.
- A regulated device to simulate the in-situ wetting and drying conditions in compacted soils was proposed and submitted for Patent approval.

8.3 Future scope.

Some possible future scope derived from this study are as follows:

- This study emphasized the role of compaction mechanisms towards hydromechanical performances of lime-treated soil. In this context, in addition to kneading action, the influence of rolling action should also be investigated in lime-treated soil, since in-situ soil on being subjected to Padfoot roller experiences both kneading and rolling actions simultaneously.
- Chapter 7 highlights that exposing lime-treated soil to fluids of different nature can bring changes in strength, physicochemical, and microstructure of the subjected soil, unique for each fluid. However, the chemical interactions of each type of fluid with the lime-treated soil is not investigated in this study. Such an investigation should be made to evaluate the mechanism that cause change in properties of lime-treated soil during W-D cycles.
- Also provided that pore-fluid nature modifies the hydromechanical performances of lime-treated soils, effect of sea water on the performances of lime-treated hydraulic structures should be investigated.

BIBLIOGRAPHY

- Addiscott, T.M., Wagenet, R.J., 1985. Concepts of solute leaching in soils: a review of modelling approaches. *Journal of soil science*, 36(3), pp.411-424. <https://doi.org/10.1111/j.1365-2389.1985.tb00347.x>
- Adefemi, B.A., Wole, A.C., 2013. Regression analysis of compaction delay on CBR and UCS of lime stabilized yellowish brown lateritic soil. *Electronic Journal of Geotechnical Engineering (EJGE)* 18, 3301–3314.
- Ajayi, E.S., 2012. Effect of Lime Variation on the Moisture Content and Dry Density of Lateritic Soil in Ilorin, Nigeria.
- Akcanca, F., Aytakin, M., 2014. Impact of wetting–drying cycles on the hydraulic conductivity of liners made of lime-stabilized sand–bentonite mixtures for sanitary landfills. *Environmental Earth Sciences* 72, 59–66. <https://doi.org/10.1007/s12665-013-2936-4>
- Akula, P., Hariharan, N., Little, D.N., Lesueur, D., Herrier, G., 2020. Evaluating the Long-Term Durability of Lime Treatment in Hydraulic Structures: Case Study on the Friant-Kern Canal. *Transportation Research Record* 0361198120919404. <https://doi.org/10.1177/0361198120919404>
- Ali, H., Mohamed, M., 2018. The effects of lime content and environmental temperature on the mechanical and hydraulic properties of extremely high plastic clays. *Applied Clay Science* 161, 203–210. <https://doi.org/10.1016/j.clay.2018.04.012>
- Ali, H., Mohamed, M., 2019. Assessment of lime treatment of expansive clays with different mineralogy at low and high temperatures. *Construction and Building Materials* 228, 116955. <https://doi.org/10.1016/j.conbuildmat.2019.116955>
- Ali, H., Mohamed, M., 2017. The effects of compaction delay and environmental temperature on the mechanical and hydraulic properties of lime-stabilized extremely high plastic clays. *Applied Clay Science* 150, 333–341. <https://doi.org/10.1016/j.clay.2017.09.019>
- Allen, R., Sun, S., 2017. Computing and comparing effective properties for flow and transport in computer-generated porous media. *Geofluids*. <https://doi.org/10.1155/2017/4517259>
- Al-Mukhtar, M., Khattab, S., Alcover, J.F., 2012. Microstructure and geotechnical properties of lime-treated expansive clayey soil. *Engineering geology* 139, 17-27. <https://doi.org/10.1016/j.enggeo.2012.04.004>
- Al-Mukhtar, M., Lasledj, A., Alcover, J.-F., 2010. Behaviour and mineralogy changes in lime-treated expansive soil at 20 C. *Applied clay science* 50, 191–198. <https://doi.org/10.1016/j.clay.2010.07.023>
- Al-Neaimi, M.S., Ahmad Hussain, H., 2011. Some Engineering Characteristics of Lime-Treated Soil of Semeel Region with Emphasis on Compaction Delay. *Al-Rafidain Engineering Journal (AREJ)* 19(5), 12-27. <http://dx.doi.org/10.33899/rengj.2011.26742>
- Al-Rawas, A.A., Goosen, M.F. eds., 2006. *Expansive soils: recent advances in characterization and treatment*.

- Anagnostopoulos, C.A., 2007. Cement–clay grouts modified with acrylic resin or methyl methacrylate ester: Physical and mechanical properties. *Construction and Building Materials*, Elsevier 21(2), 252–257. <https://doi.org/10.1016/j.conbuildmat.2005.12.007>
- Arandigoyen, M., Bicer-Simsir, B., Alvarez, J.I., Lange, D.A., 2006. Variation of microstructure with carbonation in lime and blended pastes, *Applied surface science*. 252, 7562–7571. <https://doi.org/10.1016/j.apsusc.2005.09.007>
- Army Corps of Engineers, 1984. Engineering and design-airfield flexible pavement-mobilization construction, Engineering Manual. Washington, DC, USA: Department of the Army Corps of Engineers Office of the Chief of Engineers. 1110, 3–141.
- Asgari, M.R., Dezfuli, A.B., Bayat, M., 2015. Experimental study on stabilization of a low plasticity clayey soil with cement/lime. *Arabian Journal of Geosciences* 8, 1439–1452. <https://doi.org/10.1007/s12517-013-1173-1>
- ASTM-C42-77., 1978. Standard method of obtaining and testing drilled cores and sawed beams of concrete. American Society for Testing and Materials, West Conshohocken, PA, USA.
- ASTM D2487-17e1, 1984. Standard Practice for Classification of Soils for Engineering purposes (Unified Soil Classification System).
- ASTM-D559, 2015. Standard test methods for wetting and drying compacted soil-cement mixtures.
- ASTM D6276-99a, 2006. Standard test method for using pH to estimate the soil-lime proportion requirement for soil stabilization. Annual book of ASTM Standards.
- ASTM, D2166., 2006. Standard test method for unconfined compressive strength of cohesive soil. American Society for Testing and Materials, West Conshohocken, PA, USA.
- ASTM, D2216., 2010. Standard test methods for laboratory determination of water (moisture) content of soil and rock by mass. Annual Book of ASTM Standards.
- ASTM, A, D698-12e2., 2012. Standard Test Methods for Laboratory Compaction Characteristics of Soil Using Standard Effort (12 400 Ft-Lbf/Ft³ (600 KN-m/M³)).
- ASTM, D4972-19, 2019. Standard Test Methods for pH of Soils. West Conshohocken, PA.
- Awad, M., Al-Kiki, I., Khalil, A., 2021. Permeability of Expansive Soils Modified/Stabilized with lime. *Diyala Journal of Engineering Sciences* 14, 129–140. <https://doi.org/10.24237/djes.2021.14212>
- Babu, N., Poulouse, E., 2018. Effect of lime on soil properties: A review. *microbiology* 5.
- Baghdadi, Z.A., Fatani, M.N., Sabban, N.A., 1995. Soil modification by cement kiln dust. *Journal of Materials in Civil Engineering* 7, 218–222. [https://doi.org/10.1061/\(ASCE\)0899-1561\(1995\)7:4\(218\)](https://doi.org/10.1061/(ASCE)0899-1561(1995)7:4(218))
- Bagonza, S., Peete, J.M., Newill, D., Freer-Hewish, R., 1987. Carbonation of stabilised soil-cement and soil-lime mixtures--developing countries: highway construction. Proc. of seminar held at the PTRC transport & planning summer annual meeting, Bath Univ. England 7-11 September 1987, Volume P295. Publication of: PTRC Education & Research Services Limited.

- Baldovino, J. de J.A., dos Santos Izzo, R.L., Moreira, E.B., Rose, J.L., 2019. Optimizing the evolution of strength for lime-stabilized rammed soil. *Journal of rock mechanics and geotechnical engineering* 11, 882–891. <https://doi.org/10.1016/j.jrmge.2018.10.008>
- Baldovino, J.A., Moreira, E.B., Izzo, R.L., Rose, J.L., 2018b. Empirical relationships with unconfined compressive strength and split tensile strength for the long term of a lime treated silty soil. *Journal of Materials in Civil Engineering* 30(8). [https://doi.org/10.1061/\(ASCE\)MT.1943-5533.0002378](https://doi.org/10.1061/(ASCE)MT.1943-5533.0002378).
- Baldovino, J.A., Moreira, E.B., Teixeira, W., Izzo, R.L., Rose, J.L., 2018a. Effects of lime addition on geotechnical properties of sedimentary soil in Curitiba, Brazil. *Journal of Rock Mechanics and Geotechnical Engineering* 10(1), 188-194. <https://doi.org/10.1016/j.jrmge.2017.10.001>
- Bandipally, S., Cherian, C., Arnepalli, D.N., 2018. Characterization of lime-treated bentonite using thermogravimetric analysis for assessing its short-term strength behaviour, *Indian Geotechnical Journal*. 48, 393–404, <https://doi.org/10.1007/s40098-018-0305-7>
- Barrett, E.P., Joyner, L.G., Halenda, P.P., 1951. The determination of pore volume and area distributions in porous substances. I. Computations from nitrogen isotherms. *Journal of the American Chemical society* 73, 373–380. <https://doi.org/10.1021/ja01145a126>
- Basma, A.A., Al-Homoud, A.S., Al-Tabari, E.Y., 1994. Effects of methods of drying on the engineering behavior of clays. *Applied Clay Science* 9, 151–164. [https://doi.org/10.1016/0169-1317\(94\)90017-5](https://doi.org/10.1016/0169-1317(94)90017-5)
- Beetham, P., Dijkstra, T., Dixon, N., Fleming, P., Hutchison, R., Bateman, J., 2015. Lime stabilisation for earthworks: a UK perspective. *Proceedings of the Institution of Civil Engineers-Ground Improvement* 168(2), 81-95. <https://doi.org/10.1680/grim.13.00030>
- Beetham, P., Dijkstra, T., Dixon, N., 2014. Lime diffusion and implications for lime stabilization practice (No. 14-5734).
- Bell, F.G., 1996. Lime stabilization of clay minerals and soils. *Engineering geology* 42, 223–237. [https://doi.org/10.1016/0013-7952\(96\)00028-2](https://doi.org/10.1016/0013-7952(96)00028-2)
- Bhattacharja, S.A.N.K.A.R., Bhatta, J.I., Todres, H.A., 2003. Stabilization of clay soils by Portland cement or lime—a critical review of literature. *PCA R&D Serial*, 60(1), 124-33.
- Bhuvaneshwari, S., Robinson, R.G., Gandhi, S.R., 2014. Behaviour of lime treated cured expansive soil composites. *Indian Geotechnical Journal* 44, 278–293.
- Bicalho, K. v, Boussafir, Y., Cui, Y.-J., 2018. Performance of an instrumented embankment constructed with lime-treated silty clay during four-years in the Northeast of France. *Transportation Geotechnics* 17, 100–116. <https://doi.org/10.1016/j.trgeo.2018.09.009>
- Bin, S., Zhibin, L., Yi, C., Xiaoping, Z., 2007. Micropore structure of aggregates in treated soils. *Journal of materials in civil engineering* 19, 99–104. [https://doi.org/10.1061/\(ASCE\)0899-1561\(2007\)19:1\(99\)](https://doi.org/10.1061/(ASCE)0899-1561(2007)19:1(99))
- Brandl, H., 1981. Alteration of soil parameters by stabilization with lime, in: *Proceedings of the 10th International Conference on Soil Mechanics and Foundation Engineering*, Volume 3, Stockholm.

- Brunauer, S., Emmett, P.H., Teller, E., 1938. Adsorption of gases in multimolecular layers. *Journal of the American chemical society* 60, 309–319. <https://doi.org/10.1021/ja01269a023>
- Charles, I., Herrier, G., Chevalier, C., Durand, E., 2012. An experimental full-scale hydraulic earthen structure in lime treated soil. 6th International Conference on Scour and Erosion, Paris, p. 1223–30.
- Chen, M. L., Lv, P. F., Zhang, S. L., Chen, X. Z., Zhou, J. W., 2018. Time evolution and spatial accumulation of progressive failure for Xinhua slope in the Dagangshan reservoir, Southwest China. *Landslides* 15(3), 565-580. <https://doi.org/10.1007/s10346-018-0946-8>
- Cherian, C., Arnepalli, D.N., 2015. A critical appraisal of the role of clay mineralogy in lime stabilization. *International Journal of Geosynthetics and Ground Engineering* 1, 8.
- Chittoori, B.C.S., Puppala, A.J., Wejrungsikul, T., Hoyos, L.R., 2013. Experimental studies on stabilized clays at various leaching cycles. *Journal of Geotechnical and Geoenvironmental Engineering* 139, 1665–1675. [https://doi.org/10.1061/\(ASCE\)GT.1943-5606.0000920](https://doi.org/10.1061/(ASCE)GT.1943-5606.0000920)
- Clegg, B., 1964. Kneading compaction. *Australian Road Research Board Bulletin*, 1.
- Collet, F., Bart, M., Serres, L., Miriel, J., 2008. Porous structure and water vapour sorption of hemp-based materials. *Construction and Building Materials* 22, 1271–1280. <https://doi.org/10.1016/j.conbuildmat.2007.01.018>
- Consoli, N.C, Rosa, A.D, Saldanha, R.B., 2011a. Variables governing strength of compacted soil fly ash-lime mixtures. *Journal of Materials in Civil Engineering* 23(4), 432-440. [https://doi.org/10.1061/\(ASCE\)MT.1943-5533.0000186](https://doi.org/10.1061/(ASCE)MT.1943-5533.0000186)
- Consoli, N.C., Lopes Jr, L.D.S., Prietto, P.D.M., Festugato, L., Cruz, R.C., 2011b. Variables controlling stiffness and strength of lime-stabilized soils. *Journal of geotechnical and geoenvironmental engineering* 137(6), 628-632. [https://doi.org/10.1061/\(ASCE\)GT.1943-5606.0000470](https://doi.org/10.1061/(ASCE)GT.1943-5606.0000470)
- Consoli, N.C., Prietto, P.D.M., da Silva Lopes Jr, L., Winter, D., 2014. Control factors for the long-term compressive strength of lime treated sandy clay soil. *Transportation Geotechnics* 1, 129–136. <https://doi.org/10.1016/j.trgeo.2014.07.005>
- Cristelo, N., Glendinning, S., Fernandes, L., Pinto, A.T., 2012. Effect of calcium content on soil stabilisation with alkaline activation. *Construction and Building Materials* 29, 167–174. <https://doi.org/10.1016/j.conbuildmat.2011.10.049>
- Croce, P., Russo, G., 2003. Soil-water characteristic curves of lime stabilised soil, in: *Proc Int Workshop on Geotechnics of Soft Soils–Theory and Practice*. Noordwijkerhout.
- Cuisinier, O., Auriol, J.-C., le Borgne, T., Deneele, D., 2011. Microstructure and hydraulic conductivity of a compacted lime-treated soil. *Engineering geology* 123, 187–193. <https://doi.org/10.1016/j.enggeo.2011.07.010>
- Cuisinier, O., Masroui, F., 2005. Hydromechanical behaviour of a compacted swelling soil over a wide suction range. *Engineering Geology* 81, 204–212. <https://doi.org/10.1016/j.enggeo.2005.06.008>

- Cuisinier, O., Deneele, D., 2008. Long-term behaviour of lime-treated expansive soil submitted to cyclic wetting and drying. *Unsaturated soils: advances in geoen지니어ing: proceedings of the 1st European Conference on Unsaturated Soils, EUNSAT*, 327.
- Cuisinier, O., Masrouri, F., Mehenni, A., 2020. Alteration of the Hydromechanical Performances of a Stabilized Compacted Soil Exposed to Successive Wetting–Drying Cycles. *Journal of Materials in Civil Engineering* 32, 04020349. [https://doi.org/10.1061/\(ASCE\)MT.1943-5533.0003270](https://doi.org/10.1061/(ASCE)MT.1943-5533.0003270)
- Cuisinier, O., Stoltz, G., Masrouri, F., 2014. Long-term behavior of lime-treated clayey soil exposed to successive drying and wetting, in: *Geo-Congress 2014: Geo-Characterization and Modeling for Sustainability*. pp. 4146–4155. <https://doi.org/10.1061/9780784413272.403>
- Das, G., Bharat, T.V., 2016. Shrinkage behavior of clay soil: an experimental study. In: *International conference on soil and environment, ICSE, Bangalore*, 1-8.
- Das, G., Razakamanantsoa, A., Herrier, G., Saussaye, L., Lesueur, D., Deneele, D., 2020. Evaluation of the long-term effect of lime treatment on a silty soil embankment after seven years of atmospheric exposure: Mechanical, physicochemical, and microstructural studies. *Engineering Geology* 105986. <https://doi.org/10.1016/j.enggeo.2020.105986>.
- Das, G., Razakamanantsoa, A., Herrier, G., Deneele, D., 2021. Compressive strength and microstructure evolution of lime-treated silty soil subjected to kneading action. *Transportation Geotechnics*, 29, 100568. <https://doi.org/10.1016/j.trgeo.2021.100568>
- Das, G., Razakamanantsoa, A., Herrier, G., Deneele, D., 2021. Influence of pore fluid-soil structure interactions on compacted lime-treated silty soil. *Engineering Geology*. <https://doi.org/10.1016/j.enggeo.2021.106496>
- Dash, S.K., Hussain, M., 2011. Lime stabilization of soils: reappraisal. *Journal of materials in civil engineering* 24, 707–714. [https://doi.org/10.1061/\(ASCE\)MT.1943-5533.0000431](https://doi.org/10.1061/(ASCE)MT.1943-5533.0000431)
- Davoudi, M.H., Kabir, E., 2010. The interaction of lime and sodium chloride in fine grained soils with low plastic index. *Journal of Geotechnical Geology (Applied Geology)*.
- Dawson, R.F., McDowell, C., 1961. A Study of an Old Lime-Stabilized Gravel Base. *Highway Research Board Bulletin*.
- De Bel, R., Bollens, Q., Duvigneaud, P.-H., Verbrugge, J.-C., 2005. Influence of curing time, percolation and temperature on the compressive strength of a loam treated with lime, in: *Tremti 2005*. pp. 1–10.
- De Bel, R., Correia, A.G., Verbrugge, J.-C., 2009. Contribution of loamy soil treatment to improve embankments performance, in: *Characterization, Modeling, and Performance of Geomaterials: Selected Papers From the 2009 GeoHunan International Conference*. pp. 186–191. [https://doi.org/10.1061/41041\(348\)27](https://doi.org/10.1061/41041(348)27)
- De Bel, R., Gomes Correia, A., Duvigneaud, P.-H., Francois, B., Herrier, G., Verbrugge, J.-C., 2013. Evolution mécanique et physico-chimique à long terme d'un sol limoneux traité à la chaux., in: *Colloque TerDOUEST*.

- Delage, P., Lefebvre, G., 1984. Study of the structure of a sensitive Champlain clay and of its evolution during consolidation. *Canadian Geotechnical Journal* 21, 21–35. <https://doi.org/10.1139/t84-003>
- Delage, P., Pellerin, F.M., 1984. Influence de la lyophilisation sur la structure d'une argile sensible du Québec. *Clay minerals* 19, 151–160. <https://doi.org/10.1180/claymin.1984.019.2.03>
- Delage, P., Vicol, T., Suraj de Silva, G.P.R., 1992. Suction controlled testing of non-saturated soils with an osmotic consolidometer, in: *International Conference on Expansive Soils*. pp. 206–211.
- Deneele, D., Dony, A., Colin, J., Herrier, G., Lesueur, D., 2021. The carbonation of a lime-treated soil: experimental approach. *Materials and Structures*. Springer 54(1), 1-12. <https://doi.org/10.1617/s11527-021-01617-w>
- Deneele, D., 2016. Scanning Electron Microscope (SEM) investigations in soil microstructure description.
- Deneele, D., le Runigo, B., Cui, Y.-J., Cuisinier, O., Ferber, V., 2016. Experimental assessment regarding leaching of lime-treated silt. *Construction and Building Materials* 112, 1032–1040. <https://doi.org/10.1016/j.conbuildmat.2016.03.015>
- Deneele, D., Dony, A., Colin, J., Herrier, G., Lesueur, D., 2021. The carbonation of a lime-treated soil: experimental approach, *Materials and Structures*. 54(1) 1-12. <https://doi.org/10.1617/s11527-021-01617-w>
- Dhar, S., Hussain, M., 2019. The strength and microstructural behavior of lime stabilized subgrade soil in road construction. *International Journal of Geotechnical Engineering* 1–13. <https://doi.org/10.1080/19386362.2019.1598623>
- Di Sante, M., di Buò, B., Fratolocchi, E., Länsivaara, T., 2020. Lime treatment of a soft sensitive clay: A sustainable reuse option. *Geosciences* 10, 182. <https://doi.org/10.3390/geosciences10050182>
- Di Sante, M., 2019. On the Compaction Characteristics of Soil-Lime Mixtures. *Geotechnical and Geological Engineering* 1–10. <https://doi.org/10.1007/s10706-019-01110-w>
- Di Sante, M., Fratolocchi, E., Mazzieri, F., Brianzoni, V., 2015. Influence of delayed compaction on the compressibility and hydraulic conductivity of soil–lime mixtures. *Engineering Geology* 185, 131–138. <https://doi.org/10.1016/j.enggeo.2014.12.005>
- Diamond, S., Kinter, E.B., 1965. Mechanisms of soil-lime stabilization. *Highway Research Record* 92, 83–102.
- Ding, L., Vanapalli, S.K., Zou, W., Han, Z., Wang, X., 2021. Freeze-thaw and wetting-drying effects on the hydromechanical behavior of a stabilized expansive soil. *Construction and Building Materials* 275, 122162. <https://doi.org/10.1016/j.conbuildmat.2020.122162>
- Dowling, A., O'Dwyer, J., Adley, C.C., 2015. Lime in the limelight. *Journal of cleaner production* 92, 13–22. <https://doi.org/10.1016/j.jclepro.2014.12.047>
- Eades, J.L., Grim, R.E., 1966. A quick test to determine lime requirements for lime stabilization. *Highway research record*.

- Elkady, T.Y., 2016. The effect of curing conditions on the unconfined compression strength of lime-treated expansive soils. *Road Materials and Pavement Design* 17, 52–69. <https://doi.org/10.1080/14680629.2015.1062409>
- El-Rawi, N.M., Awad, 1981. Permeability of lime stabilized soils. *Journal of Transportation Engineering, ASCE* 107, 25–35. <https://doi.org/10.1061/TPEJAN.0000907>
- Erlandsson, M., Cory, N., Köhler, S., Bishop, K., 2010. Direct and indirect effects of increasing dissolved organic carbon levels on pH in lakes recovering from acidification. *Journal of Geophysical Research: Biogeosciences* 115(G3). <https://doi.org/10.1029/2009JG001082>
- European Commission, 2014a. Energy Prices and Cost Report. SWD (2014) 20 Final/ 2. Date accessed: 11/12/2014. http://ec.europa.eu/energy/doc/2030/20140122_sw_d_prices.pdf.
- Farooq, S.M., Rouf, M.A., Hoque, S.M.A., Ashad, S.M.A., 2011. Effect of lime and curing period on unconfined compressive strength of Gazipur soil, Bangladesh, in: 4th Annual Paper Meet and 1st Civil Engineering Congress. pp. 22–24.
- Fassel, V.A., Kniseley, R.N., 1974. Inductively coupled plasma. Optical emission spectroscopy. *Analytical Chemistry*, 46(13), pp.1110A-1120a.
- Fredlund, D.G., Rahardjo, H., 1993. Soil mechanics for unsaturated soils. John Wiley & Sons.
- Gallage, C., Cochrane, M., Ramanujam, J., 2012. Effects of lime content and amelioration period in double lime application on the strength of lime treated expansive sub-grade soils. In *Advances in Transportation Geotechnics 2: Proceedings of the 2nd International Conference on Transportation Geotechnics (ICTG)* 99-104. CRC Press/Balkema.
- Gao, Y., Qian, H., Li, X., Chen, J., Jia, H., 2018. Effects of lime treatment on the hydraulic conductivity and microstructure of loess. *Environmental Earth Sciences* 77, 1–15. <https://doi.org/10.1007/s12665-018-7715-9>
- Gapak, Y., Das, G., Yerramshetty, U., Bharat, T. V., 2017. Laboratory determination of volumetric shrinkage behavior of bentonites: A critical appraisal. *Applied Clay Science* 135, 554-566. <https://doi.org/10.1016/j.clay.2016.10.038>
- Griffiths, F.J., Joshi, R.C., 1989. Change in pore size distribution due to consolidation of clays. *Geotechnique* 39, 159–167. <https://doi.org/10.1680/geot.1989.39.1.159>
- GTS - LCPC-Setra Technical Guide., 2000. Soil treatment with lime and/or hydraulic binders: Application to the Construction of fills and capping layers. LCPC Eds, Paris (France).
- Haghverdi, A., Öztürk, H. S., Durner, W., 2020. Studying Unimodal, Bimodal, PDI and Bimodal-PDI Variants of Multiple Soil Water Retention Models: II. Evaluation of Parametric Pedotransfer Functions Against Direct Fits. *Water*, 12(3), 896. <https://doi.org/10.3390/w12030900>
- Han, C., Dong, Q., Xu, X., 2021. Microstructural analysis on the variation of resilient modulus of lime modified soil under freezing–thawing action. *Road Materials and Pavement Design* 1–15. <https://doi.org/10.1080/14680629.2021.1924235>

- Hara, H., Suetsugu, D., Hayii, S., 2012. Calcium Leaching Mechanism of Lime Treated Soil Immersed in Seawater. *Journal of the Society of Materials Science, Japan* 61, 11–14.
- Hara, H., Suetsugu, D., Hayashi, S., Du, Y.J., 2008. Calcium leaching properties of lime-treated soil by infiltration of tidal river water. In the Eighteenth International Offshore and Polar Engineering Conference. International Society of Offshore and Polar Engineers.
- He, J., Wang, Y., Li, Y., Ruan, X., 2015. Effects of leachate infiltration and desiccation cracks on hydraulic conductivity of compacted clay. *Water Science and Engineering* 8, 151–157. <https://doi.org/10.1016/j.wse.2015.04.004>
- Herrier, G., Chevalier, C., Froumentin, M., Cuisinier, O., Bonelli, S., Fry, J.-J., 2012. Lime treated soil as an erosion-resistant material for hydraulic earthen structures.
- Holt, C.C., Freer-Hewish, R.J. Ghataora, G.S., 2000, November. The use of lime-treated British clays in pavement construction. Part 2: The effect of mellowing on the stabilization process. In *Proceedings of the Institution of Civil Engineers-Transport* (Vol. 141, No. 4, pp. 207-216). Thomas Telford Ltd. <https://doi.org/10.1680/itrn.1998.31194>
- Holtz, R.D, Kovacs, W.D, Sheahan, T.C., 1981. *An introduction to geotechnical engineering*, Prentice-Hall Englewood Cliffs, NJ.
- Homauoni, Z.J., Yasrobi, S.S., 2011. Stabilization of dune sand with poly (methyl methacrylate) and polyvinyl acetate using dry and wet processing. *Geotechnical and Geological Engineering* 29(4), 571-579. <https://doi.org/10.1007/s10706-011-9404-2>
- Houben, H., Guillaud, H., 1994. de l'article/du chapitre Earth construction. A comprehensive guide. distributeur Craterre-Eag.
- Hunt, A.G., Sahimi, M., 2017. Flow, transport, and reaction in porous media: Percolation scaling, critical-path analysis, and effective medium approximation. *Reviews of Geophysics* 55, 993–1078. <https://doi.org/10.1002/2017RG000558>
- Ikeagwuani, C.C., Nwonu, D.C., 2019. Emerging trends in expansive soil stabilisation: A review. *Journal of Rock Mechanics and Geotechnical Engineering* 11(2), 423-440. <https://doi.org/10.1016/j.jrmge.2018.08.013>
- Ingles, O.G., Metcalf, J.B., 1972. *Soil stabilization principles and practice*.
- James, R., Kamruzzaman, A.H.M., Haque, A., Wilkinson, A., 2008. Behaviour of lime–slag-treated clay. *Proceedings of the Institution of Civil Engineers-Ground Improvement* 161, 207–216. <https://doi.org/10.1680/grim.2008.161.4.207>
- Jan, O.Q., Mir, B.A., 2018. Strength and Micro Structural Behavior of Lime Stabilized Dredged Soil, in: *International Congress and Exhibition" Sustainable Civil Infrastructures: Innovative Infrastructure Geotechnology"*. Springer, pp. 132–153. https://doi.org/10.1007/978-3-030-01917-4_11
- Jennings, H.M., Thomas, J.J., Rothstein, D., Chen, J.J., 2002. Cements as porous materials. *Handbook of porous solids* 2971–3028.

- Jha, A.K., Sivapullaiah, P. v, 2019. Lime Stabilization of Soil: A Physico-Chemical and Micro-Mechanistic Perspective. *Indian Geotechnical Journal* 1–9. <https://doi.org/10.1007/s40098-019-00371-9>
- Joel, M. and Otse, V.O., 2016. Effect of lime pre-treatment mellowing duration on some geotechnical properties of shale treated with cement. *Global Journal of Engineering Research*, 15(1), 35-46. <https://doi.org/10.4314/gjer.v15i1.5>
- Jung, C., Bobet, A., 2008. Post-construction evaluation of lime-treated soils. *Joint Transportation Research Program* 319.
- Jia, G. W., Zhan, T. L., Chen, Y. M., Fredlund, D. G., 2009. Performance of a large-scale slope model subjected to rising and lowering water levels. *Engineering Geology* 106(1-2), 92-103. <https://doi.org/10.1016/j.enggeo.2009.03.003>
- Johansson, J., Edeskär, T., 2014. Effects of external water-level fluctuations on slope stability. *The Electronic journal of geotechnical engineering* 19(K), 2437-2463.
- Karim, M.E., Alam, M.J., Hoque, M.S., 2017. Effect of salinity of water in lime-fly ash treated sand. *International Journal of Geo-Engineering* 8(1), 1-12. <https://doi.org/10.1186/s40703-017-0052-0>
- Kassiff, G., Shalom, A. ben, 1971. Experimental relationship between swell pressure and suction. *Géotechnique* 21, 245–255. <https://doi.org/10.1680/geot.1971.21.3.245>
- Katsumi, T., Ishimori, H., Onikata, M., Fukagawa, R., 2008. Long-term barrier performance of modified bentonite materials against sodium and calcium permeant solutions. *Geotextiles and Geomembranes* 26, 14–30. <https://doi.org/10.1016/j.geotextmem.2007.04.003>
- Kenai, S., Bahar, R., Benazzoug, M., 2006. Experimental analysis of the effect of some compaction methods on mechanical properties and durability of cement stabilized soil. *Journal of Materials Science* 41(21), 6956-6964. <https://doi.org/10.1007/s10853-006-0226-1>
- Khattab, S.A., Al-Mukhtar, M., Fleureau, J.-M., 2007. Long-term stability characteristics of a lime-treated plastic soil. *Journal of materials in civil engineering* 19, 358–366. [https://doi.org/10.1061/\(ASCE\)0899-1561\(2007\)19:4\(358\)](https://doi.org/10.1061/(ASCE)0899-1561(2007)19:4(358))
- Kichou, Z., 2015. A study on the effects of lime on the mechanical properties and behaviour of London clay (Doctoral dissertation, London South Bank University).
- Kitazume, M., Takahashi, H., 2009. 27 Years' investigation on property of in-situ quicklime treated clay. In *Proceedings of the 17th International Conference on Soil Mechanics and Geotechnical Engineering* (Volumes 1, 2, 3 and 4) (pp. 2358-2361). IOS Press.
- Kolias, S., Kasselouri-Rigopoulou, V., Karahalios, A., 2005. Stabilisation of clayey soils with high calcium fly ash and cement. *Cement and Concrete Composites* 27, 301–313. <https://doi.org/10.1016/j.cemconcomp.2004.02.019>
- Kouassi, P., Breyse, D., Girard, H., Poulain, D., 2000. A new technique of kneading compaction in the laboratory. *Geotechnical Testing Journal* 23, 72–82. <https://doi.org/10.1520/GTJ11125J>
- Kosmatka, S.H., Kerkhoff, B., Panarese, W.C., 2002. Design and control of concrete mixtures (Vol. 5420, pp. 60077-1083). Skokie, IL: Portland Cement Association.

- Kumar, A., Walia, B.S., Bajaj, A., 2007. Influence of fly ash, lime, and polyester fibers on compaction and strength properties of expansive soil. *Journal of materials in civil engineering* 19, 242–248. [https://doi.org/10.1061/\(ASCE\)0899-1561\(2007\)19:3\(242\)](https://doi.org/10.1061/(ASCE)0899-1561(2007)19:3(242))
- Le Runigo, B., Cuisinier, O., Cui, Y.-J., Ferber, V., Deneele, D., 2009. Impact of initial state on the fabric and permeability of a lime-treated silt under long-term leaching. *Canadian Geotechnical Journal* 46, 1243–1257. <https://doi.org/10.1139/T09-061>
- Le Runigo, B., Ferber, V., Cui, Y.-J., Cuisinier, O., Deneele, D., 2011. Performance of lime-treated silty soil under long-term hydraulic conditions. *Engineering geology* 118, 20–28. <https://doi.org/10.1016/j.enggeo.2010.12.002>
- Lekarp, F., Isacsson, U., Dawson, A., 2000. State of the art. II: Permanent strain response of unbound aggregates. *Journal of Transportation Engineering* 126, 76–83. [https://doi.org/10.1061/\(ASCE\)0733-947X\(2000\)126:1\(76\)](https://doi.org/10.1061/(ASCE)0733-947X(2000)126:1(76))
- Lemaire, K., Deneele, D., Bonnet, S., Legret, M., 2013. Effects of lime and cement treatment on the physicochemical, microstructural and mechanical characteristics of a plastic silt. *Engineering Geology* 166, 255–261. <https://doi.org/10.1016/j.enggeo.2013.09.012>
- Liang, S., Chen, J., Guo, M., Feng, D., Liu, L., Qi, T., 2020. Utilization of pretreated municipal solid waste incineration fly ash for cement-stabilized soil. *Waste Management* 105, 425–432. <https://doi.org/10.1016/j.wasman.2020.02.017>
- Lime Manual, 2004. Lime-Treated Soil Construction Manual – Lime Stabilization and Lime Modification. published by National Lime Association, USA, Bulletin 326.
- Lipiec, J., Hajnos, M., Świeboda, R., 2012. Estimating effects of compaction on pore size distribution of soil aggregates by mercury porosimeter. *Geoderma* 179, 20–27. <https://doi.org/10.1016/j.geoderma.2012.02.014>
- Little, D.N., 2000. Evaluation of structural properties of lime stabilized soils and aggregates, Volume 3: Mixture Design and Testing Protocol for Lime Stabilized Soils. National Lime Association, <http://www.lime.org/SOIL3>. PDF, accessed February 13, 2013.
- Little, D.N., 1995. Stabilization of pavement subgrades and base courses with lime.
- Little, D.N., 1993. Evaluation of the Structural Properties of Stabilized Pavement Layers. Interim Report to the Texas Department of Transportation, Research Project 1287.
- Little, D.N., 1992. Comparison of in-situ resilient moduli of aggregate base courses with and without low percentages of lime stabilization, in: *Innovations and Uses for Lime*. ASTM International. <https://doi.org/10.1520/STP15526S>
- Little, D.N., 1987. Fundamentals of the Stabilization of Soil with Lime. National Lime Association.
- Liu, L., Li, Z., Liu, X., Li, Y., 2018 Effect of salt content on freezing temperature and unconfined compression strength of lime-treated subgrade clay. *Applied Clay Science* 158, 65-71. <https://doi.org/10.1016/j.clay.2018.03.022>

- Locat, J., Trembaly, H., Leroueil, S., 1996. Mechanical and hydraulic behaviour of a soft inorganic clay treated with lime. *Canadian geotechnical journal* 33, 654–669. <https://doi.org/10.1139/t96-090-311>
- Lucian, C., 2013. Effectiveness of mellowing time on the properties of two stage lime cement stabilized expansive soil. *International Journal of Engineering Research and Technology (IJERT)* 2(50), 623-634.
- Makki-Szymkiewicz, L., Hibouche, A., Taibi, S., Herrier, G., Lesueur, D., Fleureau, J.-M., 2015. Evolution of the properties of lime-treated silty soil in a small experimental embankment. *Engineering Geology* 191, 8–22. <https://doi.org/10.1016/j.enggeo.2015.03.008>
- Manzoor, S.O., Yousuf, A., 2020. Stabilisation of Soils with Lime: A Review.
- Massat, L., Cuisinier, O., Bihannic, I., Claret, F., Pelletier, M., Masrouri, F., Gaboreau, S., 2016. Swelling pressure development and inter-aggregate porosity evolution upon hydration of a compacted swelling clay. *Applied Clay Science, Elsevier* 124, 197–210. <https://doi.org/10.1016/j.clay.2016.01.002>
- McCallister, L.D., Petry, T.M., 1992. Leach tests on lime-treated clays. *Geotechnical testing journal* 15, 106–114. <https://doi.org/10.1520/GTJ10232J>
- McGregor, F., Heath, A., Fodde, E., Shea, A., 2014. Conditions affecting the moisture buffering measurement performed on compressed earth blocks. *Building and Environment* 75, 11–18. <https://doi.org/10.1016/j.buildenv.2014.01.009>
- Miller, G.A., Azad, S., 2000. Influence of soil type on stabilization with cement kiln dust. *Construction and building materials* 14, 89–97. [https://doi.org/10.1016/S0950-0618\(00\)00007-6](https://doi.org/10.1016/S0950-0618(00)00007-6)
- Mirzababaei, M., Yasrobi, S., Al-Rawas, A., 2009. Effect of polymers on swelling potential of expansive soils. *Proceedings of the Institution of Civil Engineers-Ground Improvement* 162(3), 111-119. <https://doi.org/10.1680/grim.2009.162.3.111>
- Mitchell, J.K., Hooper, D.R., 1961. Influence of time between mixing and compaction on properties of a lime-stabilized expansive clay. *Highway Research Board Bulletin*.
- Mitchell, J.K., Hooper, D.R., Campenella, R.G., 1965. Permeability of compacted clay. *Journal of the Soil Mechanics and Foundations Division* 91, 41–65. <https://doi.org/10.1061/JSFEAQ.0000775>
- Mitchell, J.K., Soga, K., 2005. *Fundamentals of soil behavior*. John Wiley & Sons Hoboken, NJ.
- Mitchell, J.K., McConnell, J.R., 1965. Some Characteristics of the elastic and plastic deformation of clay on initial loading. *Institute of Transportation and Traffic Engineering, University of California*.
- Mohammadi, M., Shadizadeh, S.R., Manshad, A.K., Mohammadi, A.H., 2020. Experimental study of the relationship between porosity and surface area of carbonate reservoir rocks. *Journal of Petroleum Exploration and Production Technology*, pp.1-18.
- Moghal, A.A.B., Ashfaq, M., Al-Obaid, A.A.K.H., Abbas, M.F., Al-Mahbashi, A.M., Shaker, A.A., 2020. Compaction delay and its effect on the geotechnical properties of lime treated semi-arid soils. *Road Materials and Pavement Design* 1–15. <https://doi.org/10.1080/14680629.2020.1784256>

- Mossadeghi-Björklund, M., Jarvis, N., Larsbo, M., Forkman, J., Keller, T., 2019. Effects of compaction on soil hydraulic properties, penetration resistance and water flow patterns at the soil profile scale. *Soil Use and Management* 35, 367–377. <https://doi.org/10.1111/sum.12481>
- Nabil, M., Mustapha, A., Rios, S., 2020. Impact of wetting—drying cycles on the mechanical properties of lime-stabilized soils. *International Journal of Pavement Research and Technology*. Springer 13(1), 83–92. <https://doi.org/10.1007/s42947-019-0088-y>
- Nalbantoglu, Z., Tuncer, E.R., 2001. Compressibility and hydraulic conductivity of a chemically treated expansive clay. *Canadian geotechnical journal* 38, 154–160. <https://doi.org/10.1139/t00-076>
- Nasrizar, A.A., Muttharam, M., Ilamparuthi, K., 2010. Effect of placement water content on strength of temperature cured lime treated expansive soil, in: *Ground Improvement and Geosynthetics*. pp. 174–180. [https://doi.org/10.1061/41108\(381\)23](https://doi.org/10.1061/41108(381)23)
- National Lime Association, 2020. Uses of lime. <https://www.lime.org/lime-basics/uses-of-lime/Netterberg>, F., Paige-Green, P., 1984. Carbonation of lime and cement stabilized layers in road construction.
- NF P 94-093, 1993. Détermination des caractéristiques de compactage du sol. Paris: AFNOR
- NF P11-300, 1992. Exécution des terrassements—Classification des matériaux utilisables dans la construction des remblais et des couches de forme d’infrastructures routières. AFNOR Boutique, France (in French).
- NF EN 13286-2, 2010. Unbound and hydraulically bound mixtures—part 2: test methods for laboratory reference density and water content—proctor compaction.
- Nguyen, T.T.H., Cui, Y.-J., Ferber, V., Herrier, G., Ozturk, T., Plier, F., Puiatti, D., Salager, S., Tang, A.M., 2019. Effect of freeze-thaw cycles on mechanical strength of lime-treated fine-grained soils. *Transportation Geotechnics* 21, 100281. <https://doi.org/10.1016/j.trgeo.2019.100281>
- Nguyen TTH, 2015. Stabilisation des sols traités à la chaux et leur comportement au gel.
- Ojuri, O.O., Adavi, A.A., Oluwatuyi, O.E., 2017. Geotechnical and environmental evaluation of lime–cement stabilized soil–mine tailing mixtures for highway construction. *Transportation Geotechnics* 10, 1–12. <https://doi.org/10.1016/j.trgeo.2016.10.001>
- Osinubi, K.J., Nwaiwu, C.M., 2006. Compaction delay effects on properties of lime-treated soil. *Journal of materials in Civil Engineering* 18(2), 250-258. [https://doi.org/10.1061/\(ASCE\)0899-1561\(2006\)18:2\(250\)](https://doi.org/10.1061/(ASCE)0899-1561(2006)18:2(250))
- Osinubi, K.J., 1998. Permeability of lime-treated lateritic soil. *Journal of Transportation Engineering* 124, 465–469. [https://doi.org/10.1061/\(ASCE\)0733-947X\(1998\)124:5\(465\)](https://doi.org/10.1061/(ASCE)0733-947X(1998)124:5(465))
- Osula, D.O.A., 1996. A comparative evaluation of cement and lime modification of laterite. *Engineering geology* 42, 71–81. [https://doi.org/10.1016/0013-7952\(95\)00067-4](https://doi.org/10.1016/0013-7952(95)00067-4)
- Prêt, D., 2003. Nouvelles méthodes quantitatives de cartographie de la minéralogie et de la porosité dans les matériaux argileux: application aux bentonites compactées des barrières ouvragées. Université de Poitiers, PhD diss., CEA, Grenoble.

- Prêt, D., Sammartino, S., Beaufort, D., Meunier, A., Fialin, M., Michot, L.J., 2010. A new method for quantitative petrography based on image processing of chemical element maps: Part I. Mineral mapping applied to compacted bentonites. *American Mineralogist*, GeoScienceWorld 95(10), 1379–1388. <https://doi.org/10.2138/am.2010.3431>
- Punmia, B., Jain, A.K., 2005. Soil mechanics and foundations. Firewall Media.
- Puppala, A.J., 2021. Performance Evaluation of Infrastructure on Problematic Expansive Soils: Characterization Challenges, Innovative Stabilization Designs, and Monitoring Methods. *Journal of Geotechnical and Geoenvironmental Engineering* 147, 04021053. [https://doi.org/10.1061/\(ASCE\)GT.1943-5606.0002518](https://doi.org/10.1061/(ASCE)GT.1943-5606.0002518)
- Puppala, A.J., Manosuthikij, T., Chittoori, B.C.S., 2013. Swell and shrinkage characterizations of unsaturated expansive clays from Texas. *Engineering Geology* 164, 187–194. <https://doi.org/10.1016/j.enggeo.2013.07.001>
- Raja, P.S.K., Thyagaraj, T., 2020. Effect of compaction time delay on compaction and strength behavior of lime-treated expansive soil contacted with sulfate. *Innovative Infrastructure Solutions* 5, 1–15. <https://doi.org/10.1007/s41062-020-0268-2>
- Ranaivomanana, H., Razakamanantsoa, A., Amiri, O., 2018. Effects of cement treatment on microstructural, hydraulic, and mechanical properties of compacted soils: Characterization and modelling. *International Journal of Geomechanics* 18:04018106. [https://doi.org/10.1061/\(ASCE\)GM.1943-5622.0001248](https://doi.org/10.1061/(ASCE)GM.1943-5622.0001248)
- Ranaivomanana, H., Razakamanantsoa, A., Amiri, O., 2017. Permeability prediction of soils including degree of compaction and microstructure. *International Journal of Geomechanics* 17:04016107. [https://doi.org/10.1061/\(ASCE\)GM.1943-5622.0000792](https://doi.org/10.1061/(ASCE)GM.1943-5622.0000792)
- Rajasekaran, G., Rao, S.N., 2002. Permeability characteristics of lime treated marine clay. *Ocean engineering* 29, 113–127. [https://doi.org/10.1016/S0029-8018\(01\)00017-8](https://doi.org/10.1016/S0029-8018(01)00017-8)
- Razakamanantsoa, A.R., Djeran-Maigre, I., 2016. Long term chemo-hydro-mechanical behavior of compacted soil bentonite polymer complex submitted to synthetic leachate. *Waste management* 53, 92–104. <https://doi.org/10.1016/j.wasman.2016.04.023>
- Razakamanantsoa, A.R., Barast, G., Djeran-Maigre, I., 2012. Hydraulic performance of activated calcium bentonite treated by polyionic charged polymer. *Applied Clay Science* 59, 103–114. <https://doi.org/10.1016/j.clay.2012.01.022>
- Rogers, C.D.F., Glendinning, S., 1996. Modification of clay soils using lime. *Lime Stabilisation: Proceedings of the seminar held at Loughborough University Civil & Building Engineering Department on 25 September*, Thomas Telford Publishing, p. 99–114.
- Romero, E., Simms, P.H., 2008. Microstructure investigation in unsaturated soils: a review with special attention to contribution of mercury intrusion porosimetry and environmental scanning electron microscopy. *Geotechnical and Geological Engineering* 26, 705–727.

- Rosone, M., Celauro, C., Ferrari, A., 2020. Microstructure and shear strength evolution of a lime-treated clay for use in road construction. *International Journal of Pavement Engineering* 21, 1147–1158. <https://doi.org/10.1080/10298436.2018.1524144>
- Rosone, M., Megna, B., Celauro, C., 2019. Analysis of the chemical and microstructural modifications effects on the hydro-mechanical behaviour of a lime-treated clay. *International Journal of Geotechnical Engineering* 1–14. <https://doi.org/10.1080/19386362.2019.1639351>
- Rosone, M., Ferrari, A., Celauro, C., 2018. On the hydro-mechanical behaviour of a lime-treated embankment during wetting and drying cycles. *Geomechanics for Energy and the Environment* 14, 48–60. <https://doi.org/10.1016/j.gete.2017.11.001>
- Rouquerol, J., Avnir, D., Fairbridge, C.W., Everett, D.H., Haynes, J.M., Pernicone, N., Ramsay, J.D.F., Sing, K.S.W., Unger, K.K., 1994. Recommendations for the characterization of porous solids (Technical Report). *Pure and Applied Chemistry* 66, 1739–1758.
- Russo, G., Modoni, G., 2013. Fabric changes induced by lime addition on a compacted alluvial soil. *Géotechnique Letters* 3, 93–97. <https://doi.org/10.1680/geolett.13.026>
- Russo, G., 2005. Water retention curves of lime stabilised soil. *Advanced experimental unsaturated soil mechanics* 391–396.
- Sato, K., Barast, G., Razakamanantsoa, A.R., Djeran-Maigre, I., Katsumi, T., Levacher, D., 2017. Comparison of prehydration and polymer adding effects on Na activated Ca-bentonite by free swell index test. *Applied Clay Science* 142, 69–80. <https://doi.org/10.1016/j.clay.2016.10.009>
- Shackelford, C.D., Benson, C.H., Katsumi, T., Edil, T.B., Lin, L., 2000. Evaluating the hydraulic conductivity of GCLs permeated with non-standard liquids. *Geotextiles and Geomembranes* 18, 133–161. [https://doi.org/10.1016/S0266-1144\(99\)00024-2](https://doi.org/10.1016/S0266-1144(99)00024-2)
- Show, K.-Y., Tay, J.-H., Goh, A.T.C., 2003. Reuse of incinerator fly ash in soft soil stabilization. *Journal of materials in civil engineering* 15, 335–343. [https://doi.org/10.1061/\(ASCE\)0899-1561\(2003\)15:4\(335\)](https://doi.org/10.1061/(ASCE)0899-1561(2003)15:4(335))
- Sikora, P., Cendrowski, K., Abd Elrahman, M., Chung, S-Y., Mijowska, E., Stephan, D. 2019. The effects of seawater on the hydration, microstructure and strength development of Portland cement pastes incorporating colloidal silica. *Applied Nanoscience*, Springer 1–12.
- Sivapullaiah, P. v, Prashanth, J.P., Sridharan, A., 1998. Delay in compaction and importance of the lime fixation point on the strength and compaction characteristics of soil. *Proceedings of the Institution of Civil Engineers-Ground Improvement* 2, 27–32. <https://doi.org/10.1680/gi.1998.020105>
- Sotomayor, F.J, Cychosz, K.A, Thommes, M., 2018. Characterization of micro/mesoporous materials by physisorption: concepts and case studies, *Accounts of Materials & Surface Research* 2, 36-37.
- Srisutthiyakorn, N., Mavko, G., 2016. Hydraulic tortuosity: From artificial packs to natural rocks, in: *SEG Technical Program Expanded Abstracts 2016*. Society of Exploration Geophysicists, pp. 3133–3137. <https://doi.org/10.1190/segam2016-13966753.1>

- Stockdale, A., Tipping, E., Lofts, S., Mortimer, R.J., 2016. Effect of ocean acidification on organic and inorganic speciation of trace metals. *Environmental Science & Technology* 50(4), 1906-1913. <https://doi.org/10.1021/acs.est.5b05624>
- Stoltz, G., Cuisinier, O., Masrouri, F., 2014. Weathering of a lime-treated clayey soil by drying and wetting cycles. *Engineering Geology* 181, 281–289. <https://doi.org/10.1016/j.enggeo.2014.08.013>
- Stoltz, G., Cuisinier, O., Masrouri, F., 2012. Multi-scale analysis of the swelling and shrinkage of a lime-treated expansive clayey soil. *Applied clay science* 61, 44–51. <https://doi.org/10.1016/j.clay.2012.04.001>
- Sunil, B.M., Deepa, A. v, 2016. Influence of drying temperature on three soils physical properties. *Geotechnical and Geological Engineering* 34, 777–788. <https://doi.org/10.1007/s10706-016-0001-2>
- Sweeney, D. A., Wong, D. K. H., Fredlund, D. G., 1988. Effect of lime on highly plastic clay with special emphasis on aging. *Transportation Research Record* 1190, 13-23.
- Talluri, N., Puppala, A.J., Chittoori, B.C., Gaily, A.H. and Harris, P., 2013. Stabilization of high-sulfate soils by extended mellowing. *Transportation research record*, 2363(1), 96-104. <https://doi.org/10.3141/2363-11>
- Todingrara, Y.T., Tjaronge, M.W., Harianto, T., Ramli, M., 2017. Performance of laterite soil stabilized with lime and cement as a road foundation. *International Journal of Applied Engineering Research* 12, 4699–4707.
- Tran, T.D., Cui, Y.-J., Tang, A.M., Audiguier, M., Cojean, R., 2014a. Effects of lime treatment on the microstructure and hydraulic conductivity of Héricourt clay. *Journal of Rock Mechanics and Geotechnical Engineering* 6, 399–404. <https://doi.org/10.1016/j.jrmge.2014.07.001>
- Tran-Nguyen, H.H., Wong, H., Ragueneau, F., Ha-Minh, C. eds., 2017. *Proceedings of the 4th Congrès International de Géotechnique-Ouvrages-Structures: CIGOS 2017*, 26-27 October, Ho Chi Minh City, Vietnam (Vol. 8). Springer.
- Ural, N., 2021. The significance of scanning electron microscopy (SEM) analysis on the microstructure of improved clay: An overview. *Open Geosciences* 13, 197–218. <https://doi.org/10.1515/geo-2020-0145>
- Verbrugge, J.-C., de Bel, R., Correia, A.G., Duvigneaud, P.-H., Herrier, G., 2011. Strength and micro observations on a lime treated silty soil, in: *Road Materials and New Innovations in Pavement Engineering*. pp. 89–96. [https://doi.org/10.1061/47634\(413\)12](https://doi.org/10.1061/47634(413)12)
- Le Vern, M., Sediki, O., Razakamanantsoa, A., Murzyn, F., Larrarte, F., 2020. Experimental study of particle lift initiation on roller-compacted sand–clay mixtures. *Environmental Geotechnics*, 1–12. <https://doi.org/10.1680/jenge.19.00172>
- Vaverková, M.D., Elbl, J., Koda, E., Adamcová, D., Bilgin, A., Lukas, V., Podlasek, A., Kintl, A., Wdowska, M., Brtnický, M., 2020. Chemical Composition and Hazardous Effects of Leachate from the Active Municipal Solid Waste Landfill Surrounded by Farmlands. *Sustainability* 12, 4531. <https://doi.org/10.3390/su12114531>

- Vitale, E., 2016. Chemo-Physical evolution and Hydro-mechanical behavior of lime-treated clays, PhD thesis, University of Cassino and Southern Lazio, Italy.
- Vitale, E., Deneele, D., Paris, M., Russo, G., 2017. Multi-scale analysis and time evolution of pozzolanic activity of lime treated clays. *Applied Clay Science* 141, 36–45. <https://doi.org/10.1016/j.clay.2017.02.013>
- Vitale, E., Russo, G., Deneele, D., 2018. Carbonation of lime treated fine grained soils, in: Proc. of 7th International Conference on Unsaturated Soils (UNSAT2018), Hong Kong, China. pp. 3–5.
- Vitale, E., Deneele, D., Russo, G., 2020. Microstructural investigations on plasticity of lime-treated soils. *Minerals* 10, 386. <https://doi.org/10.3390/min10050386>
- Wang, J., Liu, E., Li, L., 2018. Multiscale investigations on hydration mechanisms in seawater OPC paste. *Construction and Building Materials*, Elsevier 191, 891–903. <https://doi.org/10.1016/j.conbuildmat.2018.10.010>
- Wang, D., Zentar, R., Abriak, N.E., 2017. Temperature-accelerated strength development in stabilized marine soils as road construction materials. *Journal of Materials in Civil Engineering* 29, 04016281. [https://doi.org/10.1061/\(ASCE\)MT.1943-5533.0001778](https://doi.org/10.1061/(ASCE)MT.1943-5533.0001778)
- Wang, Y., Cui, Y.-J., Tang, A.M., Benahmed, N., 2016. Aggregate size effect on the water retention properties of a lime-treated compacted silt during curing, in: E3S Web of Conferences. EDP Sciences, p. 11013. <https://doi.org/10.1051/e3sconf/20160911013>
- Watabe, Y., Leroueil, S., le Bihan, J-P., 2000. Influence of compaction conditions on pore-size distribution and saturated hydraulic conductivity of a glacial till. *Canadian Geotechnical Journal* 2000 37:1184–1194. <https://doi.org/10.1139/t00-053>
- Westermarck, S., 2000. Use of mercury porosimetry and nitrogen adsorption in characterisation of the pore structure of mannitol and microcrystalline cellulose powders, granules and tablets.
- Williams, J., Shaykewich, C.F., 1969. An evaluation of polyethylene glycol (PEG) 6000 and PEG 20,000 in the osmotic control of soil water matric potential. *Canadian Journal of Soil Science* 49, 397–401. <https://doi.org/10.4141/cjss69-054>
- Xiong, X., Zhenming, S., Yonglin, M. P., Xiaolong, M., Feng Z., 2019. Unsaturated slope stability around the Three Gorges Reservoir under various combinations of rainfall and water level fluctuation. *Engineering Geology* 261, 105231. <https://doi.org/10.1016/j.enggeo.2019.105231>
- Xu, L., Zha, F., Liu, C., Kang, B., Liu, J., Yu, C., 2020. Experimental Investigation on Carbonation Behavior in Lime-Stabilized Expansive Soil. *Advances in Civil Engineering* 2020. <https://doi.org/10.1155/2020/7865469>
- Yin, C., Zhang, W., Jiang, X., Huang, Z., 2018. Effects of initial water content on microstructure and mechanical properties of lean clay soil stabilized by compound calcium-based stabilizer. *Materials* 11, 1933. <https://doi.org/10.3390/ma11101933>
- Young, R., 2012. Soil properties and behaviour. Elsevier.

Yunus, N.Z.M., Wanatowski, D., Stace, R., Marto, A., Abdullah, R.A., Mashros, N., 2014. A short review of the factors influencing lime-clay reactions. *Electron. J. Geotech. Eng* 19, 6269–6282.

Zhang, M., Guo, H., El-Korchi, T., Zhang, G., Tao, M., 2013. Experimental feasibility study of geopolymer as the next-generation soil stabilizer. *Construction and Building Materials* 47, 1468–1478. <https://doi.org/10.1016/j.conbuildmat.2013.06.017>

Zhang, Y., Daniels, J.L., Cetin, B., Baucom, I.K., 2020. Effect of Temperature on pH, Conductivity, and Strength of Lime-Stabilized Soil. *Journal of Materials in Civil Engineering* 32, 04019380. [https://doi.org/10.1061/\(ASCE\)MT.1943-5533.0003062](https://doi.org/10.1061/(ASCE)MT.1943-5533.0003062)

Zielinski, J.M, Kettle, L., 2013. *Physical characterization: surface area and porosity*. London: Intertek.

APPENDIX-I

Peer reviewed Journals

Published

- **Das, G.**, Razakamanantsoa, A., Herrier, G., Saussaye, L., Lesueur, D., & Deneele, D. (2021). Evaluation of the long-term effect of lime treatment on a silty soil embankment after seven years of atmospheric exposure: Mechanical, physicochemical, and microstructural studies. *Engineering Geology*, 281, 105986. <https://doi.org/10.1016/j.enggeo.2020.105986>
- **Das, G.**, Razakamanantsoa, A., Herrier, G., & Deneele, D. (2021). Compressive strength and microstructure evolution of lime-treated silty soil subjected to kneading action. *Transportation Geotechnics*, 29, <https://doi.org/10.1016/j.trgeo.2021.100568>
- **Das, G.**, Razakamanantsoa, A., Herrier, G., & Deneele, D. (2021). Influence of pore fluid-soil structure interactions on compacted lime-treated silty soil. *Engineering Geology*. <https://doi.org/10.1016/j.enggeo.2021.106496>.

Under review

- Ranaivomanana, H., **Das, G.**, & Razakamanantsoa, A. Modelling of hysteretic behaviour of soil-water retention curves using an original pore network model. *Transport in Porous Media*.
- **Das, G.**, Razakamanantsoa, A., Herrier, G., & Deneele, D. Physicochemical and microstructure evaluation in lime-treated silty soil exposed to successive wetting-drying cycles using different testing conditions. *Journal of Materials in Civil Engineering*.
- **Das, G.**, Razakamanantsoa, A., Herrier, G., & Deneele, D. Influence of wetting fluids on the compressive strength, physicochemical, and pore-structure evolution in lime-treated silty soil subjected to wetting and drying cycles. *Bulletin of Engineering Geology and the Environment*.
- **Das, G.**, Razakamanantsoa, A., Herrier, G., & Deneele, D. Soil improvement by lime treatment: A review. *Journal of Rock Mechanics and Geotechnical Engineering*.

Conferences (National & International)

- Saussaye, L., **Das, G.**, Razakamanantsoa, A., Rayssac, E., Deneele, D., Chevalier, C., ... & Ranaivomanana, H. (2020, November). Dignes expérimentales du CER de Rouen en sol limoneux traité à la chaux et non traité: évaluation après 7 ans. In Journées Nationales de Géotechnique et de Géologie de l'Ingénieur (pp. 9-p).
- **Das, G.**, Razakamanantsoa, A., Herrier, G., & Deneele, D. (2022). Hydraulic performance and microstructure evolution of kneading compacted lime-treated silty soil permeated with low-ionic strength solution. Proceedings of the 20th International Conference on Soil Mechanics and Geotechnical Engineering, Sydney. (Accepted)
- **Das, G.**, Razakamanantsoa, A., Herrier, G., & Deneele, D. (2022). Hydromechanical and pore-structure evolution in lime-treated kneading compacted soil. ASCE Geo-Congress, Charlotte. (Accepted)

Patent

- **Das, G.**, Razakamanantsoa, A., & Rayssac, E. A regulated device to simulate the in-situ wetting and drying conditions in compacted soil (filed on 2nd December, 2021).

Titre : Évaluation du compactage par pétrissage et des performances à long terme des sols traités à la chaux.

Mots clés : traitement à la chaux, pétrissage, microstructure, fluide d'essai, humidification et séchage.

Résumé : L'étude du comportement des sols traités à la chaux est axée sur l'analyse de l'influence des conditions de mise en œuvre en laboratoire et in situ avec une attention particulière sur l'évolution de la microstructure.

Les échantillons de sol prélevés dans un remblai constitué d'un sol traité à la chaux, soumis à l'exposition atmosphérique pendant 7 ans, montrent une évolution significative des performances du matériau, notamment sa résistance à la compression. Ces résultats mettent en évidence l'influence du traitement à la chaux sur le long terme. Le remblai étudié a été mis en œuvre par "compactage par pétrissage", dont le mécanisme est moins étudié dans la littérature. Le pétrissage semble améliorer la dispersion de la chaux dans le sol, ainsi que sa structuration. Cette propriété est favorable à l'hydratation de composés cimentaires, particulièrement, en cas de présence d'eau disponible. L'effet du fluide interstitiel sur la performance hydraulique des

sols traités à la chaux, et le mécanisme de lixiviation associé sont étudiés en fonction du volume des pores traversés par le fluide. Le nombre de volume de pore traversé s'avère être un paramètre clé pour l'étude de la durabilité des performances des sols traités. L'eau déminéralisée s'avère être plus agressive qu'une solution à faible force ionique. Cela démontre l'importance de prendre en compte le type de solution perméante.

La performance à long terme du sol traité à la chaux soumis au cycle d'humidification-séchage, sous différentes conditions d'essai et différents fluides, est évaluée. L'étude a révélé la contribution de la nature du fluide d'imbibition et des effets de la température sur l'évolution des propriétés physico-chimiques et microstructurales du sol traité à la chaux.

Ainsi, la condition de compactage mise en œuvre, la nature du fluide d'essai et les conditions d'essai à l'échelle du laboratoire doivent se rapprocher de la situation sur le terrain.

Title: Evaluation of kneading compaction method and the long-term performances of lime-treated soils.

Keywords: Lime-treated soil, kneading compaction, microstructure, Pore fluids, durability, wetting-drying cycles.

Abstract: Investigation of the behavior of lime-treated soil with emphasis on laboratory and field implementation technics and microstructural observations is made.

Field investigation of a 7-year atmospherically cured embankment, thanks to measurement of sampled materials performances, shows a significant evolution in compressive strength, evidencing the long-term benefits of lime treatment. This embankment was subjected to 'kneading compaction', which mechanism is less investigated. At laboratory scale, 'kneading compaction' is found to improve lime-dispersion and soil fabric. Such features, if accompanied by available water, favors the development of cementitious compounds. The effect of pore fluid on the hydraulic conductivity, k evolution, and leaching mechanism of kneaded lime-treated soil is studied. Using demineralized

water as pore fluid is found to be comparatively aggressive than a low-ionic strength solution. Thus, demonstrating the importance of consideration of the type of permeant solution.

Long-term performance of lime-treated soil by subjecting them to wetting-drying cycle using different testing conditions and different wetting fluids is evaluated. The evaluation revealed the importance of consideration of the nature of wetting fluid and temperature effects on the physicochemical and microstructure evolution of lime-treated soil.

Thus, the reproduced compaction procedure, nature of the permeant solution, and testing conditions in the laboratory scale must be closer to the field situation.